THE GENERATION AND TRANSMISSION OF PRESSURE FLUCTUATIONS IN PUMP SUCTION LINES

submitted by

Francisco J. T. de Freitas

for the degree of PhD of the University of Bath 1982

SUMMARY

A thorough study of standing waves in hydraulic lines is carried out using transmission line theory. Special emphasis is attached to the representation of standing wave patterns of different systems by three dimensional graphs. From this study a new experimental test method has been developed for evaluating the fluid borne noise characteristics of pumps and other hydraulic components. The validity and accuracy of this test method, named the "tuned length method", was assessed by comparison with other existing methods. Unlike many other experimental methods, the tuned length method is capable of testing hydraulic components at low mean pressures.

The "tuned length method" was used to evaluate the inlet fluid borne noise characteristics of three gear pumps and an axial piston pump. A purpose built pressurized reservoir was used to control pump inlet conditions. Large pressure fluctuations were measured at some positions in pressurized suction lines and were found to be similar to fluctuations measured in pump discharge lines. The levels of pressure ripple in a pump suction line were found to have a significant affect on the air borne levels generated by the hydraulic system.

There is strong evidence of air release occurring in the pump inlet passageway under normal operating conditions. This accounts for the very low pressure ripples in the suction line of a normally aspirated pump. However, this does not affect the volumetric efficiency of the pump. When the pump inlet is pressurized air release is inhibited and the pressure ripple can be very large.

An axial piston pump was tested when boosted by another piston pump and the inlet characteristics were evaluated. These characteristics are very similar to those obtained when the pump is supplied by a pressurized reservoir.

In order to maintain low fluid borne noise in pump suction lines the mean inlet pressure must be kept as low as possible. The existence of air disolved in the fluid in small quantities is favourable as it prevents very low instantaneous pressures and hence limit the possibility of cavitation. The use of a pressurized reservoir is recommended for this purpose, as long as steps are taken to avoid solution of additional quantities of air.

ACKNOWLEDGEMENTS

The author wishes to thank everyone who helped making this thesis a reality.

This thesis would never have been written without the help and continuous guidance of Prof. D.E. Bowns, Head of School of Engineering and the financial support of the Fluid Power Centre of the University of Bath. The author is most grateful to his supervisor, Dr. K.A. Edge for his tireless help and encouragement, and to Dr. D.G. Tilley, Mr. B. Lipscombe and Mr. T. Wing for the very fruitful 'coffee break' discussions.

The implementation of the test rig was possible with the practical assistance of the staff of the laboratory of the Fluid Power Centre.

The author would also like to thank Dr. R.A. Sarmento, of the University of Porto, for allowing the undertaking of this research study.

The word processing and printing of this thesis was possible with the kind permission and co-operation of Mr. D. Cunningham, Dr. A. Bowyer and Dr. I. Holyer of the Computer Unit of the University of Bath.

Finally, I would like to thank my wife, Prazeres, for her moral support throughout this work which made it all worthwhile.

NOTATION

a	local speed of sound in the fluid	[m/s]
A	internal area of pipe	[m^2]
b	gear width	[m]
c	coefficient	-
d	internal diameter of pipe	[m]
d	piston diameter(section 3.6.1)	[m]
D	displacement ripple of pump	[m^3/rad]
flowi	instantaneous flow delivery by ith piston	[m^3/s]
g	acceleration due to gravity	[m/s^2]
j	complex operator	-
n	exponential coefficient	-
n	number of pistons (section 3.6.1)	-
P_J	pressure fluctuations at junction	[N/m^2]
P_o	pressure fluctuations measured at pump flange	[N/m^2]
P_m	pressure fluctuations due to motor flow ripple	[N/m^2]
P_{mx}	Pm measured at distance x from pump	[N/m^2]
P_{px}	press. fluct. due to pump ripple measured at point x	[N/m^2]
P_x	pressure fluctuation at distance x from source	[N/m^2]
Q_J	flow ripple at junction	[m^3/s]
Q_L	mean leakage flow	[m^3/s]
Q_s	source flow fluctuation of pump	[m^3/s]
Q_{sm}	motor flow ripple	[m^3/s]
Q_{sp}	pump flow ripple	[m^3/s]
Q_1	flow ripple at entrance to branch 1	[m^3/s]
Q_2	flow ripple at entrance to branch 2	[m^3/s]
R	pressure drop in pipe/unit length/unit flow	[Ns/m^6]
s	laplace transform operator	[1/s]

v	velocity	[m/s]
V	volume of oil	[m^3]
V_p	volume of oil inside pump outlet chamber	[m^3]
x	distance between source and point in line	[m]
z	number of teeth per gear	-
Z	impedance	[Ns/m^5]
Z_E	entry impedance	[Ns/m^5]
Z_{eq}	equivalent impedance of two impedances in parallel	[Ns/m^5]
Z_i	inductive impedance	[Ns/m^5]
Z_L	leakage impedance	[Ns/m^5]
Z_o	line impedance	[Ns/m^5]
Z_s	source impedance	[Ns/m^5]
Z_{sm}	source impedance of motor	[Ns/m^5]
Z_{sp}	source impedance of pump	[Ns/m^5]
Z_t	termination impedance	[Ns/m^5]
Z_1	entry impedance to branch 1	[Ns/m^5]
Z_2	entry impedance to branch 2	[Ns/m^5]
α	pump swash angle	[rad]
β	bulk modulus of fluid	[N/m^2]
ΔT	variation in temperature	[K]
ΔV	variation in volume	[m^3]
γ	propagation constant	-
μ	dynamic viscosity of oil	[Ns/m^2]
ℓ	length of line	[m]
λ	wave length	[m]
ρ	density of oil	[Kg/m^3]
ρ_s	source reflection coefficient	-
ρ_t	termination reflection coefficient	-
ρ_{tm}	termination reflection coeff. at motor harmonics	-
ρ_{tp}	termination reflection coeff. at pump harmonics	-

θ	pump shaft angle of rotation	[rad]
ω	frequency	[rad/s]

CONTENTS PAGE

FIGURES PAGE

CHAPTER I

INTRODUCTION

1.1 – GENERAL BACKGROUND

1.2 – OBJECTIVE OF THE WORK

1.3 – SCOPE OF THE THESIS

1.1 GENERAL BACKGROUND

In recent years hydraulic component manufacturers have been confronted with customers taking the noise aspect of systems much more seriously than in the past. It is quite common these days to decide to purchase a pump on the basis of a low noise generating potential rather than on a marginal price difference. This is mainly a consequence of the action undertaken by most western nations, and in particular E.E.C. countries, to set maximum limits on noise levels acceptable in industrial environments. It is also a reflection of the wide usage of hydraulics in fields where low noise levels are extremely important, such as hospitals, lifts and defence applications (submarines).

The noise radiated from hydraulic systems can be intermittent, as when a directional control valve opens or closes a line, or can be continuous as in the case of a pump, the discharge of a relief valve or the oscillation caused by the actuation of a servomechanism. In a great majority of systems, however, it is the pump that is considered the main component responsible for system noise. This is not only because the pump is noisy in its own right, due to the motion of its elements, but also because the pump is capable of inducing vibration in the whole system. This vibration can take two forms: fluid borne or structure borne vibration, more commonly known as fluid borne noise or structure borne noise.

When a pump is mounted rigidly on a supporting structure, the

vibration generated in the pump is propagated to the base and all attached components creating structural vibration. Furthermore, in many systems the pump is rigidly attached to the hydraulic reservoir, and rigidly connected to the system by rigid pipes. In these circumstances the system as a whole may resonate in sympathy with the excitation generated by the pump. The air borne noise produced as a result may in some cases be greater than the noise generated by the pump. Research work carried out in this field has resulted in the formation of guidelines for the reduction of structure borne noise, such as the efficient use of flexible mounting arrangements [1] and the use of flexible hoses.

Fluid borne noise is the oscillation induced in the fluid by the unsteady flow generated by positive displacement hydraulic pumps. This oscillation is propagated through rigid pipes and flexible hoses and therefore is present at any point in the system. It is usually measured in terms of the pressure fluctuation of the fluid. Needless to say, the fluid pressure fluctuation acting on the system and attached components may generate structural vibration even at points quite remote from the pump. Unlike structural vibration, it is difficult to prevent fluid borne noise from propagating to all parts of the system. Some attempts have been made at designing suitable 'silencers' to attach to pumps which can remove a considerable amount of pressure ripple and hence isolate the pump from the system. These silencers are either based on similar principles to those used in the design of car exhaust silencers [2], or on the use of long flexible hoses due to their damping characteristics [3]. These solutions have some disadvantages such as the large power losses associated with acoustic silencers and the length of flexible hoses necessary to reduce significantly pressure ripple in systems over a large frequency range.

The need for reducing fluid borne noise in hydraulic systems makes an understanding of the mechanism of the generation and transmission of pressure fluctuations of the utmost importance. In recent years a great deal of research has been put into the study of the generation and propagation of pressure waves in systems [4][5][6][7] and the relationship between fluid pressure fluctuations and air borne noise [8]. The vast majority of this research work has concentrated on high pressure lines as fluid borne noise has always been associated with the existence of a high mean pressure in a line. Indeed, the higher the mean pressure in a system, the larger the pressure fluctuations generally are. Peak-to-peak pressure variations of around 30 bar have been recorded in hydraulic pressure lines [9] which must lead to concern about the behaviour of some of the most fragile components in the system when subjected to such excitation.

When the unsteady flow produced by positive displacement hydraulic pumps is discharged into a loading system, the pressure in the system varies according to that change in flow. In the light of this, it would appear that a pump that produces large flow variations is likely to generate high values of pressure fluctuations in a system. Moreover, steps have been taken to develop experimental methods to measure pump fluid borne noise generating potential in unique terms [10].

In a previous work [11] the author reported the study of pressure fluctuations in the boost line of an axial piston pump. It was found that the level of pressure ripple measured in a boost line could be as large as that measured on the pump outlet line, even though the fluctuations were superimposed on a much lower mean pressure. Indeed, it was found that the peak-to-peak pressure variation could be higher than the value of the mean pressure in the line. The

pressure fluctuations generated in the boost line of a pump are due to two sources: the unsteady flow delivered by the boost pump and the unsteady flow drawn in by the boosted pump. The flow fluctuations generated on the inlet of a piston pump were found to be of the same order of magnitude as those produced by its outlet. This suggests that if a pump is working at low inlet pressures, indeed even if unboosted, it may still create pressure fluctuations in the inlet line of a similar magnitude to its outlet line. This conclusion is difficult to accept as very large pressure variations cannot occur around a mean pressure of, say, 1 bar absolute because this would result in the creation of very low instantaneous pressures causing cavitation or air release in the inlet line.

Research work carried out by Lindsay [12] on the suction line of a gear pump revealed that the pressure pulsations in the line were not sufficiently stable for accurate theoretical analysis to be undertaken. Furthermore, the use of a transparent pipe in the same test rig revealed the formation of air bubbles even at mean inlet pressures within normal pump operating conditions [13].

To summarize, fluid pressure pulsations in the inlet line of a positive displacement pump may not only assume values comparable to those typical of high pressure lines, and hence cause structure and air borne noise, but may also create conditions of air release and cavitation with the possibility of pump early degradation.

1.2 OBJECTIVE OF THE WORK

Some of the shortcomings of previous research work [11][12] were related to both theoretical and experimental approaches. Theoretical studies of fluid borne noise in hydraulic lines have been undertaken in recent years and methods of analysing and predicting pressure

ripple have been proposed, for high pressure lines, but have proved to be either relatively inaccurate or involved lengthy experimental testing of systems. Therefore, the available methods were not regarded as suitable for analysis of pressure ripple in low mean pressure lines where the stability of the pressure waveform is known to be relatively poor [12]. One objective of the present work is to give an explanation to the theoretical difficulties reported in references [11] and [12] on pressure wave behaviour in hydraulic pump suction lines.

In terms of the experimental approach, researchers have always faced difficulties when trying to simulate different suction conditions on pumps suction lines. Intrusive solutions have normally been adopted for the purpose, and as a consequence in-line restrictor valves have been used to control mean inlet pressure [12] or as in the case of [14] a boost pump was used to 'starve' of fluid the pump under test. In the latter case the mean pressure was controlled by a restrictor valve positioned in a branch line drawing flow from a reservoir. In the work reported in this thesis a purpose built pressurized reservoir was used to produce a wide range of conditions on the suction line of pumps. This choice is in strict agreement with the increasing use of pressurized reservoirs in practical applications, namely in aircraft and mobile equipment hydraulic circuits. The use of pressurized reservoirs or boost pump to prevent the occurrence of cavitation on the inlet of pumps has received little attention from the fluid borne noise point of view. The testing of hydraulic pumps using these two approaches allowed the pump inlet characteristics to be examined in detail.

1.3 SCOPE OF THE THESIS

This thesis starts with a fundamental study of the application of wave propagation theory to hydraulic lines. Extensive use of graphical representations of pressure standing waves is employed (chapter II).

In chapter III, wave propagation theory is used to develop a new experimental test method for evaluating the fluid borne noise characteristics of hydraulic components.

Chapter IV presents an analysis of the suction performance of pumps together with a discussion of the generation of inlet flow fluctuations. This is followed by a description of how the experimental test method can be adapted to suction line work.

In Chapter V, a detailed review of hydraulic tank design is given. A purpose built pressurized reservoir based on this review and on the requirements of the test method is, then, described.

Chapters VI and VII describe the experimental tests performed on the inlet lines of axial piston and external gear pumps under unboosted and boosted suction conditions.

Appendices I to IV present a detailed documentation of the digital computer program, which was used to implement the test method, together with the related sub-programs. Appendix V gives a worked example of the sizing of a reservoir and appendix VII presents details of the hydraulic components tested during the experimental work.

CHAPTER II

ANALYSIS OF STANDING WAVES IN HYDRAULIC SYSTEMS

2.1 PRESSURE FLUCTUATIONS GENERATED IN A SIMPLE SYSTEM

Fig.2.1 shows three pressure signals recorded from a system composed of an axial piston pump, a rigid steel pipe and a restrictor valve at the end. These signals, which were measured with piezoelectric transducers, are all periodic repeating at piston frequency. However, there are considerable differences in waveform shape and peak-to-peak amplitude, even though all signals were recorded at identical conditions (i.e. same mean pressure, temperature and pump speed). The differences, as shown in fig.2.1, are due to the fact that the pressures were measured at different positions in a line (case cases a and b) or in a system with a different pipe configuration (case c). The values of peak-to-peak pressure variation shown in the figure are typical of pressurized hydraulic lines (up to 15 bar), but larger values of pressure ripple have been recorded (above 30 bar) [9].

Although all pressure signals are a consequence of the flow fluctuation created by the pump, they can be understood to be modified images of the flow depending upon the characteristics of the circuit connected to it and the position in the system where the pressure fluctuation is measured.

As the pump fluctuating potential and loading system characteristic are dependent upon running conditions the pressure fluctuations in the system will also vary with these parameters. This makes any analysis of fluid borne noise only valid for a

specified system at the stated running conditions.

Fig.2.2 shows the flow ripple generated by the piston pump which was responsible for the pressure signals shown in fig.2.1. Both pressure and flow signals show the same fundamental frequency which is identified in this case by sharp variations at regular intervals. The flow fluctuation of the piston pump shows the port plate timing effects, indicated by the sharp fall in outlet flow when a piston filled with low pressure fluid is opened to the pressurized line. These changes create the mentioned sharp variations in the pressure signals and are typical of piston pumps. The pressure signals are, in general, very repeatable and steady.

The pressure fluctuations created by an external gear pump are very different in shape from those typical of axial piston pumps. Nevertheless they retain the same essential properties with a well defined fundamental frequency, and a very stable waveform. These pressure waveforms, as shown in fig.2.3, have a much smoother shape. Under some circumstances these signals may even approach almost sinusoidal shapes. This is a consequence of the flow ripple generated by external gear pump, which generally exhibits a smoother waveform than an axial piston pump (fig.3.16).

Instantaneous pressure fluctuations can be easily measured at virtually any point in a hydraulic system with great accuracy by means of suitable pressure transducers. However, instantaneous readings of flow fluctuations are not as simple to measure. Hot film anemometers or laser anemometers have a sufficiently good frequency response, but such methods are expensive. Even when such techniques are employed, though, it is often extremely difficult to measure flow ripples at certain locations, as for example inside the pump. Nevertheless, using plane wave propagation theory [5] it is possible

to establish a mathematical relationship between pressure fluctuations and flow fluctuations in a system. In order to do this it is necessary to have means of representing, in mathematical terms, the measured pressure ripple.

The pressure fluctuations often exhibit rather complex waveforms, but because they are periodic it is possible to analyse them in terms of harmonic components, using Fourier Analysis. Each individual signal of pressure fluctuation (or indeed flow fluctuation) can be considered as the sum of several sinusoidal waves. These sinusoidal functions must have frequencies at integer multiples of the pressure signal fundamental frequency. For example, fig.2.4 shows how ten sine functions, when summed together, compose a signal which can be compared with the actual recorded pressure signal generated by an axial piston pump in a system. On the left hand side column of fig.2.4 the individual sine waves are represented, whilst on the right hand side these functions are summed one at a time until the tenth is reached. A satisfactory agreement was reached between the mathematical model and the actual signal, as presented at the bottom of the figure. Consideration of ten harmonics has been found to be satisfactory to describe most piston pump generated pressure signals. Although this particular signal has very strong 6th and 8th harmonic components, other signals generated at other positions in the system may reveal a rather different composition.

Due to the smoother shapes of flow ripples generated by external gear pumps, it is generally sufficient to use only six harmonics to define pressure fluctuations generated by them.

A frequency spectrum of a signal gives a clear understanding of the relative magnitude of the components which are necessary to characterize it. Fig.2.5 shows a frequency spectrum of the signal

shown in fig.2.4. The signal is described by the amplitude and phase of its harmonic components. The consideration of the phase of each harmonic component is very important. Depending upon the relative phasing of the individual sine waves the synthesized signal may either exhibit very large peak-to-peak amplitudes or very low amplitudes. This is because the relative phasing of the harmonic components may allow them to be added to one another but may, as well, contribute to each others partial cancellation.

2.2 THE STANDING WAVE.

In most cases the representation of a pressure waveform in its Fourier components is acceptable, as the synthesis of these generates an accurate reproduction of the pressure signal. Hence, the study of pressure fluctuations in a system can be simplified considerably, since it is possible to examine each sinusoidal pressure wave in isolation, and determine its relationship with the sinusoidal component of the flow ripple generated by the pump.

In the following paragraphs the terms "pressure and flow fluctuation" will be understood to mean one harmonic component of the actual pressure or flow signal. According to this simplified analysis any simple hydraulic system can be modelled as if it were as shown in fig.2.6. Here an ideal sinusoidal flow fluctuation is generated at one end of a line and therefore fluctuations of pressure are created about a mean level in the line.

As the fluid is compressed by the sinusoidal movement of the piston, the pressure varies accordingly, starting at the piston face and being propagated along the line, of length ℓ, at the speed of sound in the fluid ($\approx$1400 m/s). This wave, named the incident wave, propagates to the end of the line where it is reflected back towards

the pump, not necessarily with the same strength, as some energy has invariably been lost at the termination. This reflection can be represented by a complex variable, named the 'termination reflection coefficient' (ρ_t), the amplitude of which shows how much of the incident wave has been reflected, and the phase indicates how much the reflected wave is lagging the incident one. The reflected wave travels back towards the pump where a further reflection occurs as determined by the, "source reflection coefficient" (ρ_s). This process continues indefinitely. For all practical purposes, however, after a small number of further reflections they are of such small amplitude that they may be considered negligible in comparison with the incident wave. This is due to the continuous loss of energy when the wave is reflected several times at the source and the termination and also due to the friction in the pipe.

Both the incident wave and the subsequent reflections have the same frequency although different amplitudes and phases. Furthermore, they travel in opposite directions interacting with one another and hence the result is a "standing wave", as detailed in fig.2.7. In this example, the incident wave (top left) is propagated from the source to the termination with an amplitude (top centre) which is continuously decreased by pipe friction. The phase (top right) decreases linearly with the distance travelled. The first reflected wave, of lower amplitude, when added to the incident, generates at some positions in the line larger values of amplitude than the incident wave alone. At other positions the amplitude is, however, smaller. The phase graph is also affected so that the phase ceases to vary uniformly along the line. The consideration of further reflections results in better defined amplitude and phase graphs of the standing wave. In this example, the 7th reflection was of sufficiently low amplitude for any further reflections to be

considered negligible. Clearly the formation of the standing wave in a length of line reveals positions where very large variations of pressure occur (anti-nodes) and others where the fluctuations are very low (nodes). If the length of line is such that the standing wave has a complete period, then this length is called a wavelength (λ). In general, if a length is shorter than 1/20th of a wavelength for a given frequency, the standing wave effects can be neglected. Nodes are half a wavelength apart ($\lambda/2$) along a line. This distance is generally less than 5m for the fundamental frequency of many hydraulic pumps. At each node the phase of the standing wave changes its sign, which means that the instantaneous pressure varies from a value above the mean instantaneous pressure level to below it, or viceversa.

As the pressure at the source varies in time, at each point in the line the pressure is continuously changing. If a discrete number of successive waves are represented on one figure a clearer view of the standing wave can be obtained, as shown in fig.2.8. This figure demonstrates how the wave actually behaves, passing from above to below the mean pressure line, and how all successive waves follow the same envelope.

When different line lengths are used in a system, keeping source and termination characteristics constant, the standing wave pattern changes. If the pressure is monitored at one point in the line, say at a fixed distance from the pump, and several tests are performed with different line lengths, the envelope of the standing wave could be as in fig.2.9. For this particular system the position considered in the line was close to the pump flange. This position coincided with a node when the line length was around 0.6, 1.9 or 3.2m and hence the pressure fluctuations there were very low (0.2 bar), but

amplitudes over twenty times larger (4 bar) were measured when the length was around 1.0 or 2.4m. These lengths are usually referred as resonant lengths for the system at the considered frequency (in this case ≈300Hz). Resonant lengths are half a wavelength apart.

This study of the standing wave can give some indication of how line lengths should be chosen to produce low levels of fluctuations. It must be emphasized that this description of the standing wave refers to one frequency only and several harmonic frequencies must be considered in fluid borne noise analysis. Consequently, line lengths that generate low amplitudes at one frequency may correspond to resonant lengths at others, and in the design of low noise systems a compromise must be found [16].

2.3 THEORETICAL MODEL OF A SIMPLE SYSTEM

Plane wave propagation theory was used by Bowns et al [5] to interpret the behaviour of the pressure fluctuations in hydraulic lines. This study was similar to that used by Electrical Engineers in telecommunications and power transmission through electrical lines. The analogy is made between current and flow, and voltage and pressure. The pump (transmitter) is characterized by its "source flow" fluctuation (Q_s), as described above, and its "source impedance" characteristic (Z_s). At this stage the source impedance may be considered as a capacitance due to the volume of oil held inside the pump. A further discussion on source impedance will be given in a later section (chapter III). The electric cable, of a known impedance, is substituted by the pipe line filled with oil at a mean pressure and represented by its "characteristic impedance" (Z_o). This is a function of the dimensions of the pipe and its roughness as described below. At the end of the line, the hydraulic valve, or the

receiver in electrical systems, offers an impedance to the system, known as the "termination impedance" (Z_t). The phase shift and attenuation of the transmitted wave along the line are characterized by the "wave propagation constant" (γ), which is dependent upon line dimensions and running conditions.

The frequencies involved in electrical systems, from 50Hz (power transmission) to several gigahertz (microwaves) cover a very wide range which is not typical of fluid borne noise work. As fluid borne noise is mainly studied in connection with its air borne noise generating potential the range of frequencies of interest generally lies between 100Hz and 10kHz, which are audible frequencies. In some special cases, as in submarine applications, lower frequencies may also be important. The velocity of propagation of electrical signals ($\approx 3*10^8$ m/s) is again very different from the speed of sound in fluids ($\approx$1400m/s for oil).

LINE DEPENDENT PARAMETERS

In a hydraulic system, the line dependent parameters (γ and Z_o) can be determined from the fluid properties, pipe dimensions and running conditions. The line characteristic impedance is given by [5]:

$$Z_o = \left[\frac{R + \frac{\rho}{A} j\omega}{\frac{A}{\beta} j\omega} \right]^{1/2} \qquad (2.1)$$

where: R - pres. drop/unit length/unit flow [Ns/m^6]

ρ - fluid density [Kg/m^3]

A - pipe cross-sectional area [m^2]

β - fluid bulk modulus [N/m^2]

j - complex operator -

ω - frequency [rad/s]

Hydraulic lines usually have smooth internal walls which results in low pipe friction and consequently, the friction term (R), in eq.2.1, can be considered negligible. Hence, eq.2.1 can be simplified for a lossless case:

$$Z_o = \frac{1}{A} \cdot [\ \rho\ \beta\ ]^{1/2} \qquad (2.2)$$

The characteristic impedance is, then, inversely proportional to the pipe area, and may be represented in the simplified case by a real value instead of a complex one.

The wave propagation constant (γ) is given by [5]:

$$\gamma = \left[\frac{A}{\beta}\ j\ \omega \left(R + \frac{\rho}{A}\ j\ \omega \right) \right]^{1/2} \qquad (2.3)$$

where A, β, R, ρ, j and ω are as in eq.2.1. For a lossless line, with R=0:

$$\gamma = j\ \omega \left(\frac{\rho}{\beta} \right)^{1/2} \qquad (2.4)$$

as the speed of sound in a fluid is given by $a= (\beta/\rho)^{1/2}$, eq.2.4 can be written as follows:

$$\gamma = j\ \frac{\omega}{a} \qquad (2.5)$$

In normal hydraulic lines the lossless condition applies (the attenuation is negligible unless the line is very long) and eq.2.5 is acceptable. In this case the value of γ is imaginary.

A computer subroutine was written to evaluate the line dependent parameters (Z_o and γ) and is documented in appendix II. The properties of hydraulic fluid necessary for the calculations were evaluated using another subroutine presented in appendix I.

TRANSMISSION LINE EQUATION

The fluctuation of pressure in a simple system measured at a distance x from the source, as shown in fig.2.6, is a function of the pump and termination characteristics and the line dependent parameters. It is given according to the following equation:

$$P_x = \underbrace{\frac{Q_s Z_s Z_o}{Z_s + Z_o}}_{A} \cdot \underbrace{\frac{e^{-\gamma x} + \rho_t e^{-\gamma(2\ell - x)}}{1 - \rho_s \rho_t e^{-2\gamma\ell}}}_{B} \qquad (2.6)$$

This equation is the key to most of the work related to pressure standing waves in a line and consequently a large part of this chapter will be devoted to its understanding. The derivation of this equation may be found in reference [5].

Equation 2.6 is valid for a single frequency (ω) only, as considered in the previous section. The variables are defined as follows: (* denotes a complex variable)

- P_x - press. fluct. at distance x from source at frequency ω *
- Q_s - source flow fluct. at frequency ω *
- x - distance from measurement position to source
- Z_o - line impedance at frequency ω *
- Z_s - source impedance at frequency ω *
- γ - wave propagation constant evaluated at frequency ω *
- ℓ - length of line
- ρ_s - source reflection coeff. evaluated at frequency ω *
- ρ_t - termination reflection coeff. evaluated at frequency ω *

The reflection coefficients are given as a function of the line

and end impedances,

$$\rho_s = \frac{Z_s - Z_o}{Z_s + Z_o} \quad (2.7) \qquad \text{and} \qquad \rho_t = \frac{Z_t - Z_o}{Z_t + Z_o} \quad (2.8)$$

The values of the reflection coefficients are limited to amplitude values ≤ 1, which simply means that a reflected wave cannot have an amplitude greater than the incident which caused it.

Eq.2.6 has two distinct groups of terms: one which has the units of a pressure (flow x impedance) (factor A) and the second which is a dimensionless complex quantity (factor B).

The value of factor A does not vary with line length or position of measurement on the line and hence establishes a mean level of fluctuation in the line by which the second factor is multiplied. The second part of equation 2.6 characterizes the formation of the standing wave in the line. Here, the term $e^{-\gamma x}$ characterizes the incident wave at a distance x from the source. The wave propagation constant γ is a complex variable ($\alpha+j\beta$), and its real part α determines the attenuation of the wave as it travels along the line, due to friction. This effect although negligible in most hydraulic lines, can be seen in the top graph of fig.2.8, where the amplitude of the wave at the source is larger than at the termination. The imaginary part β of the wave propagation constant determines the rate of variation of the phase of the wave along the line. When the phase shift reaches 2π the wave has travelled one wavelength.

The term $\rho_t . e^{-\gamma(2\ell - x)}$ characterizes the reflected wave at a distance x from the source ($2\ell - x$ is the distance the wave has already travelled since it was created at the source). The existence of ρ_t in this term means that the wave has been reflected once at the termination. The factor $(1-\rho_s\rho_t e^{-2\gamma\ell})^{-1}$ can be expanded into an

infinite series of terms which when multiplied to the incident and 1st reflected wave terms takes into consideration all the subsequent reflections existent in the line.

GRAPHICAL REPRESENTATION OF STANDING WAVE PATTERN

Using eq.2.6 it is possible to predict the pressure at any point in a simple system. As most of the variables involved in the equation are complex numbers, including the resultant pressure, it is difficult to appreciate the sort of values the equation can produce unless some constraints are imposed on it. If the values of Q_s, Z_s, Z_t, Z_o and γ are fixed at realistic levels for hydraulic systems, eq.2.6 becomes a function of x and ℓ and consequently the results of pressure describe the standing wave pattern along any length ℓ of line. These effects can best be understood if plotted in the form of two three-dimensional surfaces. One surface characterizes the behaviour of amplitude whilst the other describes the phase of the pressure fluctuations, as shown in fig.2.11. These three-dimensional surfaces have a triangular base (fig.2.10) due to the impossibility of placing a transducer beyond the end of the line. The values used in this example are typical of the second harmonic component (400 Hz) of an external gear pump of medium size (≈36cc/rev), with a source flow $Q_s=5*10^{-5}m^3/s;\angle 0deg$ and source impedance $Z_s=3*10^{11}Ns/m^5;\angle -90deg$. The termination value ($Z_t=2*10^{10}Ns/m^5;\angle 0deg$) represents the impedance of a restrictor valve creating 200 bar mean pressure in the system corresponding to the mean flow delivered by the pump. The pipe internal diameter was chosen to be 25mm for which the corresponding value of Z_o is about $2*10^9Ns/m^5;\angle 0deg$.

Using these values for the system, the length of the line between source and termination was varied from 0 to 4m and the pressures were predicted using eq.2.6. The top graph in fig.2.11 shows the

behaviour of the amplitude of the pressure fluctuations in such system. Each line parallel to the "TRANSDUCER POSITION" axis represents the values of amplitude of the standing wave along a length of line. The lines parallel to the "LINE LENGTH" axis indicate the values of amplitude at a fixed position from source for different lengths of line used in the system. The amplitude of the pressure ripple reaches values as high as 6 bar and as low as 0.1 bar. The range of lengths chosen covers in excess of a wavelength of the standing wave (λ=3.3m). If longer lengths of line were to be considered the graph would be virtually a continuous repetition of itself at intervals of half a wavelength. Line lengths of 1.65 and 3.30m coincide with resonant lengths creating large fluctuations, whereas 0.8 and 2.45m lengths coincide with anti-resonant conditions. Furthermore, for all line lengths there are positions along the line where the amplitude of the fluctuation is always very low which are found at fixed distances from the termination. In fig.2.11 they are found 0.8m and 2.45m away from the termination. One important feature of this amplitude plot is the way it shows how accurate a length needs to be defined to achieve resonant conditions. Minor changes in length can decrease the overall level of pressure fluctuations in a line to well below 40% of the resonant levels.

The bottom graph in fig.2.11 shows the behaviour of the phase of the pressure fluctuations corresponding to the amplitudes in the top graph. In this figure the phase is not made to be confined to a fixed interval ([-180.,+180.] as in fig.2.7) but is plotted on a continuous phase shift scale with line length. this scale interprets correctly the actual behaviour of the phase of the standing wave. This justifies the scale used which starts at an uncommon value of 800 deg and decreases until 0 deg. By using this continuous phase scale the phase plot is represented by a smooth surface, very much

like a waterfall. In this particular example, the phase varies along a length of line in "steps". Two steps are about half a wavelength apart. This view of the phase plot does not provide enough information about the variation of the phase at fixed positions away from the source, because part of the surface is obscured. Nevertheless, if the position close to the source is considered, the variation of phase for different lengths of line is very large. This may not appear to be significant when considering fluid borne noise in a system but it is important to remember that when the pressure wave is synthesized from the harmonic components, the relative phases are very significant in the determination of the peak-to-peak amplitude variation of the signal.

Further information can be obtained from the plot shown in fig.2.11, if it is rotated around its pressure axis, as shown in fig.2.12. Fig.2.12a is a reproduction of fig.2.11 and is taken as the basis for comparison. Fig.2.12b is the view of the same surface from the side. This gives a perfect view of the standing wave at fixed distances from the termination. Clearly, the standing wave does not move in relation to the termination when the line length is altered, and hence conditions of maximum and minimum values of the amplitude of fluctuations are always positioned at fixed distances from the termination. The phase of the standing wave follows, again, a pattern that is fixed relative to the termination, with the changes in "step" occurring at the positions where the amplitude pattern shows an anti-resonant condition. This graph of phase provides a clarification of the way the phase behaves at fixed distances from the source. Although close to the source the phase varies over a wide range of values, at a position about 0.8m from the source the phase is virtually unchanged for any length of line used.

In fig.2.12c the two surfaces of fig.2.12a are seen from behind. The amplitude plot shows at the forefront plane the variation of the standing wave at the termination, which in this example never falls below 1.0 bar. This is because the termination coincides with an anti-nodal position on the standing wave.

Figs.2.11 and 2.12 were produced from eq.2.6 for fixed values of Q_s, Z_s, Z_t, γ and Z_o. The surface is changed considerably by the variation of one or more of these variables.

The use of a 3D representation of the standing wave will be found to be particularly useful in examining the effects of system parameters on pressure ripple levels. By a simple computer simulation of a pressure standing wave pattern, a complete view of the pressure ripple in the system is obtained.

2.4 THE INFLUENCE OF PUMP AND SYSTEM CHARACTERISTICS ON THE STANDING WAVE.

2.4.1 Standing wave pattern parameters. When a designer is faced with the task of trying to reduce standing wave effects in a system by selecting appropriate components, he must look for indicators that reflect the characteristics of the pattern of the standing wave. One very important indicator to consider is the pressure standing wave ratio (PSWR). This is normally defined as the ratio between the maximum and minimum values of the pressure amplitude of the standing wave pattern for a given length of line. In this work, when examining the standing wave pattern on a three-dimensional basis, the maximum value of PSWR, which occurs for the resonant lengths, will be considered. The value of PSWR is dependent upon the values assumed by factor B, in eq.2.6. The value of PSWR can vary from a minimum value of 1 to maximum values that, theoretically, tend to ∞. A

second point to consider is the average level of fluctuations in the line as given by factor A of eq.2.6. This does not interfere with the PSWR but if it is a small value it ensures that the overall pressure ripple in the system is reduced.

The value of the wavelength is another parameter to consider as it gives the period of the standing wave. The position where nodes and anti-nodes occur in the line is also very important, as they can turn resonant lines into anti-resonant lines or viceversa.

2.4.2 Variation of termination characteristics. In section 2.3 the special relationship between the position of the standing wave pattern and the termination characteristic was stressed. In transmission line studies, the termination is represented by its impedance Z_t, which is generally a complex variable. Its value may vary considerably with the type of element used for termination and with running conditions. For example, if a restrictor valve is placed as termination, its impedance can be calculated by the formula:

$$Z_t = n \frac{P}{Q} \qquad (2.9)$$

where: n - coefficient $1 \leq n \leq 2$

P - mean pressure

Q - mean flow

This is only an approximation and is only valid for low frequencies; further details of restrictor valve impedance characteristics will be given in section 3.6.3. However, it is clear from eq.2.9 that a variation in mean pressure or flow through the valve alters the value of impedance. In this section this and other changes in termination impedance will be studied for its influence on

the standing wave pattern.

RELATION BETWEEN Z_t AND ρ_t

Although the termination impedance is the characteristic intrinsic to the component used, this variable is found only implicitly in part B of eq.2.6 as a constituent of the termination reflection coefficient (ρ_t). This means that the termination impedance does not have a direct affect on the standing wave. It is the relationship between Z_t and Z_o (line impedance), as given by ρ_t, which alters the standing wave pattern.

The line characteristic impedance (Z_o) is given by a real value for the case where the pipe friction is negligible (eq.2.2), i.e. the phase of Z_o=0. degrees. Hence, it is possible to establish a relationship between Z_t and ρ_t from eq.2.8, knowing $|Z_o|$, as follows:

$$Z_t = |Z_o| \quad \frac{1 + \rho_t}{1 - \rho_t} \qquad (2.10)$$

A graphical representation of this equation is shown in fig.2.13. This figure shows the values of ρ_t represented by numerical symbols. Different symbols ('0' to '9') correspond to different values of $|\rho_t|$ as indicated on the right hand table. The phases of ρ_t are given by the dotted lines which link points of equal phase of ρ_t ($-180. \leq \angle\rho_t \leq +180.$), in 10 deg steps. The amplitudes of ρ_t considered are not only the realistic values ($0 \leq |\rho_t| \leq 1$), but are extended up to 1.6 for reasons that will become clear later. In fig.2.13 the value of $|Z_o|$ was chosen to correspond to that of a pipe of internal diameter =0.025 m ($|Z_o| = 2*10^9$ Ns/m^5 or $|Z_o|$=187 dB). This value (187dB;0.deg) is the centre of the graph, meaning that when $|\rho_t|$=0 (symbol '0') the value of Z_t is equal to Z_o. As the values of Z_t corresponding to the different values of ρ_t vary in magnitude over a very wide range of values, the amplitude axis of Z_t was plotted on a

logarithmic scale (dB=20.*$\log_{10}$(amplitude(Ns/m^5))).

All the values of ρ_t which are realistic (symbols '0' to 'x') lead to values of $\angle Z_t$ which are limited to the range -90 to +90 degrees. If $|\rho_t|>1.0$ the phase of Z_t lies outside this range. This means that the impedance values cannot assume values outside this interval, otherwise $|\rho_t|$ would be >1.0.

As the value of $|\rho_t|$ is varied from 0.0 to 1.0 the corresponding values of Z_t move further away from Z_o, either in amplitude or in phase or both. For example, when ρ_t=0.8;$\angle$0.deg the corresponding value of Z_t is 206dB;$\angle$0.deg and when ρ_t=0.6;$\angle$-90.deg the value of Z_t becomes 187dB;$\angle$-63deg. When the phase of Z_t approaches +90deg or -90deg the amplitude of ρ_t is always very close to unity, although the reverse is not true. It is possible to achieve $|\rho_t|$=1.0 with very large or very small values of $|Z_t|$, without having $\angle Z_t$=-90 or +90 deg. Moreover, when the value of $\angle\rho_t$ is close to 0 or 180 deg small changes in ρ_t affect the values of Z_t significantly. When $\angle\rho_t$ approaches +90 or -90 deg very large changes in $|\rho_t|$ do not alter $|Z_t|$, but only the value of $\angle Z_t$.

This figure enables a quick assessment of the magnitude of the reflection coefficient from typical termination impedances. For example, as a phase of -90 deg is characteristic of a volume, a volume located at the termination will create very large reflections of the pressure wave.

Impedance at other points in a line

It is sometimes convenient to refer to the impedance at a point in

a line, say at a distance x from the actual valve,

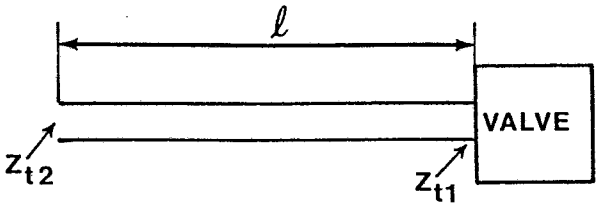

The impedance Z_{t2} is given by [5]:

$$Z_{t2} = Z_o \frac{1 + \rho_{t1} e^{-2\gamma x}}{1 - \rho_{t1} e^{-2\gamma x}} \qquad (2.11)$$

In essence, Z_{t2} is the impedance of a length of line (x) with the impedance of the valve (Z_{t1}) at the end. If this sub-system is connected to the end of a line of impedance Z_o, the termination reflection coefficient at that point is, as in eq.2.8:

$$\rho_{t2} = \frac{Z_{t2} - Z_o}{Z_{t2} + Z_o} \qquad (2.12)$$

As eq.2.12 is similar to eq.2.10, it means that the impedance Z_{t2} must have, again, a phase $\epsilon[-90.,+90.]$, otherwise the reflection coefficient at that point would be greater than unity. Hence, the impedance values at a point in a system, can theoretically have values of amplitude in the interval $]0,+\infty[$, whilst the phase must be between -90 and 90 degrees. Later in this chapter, the impedance as defined for Z_{t2} will be referred as an entry impedance to the sub-system.

VARIATION OF $|Z_t|$

When these concepts are applied to the standing wave equation the value of ρ_t can change the levels of fluctuation in the line considerably. In fact, as shown before, the very existence of a standing wave is due to the existence of ρ_t. Indeed, if in eq.2.6 $\rho_s \to 1.0;\measuredangle 0.$, $\rho_t \to 1.0;\measuredangle 0.$ and $e^{-\gamma \ell} \to 1.0;\measuredangle 0.$ the denominator of the

equation assumes a very small value and the pressure becomes extremely large.

The influence of the termination values on the pressure levels will now be examined, using the standing wave pattern shown in fig.2.11 as a basis for comparison, as reproduced in fig.2.14a. In this example the value of the reflection coefficient is ρ_t=0.8;40. The value of $|Z_t|$ was increased by a factor of 5, as would occur if the mean flow was increased by a factor of 5 at the same mean system pressure. Supposing that the pump characteristics remained unchanged, the effect of this variation of $|Z_t|$ on the standing wave is shown in fig.2.14b. The value of ρ_t increased to 0.95;40. Due to the low value of the phase of ρ_t it would be necessary to increase the amplitude of Z_t to much higher levels to achieve values of $|\rho_t|$ closer to unity (see fig.2.13). The standing wave values of amplitude increase at the anti-nodes and decrease at the nodes. Hence, the PSWR increases substantially and the maximum value of pressure ripple reaches about 18 bar. The position of the nodes and anti-nodes remained unchanged with this case of variation of $|Z_t|$.

VARIATION OF PHASE OF Z_t

Consider now a volume of liquid is introduced very close to the termination such that the impedance phase to change to -90 deg, but $|Z_t|$ remains at the original value of $2*10^{10}$ Ns/m^5. The changes incurred in the standing wave are as shown in fig.2.14c. The value of $|\rho_t|$ changes to unity and hence the maximum levels of fluctuation in the system increased dramatically, reaching much higher levels than those shown in fig.2.14b. The amplitude scale has been changed to accommodate these increases. Maximum values of 27 bar are reached compared to just 18 bar in the previous figure. This is solely due to the difference between the reflection coefficients: $|\rho_t|$=0.95 and

$|\rho_t|=1$. Although the change in phase of Z_t was very large its effect on the phase of ρ_t was small due to the large difference between the values of $|Z_t|$ and $|Z_o|$. It was mentioned earlier that when the value of $|Z_t|$ is much larger (or smaller) than $|Z_o|$ the phase of ρ_t is very insensitive to variations in phase of Z_t (see fig.2.13). Nevertheless the small phase variation of ρ_t ($\approx$10 deg) is reflected in a minor shift in the position of the nodes and anti-nodes. They are now positioned 0.2m further away from the termination. By comparing figs.2.14b and 2.14c it is clear that there is no simple relationship between Z_t and the standing wave. Large changes in the amplitude of Z_t do not produce corresponding changes in the amplitude of the standing wave. The important factor is the reflection coefficient.

In the cases shown in fig.2.14b and c, $\angle\rho_t$ always remained very close to 0 because the values of $|Z_t|$ are much greater than $|Z_o|$. As a result, the nodes are found at positions in the line corresponding to odd multiples of a quarter of a wavelength away from the termination. If the phase of ρ_t is changed by 180 deg for example, the position of the nodes and anti-nodes are shifted away from the termination by a quarter of a wavelength. This case occurs when the values of termination impedance are relatively low in amplitude and is shown in fig.2.14d. This example will be recalled later as it is typical of pump suction lines, but it is convenient now to stress that although the impedance amplitude chosen was ten times smaller than $|Z_o|$ the pressure ripple levels in the line were not significantly decreased.

REFLECTIONLESS TERMINATION

A reflectionless condition is obtained when Z_t equals Z_o. No wave is reflected under these conditions and $|\rho_t|=0$. For a

reflectionless termination, fig.2.14e shows that the amplitude of the wave is constant along the line, regardless of which length of line happens to have been chosen. This constant value of fluctuation is determined by the value of factor A in eq.2.6, as factor B is reduced to unity.

2.4.3. Variation of the source characteristics. The source characteristics are defined as the source flow (Q_s) which represents the disturbance input to the system and the source impedance (Z_s).

VARIATION OF Q_s

The source flow is included in factor A of eq.2.6 and may be considered as a term by which the whole equation is multiplied. Hence, the magnitude of the pressure fluctuations anywhere in the system is directly proportional to the values of the flow ripple generated by the pump. Obviously, if the source flow produced by the pump could be reduced to zero no variations of pressure will occur in the system. As factor B is unchanged, the PSWR and the nodal positions of the standing wave are not altered.

Alterations in Q_s may occur if the pump speed is changed or if the mean system pressure is varied, for example.

VARIATION OF Z_s

The source impedance is present in eq.2.6 in two forms: explicitly in factor A and implicitly in the term ρ_s in factor B.

The ratio $(Z_s.Z_o)/(Z_s+Z_o)$ in factor A was studied to examine the effect of different values of the variables. The value of Z_o was once again chosen to be characteristic of a 25mm pipe diameter (Z_o=187dB) and the values of Z_s were made to vary over a wide range of values (1000:1). The results are presented in fig.2.15. This

graph was constructed in a similar manner to fig.2.13 with the amplitude axis on a logarithmic scale and the phase axis covering the interval [-180.,+180.] degrees. The lines of constant value of $|Z_t|/|Z_o|$ are defined by the same numerical symbol and the dotted lines represent the contour of constant phase of Z_s. As Z_s cannot assume values of phase outside the interval [-90.,90.], given that $|\rho_s|$ cannot assume values greater than unity, these values are cross-hatched in the picture. The remaining surface is delimited by the two lines of constant phase, $\measuredangle Z_s = \pm 90$ deg. When the value of $|Z_s|$ is very much smaller than $|Z_o|$, as in case corresponding to symbol "0", the value of the fraction strictly follows the value of Z_s, both in terms of amplitude and phase. For larger values of $|Z_s|$ the values of the fraction increase in amplitude but not without limit. When the value of $|Z_s|$ approaches and exceeds the value of $|Z_o|$ the value of factor A ceases being very dependent upon Z_s and the results start getting closer and closer to a constant value ($|Z_o|$) which is never exceeded.

To summarize, the value of factor A of eq.2.6 may vary from $Q_s.Z_s$, for low values of $|Z_s|$ in relation to $|Z_o|$, to $Q_s.Z_o$ for values of $|Z_s|$ much greater than $|Z_o|$. This value ($Q_s.Z_o$) is the maximum the factor can assume. As factor A determines the average level of fluctuation in a line a reduction of $|Z_s|$ below the value of $|Z_o|$ will have a significant affect on the standing wave. This however is not easy to achieve because, typically, the source impedance of pumps is always very much larger than the line impedance.

It is important at this stage to stress the relative insensitivity of factor A to changes in phase of Z_s. This will prove to be important when discussing experimental methods of determining pump source impedances and will be raised again in chapter III.

Case of $|Z_s| > |Z_o|$

In general, compact pumps have very large source impedance amplitudes, whilst pumps that have large volume chambers near the outlet port show lower values of source impedance.

A simulation of such conditions was carried out using three dimensional plots to characterize the standing wave. The original value of Z_s (fig.2.16a is a reproduction of fig.2.11) is $Z_s = 5*10^{10} Ns/m^5 ; \angle -90deg$ which corresponds to a very large value of source reflection coefficient ($|\rho_s| = 1.0$) and a relatively low phase given that the value of $|Z_o|$ is 25 times smaller than $|Z_s|$. The pressure standing wave pattern would not change if $|Z_s|$ were increased from the original value as neither factor A nor ρ_s would be significantly varied. Consequently, fig.2.16b shows the standing wave pattern corresponding to a decrease of $|Z_s|$ by a factor of 10 ($Z_s = 5*10^9 Ns/m^5 ; \angle -90deg$). As $|Z_s|$ is still larger than $|Z_o|$ the value of factor A was not considerably altered but the standing wave shows quite a different pattern. This variation in the standing wave is, hence, almost solely due to the variation in ρ_s. At first sight it would appear that the effect of ρ_s on the standing wave would be of secondary importance, as it concerns only the introduction of reflections after the first termination reflection on the standing wave. However, in this case the value of $|\rho_s|$ changed from 1 to 0.55. This resulted in a large 'smoothing' effect on the standing wave. The important modification in this figure is that resonant conditions are no longer of major importance and the PSWR is very much reduced. When the value of $|\rho_s|$ is decreased the term $\rho_s . \rho_t . e^{-2\gamma \ell}$ in factor B assumes values which are no longer close to unity regardless of the length ℓ, and the denominator of factor B cannot reach values very close to zero. Consequently, resonant lengths will not produce very large values of pressure ripple in the

line.

Case of $|Z_s| < |Z_o|$

The value of Z_s was reduced then to $5*10^8 Ns/m^5$; $\angle -90deg$, such that the amplitude was lower than $|Z_o|$. This variation of Z_s caused not only a decrease in the value of factor A but also a variation in $\angle\rho_s$ without any change to the value of $|\rho_s|$. The effect on the standing wave is shown in fig.2.16c. As $\angle\rho_s$ changes by around 160 deg, the resonant lengths change by about $\lambda/4$. Hence, a resonant length of 1.75m in fig.2.16a is anti-resonant in fig.2.16c, whilst the anti-resonant length of 0.75m in fig.2.16a is resonant in fig.2.16c. The huge difference in amplitude levels of these two figures is due to the change in Z_s such that $|Z_s| \ll |Z_o|$. This leads to a drastic change in the value of factor A. However, the PSWR remains constant as $|\rho_s|$ did not change.

To summarize, when the value of $|Z_s|$ is below the value of $|Z_o|$ the standing wave is very sensitive to any changes in $|Z_s|$. Hence these conditions, if it is possible to achieve these conditions, a considerable reduction in pressure standing wave in hydraulic lines can be obtained by pump source impedance modification.

2.4.4 Variation of line parameters. The line parameters in eq.2.2 are the line characteristic impedance (Z_o) and the wave propagation constant (γ). As these are dependent upon line dimensions and running conditions, a variation of their values, if effective on the standing wave behaviour, may be relatively easy to achieve.

VARIATION OF Z_o

By changing the value of Z_o the standing wave in a hydraulic line changes considerably as it varies both factors A and B (see eq.2.6). The relationship between the reflection coefficient (ρ_t) and Z_t, seen

in fig.2.13, for a constant value of $|Z_o|$=187dB, is located on the value of Z_o and, hence, by varying Z_o it is possible to modify the value of ρ_t for a given value of Z_t to achieve high or low values of ρ_t (the same applies to ρ_s). A suitably selected Z_o (by choosing an appropriate pipe diameter) could in this way transform large reflections into small reflections. As factor A in eq.2.6 is also very much dependent upon Z_o (when $|Z_s| > |Z_o|$ the value of factor A tends to $Q_s.Z_o$), a larger pipe diameter (small Z_o) results in a lower pressure ripple. If $|Z_o|$ is very much greater than $|Z_s|$, then factor A remains very nearly constant irrespective of any variations in $|Z_o|$.

A particularly important condition is obtained if the pump is connected to a pipe of sufficiently small diameter such that $|Z_o| \ll |Z_s|$. Eq.2.6 becomes, then:

$$P_x = Q_s \cdot Z_s \frac{Z_o}{Z_s + Z_o} \frac{e^{-\gamma x} + \rho_t e^{-\gamma(2\ell - x)}}{1 - \rho_s \rho_t e^{-2\gamma\ell}}$$

or

$$P_x = Q_s \cdot Z_s \frac{e^{-\gamma x} + \rho_t e^{-\gamma(2\ell - x)}}{1 - \rho_t e^{-2\gamma\ell}} \qquad (2.13)$$

if the pressure is measured at the pump flange, x=0:

$$P_o = Q_s \cdot Z_s \frac{1 + \rho_t e^{-2\gamma\ell}}{1 - \rho_t e^{-2\gamma\ell}}$$

or

$$P_o = Q_s \cdot Z_s \qquad (2.14)$$

this result means that it is possible to find the product of the pump characteristics (Q_s & Z_s) by measuring the pressure fluctuation at the pump flange, provided the pipe attached to it has an impedance characteristic $|Z_o| \ll |Z_s|$. This point will be raised again later in

section 3.3.3.

To summarize, the mean levels of pressure fluctuation in a line increase with decreasing diameter (i.e. increasing Z_o) but remain unaltered when $|Z_o|$ is well above the value of $|Z_s|$. However, although the fluid borne noise decreases with Z_o, the air borne noise and the vibration of the pipe may not necessarily decrease because the pipe area over which these fluctuations act is considerably larger.

VARIATION OF γ

Fig.2.16d presents the case of halving the frequency (200Hz), which corresponds to a doubling of the wavelength, and hence a comparison between figs.2.16a and d shows that the levels remain the same but the base scale, which has changed by a factor of 2. This makes nodes become anti-nodes and resonant lengths anti-resonant.

2.5 MODELLING MORE GENERAL SYSTEMS

2.5.1 Description of a more general system. The system that has been under consideration (fig.2.7) shows little resemblance to most realistic hydraulic systems. However, the theory can be adapted to cope with more complicated circuits.

A more realistic system (fig.2.17) may contain pumps, rigid lines, flexible hoses, branches, elbows, valves, hydraulic motors, etc. This type of system can also be modelled using wave propagation theory and good agreement between experimental and predicted results is found if some of the basic requirements such as mean temperature and pressure in the system are kept constant [17]. Furthermore, mechanical vibration of the system must be kept to a minimum as the oscillation of components may result in spurious fluctuating flow

sources, particularly when their frequencies are of the same order as the fluctuation generated by the pump [9].

In the following paragraphs several different systems will be studied which, when combined, constitute the basis of most circuits.

2.5.2 Pump-Motor Systems. In much the same manner as a pump behaves as a flow ripple generator, a hydraulic motor is also a flow ripple generator. Consequently a motor is capable of generating pressure fluctuations in a system as a pump when presented with load and identical running conditions.

Whereas pumps tend to work at constant speed in a system, the speed of hydraulic motors is dependent upon mean flow and load. Therefore, even if a pump-motor system is composed of two similar reversible units (fig.2.18), the speed of the pump is unlikely to be the same as the motor, particularly under load, due to unavoidable leakage effects.

The source flow (Q_{sp}) and the source impedance (Z_{sp}) of a pump were defined as characteristics whose values are given at the discrete frequencies of pump fundamental and its harmonics. Therefore, the pressure fluctuations measured in a system reveal those particular frequencies as their components. If in addition a hydraulic motor also generates a source flow (Q_{sm}) and has a source impedance (Z_{sm}), defined at the harmonic frequencies associated with the motor the pressure fluctuations generated in the system by the motor are given at those frequencies only. If a system contains, say, two flow generators, the principle of superposition may be applied and the pressure fluctuation at each point in the line can be given as the sum of the pressure fluctuations generated by each flow

ripple source at that point. Hence,

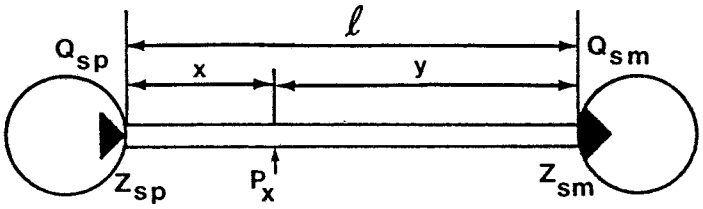

$$P_x = P_{px} + P_{mx} \qquad (2.14)$$

where: P_x - press. fluct. at distance x from pump

P_{px} - press. fluct. generated at x by pump only

P_{mx} - press. fluct. generated at x by motor only

The pump-motor system may, then, be divided into two separate simple systems:

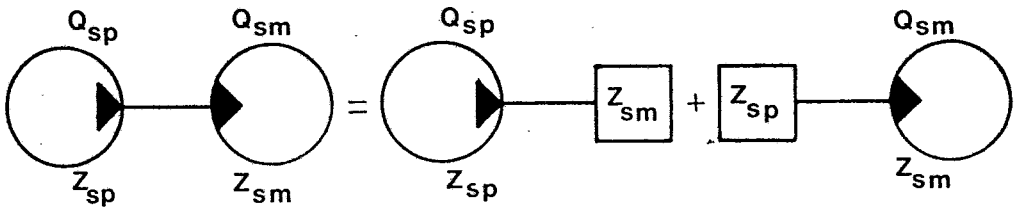

where :

$$P_{px} = \frac{Q_{sp}\, Z_{sp}\, Z_o}{Z_{sp} + Z_o} \cdot \frac{e^{-\gamma x} + \rho_{tm}\, e^{-\gamma(2\ell - x)}}{1 - \rho_{sp}\, \rho_{tm}\, e^{-2\gamma\ell}} \qquad (2.16)$$

and:

$$P_{mx} = \frac{Q_{sm}\, Z_{sm}\, Z_o}{Z_{sm} + Z_o} \cdot \frac{e^{-\gamma(\ell - x)} + \rho_{tp}\, e^{-\gamma(\ell + x)}}{1 - \rho_{sm}\, \rho_{tp}\, e^{-2\gamma\ell}} \qquad (2.17)$$

If the pump and motor frequencies involved are the same, then it is impossible to differentiate between the individual effects.

However, if the frequencies of pump and motor harmonics are different, then the harmonics of a pressure signal will reveal the individual components of each generator, and so P_{px} and P_{mx} can be measured, as shown in fig.2.19. In this case, eq.2.16 and 2.17 will refer to different frequencies. The values of ρ_{tm} must be given at pump harmonic frequencies whilst the values of ρ_{tp} must be referred to motor frequencies. This creates an apparent contradiction because the reflection coefficient at the motor end is only known, from the motor impedance, at motor harmonics. In order to find the values at other frequencies, interpolation must be performed.

When two standing waves are added together, as in this case, the result is only a standing wave if their harmonic frequencies are equal. This is very seldom the case, and when the frequencies differ a beat phenomenon takes place [17]. This is characterized by very large variations of the overall fluctuation repeating themselves at frequencies equal to half of the difference between the individual component frequencies. This phenomena when involving relatively low frequency beating of large amplitude components can create conditions leading to serious structural vibration. The beating is frequently accompanied by a characteristic noise which tends to be very annoying for the human ear. Fig.2.20 shows a typical beat phenomenon for piston pump and motor generated pressure ripples.

2.5.3 Branch line systems. The existence of branches in hydraulic systems is very common, dividing a flow into two lines. In terms of pressure and flow fluctuations the electrical analogy is very helpful. Kirchoff's 1st law states that at the junction the sum of all the currents is equal to zero. Using the hydraulic analogy:

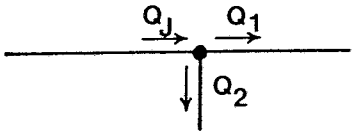

$$Q_J = Q_1 + Q_2 \qquad (2.18)$$

where: Q_J, Q_1 and Q_2 represent the flow fluctuations at the junction and into each line, respectively.

The relative magnitudes of Q_1 and Q_2 will depend upon the impedance of each branch measured at the entry:

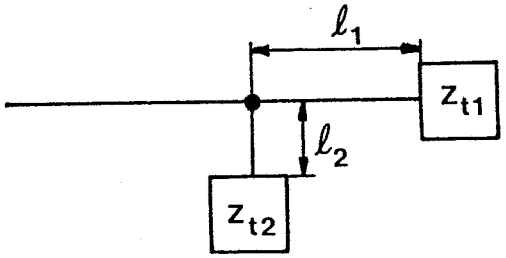

Using eq.2.11, the entry impedance for each line branch line is:

$$Z_{E1} = Z_o \frac{1 + \rho_{t1} e^{-2\gamma \ell 1}}{1 - \rho_{t1} e^{-2\gamma \ell 1}} \qquad (2.19)$$

and,

$$Z_{E2} = Z_o \frac{1 + \rho_{t2} e^{-2\gamma \ell 2}}{1 - \rho_{t2} e^{-2\gamma \ell 2}} \qquad (2.20)$$

Hence, as the pressure at the junction is common to both branches:

$$Q_1 = \frac{P_J}{Z_{E1}} \quad \text{and} \quad Q_2 = \frac{P_J}{Z_{E2}}$$

and,

$$Q_J = P_J \frac{1}{Z_{E1}} + \frac{1}{Z_{E2}} \qquad (2.21)$$

Representing the impedance at the junction by Z_J, then:

$$Q_J = \frac{P_J}{Z_J} \qquad \text{where,} \quad \frac{1}{Z_J} = \frac{1}{Z_{E1}} + \frac{1}{Z_{E2}} \qquad (2.22)$$

Tests carried out at Bath University [17] have shown that extra reflections that occur at the junction, due to turbulence and wall effects, are of secondary importance when compared to the source and

termination reflections and therefore may be ignored in the analysis. Furthermore, when tests were performed before and after changing over two branch lines it was revealed that the direction of the branch does not change the fluctuations in the line significantly. The use of bends and elbows in circuits , also has very little effect [17] on the propagation of the wave provided that the radius of the bend is of higher order of magnitude than the pipe diameter.

2.5.4 Systems with hoses. The introduction of flexible hoses in systems introduces an additional and important secondary effect: there is a significant movement of the hose wall which can have a considerable effect on the pressure ripple levels. Even with rigid pipes movement of the walls exist, but these are negligible compared with the fluid vibration, and the transmission of the wave through the pipe walls occurs at speeds far greater than the speed of sound in the fluid. With flexible hoses, however, the two waves can be considered to have speeds of a similar order of magnitude (a ratio of approximately two to one) [3].

The movement of the walls and the damping properties of hose materials contribute to the loss of energy and so hoses may be regarded as attenuators of both structure borne and fluid borne noise [3].

The theoretical interpretation of fluid borne noise in hydraulic hoses involves spatial wave propagation theory which is not within the scope of this work but can be found in refs. [3][18] and [19].

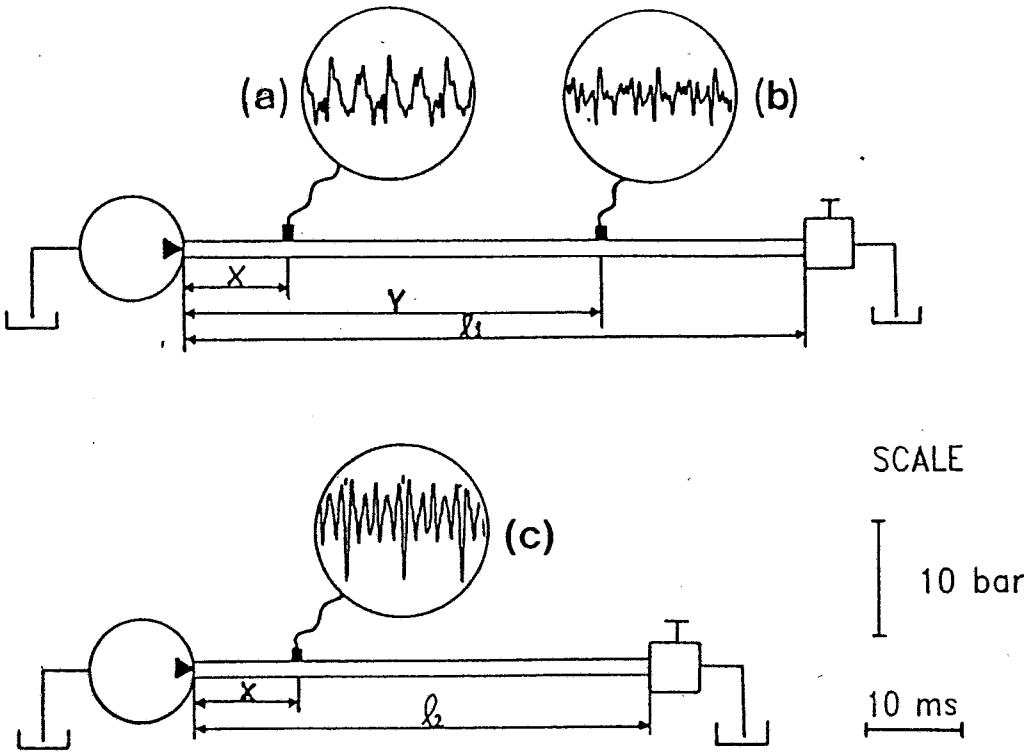

Fig. 2.1 Piston pump generated pressure signals in a system (n=1500 rev/min; p=100 bar)

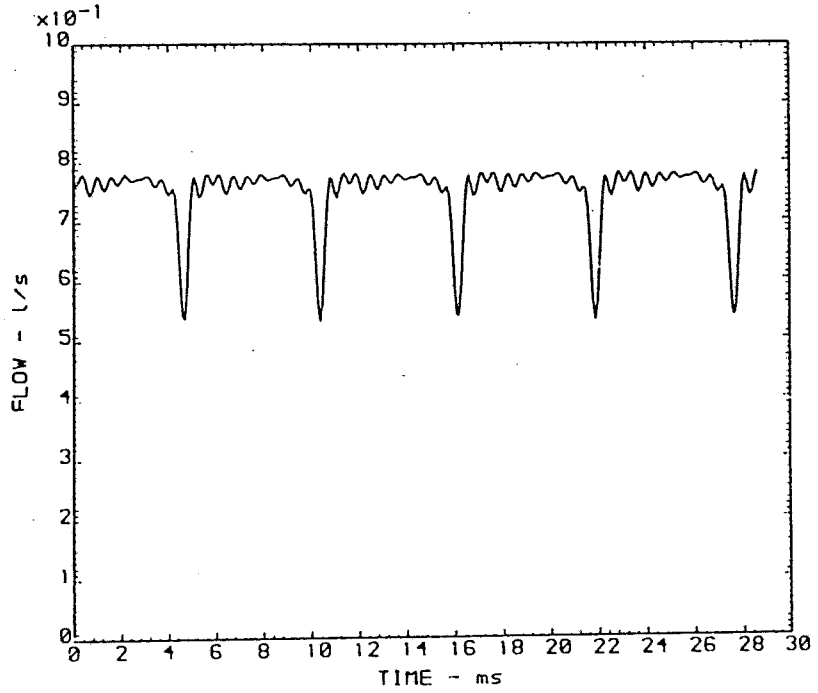

Fig. 2.2 Flow fluctuation generated by an axial piston pump (n=1500 rev/min; p=100 bar)

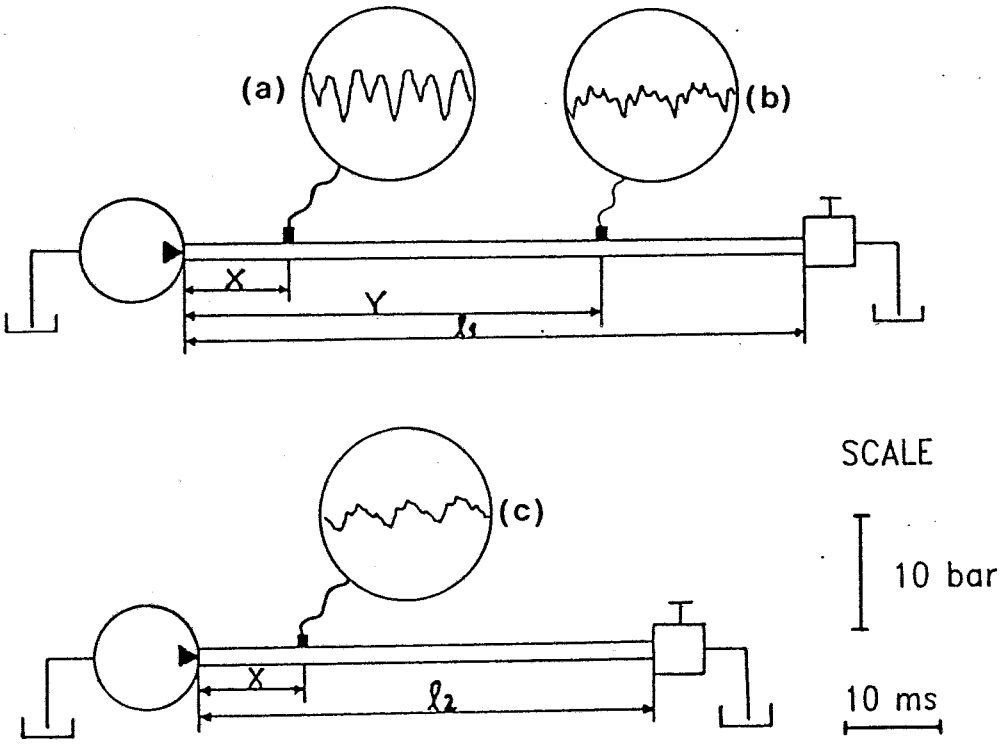

Fig. 2.3 Gear pump generated pressure signals in a system (n=1500 rev/min; p=50 bar)

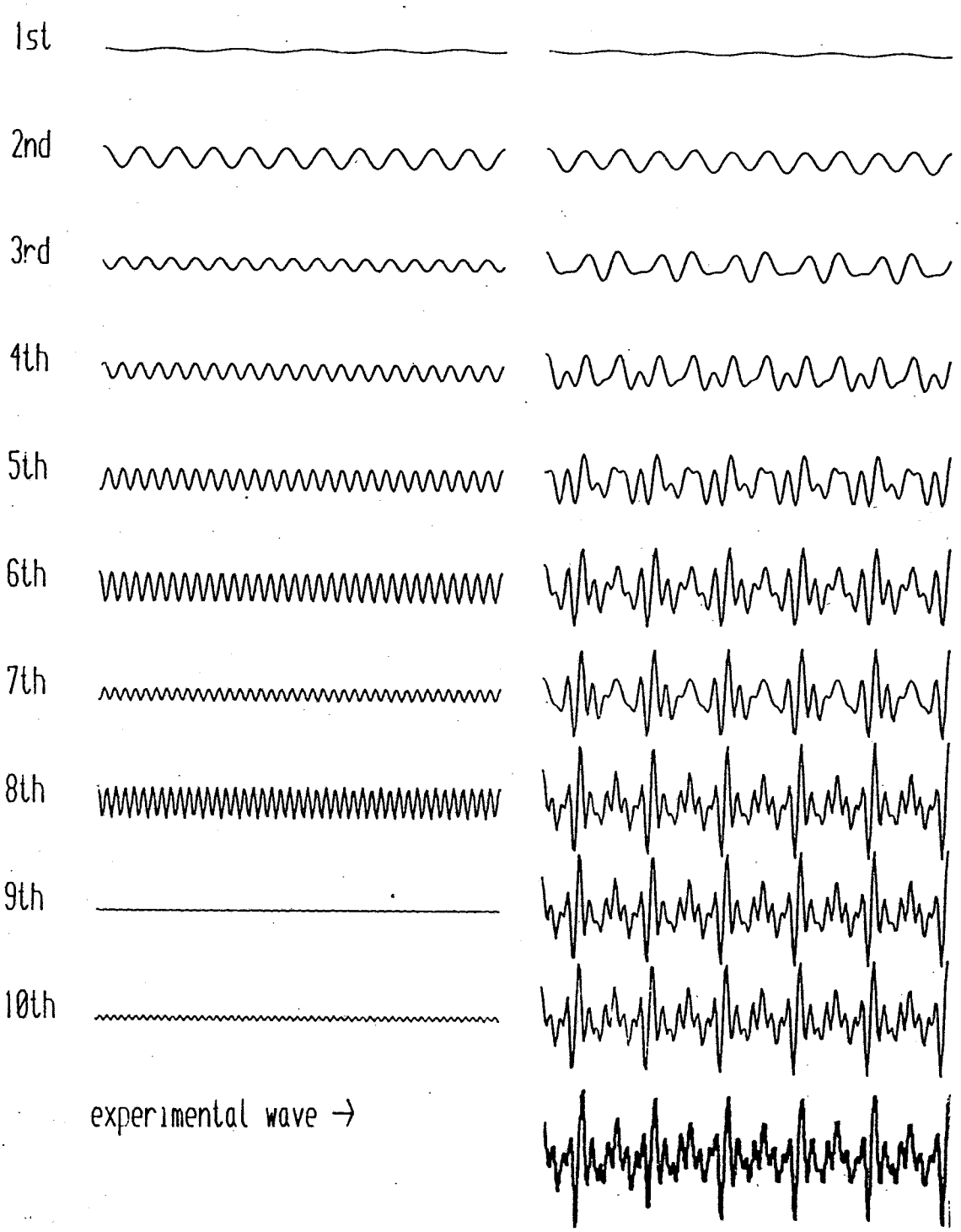

Fig. 2.4 Fourier synthesis of a piston pump generated pressure wave and comparison with experimental trace

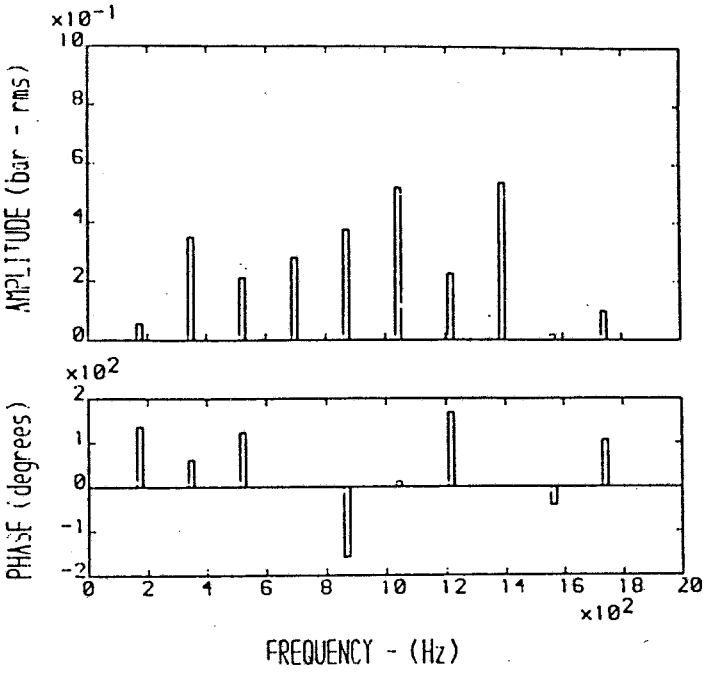

Fig. 2.5 Frequency spectrum of piston pump generated pressure signal

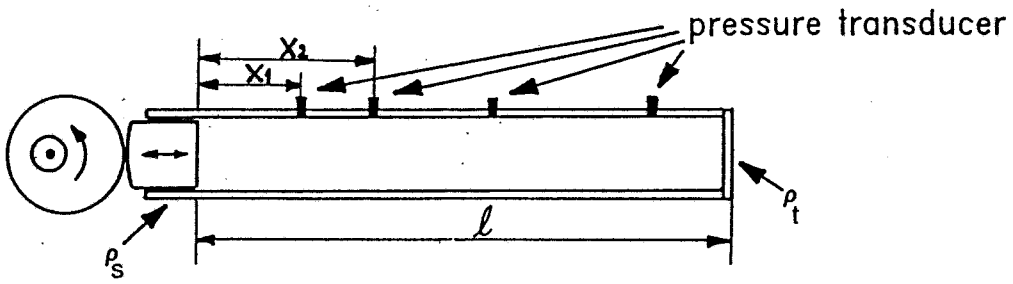

Fig. 2.6 Model of an ideal sinusoidal flow fluctuation in a hydraulic system

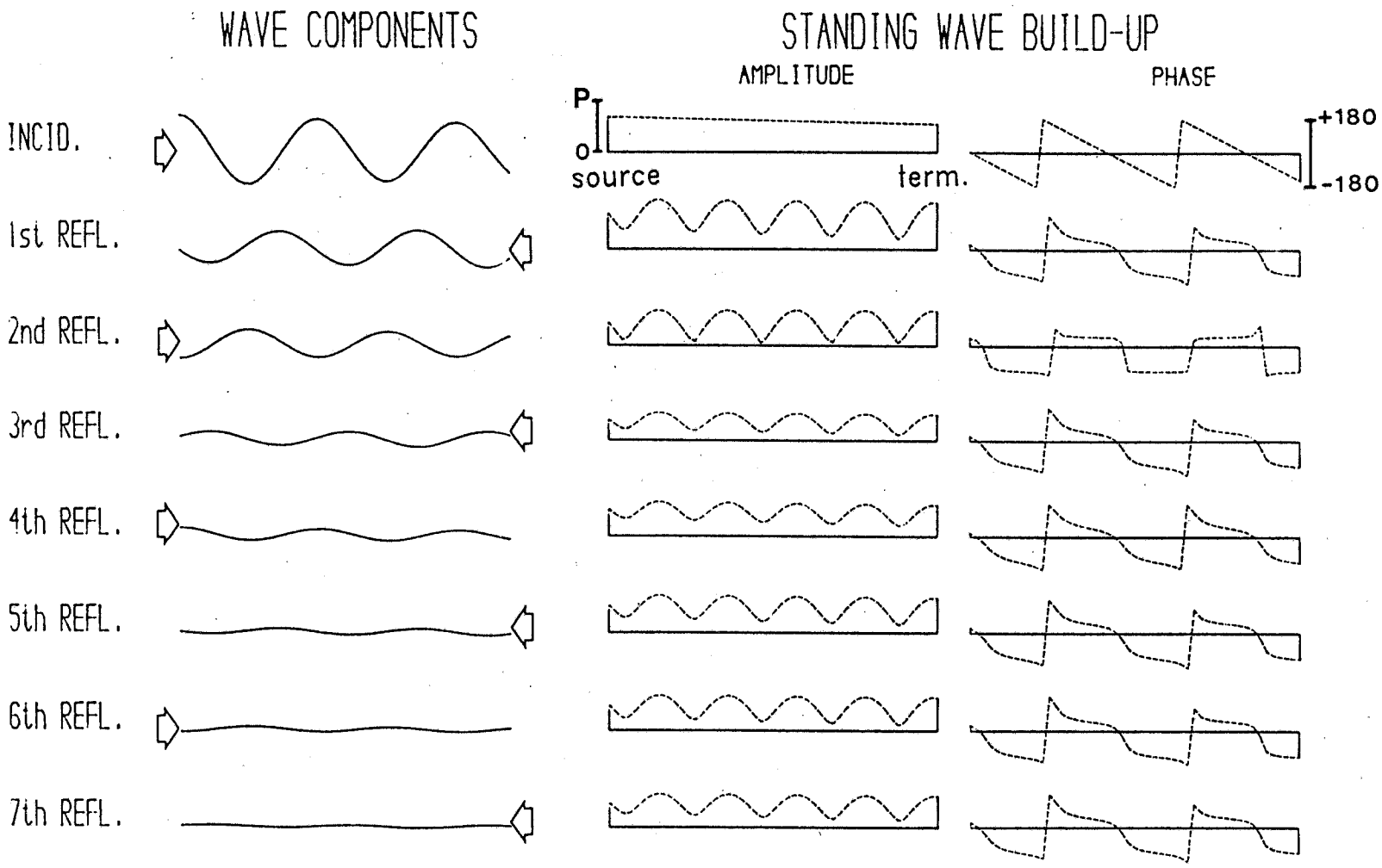

Fig. 2.7 Standing wave build-up pattern with 7 reflections (one wave)

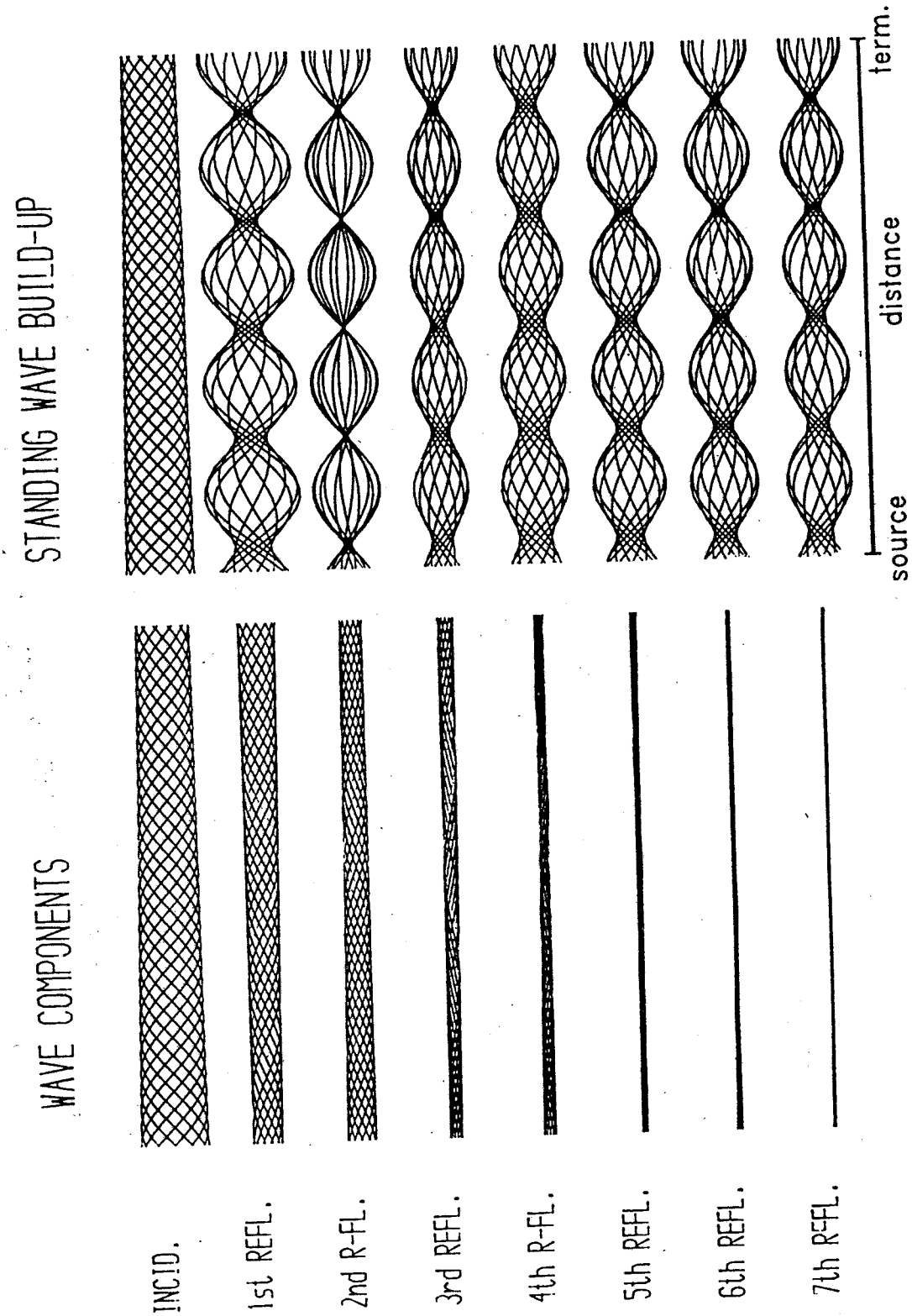

Fig. 2.8 Standing wave build-up pattern with 7 reflections (several waves)

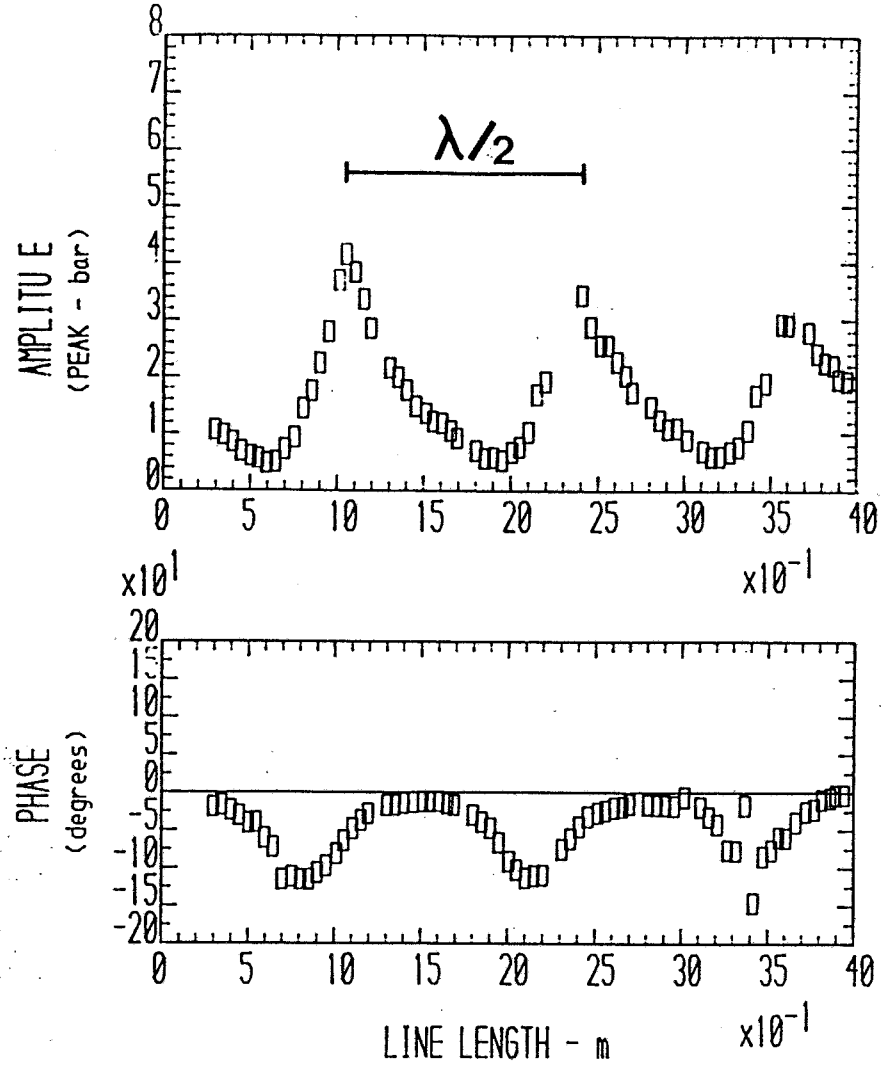

Fig. 2.9 Variation of pressure at fixed position from pump for varying line lengths

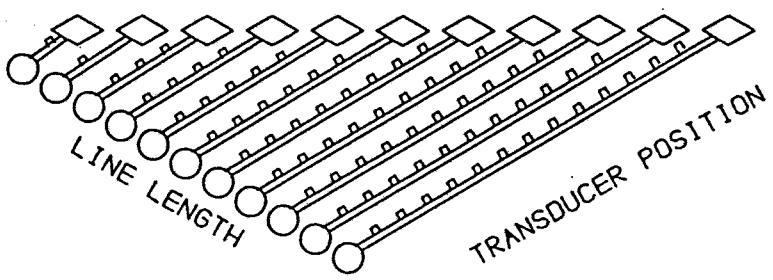

Fig. 2.10 Base-plane for three dimensional plot

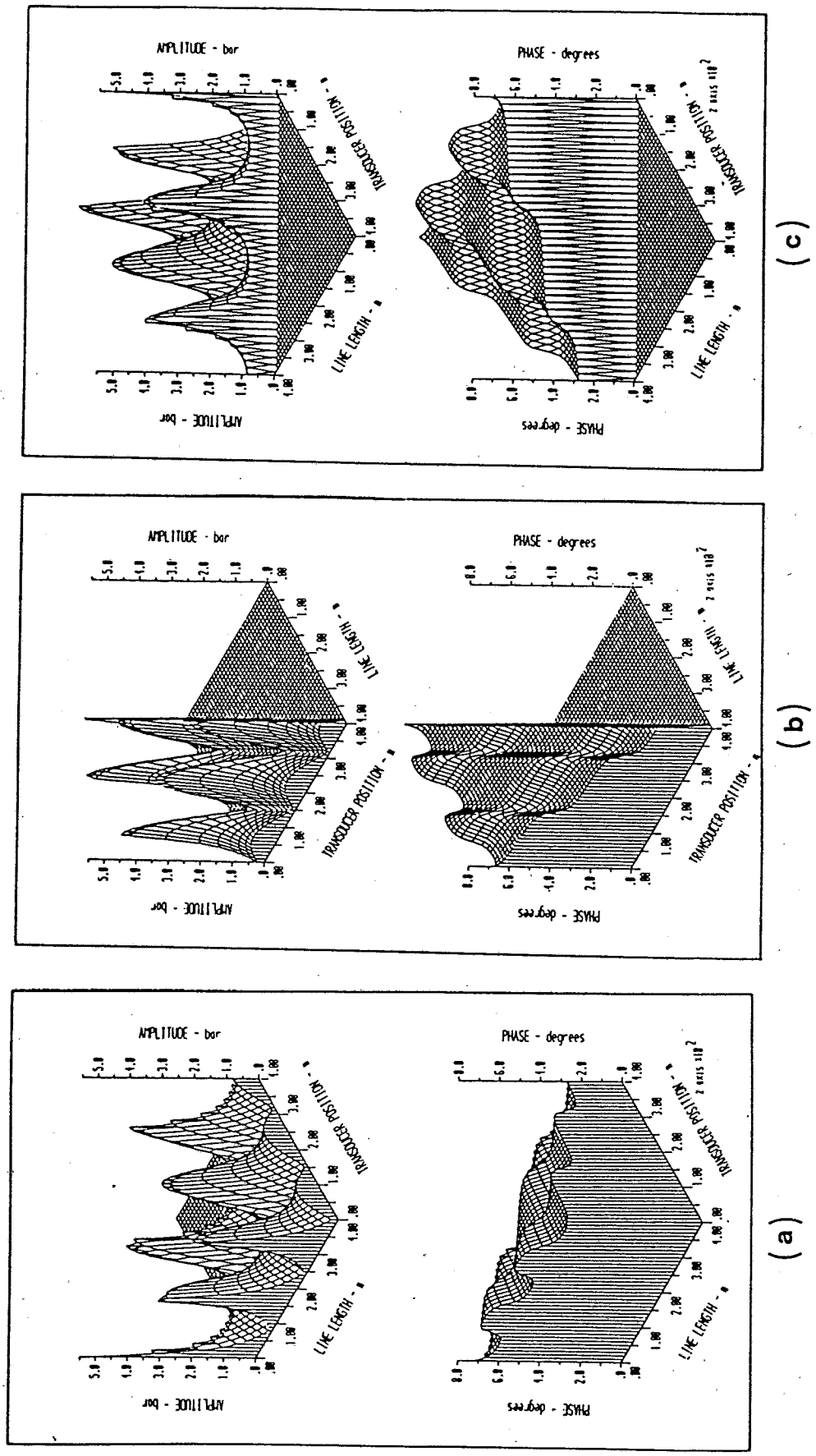

Fig. 2.12 Rotated views of three dimensional plot of standing wave pattern

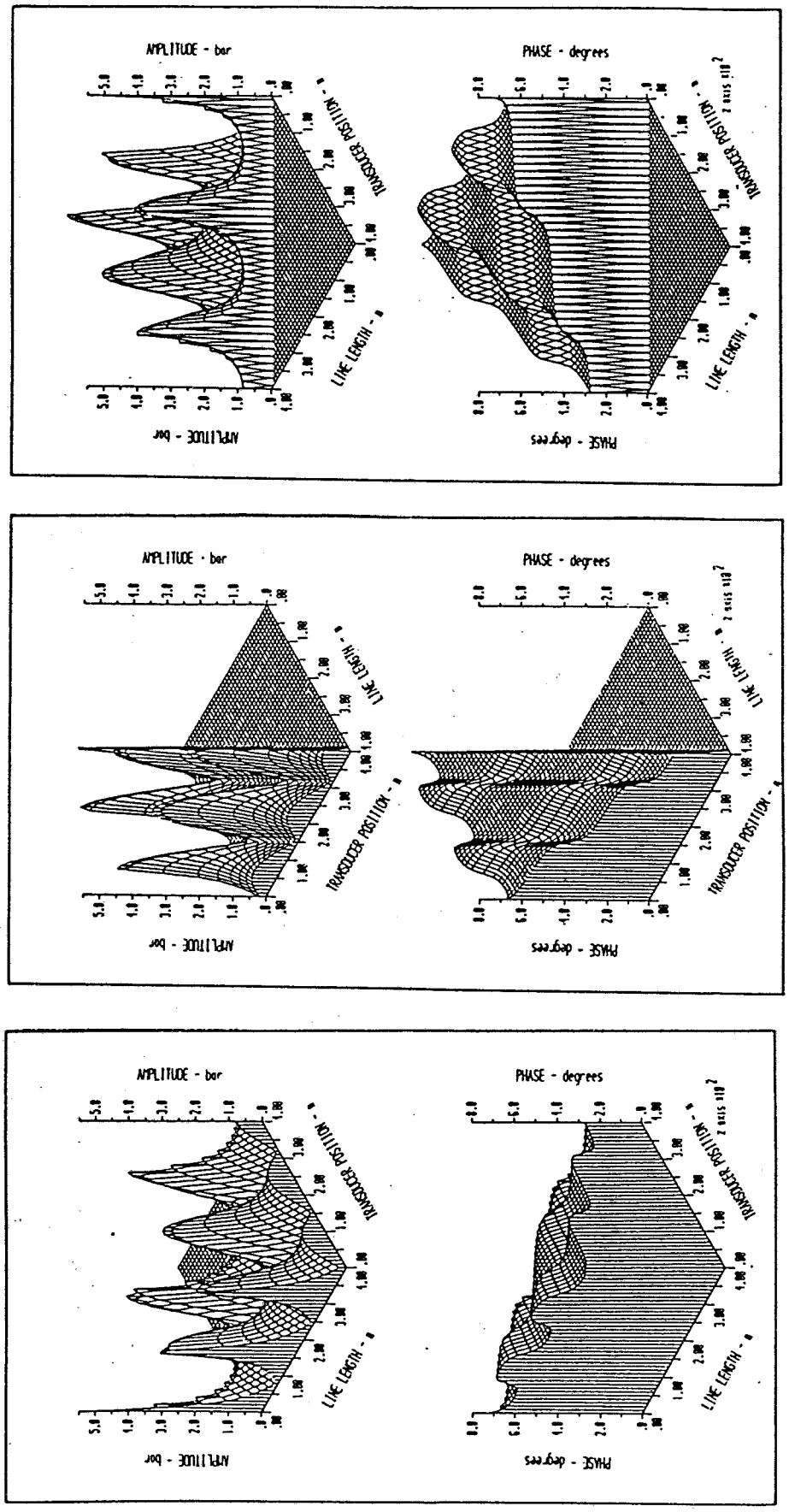

Fig. 2.12 Rotated views of three dimensional plot of standing wave pattern

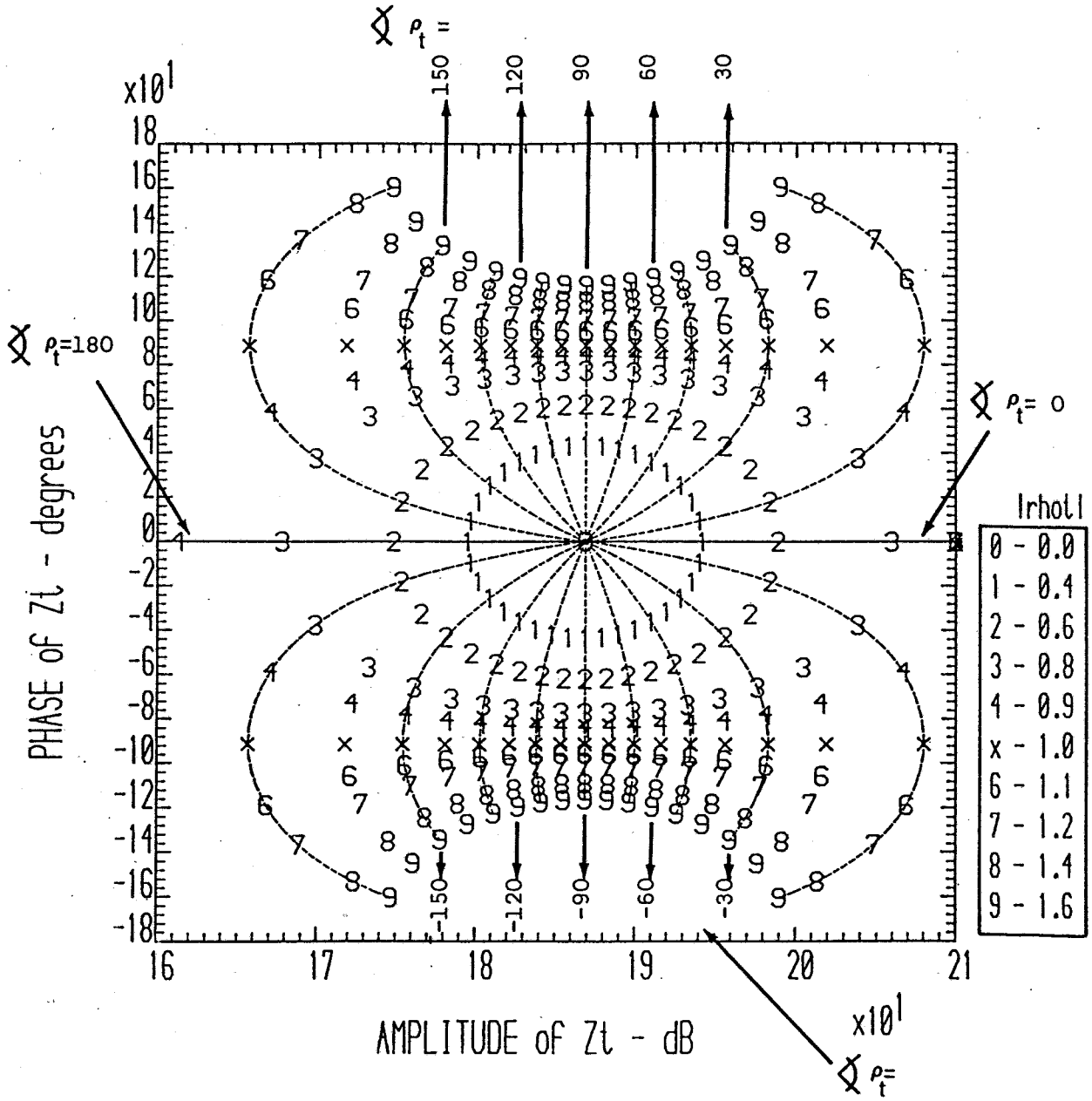

Fig. 2.13 Variation of Zt with ρ_t
(|Zo|=2e9 Ns/m5 = 187 dB)

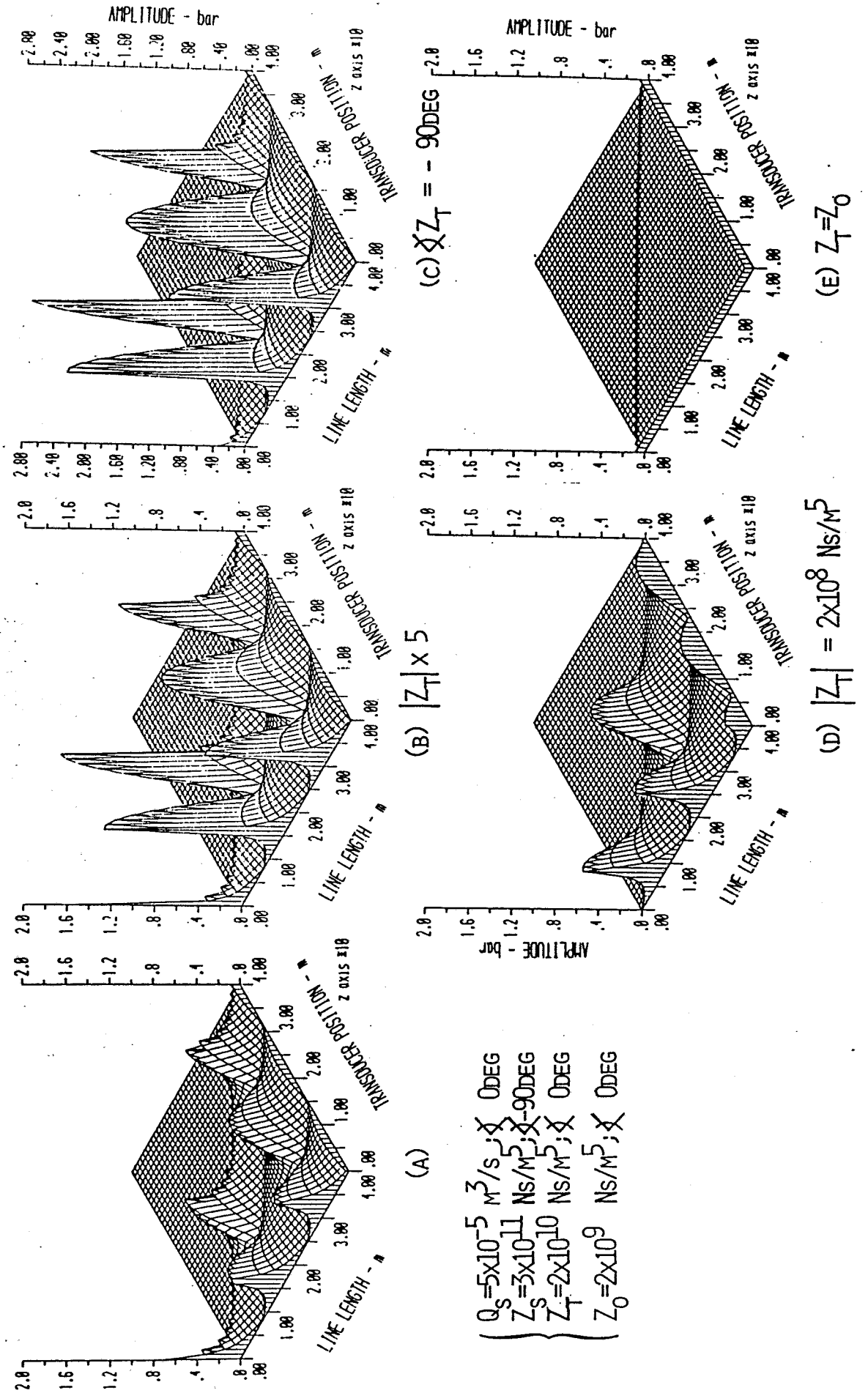

Fig. 2.14 Effect of variation of Zt on the standing wave

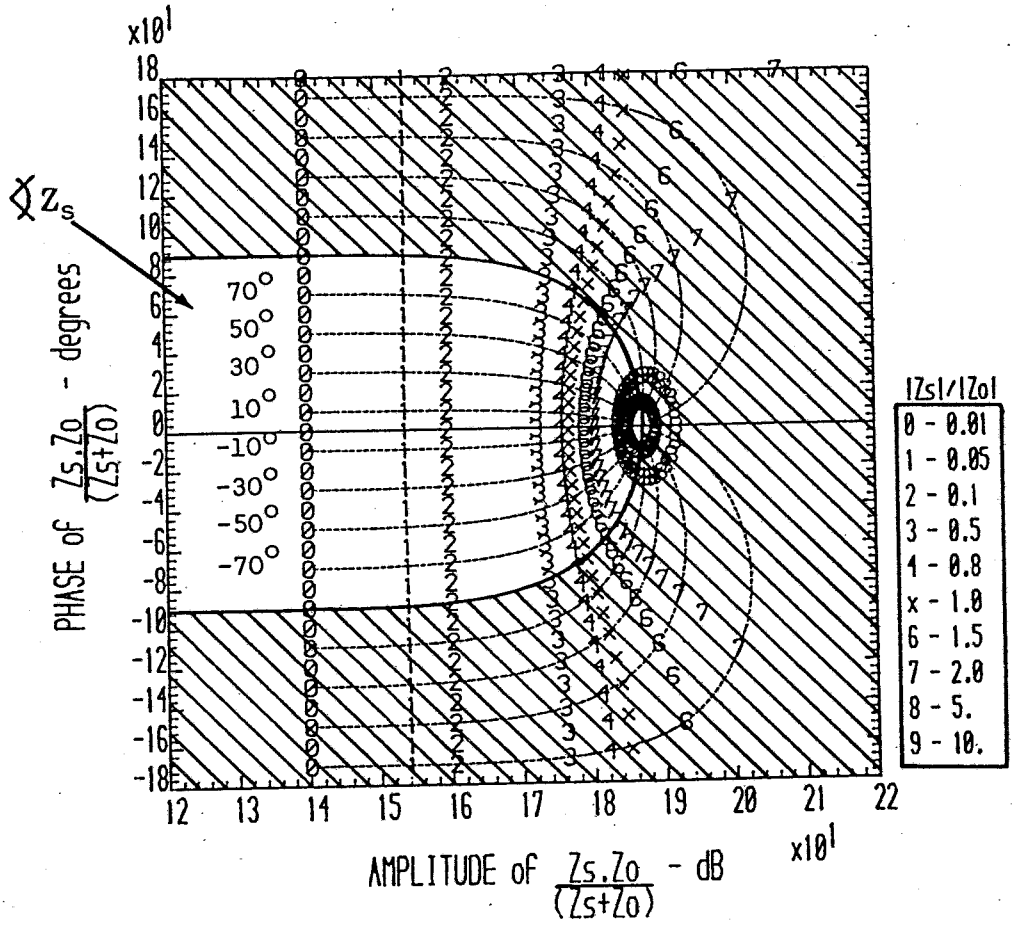

Fig. 2.15 Variation of Zs.Zo/(Zs+Zo) with Zs
(|Zo|=2e9 Ns/m5 = 187 dB)

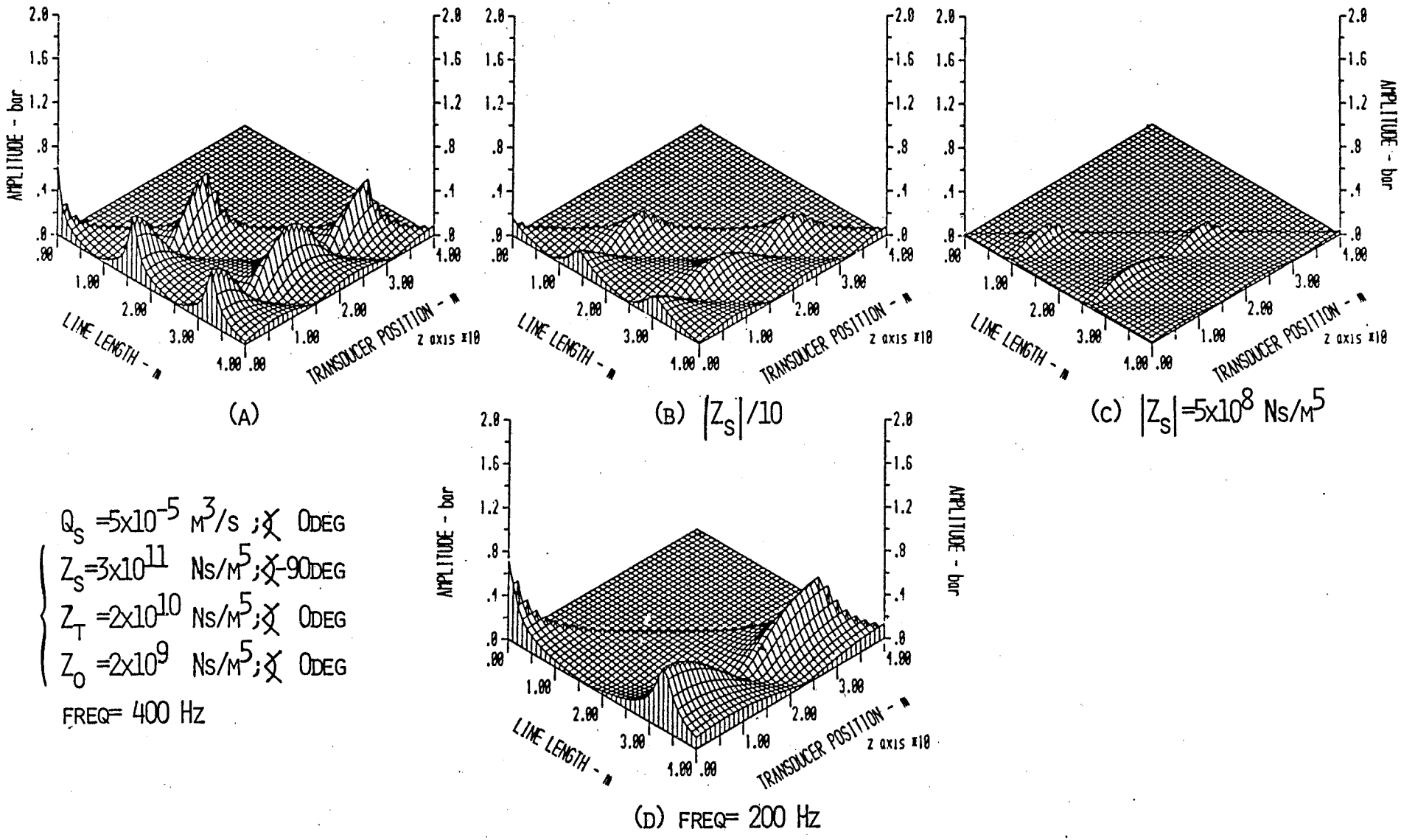

Fig. 2.16 Effect of variation of Zs and γ on standing wave

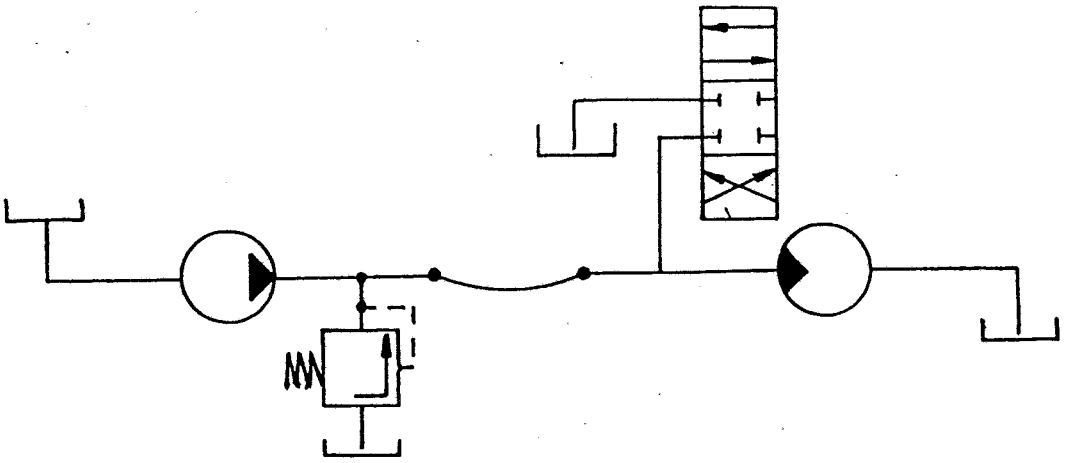

Fig. 2.17 Example of complex system for fluid borne noise analysis

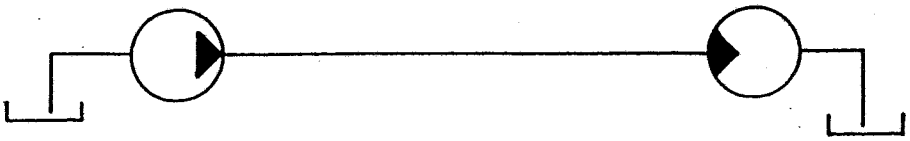

Fig. 2.18 Pump-motor system

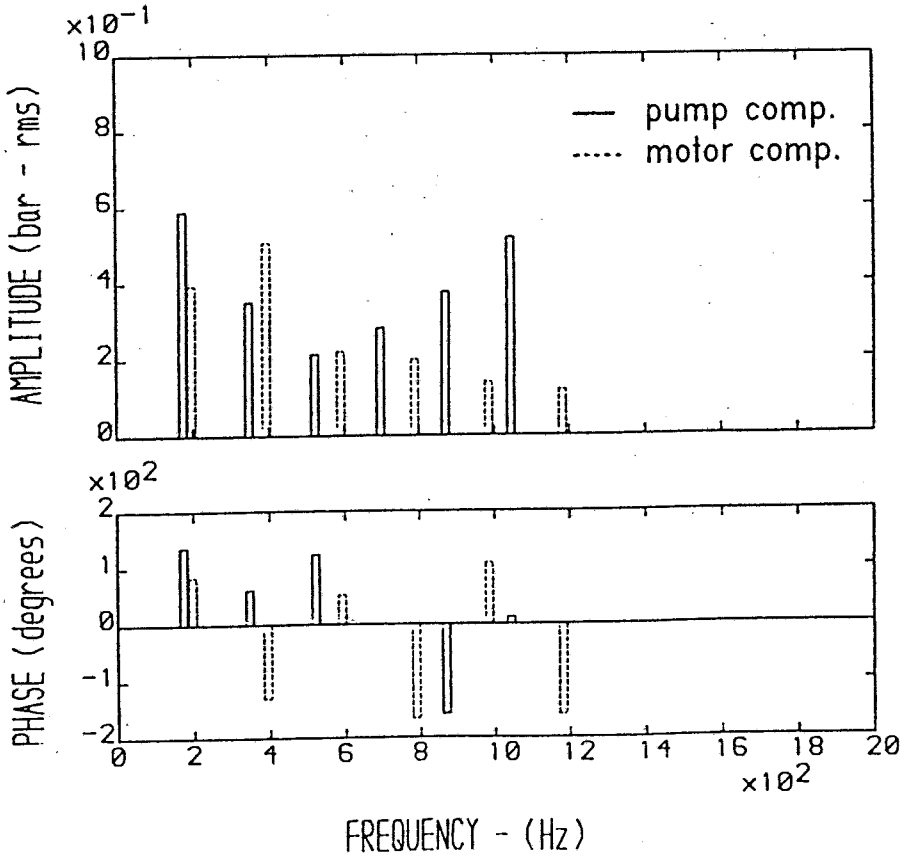

Fig. 2.19 Spectrum of pressure signal in pump-motor system

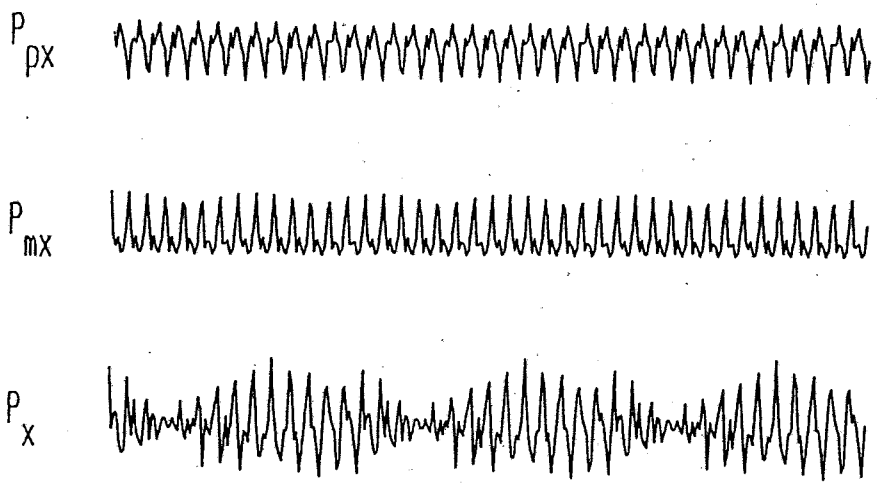

Fig. 2.20 Example of beat phenomena in a pump-motor system (ffreq. of Ppx=240Hz ; ffreq. of Pmx=260Hz)

CHAPTER III

METHODS OF DETERMINING HYDRAULIC COMPONENTS CHARACTERISTICS

3.1 INTRODUCTION

As described in the previous chapter, plane wave propagation theory can be used to predict the behaviour of the pressure fluctuations in hydraulic systems. Knowing the characteristics of the hydraulic components, it is possible to predict the pressure ripple at any point in a system with a high degree of confidence. However, in most systems the fluid borne noise characteristics of components are unknown, and cannot, in general, be accurately predicted from their design details. The characteristics of components will also vary with several factors such as pressure, temperature, frequency and wear.

Although it is possible to develop theoretical models of the instantaneous flow delivered by positive displacement pumps [6] [20] these models may not be accurate in predicting instantaneous effects of leakages, pressure pulses, timing effects and relieving grooves. The same criticism applies to the prediction of the impedance of components. In some cases the impedance can be predicted from the steady state characteristics but this is only satisfactory for low frequency studies [21] (this subject will be discussed in section 3.3.1).

It is, therefore, important to find methods of determining whether a component has suitable dynamic characteristics to use in a system in order to reduce fluid borne noise.

In this chapter some methods of evaluating the fluid borne noise characteristics of hydraulic components are described. Some of these methods are directed at pumps, since they are the main source of fluid borne noise. Indeed, there has been a great demand to find a straightforward test to define, in simple terms, the fluid borne noise generating potential of pumps.

The methods described below are mainly related to the evaluation of components characteristics in pressurized lines. From a clear understanding of these methods it will be possible to choose a suitable method for testing systems under low mean pressure, as in the case of pump suction lines.

The methods described below are based on the assumption that it is possible to measure the fluctuations of pressure at required points in a system. Since equations exist to predict the pressure fluctuations at those points in the system as a function of components characteristics, the same equations must provide values for components characteristics if the pressure fluctuations are known.

3.2 DATA ACQUISITION

The measurement of pressure fluctuations in a hydraulic system must be regarded as an essential part of all test methods and the reliability of the end result is very much a function of the quality of data acquired.

A pressure transducer appropriate for this task must be able to work at very high pressures (up to 400bar or 50% above maximum working pressure), to cope with high temperatures (120C), to be reliable and to be insensitive to temperature variations and

mechanical vibration. In addition it must have good linearity and resolution, with low hysteresis, and have very good repeatability. It is not desirable to read mean pressure because this would lead to a reduced sensitivity when measuring fluctuations around a high mean pressure, particularly if the fluctuating component is a small percentage of the overall signal. Most important of all, the transducer must have high frequency response (well above maximum audible frequency) and be sufficiently small to be able to locate it at any point in the system where the pressure must be measured.

Piezoelectric pressure transducers are an appropriate choice for this type of work. The material most commonly used as the basis of these transducers, quartz, has excellent piezoelectric properties. A number of tiny discs of quartz, joined together in between a diaphragm and the transducer body, become electrically charged in proportion to the force applied to the diaphragm. However, this charge decays gradually preventing the transducer from measuring mean pressure. Quartz has most of the properties desired for the transducer. Fig.3.1 shows a typical transducer. These devices have, nevertheless two disadvantages which must be taken into consideration: their cost is high and, due to their small size, they are relatively fragile.

Charge amplifiers are normally used in conjunction with this type of transducer as opposed to voltage amplifiers as the calibration of the latter is dependent upon cable length. However, care must be taken to make sure that the charge generated at the transducer reaches the amplifier unaffected by the capacitance of the cable. It is particularly important to be aware that the capacitance of most cables varies slightly with the mechanical vibration of the cable, which is sufficient to interfere with the measurements. This is

called triboelectric noise.

The output of the charge amplifier is a voltage which can be readily displayed on an oscilloscope. However, as shown in chapter II, it is useful to filter the signal in order to examine individual harmonic components, in terms of their amplitude and phase. For this purpose, it is common to use either a discrete frequency analyser (Frequency Response Analyser), a continuous frequency analyser (Spectrum Analyser), or an on-line (mini) computer with fast Fourier transform (F.F.T.) algorithm and data acquisition capabilities.

Determining the amplitude components of a signal is relatively easy to achieve, as basically it is only necessary to use a narrow-band filter centered at the desired harmonic frequency. However, finding the phase of a Fourier component requires a reference signal to which all phases must be related.

The reference signal must be of the same frequency as the pump fundamental and mechanically linked to the pump shaft, so that it follows any variation in pump speed exactly, as well as maintaining a fixed relationship to each pumping element. The reference signal is generally produced by a proximity detector (magnetic pick-off) activated by a toothed wheel positioned on the pump drive shaft, with the number of teeth corresponding to the number of pumping elements. As the signal from the magnetic pick-off might be of low amplitude, or noisy, a Schmitt trigger network is used to convert the signal into a buffered square wave of the same frequency which is fed in turn to the frequency response analyser (fig.3.2). Care must be exercised in the machining of the toothed wheel in order to ensure a precise division and sharp edges, otherwise the intervals between teeth will not have the same length of arc leading to slightly different step lengths on the square wave. As the analyser reads the

frequency of each cycle on the square wave, inaccuracies on the machining of the wheel will be converted into wrong frequency information by the analyser.

For fluid borne noise measurements a maximum frequency variation of ±2Hz can be accepted at the fundamental. The frequency response analyser generates sine waves perfectly synchronised with the reference at fundamental and harmonic frequencies and performs the Fourier analysis.

During experimental tests of fluid borne noise the values of amplitude and phase of the pressure readings tend to fluctuate around a mean value due to some variations of the pressure waveform. In chapter II it was stated that pressure signals are assumed to be periodic with a fundamental frequency equal to pumping frequency. This may not be completely accurate as each successive cycle of the pressure ripple is due to a different pumping element. Slight differences in tolerances during machining and increased local clearances due to wear may result in the flow ripple and source impedance of a pump being different from one pumping element to another. Fig.3.3 shows the case of pressure signal produced by a piston pump with one faulty piston. Fortunately, the result shown in fig.3.3 refers to an extreme case and usually only minor differencies are found in each individual cycle. In the analysis of the signal this is mainly revealed by some scatter in the readings at the higher harmonics.

A representative value of the pressure fluctuation is generally found by a simple averaging process of, say, five or ten successive readings. There is no easy way of determining a priori how lengthy or detailed the analysis should be as this is, generally, not a function of the analyser but, rather, of the signal being analysed

and the reference signal. Other type of errors can also be incurred. Results of tests performed at different times cannot be expected to agree unless running conditions are closely reconstructed. In general, fluid borne noise measurements are repeatable if test conditions are similar, within the following limits:

a) mean pressure ±2%

b) mean flow ±2%

c) mean pump speed ±2%

d) mean temperature ±2C

Mechanical vibration of pipes and components must also be kept to a minimum as they can affect the results considerably [9].

3.3 METHODS FOR THE DETERMINATION OF PUMP CHARACTERISTICS

When proposing a test method for determining characteristics of components, it is important that the technique is relatively straightforward, uses widely accessible instrumentation and is of reasonable low cost. From chapter II it is apparent that the relationship between system component characteristics and pressure ripple is very complex indeed. Devising a simple test to express such relationship appears to be quite difficult. A number of different methods for testing pumps will be reviewed. Each of the methods uses a special loading system connected to the pump which, according to the authors, allows the pump characteristics to be determined. Several attempts at measuring pump characteristics using only one transducer (simple and of low cost) have been made, and four methods will now be described and assessed. The most difficult problem to solve in any of these methods is to find a loading system which reveals a representative noise characteristic for the pump. If this happens, then if the pump is 'noisy' in such a system it will be

noisy in any circuit and vice versa.

3.3.1 Unruh's and Szerlag's Methods. The methods of testing hydraulic pumps developed independently by Unruh [22] and Szerlag [23] are similar as they require the same type of loading system. These researchers decided upon a simple loading system connected to the pump as a method of obtaining its fluid borne noise characteristics. The load consisted of a very short line (to avoid the need for distributed parameter theory), terminated by a restrictor valve.

Both methods are based on the assumption that the characteristics of the restrictor valve are known and are identical to its steady state impedance (nP/Q). It is also assumed that the pump impedance is that of a lumped volume equal to the internal volume of the pump, plus the leakage impedance of the pump. Under such conditions, the source flow ($|Q_s|$) can be obtained by measuring the pressure fluctuation at the pump outlet, and using the equation:

$$|Q_s| = \frac{|P_o|}{Z} \qquad (3.1)$$

where: $|Q_s|$ - amplitude of source flow

$|P_o|$ - amplitude of pressure fluctuation

Z - calculated effective impedance of pump, line and termination

This equation is only valid if standing wave effects are negligibly small in the line. This can be achieved with a length of line shorter than 1/20th of the wavelength of the highest frequency considered during the analysis.

This is a simple method of predicting $|Q_s|$, which is considered by

Unruh and Szerlag as the relevant parameter to define a pump. However, as the technique is based on assumptions concerning pump and termination impedances considerable errors can be incurred. Results of tests performed at Bath University [17] have shown that the source impedance of pumps evaluated by consideration of volume and leakage in the pump produces values which are much higher than obtained experimentally. In addition, it was found that the assumption of an ideal orifice for the impedance characteristics of a restrictor valve is incorrect. The characteristic impedance of a restrictor valve actually shows some dependency on frequency. This will be explained in section 3.6.3.

3.3.2 Reflectionless Termination Method. The reflectionless termination case (ρ_t=0.) has been already referred to in chapter II. In such circumstances the general equation for the standing wave in a line is simplified to:

$$P_x = \frac{Q_s Z_s Z_o}{Z_s + Z_o} \quad e^{-\gamma x} \qquad (3.2)$$

and if the pressure ripple is considered at the pump flange:

$$P_x = \frac{Q_s Z_s Z_o}{Z_s + Z_o} \qquad (3.3)$$

Individual values of Q_s and Z_s can be obtained by carrying out a second test, with a different value of Z_o, i.e. a different pipe diameter. The pressures thus obtained are given by:

$$P_{o1} = \frac{Q_s Z_s Z_{o1}}{Z_s + Z_{o1}} \quad \text{and} \quad P_{o2} = \frac{Q_s Z_s Z_{o2}}{Z_s + Z_{o2}}$$

hence,

$$Z_s = Z_{o1} Z_{o2} \quad \frac{P_{o2} - P_{o1}}{Z_{o2} P_{o1} - P_{o2} Z_{o1}} \qquad (3.4)$$

and

$$Q_s = \frac{P_{o2}}{Z_{o1}} + \frac{P_{o2} Z_{o2} (Z_{o2} P_{o1} - Z_{o1} P_{o2})}{Z_{o1} (P_{o2} - P_{o1})} \qquad (3.5)$$

At first sight, this method appears to be extremely simple and powerful, with no assumptions except for the condition of a non-reflection termination. The difficulty lies in achieving a loading system which is reflectionless at all pumping frequencies. This can, however, be obtained in two ways:

a) a very long line - If a very long line is used so that the wave is attenuated completely before reaching the termination, then there will be no reflection regardless of the characteristics of the actual termination. This is best implemented by a long length of hydraulic hose which inherently has good attenuating properties. Tests carried out at Bath University [17] have shown that lengths of over 30m would be necessary for a near reflectionless case. However, even with the use of double braided hoses the results were not very reliable due to problems of waves in the hose wall. Another difficulty experienced was the accurate prediction of Z_o for the flexible hose.

b) a matched termination valve such that $Z_t=Z_o$ - It is very difficult to match the values of line impedance with a valve under different loading conditions and over a large range of frequencies. Recently though, Theissen [24] developed a valve in an attempt to achieve such conditions. As the valve must be finely adjusted for each particular test, the only way of checking whether reflectionless conditions have been achieved is by measuring the pressure fluctuations at several points along the line and verify that they show identical signals. This involves the use of at least two transducers for the set-up, although only one is used for calculations. This valve is claimed to be reflectionless over the normal range of harmonic

frequencies of hydraulic pumps. The tuning of the valve at the beginning of each test and the constant checking of its effectiveness makes this method rather awkward to use.

3.3.3 High Impedance Pipe Method - This method was developed at Bath University [21], and is based on the argument proposed in section 2.4.4. By using a small bore pipe attached to a pump, a high entry impedance is achieved and the value of the pressure reading at the pump flange is given by:

$$P_o = Q_s \cdot Z_s \qquad (3.6)$$

Hence, by a simple pressure reading it is possible to measure the product of the source flow and the source impedance of the pump.

A difficulty in the application of this method arises, however, in that if Z_s is unknown, it is only possible to decide what pipe diameter is required by experiment. Tests are carried out with different diameter pipes until a constant value of pressure is reached regardless of any further reduction in pipe diameter. If a pump has relatively low values of source impedance amplitude at some harmonic frequencies, two tests with different diameter pipes could be sufficient. However, for higher source impedance values the pipe diameters required would have to be so small that they would be impracticable. This problem may be solved by examining the effects of pipe length on the load system entry impedance. If eq.2.6 is rewritten in terms of the entry impedance (Z_E), then the pressure at the pump outlet is [21]:

$$P_o = \frac{Q_s Z_s Z_E}{Z_s + Z_E} \qquad (3.7)$$

where,

$$Z_E = Z_o \frac{1 + \rho_t e^{-2\gamma \ell}}{1 - \rho_t e^{-2\gamma \ell}} \qquad (3.8)$$

If $|Z_E| >> |Z_s|$, eq.3.7 is reduced to eq.3.6. Z_E is, therefore, a function of both Z_o and γ an for a frictionless case can be obtained from eq.3.8:

$$Z_E = Z_o \frac{(Z_t + Z_o\, j \tan(\gamma \ell/a))}{(Z_t\, j \tan(\gamma \ell/a) + Z_o)} \qquad (3.9)$$

The value of Z_E tends to:

$$Z_E \longrightarrow \frac{Z_o^2}{Z_t}, \text{ when } \tan(\gamma \ell/a) \longrightarrow \infty \qquad (a)$$

and, $$Z_E \longrightarrow Z_t, \text{ when } \tan(\gamma \ell/a) \longrightarrow 0 \qquad (b)$$

As $|Z_o|$ has a large value for a high impedance pipe, and is usually greater than $|Z_t|$, condition a) produces maximum values of Z_E which are far greater than $|Z_o|$. Therefore, by choosing a high impedance pipe of suitable length it is possible to obtain $|Z_E| \gg |Z_s|$ even if the source impedance of the pump is very large. The only inconvenience of this solution is that the length ℓ is a function of pressure, temperature and, most important of all, frequency. A length which suits the odd harmonics of the pump will generate low values of Z_E for the even harmonics, which means that several pipe diameter and pipe length combinations must be used to test one pump.

Fig.3.4 shows a typical set-up for the high impedance pipe test of a pump, and fig.3.5 presents some results for different diameter pipes. As the values of Z_s for the higher harmonics are relatively low, the pressure readings are virtually constant for all pipe diameters. The 1st and 2nd harmonics require larger values of Z_E (smaller pipe diameters) to obtain constant values on the pressure curve.

Once the values of $|Q_s.Z_s|$ are evaluated for all harmonics, the pump can be characterized by the RMS value of all harmonics, according to the following equation:

$$\text{R.M.S.} = \sqrt{\sum_{i=1}^{n} |Q_s \cdot Z_s|^2} \quad , \text{ i= harm. number} \qquad (3.10)$$

Bath University proposed this method as a draft British Standard for measuring fluid borne noise generating potential of pumps. A full description of this method can be found in [25].

The product of the source flow and the source impedance as a measure of the fluid borne noise potential of a pump is in marked contrast with Unruh's and Szerlag's methods which consider the source flow only as the important fluid borne noise characteristic of a pump. In fact this latter point of view is in accordance with the study presented in section 2.4.4 where it was verified that Z_s is only significant in determining the fluid borne noise generating potential of a pump if it has a value $|Z_s| < |Z_o|$. As this condition is very seldom the case, at least for the lower harmonics unless an uncommonly small diameter pipe is attached to the pump, the important characteristic of the pump must be considered Q_s. Consequently, the results of this method do not provide a true reflection of the fluid borne noise generating potential of a pump in a real system. This can be understood by the following simple example: Two pumps have similar values of $Q_s.Z_s$ but one has a source impedance twice as large as the other (hence half the value of Q_s). If both pumps are attached to a system with a value of $|Z_o|$ lower than either of the source impedances, the pump with half the value of Q_s would generate about half the pressure ripple in the system as the other. The $Q_s.Z_s$ rating of the pumps does not provide, in this case, an accurate reflection of the pump fluid borne noise generating potential.

3.3.4 Additional Capacity Method. The high impedance pipe method allows for the evaluation of pump parameters, in the form of the product $Q_s.Z_s$ only. This may be regarded only as a first step in the

determination of the pump fluid borne noise potential. For a more detailed analysis of the pump it is necessary to know the characteristics Q_s and Z_s separately. In order to separate the two terms, a supplementary method was suggested [10].

This method is based upon the assumption that the source impedance of a pump is mainly characterized by the behaviour of a lumped volume, the volume of the pump outlet chamber. If the impedance is modified by attaching to the pump outlet a known volume of oil (V), in the form of an expansion chamber, then the new source impedance will be:

$$Z_s' = \frac{Z_s \cdot Z_v}{Z_s + Z_v} \qquad (3.11)$$

where,

$$Z_v = \frac{\beta}{j \omega V} \qquad (3.12)$$

where: Z_s - pump source impedance

Z_s' - source impedance of modified pump

Z_v - impedance of volume V, at freq. ω

If a high impedance pipe test is carried out on the modified pump, then the value of $P'=Q_s.Z_s'$ will be measured. Using the results of the high impedance pipe on the pump alone and the results of tests on the modified pump, it is possible to separate the values of Q_s and Z_s, according to the following formula:

$$Z_s = \frac{(P - P')}{P'} \cdot Z_v \qquad (3.13)$$

and,

$$Q_s = \frac{P}{Z_s} \qquad (3.14)$$

This method can be difficult to apply as large volumes are sometimes necessary to modify the pump impedance sufficiently. This

introduces the possibility of standing waves within the chamber, and inevitably will create errors at the higher harmonics. Other errors may result from the vibration of chamber walls. Experiments performed on expansion chambers by Wing [26] demonstrated that these effects may cause the impedance of the chamber to be substantially different from the impedance of the volume contained in it. This creates some doubts about the effectiveness of this method.

Summarizing, the additional capacity method is a complement to the high impedance method described in the previous section. If the difficulties inherent to each method are considered it becomes evident that the end result cannot be expected to be particularly accurate.

3.4 SYSTEM TESTING METHODS USING TWO TRANSDUCERS

The various methods described above fail to agree on the way of representing pump fluid borne noise behaviour. It is important on one hand to make sure that the results obtained from a method are represented in terms of pressure. This is not easy, however, due to the complex behaviour of the pressure fluctuations in a system as explained in chapter II. On the other hand, reflecting the pump fluid borne noise generating potential in terms of flow ripple (Q_s) may be misleading as it states nothing in terms of the pump source impedance. In the view of the author, there is no simple way of defining pump fluid borne noise potential and consequently it should be defined by both the pump source flow (Q_s) and source impedance (Z_s) frequency spectra.

The methods described below aim at determining these characteristics not only for pumps but for motors as well. The same methods may also be used to find the characteristics of passive

components in a system such as valves and actuators.

It is at this point that the requirements of a simple test must be relinquished, and so two transducer or multi transducer methods may be considered. Various proposals will now be described, and their advantages and disadvantages examined.

3.4.1 Extending Pipe Length Method. If two pressure transducers are connected in a system composed of a pump, a pipe and a termination valve, the pressure fluctuations (P_1 and P_2) can be given, according to eq.2.6:

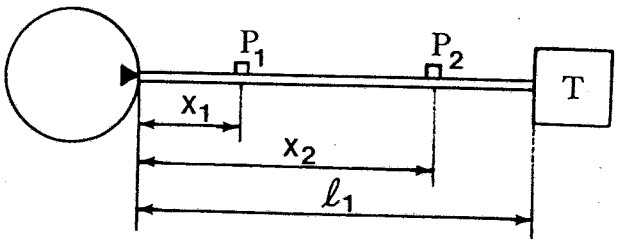

$$P_1 = \frac{Q_s Z_s Z_o}{Z_s + Z_o} \cdot \frac{e^{-\gamma x_1} + \rho_t e^{-\gamma(2\ell_1 - x_1)}}{1 - \rho_s \rho_t e^{-2\gamma \ell_1}} \qquad (3.15)$$

$$P_2 = \frac{Q_s Z_s Z_o}{Z_s + Z_o} \cdot \frac{e^{-\gamma x_2} + \rho_t e^{-\gamma(2\ell_1 - x_2)}}{1 - \rho_s \rho_t e^{-2\gamma \ell_1}} \qquad (3.16)$$

If a ratio of the two pressures is formed, the resulting equation is independent of the pump parameters:

$$\frac{P_2}{P_1} = \frac{e^{-\gamma x_2} + \rho_t e^{-\gamma(2\ell_1 - x_2)}}{e^{-\gamma x_1} + \rho_t e^{-\gamma(2\ell_1 - x_1)}} \qquad (3.17)$$

Eq.3.17 is, however, a function of ρ_t and hence a function of Z_t. Therefore, with two readings of pressure along a line it is possible

to evaluate the termination impedance (Z_t), provided Z_o and γ have been calculated (as in section 2.3). By this very simple test, it is possible to evaluate the characteristics of valves or any other passive components positioned at the end of the pipeline. Once ρ_t is known, eqs.3.15 and 3.16 become dependent upon pump parameters only (Q_s and Z_s).

If a second test is carried out with a different line length (ℓ_2) and the pressure is measured at a distance x_3 from the pump:

$$P_3 = \frac{Q_s Z_s Z_o}{Z_s + Z_o} \cdot \frac{e^{-\gamma x_3} + \rho_t e^{-\gamma(2\ell_2 - x_3)}}{1 - \rho_s \rho_t e^{-2\gamma \ell_2}} \qquad (3.18)$$

Forming the ratio between P_1 and P_3:

$$\frac{P_3}{P_1} = \frac{\dfrac{e^{-\gamma x_3} + \rho_t e^{-\gamma(2\ell_2 - x_3)}}{1 - \rho_s \rho_t e^{-2\gamma \ell_2}}}{\dfrac{e^{-\gamma x_1} + \rho_t e^{-\gamma(2\ell_1 - x_1)}}{1 - \rho_s \rho_t e^{-2\gamma \ell_1}}} \qquad (3.19)$$

This equation is only dependent upon ρ_s (as ρ_t is known) and, hence, Z_s can be obtained. Finally, using eqs.3.15, or 3.16 or 3.18, the value of Q_s can be readily evaluated.

Theoretically, two line length tests, comprising two pressure readings on the first test and only one on the second, should be enough to evaluate Q_s, Z_s and Z_t at each harmonic frequency. However, in practice, small experimental scatter on the pressure readings can generate large errors in the predicted values.

This method was used by McCandlish et al [16] to verify wave

propagation theory and obtain pump and termination parameters. In order to avoid erroneous results, it was found that a large number of pipe lengths had to be used and statistical analysis employed to obtain mean values of Q_s, Z_s and Z_t. This is, indeed, a lengthy process which is only eased by the use of on-line computer data acquisition. This method provided satisfactory results, mainly when predicting Q_s and Z_t, as presented in reference [16]. The results relating to the source impedance of pumps were particularly inconsistent at the lower harmonic frequencies, and many different line lengths tests were required to provide meaningful results.

3.4.2 Tuned Lengths Method. The difficulties experienced during the extended pipe length tests justified the need for a careful study of the inaccuracies encountered, as the method is theoretically sound. One obvious shortcoming is the assumption that a very complicated function, as eq.3.19, can be defined by only two data points. This can prove disastrous if if any scatter is associated with the measurements.

In the case of the extending pipe length method the experimental errors mentioned in section 3.2 are partially responsible for scatter, but some other errors must also be considered: instrumentation errors and test procedure errors. The analysers commonly used for fluid borne noise measurement are accurate to within ±1dB on amplitude and ±5 degrees on phase. Test procedure errors can also occur since the pump must be stopped to change the length of the pipe, and it is difficult to ensure that identical conditions are maintained from one test to another.

It will now be shown that the length of pipeline selected for the tests is extremely important and the effects of experimental scatter

can be minimized by a judicious choice of the line lengths.

EVALUATION OF ρ_t

Eq.3.17 may be simplified considerably if a particular case is chosen: one transducer is positioned near the pump flange ($x_1=0$) and the other is placed near the termination ($x_2=\ell$). This case is particularly attractive in practice as the transducers can be located in blocks directly attached to the pump and termination. Equation 3.17 becomes,

$$\frac{P_2}{P_1} = e^{-\gamma \ell} \frac{1 + \rho_t}{1 + \rho_t \, e^{-2\gamma \ell}} \qquad (3.20)$$

If the line is considered frictionless, $\gamma=j\omega/a$

$$\frac{P_2}{P_1} = e^{-j(\omega \ell/a)} \frac{1 + \rho_t}{1 + \rho_t \, e^{-2j(\omega \ell/a)}} \qquad (3.21)$$

This equation is a periodic function with $\omega\ell/a$, with a period of $\omega\ell/a=2\pi$. This equation assumes particular values when $\omega\ell/a=n\pi$, with n=0,1,2,etc. Then:

$$\frac{P_2}{P_1} = +1 \quad \text{,for n even number}$$

$$\frac{P_2}{P_1} = -1 \quad \text{,for n odd number} \qquad (3.22)$$

Therefore, the pressure fluctuation at points separated by integer multiples of a half wavelength must have the same amplitude and either equal phase angles or phases 180 degrees apart. Under such conditions, any value of ρ_t is acceptable as a solution of the equation. This is clearly a hopeless situation.

Consider now values of $\omega\ell/a$ equal to $\pi/8$, $\pi/4$ and $\pi/2$ (due to the cyclic variation of the exponential function of eq.3.20, only these values of $\omega\ell/a$ are necessary to understand the relationship between

the pressure ratio and ρ_t). These cases are represented graphically in fig.3.6. The amplitude of pressure ratio is presented on a logarithmic scale whilst the phase has a linear scale in the interval [-180.,180.] degrees. The value of ρ_t was varied both in amplitude and phase over a large range of values. Each numerical symbol represents a constant $|\rho_t|$ (according to the key in figure) and the dotted lines represent lines of constant $\measuredangle\rho_t$. These figures will be examined to obtain the importance of the line length in a qualitative, rather than a quantitative manner.

For $\omega\ell/a$ equal to $\pi/4$ (fig.3.6a) the solutions mainly occupy only a small part of the graph, around $P_2/P_1=1$. This indicates that small errors in measured pressure ratios around unity can lead to large errors in the evaluation of ρ_t. For $\omega\ell/a=\pi/4$ the solutions of the equation occupy a larger area of the pressure ratio plane (fig.3.6b), but it is only when $\omega\ell/a$ reaches the value $\pi/2$ that the solutions for ρ_t are evenly distributed in the graph (fig.3.6c). Here, the values of ρ_t are relatively insensitive to small variations in pressure ratio. Case b) may be considered as a limiting case between conditions of high and low sensitivity to data errors.

From these examples, if the cyclic behaviour of the exponential functions is taken into consideration, it is possible to conclude that the prediction of ρ_t is least sensitive to errors in data when the line lengths tested are odd integer multiples of a quarter of the wavelength of the harmonic considered. Furthermore, it is possible to specify ranges of values of $\omega\ell/a$ over which the results of ρ_t can be predicted with reasonable accuracy. From numerous tests, experience has proved that this range, centered at values $\omega\ell/a=n\pi/2$, should be:

$$\pi/4 + n\pi < \gamma \ell/a < 3\pi/4 + n\pi \text{ , for } n=0,1,2,... \qquad (3.23)$$

or, in terms of wavelengths,

$$\lambda/8 + n\lambda/2 < \ell < 3\lambda/8 + n\lambda/2 \text{ , for } n=0,1,2,... \qquad (3.24)$$

If the positions of the pressure transducers (x_1 and x_2) are not constrained to the extreme values of 0 and ℓ, eq.3.17 can be written as:

$$\frac{P_2}{P_1} = e^{-\gamma(x_2-x_1)} \frac{e^{2\gamma(\ell_1-x_2)} + \rho_t}{e^{2\gamma(\ell_1-x_2)} + \rho_t e^{-2\gamma(x_2-x_1)}} \qquad (3.25)$$

This shows that the sensitivity of the prediction of ρ_t to errors in P_2/P_1 is, in fact, only dependent upon the distance between the points of measurement (x_2-x_1) and the actual length of the line is unimportant.

EVALUATION OF ρ_s

The evaluation of ρ_s using eq.3.19, is only possible if ρ_t is known as explained in the previous section. The equation is based on the results of the pressure fluctuations measured at one point in a system for two different line length tests. It is particularly convenient, not only from the analysis point of view but from the testing procedure as well, to keep the position of measurement fixed in relation to the pump from one test to another. Assuming the position of the pressure transducers is $x_1=x_3=0.$, eq.3.19 simplifies to:

$$\frac{P_3}{P_1} = \frac{e^{2\gamma\ell_1} + \rho_t e^{-2\gamma(\ell_2-\ell_1)}}{e^{2\gamma\ell_1} + \rho_t} \cdot \frac{e^{2\gamma\ell_1} - \rho_s \rho_t}{e^{2\gamma\ell_1} - \rho_s \rho_t e^{2\gamma(\ell_2-\ell_1)}} \qquad (3.26)$$

This equation is more difficult to examine than eq.3.20, in as much as the evaluation of ρ_s is a function of both ρ_t and the

experimental results P_1 and P_3. Hence, the prediction of ρ_s will be affected not only by data errors but also by the inaccuracies in the prediction of ρ_t. If the recommendations above are followed, however, the determination of ρ_t should be regarded as fairly accurate.

The sensitivity of the prediction of ρ_s to values of the pressure ratio depends upon the values of ρ_t and the propagation term $e^{-2\gamma(\ell 2-\ell 1)}$. The effects of these will now be discussed.

Influence of ρ_t

Firstly consider the effect of a reflectionless termination. Although a such a condition is not sought during this test, it may occur at a particular harmonic frequency, causing eq.3.26 to be reduced to:

$$\frac{P_3}{P_1} = \pm 1 \quad , \text{ for } |\rho_t|=0. \qquad (3.27)$$

In this case, any value of ρ_s is feasable as a solution of this equation, and again this is a hopeless situation.

Consider now the effects of different reflecting terminations. Fig.3.7 shows the relationship between ρ_s and the pressure ratio (P_3/P_1) for three values of $|\rho_t|$ and constant value of $\omega(\ell 2-\ell 1)/a$. The first value shown in fig.3.7a is $|\rho_t|=0.3$, which corresponds to a low reflection and hence low resonances on the standing wave pattern. Consequently, the values of P_3/P_1 possible in the system (corresponding to $|\rho_s|<1$) are concentrated in a small area of the graph. Any error in the values of P_3 or P_1 may result in large errors in the prediction of ρ_s. When the value of $|\rho_t|$ is increased to 0.6 (fig.3.7b) the range of possible values of pressure ratio is enlarged. This is even more pronounced in the final case, when

$|\rho_t|=0.9$ (fig.3.7c). Hence, the prediction of ρ_s is least sensitive to experimental data errors when $|\rho_t|$ is as large as possible.

Influence of the propagation term $e^{-2\gamma(\ell 2-\ell 1)}$

For simplicity, the frictionless case will be considered, and $e^{-2\gamma(\ell 2-\ell 1)}$ becomes $e^{-2j\omega(\ell 2-\ell 1)/a}$. For each value of $|\rho_t|$, the relation between P_3/P_1 and ρ_s is dependent upon the value of $\omega(\ell 2-\ell 1)/a$. In fact, when the term $e^{-2j\omega(\ell 2-\ell 1)/a}$ assumes the real value of 1. (i.e. when $\omega(\ell 2-\ell 1)/a=n\pi$, with n=0,1,2,...) eq.3.26 is independent of ρ_s and therefore any value of ρ_s is a possible solution of the equation. Yet again a hopeless case.

Other values of $\omega(\ell 2-\ell 1)/a$ will now be examined. In fig.3.8 the value of $|\rho_t|$ was fixed at 0.7 and $\omega(\ell 2-\ell 1)$ was varied. The three cases are shown for $\omega(\ell 2-\ell 1)/a = \pi/8$, $\pi/4$ and $\pi/2$. When the value of $\omega(\ell 2-\ell 1)/a$ is very small (fig.3.8a) the pressure values (P_1 and P_3) are very close. All the solutions of ρ_s ($|\rho_s|<1$) correspond to a very small band of values of pressure ratio of amplitude close to unity. It is only when $\omega(\ell 2-\ell 1)/a$ reaches $\pi/2$ that there is an uniform distribution of the solutions (ρ_s) of the equation. In this case, any minor variation in data values due to experimental scatter will not lead to a drastic change in the prediction of ρ_s. The value $\pi/4$ (fig.3.8b) represents a satisfactory limiting condition between high and low sensitivity of results to data errors.

The condition that must be satisfied for accurate prediction of ρ_s is that the two line lengths must be a quarter of wavelength different or, in general, if ranges of conditions are considered:

$$\pi/8 + n\pi < \gamma(\ell_2-\ell_1)/a < 3\pi/4 + n\pi \quad , \text{ for } n=0,1,2,... \qquad (3.28)$$

or,

$$\lambda/8 + n\lambda/2 < \ell_2-\ell_1 < 3\lambda/8 + n\lambda/2 \quad , \text{ for } n=0,1,2,... \qquad (3.29)$$

This study was made under the assumption that $x_1=x_3=0$, i.e. both pressure transducers were placed at the pump flange. However, the same conclusions can be reached for x_1 and x_3 being at any position in the lines. If eq.3.19 is presented in an alternative form,

$$\frac{P_3}{P_1} = \frac{e^{-\gamma x_3} + \rho_t\, e^{-\gamma(2\ell_2 - x_3)}}{e^{-\gamma x_1} + \rho_t\, e^{-\gamma(2\ell_1 - x_1)}} \cdot \frac{e^{2\gamma\ell_2} - \rho_s\,\rho_t}{e^{2\gamma\ell_2} - \rho_s\,\rho_t\, e^{-2\gamma(\ell_2-\ell_1)}} \quad (3.30)$$

the factors that ρ_s is multiplied by (and hence influence the sensitivity to the pressure ratio variations) are still the same: ρ_t and $e^{-2\gamma(\ell 2-\ell 1)}$. All the other differences between eq.3.30 and eq.3.26 only affect the relative values of P_3/P_1 in relation to ρ_s. The sensitivity of ρ_s to experimental scatter is unaffected.

IMPLEMENTATION OF THE TEST METHOD

According to the study presented above, it is possible to improve the accuracy of the extended pipe length test method considerably simply by avoiding some conditions that can generate erroneous results out of small scatter in the data acquired. This means that the number of tests required to obtain the characteristics of the pump are substantially reduced. For each test the two transducers should, ideally, be separated by an odd integer multiple of a quarter of a wavelength. Successive line length tests must have lengths that also differ by about an odd integer multiple of a quarter of a wavelength. As the whole method is based upon the standing wave equation, the method fails if there is no standing wave in the line ($|\rho_t|=0.$). Therefore, the termination characteristic must be such that it provides a large value of $|\rho_t|$. In section 2.4.2 it was stated that such values of $|\rho_t|$ can be achieved either by large values of $|Z_t|$ (a restrictor valve creating a large mean pressure in the system for a low mean flow), or by the use of a volume at the termination which makes $\measuredangle Z_t$ approach -90 degrees and hence $|\rho_t| \to 1$.

When the relations given in eq.3.24 and 3.29 are applied to a pump under test, they must be considered for each harmonic of the pump. There are, therefore, many different line lengths and transducer positions necessary to satisfy the conditions at all harmonics. However, as the harmonic frequencies are integer multiples of the fundamental frequency, conditions suitable for one harmonic may be suitable for other harmonics, which reduces the number of tests considerably. In order to determine suitable pipelengths which meet the requirements given above, an interactive computer program was written.

When the program is supplied with test data characterizing the running conditions (mean pressure, temperature, frequency, etc.) the program advises on line lengths that are are suitable for the test. For 10 harmonics of pumping frequency, for example, about eight lengths would be required. When loaded with the actual test measurements the program then selects all the conditions that are appropr

This method was compared with the extended pipe length method on results from early tests carried out by McCandlish [16]. The new approach was found to be superior, both in terms of accuracy and simplicity. As a result it was selected as the standard method for the work reported in chapters VI and VII. A full description of the computer program used for the tuned length method is given in appendix III.

3.5 MULTI TRANSDUCER METHOD.

Recently, a method has been developed by Wing [26], which although based upon the wave propagation theory used for the two transducer methods, takes the experimental work one stage further and attempts

to define the standing wave 'surface', of the type shown in fig.2.11, using more than two sources of information (transducers).

Monitoring, for example, the pressure fluctuations at four positions in a system composed of pump, pipe line and termination valve, the standing wave can be defined much better than if only two transducers were used. Successive tests of different line lengths, should provide sufficient information to define the two surfaces (amplitude and phase) that describe the standing wave pattern in the line in an unique way. As the pressure measurements are subjected to the same errors reported previously a least square fit is carried out in order to find the best surfaces to represent all measurements.

For each pair of surfaces which define the standing wave, there is a unique value for each of the characteristics Q_s, Z_s and Z_t. The greater the number of pressure transducers used in a line and the greater the number of line lengths tested, the better the standing wave pattern is described. Consequently the probability of finding the correct values of pump and termination characteristics is higher.

It is a manifestly difficult task to examine, with only four transducers, one wavelength of the standing wave for all harmonic frequencies. This is simply because the corresponding wavelengths may vary from, say, 6 metres (for the fundamental frequency) to .6 metres (for the 10th harmonic). If the transducers are, say, 0.15m apart they should define the pattern of the standing wave corresponding to the 10th harmonic well. However, only a small part of the 1st harmonic is covered. If the transducers remain at a fixed distance from the pump when different line lengths are tested, they will always be positioned at different points on the standing wave. Hence, it is possible to compensate for the lack of definition of one harmonic cycle by examining the pressures for a number of different

line lengths. Of course, a large variation in lengths has to be covered to describe the wave pattern completely. Alternatively, the greater the number of pressure transducers used in a line, the fewer the number of line lengths required.

In order to make this method feasible, an instrument was developed by Wing [26] to facilitate the experimental process. It is based on a telescopic tube arrangement ('hydraulic trombone' fig.3.9) which facilitates a change of length of line without actually having to disconnect pipes. The transducers are always mounted in the fixed part of the trombone and so remain at fixed distance from the pump. Wing suggested that up to 9 line lengths may be necessary to produce acceptable results.

Bearing in mind that the method is based upon the existence of a standing wave in a pipe, it may produce poor accuracy when the termination impedance is low or zero.

In the two transducer methods previously described, anechoic or near-anechoic conditions were avoided by the use of a restrictor or relief valves as a termination. With the hydraulic trombone solution, the 'termination' consists of a length of line terminated by a valve. The entry impedance to the smaller tube is likely to assume values close to the line impedance at some frequencies. Provided conditions of low value of $|\rho_t|$ are avoided this method proves to be very successful and practical [26].

A slightly modified version of this method was used to produce some of the results reported in chapter VI.

3.6 EVALUATION OF CHARACTERISTICS OF HYDRAULIC COMPONENTS

A large experimental program was carried out to assess the potential and accuracy of the two previously described methods of evaluating characteristics of hydraulic components in pressurized lines. Indeed, no attempt could be made at using the methods under low pressure conditions (pump suction lines) without a thorough test of their validity under pressurized conditions. Pumps, motors and valves were the main components tested, over a range of running conditions; a summary of the results obtained is presented in the following paragraphs. The testing of suction lines is reported in chapter VI.

3.6.1 Evaluation of source flow. The 'tuned lengths' and the 'hydraulic trombone' methods were used to test an axial piston pump (pump A described in appendix VI) at a fixed rotation speed and a constant mean outlet pressure (100 bar). The results, presented in fig.3.10 in the form of frequency spectra, show that both methods agree very well both in terms of amplitude and phase, for at least the first six harmonics. When the harmonic values are synthesized for both sets of results (fig.3.11) the agreement is still marked. This comparison of the synthesized values is a very severe test of accuracy of the prediction of Q_s as it reflects in one only trace the accuracy of all the harmonic components both in amplitude and phase.

Fig.3.11 shows clearly the backflows that occur each time a piston comes into contact with the outlet line, due to portplate timing mismatch. If the result of source flow, shown in fig.3.11a, is plotted as volume variation (volume ripple) delivered by the pump (fig.3.12) as a function of pump angle of rotation, it is possible to quantify the volume of fluid that was compressed in the piston chamber, as shown by the cross-hatched area. This area is delimited by the measured volume ripple and the ripple delivered by the pump if

ideal timing existed.

These results shown above for pump source flow were typical of the agreement that can be expected between the two methods and hence in the following results no comparison of the two methods is made.

Pump A was tested at different mean pressures and the results are shown in fig.3.13 as volume ripple. As expected, due to timing mismatch, the higher the mean system pressure the larger the volume of oil compressed. Furthermore, when the system pressure increases the rate of compression of oil increases, i.e. the change in volume with pump angle of rotation is steeper.

The effects of pump shaft speed on backflow was examined by Wing [26]. Fig.3.14 shows the results obtained by Wing for flow fluctuations generated by an axial piston pump (pump B, as described in appendix VI) at 850, 1300, 1700 and 2150 rev/min as a function of time. The source flow plots are superimposed on different mean flows and the number of cycles per unit time is different from one trace to another. This makes any comparison of results difficult. A better comparison of the four sets of results can be made if they are plotted as volume ripple as a function of pump angle of rotation (fig.3.15). In this figure all the plots are superimposed, because the displacement per radian is the same. The only difference between the results is in the compressed volumes. Of course the compressed volumes ought to be the same regardless of the pump speed and this is shown by the very similar volumes of backflow. However, when the pump is running at the slowest speed of 850rev/min, the backflow exists over a smaller angle of rotation of the pump. Although all compressions start at the very same angular position, the compression rate is a function of time and not of angular rotation of the shaft.

An external gear pump was also tested at different pressures (pump C, as described in appendix VI). Although the values of pressure ripple in the line vary considerably with mean pressure the results of source flow (fig.3.16) for the pump are virtually identical regardless of the mean pressure. As external gear pumps have no valve plate timing effects, the instantaneous flow ripple is virtually constant despite having been tested at pressures as different as 50 bar and 200 bar.

The tuned lengths method was used to test the inlet source flow generated by hydraulic motors. This was a vital exercise in preparation for pumps suction line work due to the resemblance between inlet side of motors and pumps (apart from the differences in mean pressure). The approach used to evaluate the inlet source flow was explained in section 2.5.2. The results of tests on an axial piston motor (same dimensions as pump A) are presented in fig.3.17. The negative mean flow is taken to mean fluid entering the motor. The results show that in this case no backflows exist in the motor. Indeed, the opposite occurs. The pump instantaneous flow trace is characterized by instantaneous drop of flow delivered occurring each time a piston opens to the pressure line. The instantaneous flow admitted by the motor is characterized by a momentarily sharp increase in flow when a piston opens to the inlet line. This peak of flow increases with mean pressure again due to the portplate timing mismatch.

An external gear motor (motor D) was also tested under different running conditions, two different mean pressures and two different running speeds. The flow fluctuation was always very similar (fig.3.18) regardless of the test conditions.

The details that can be extracted from the previous examples of pump and motor instantaneous flows under very different running conditions reflects the degree of accuracy with which the source flow characteristic can be evaluated by using the tuned length or the 'hydraulic trombone' methods. In general, it has been found that the prediction of Q_s is not significantly affected by experimental scatter. This is due to the fact that the value of Q_s is related to the 'mean' level of the standing wave pattern (see section 2.4.3) and not to values of resonant or anti-resonant conditions in the line.

3.6.2 Evaluation of source impedance. This proved to be the most difficult characteristic to predict accurately and consistently throughout all the tests. Even results of the two methods used did not fully agree in some cases, as will be shown below.

The results of source impedance are represented as frequency spectra. The source impedance of the axial piston pump (pump A) at 100 bar mean pressure was evaluated using both testing methods and the results are shown in fig.3.19. The results reveal that the pump source impedance has a characteristic equivalent to a lumped volume, i.e. a phase close to -90 degrees and an amplitude that decreases with frequency at a rate of about 20dB/decade. There is however, a detail that is quite important to consider: The result of phase of the 1st harmonic obtained from the trombone method cannot be correct (-120 degrees), because the phase must lie within the range [-90.,+90.] degrees. At first sight this would suggest that the method did not work correctly for this case. However, the reason lies in a more basic problem. Due to the mechanical construction of the hydraulic trombone (with one piston sliding inside a tube) the internal diameter of the pipeline that was attached to the pump was 32mm ($|Z_o|=1.3x10^9$ $Ns/m^5=183dB$). The amplitude of the first harmonic

of the pump impedance is about 205dB (2.2×10^{10} Ns/m^5), giving a ratio between the two values of 17:1. In section 2.4.3 it was shown that under these circumstances any variation in Z_s amplitude or phase had little effect on the pressure standing wave. Consequently, the mathematical approximation could not finding the actually true value because of the insensitivity of the standing wave pattern to changes in Z_s. The same circumstances did not occur with the tuned length method as a 17.5mm internal diameter pipe was used, which has a much larger value of line impedance ($|Z_o| = 4.5 \times 10^9$ Ns/m^5=193dB). If a larger diameter pipe were to be used with this method the same difficulties experienced with the trombone method would be encountered.

The results of the source impedance of the external gear pump (pump C) when tested at different mean pressures (fig.3.20) show an invariance of results with mean system pressure. This is in strict agreement with the assumption that the pump behaves as a lumped volume. The mean pressure has a small effect on the bulk modulus of the oil, but this is sufficiently small to be undetectable in the impedance characteristic. A comparison of the two methods shows yet again the difficulty of predicting the values of the larger amplitude harmonics with the hydraulic trombone.

The axial piston pump (pump B) which was tested at different running speeds is a much larger unit than either pump A or C. This unit when tested by Wing using the hydraulic trombone (fig.3.21) shows that the spectrum of the source impedance of a pump follows the same pattern regardless of the speed at which it is tested. Furthermore, the amplitude spectrum shows an anti-resonant point at around 1.5kHz after which the amplitude values start increasing. This is accompanied by a shift in phase values from -90deg to 90deg.

These results can be interpreted, nevertheless, if the pump is modelled by distributed parameter theory as explained by Edge [27]. In the case of pump B the difficulties in the evaluation of some harmonics of pump impedance, described above, did not occur. This was due to the low values of impedance (≈195dB maximum) compared with the previous pumps. In other words, the size of the pipe used in the hydraulic trombone was compatible with the impedance of the pump under test.

Unit A was also tested when running as a motor at low swash setting. The results of source impedance at 40 and 60 bar mean pressure are represented in fig.3.22. The values of both amplitude and phase coincide with those obtained when the unit was running as a pump at 100 bar (fig.3.19). (There is a slight discrepancy at the 1st harmonic component at 40 bar; this would not occur if a smaller diameter pipe were used).

Summarizing, the prediction of source impedance for pumps or motors is somewhat more difficult than evaluating the source flow. The main difficulty is experienced when testing pumps that are very compact and hence have very high values of source impedance amplitude. This is due to the fact that these large values of impedance, under some conditions, may not alter the pressure standing wave pattern significantly. If these conditions are avoided, by selecting a pipe diameter such that the pipe impedance is of the same order of magnitude as the impedance of the unit under test, the results obtained are very satisfactory.

3.6.3 Evaluation of a termination impedance. When the tuned length method was used to obtain pump characteristics a restrictor valve was used as the termination. The impedance of the valve was

evaluated as part of the analysis procedure. The 'trombone' method did not provide termination results when the pump was tested, due to the physical arrangement used for its implementation. Consequently, no comparison of termination characteristics obtained from the two methods will be presented below.

The restrictor valve (1" size), was tested when passing 27 l/min mean flow. The results for 50, 100, 150 and 200 bar mean pressure are plotted in fig.3.23. The values show a mainly resistive type characteristic with increasing magnitude as mean pressure is increased. Indeed, when the mean pressure was changed from 50 to 100 bar the 1st harmonic of the valve impedance increased by 6 dB, which corresponds to a doubled impedance value. Furthermore, when the mean pressure was raised to 150 bar the impedance had a further increase of about 4 dB (1.5 times increase). These results vary, hence, in the same manner as described by eq.2.9. It is nevertheless important to notice the significant phase shift present at the higher harmonics. When testing the restrictor valve at lower mean pressures the impedance results obtained were much lower and did not present the same pattern (fig.3.24) as the above results. The values plotted in fig.3.24 show a considerable amount of scatter. This is due to the low values of reflection coefficient ($|\rho_t| < 0.3$) which existed.

Fig.3.25 shows the impedance results for the same restrictor valve when tested at a constant mean system pressure. (50 bar) and different mean flows. The amplitude results increase with decreasing mean flow, but not in the same manner as in fig.3.23. The amplitude of the high frequency harmonics appears to be very insensitive to changes in mean flow conditions. The trend of the low frequency harmonic amplitudes, nevertheless, if extrapolated to the steady state values would follow closely the relation given by eq.2.9 (but

only for the steady state values). The phase spectrum corresponding to the lowest mean flow, however, is considerably shifted from the zero phase line. This is consistent with the amplitude results which decrease with frequency, suggesting the presence of a capacitive component.

In conclusion, the tuned lengths method was found to be suitable for evaluating the termination characteristics as well as the fluid borne noise characteristics of the source. In general, the prediction of the termination characteristics does not create any difficulties because of the sensitivity of the pressure standing wave in the line to the termination impedance. Some difficulties may arise, however, when the relation between Z_t and Z_o is such that $|\rho_t|$ becomes very small. In this case the pipe diameter used in the tests must be modified in order to increase the value of the reflection coefficient.

The results obtained for the restrictor valve at the higher harmonic components clearly demonstrates how difficult it is to predict the impedance spectrum of a restrictor valve from the steady state performance. In this respect, these results prove how inaccurate the results of the test methods proposed by Unruh and Szerlag can be for the high frequency components.

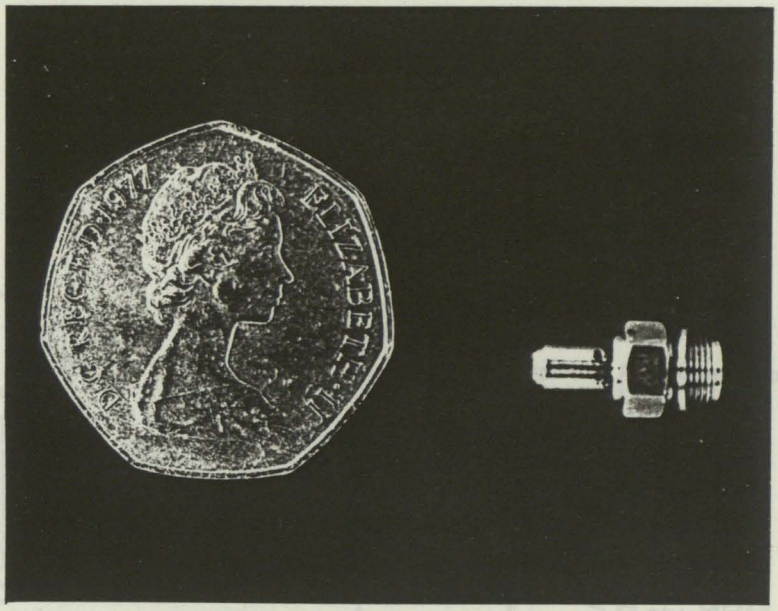

Fig. 3.1 Piezoelectric pressure transducer used for fluid borne noise tests

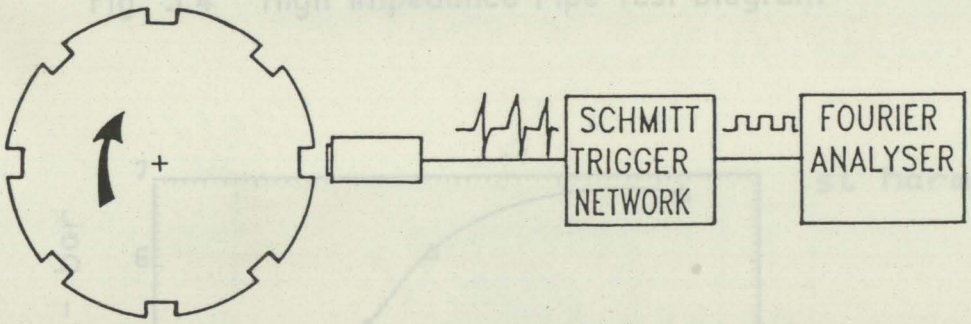

Fig. 3.2 Generation of phase reference signal

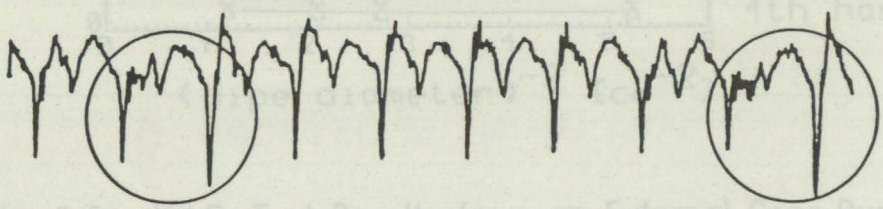

Fig. 3.3 Pressure signal showing faulty piston on a 7-piston pump

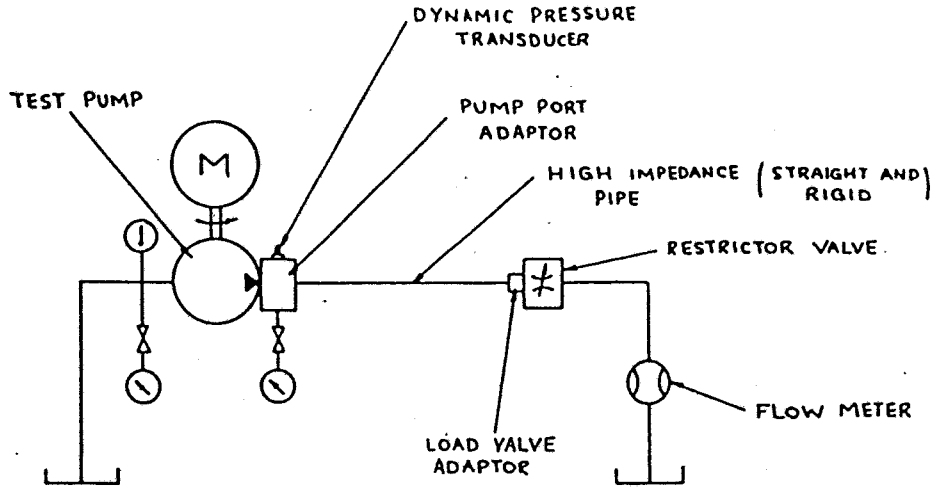

Fig. 3.4 High Impedance Pipe Test Diagram

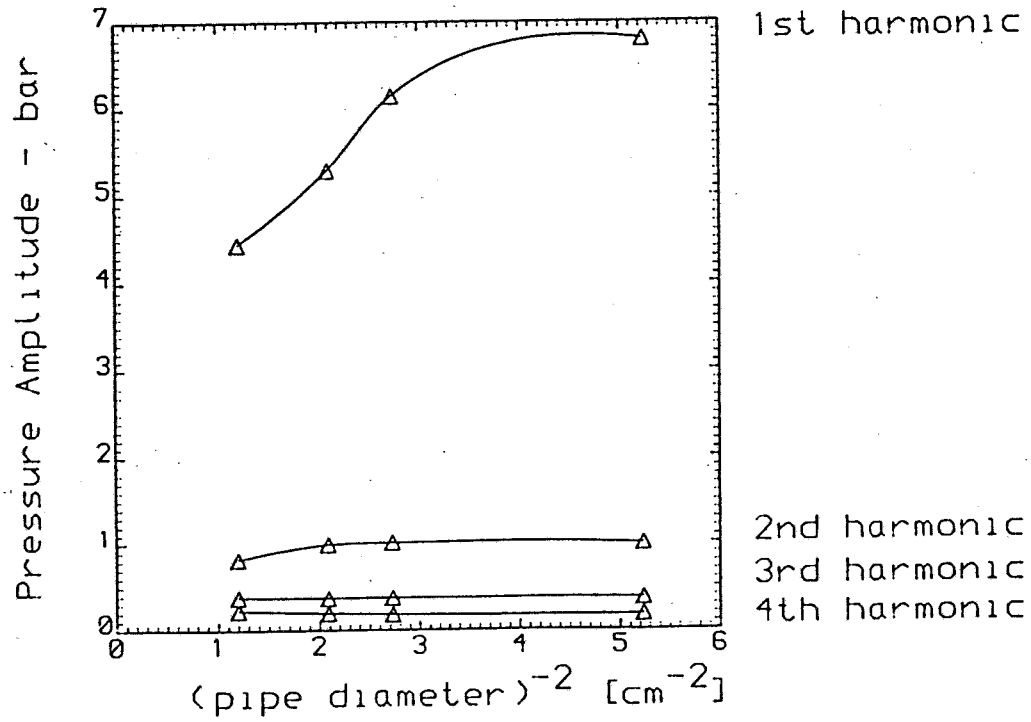

Fig. 3.5 H.I.P. Test Results from an External Gear Pump (p=80 bar; n=1500 rpm)

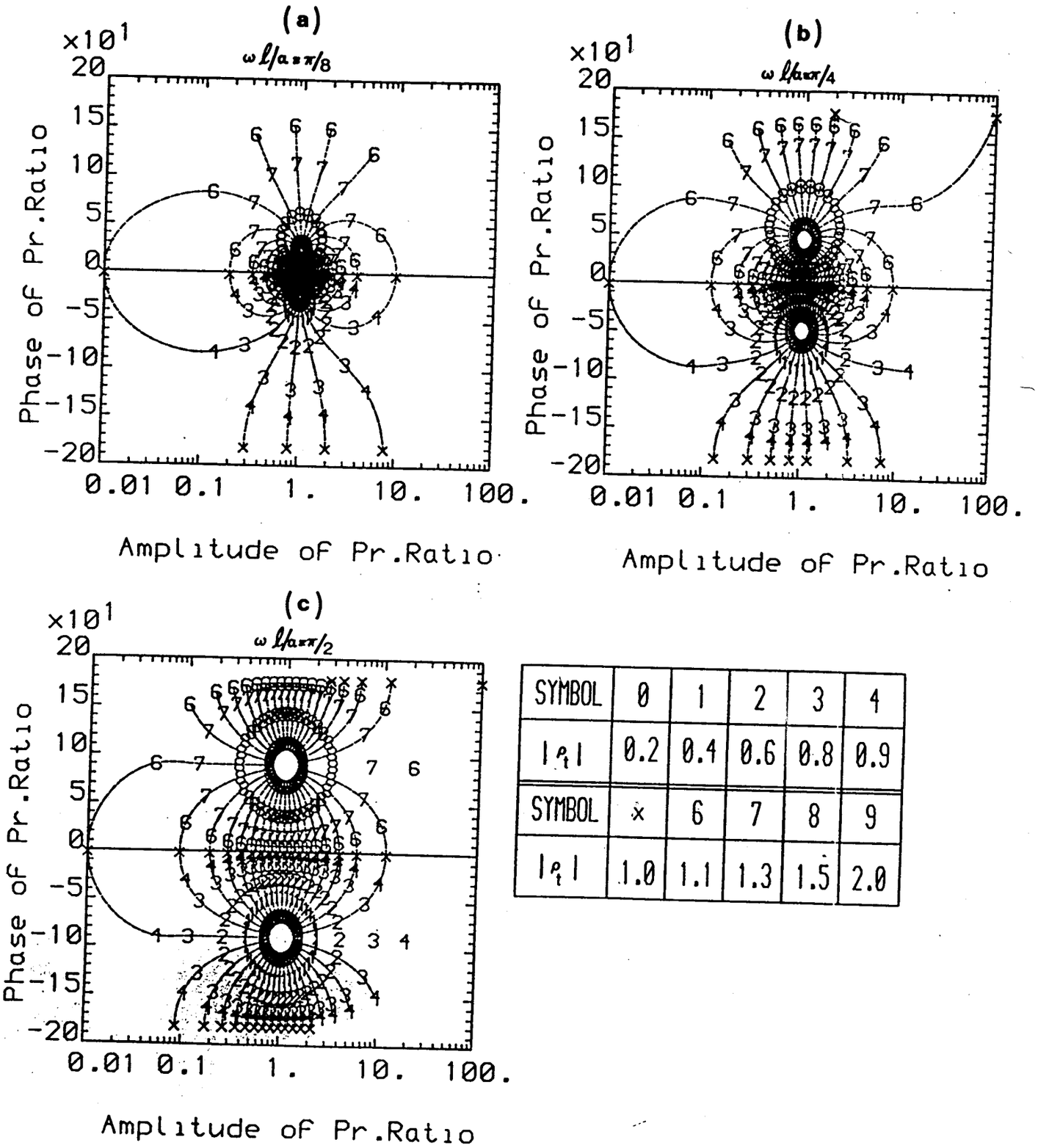

SYMBOL	0	1	2	3	4
$\lvert\rho_t\rvert$	0.2	0.4	0.6	0.8	0.9
SYMBOL	x	6	7	8	9
$\lvert\rho_t\rvert$	1.0	1.1	1.3	1.5	2.0

Fig. 3.6 Relation between "Pressure Ratio" and ρ_t

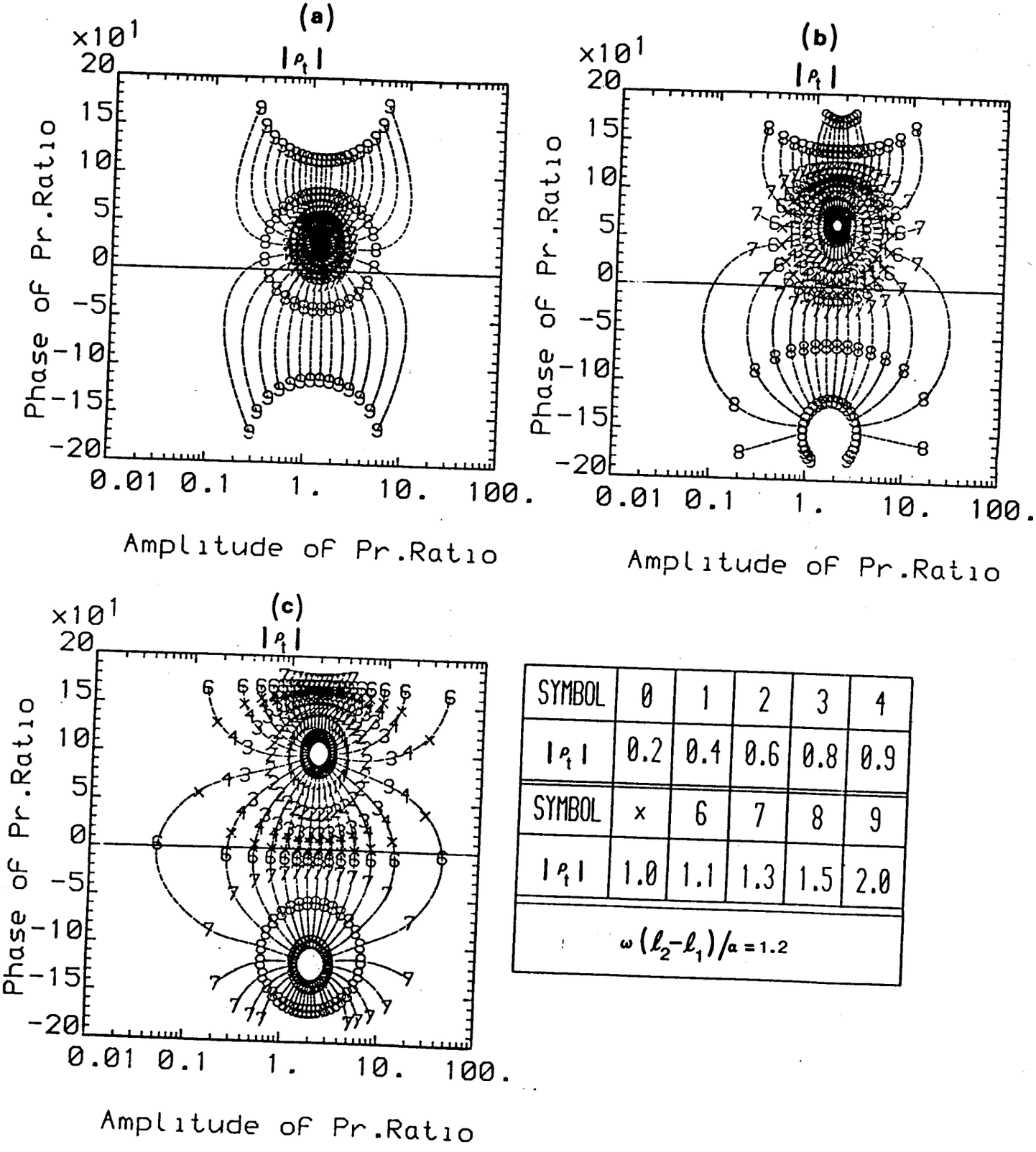

SYMBOL	0	1	2	3	4
$\lvert\rho_t\rvert$	0.2	0.4	0.6	0.8	0.9
SYMBOL	x	6	7	8	9
$\lvert\rho_t\rvert$	1.0	1.1	1.3	1.5	2.0

$\omega(\ell_2-\ell_1)/a = 1.2$

Fig. 3.7 Relation between "Pressure Ratio" and ρ_s for different values of ρ_t

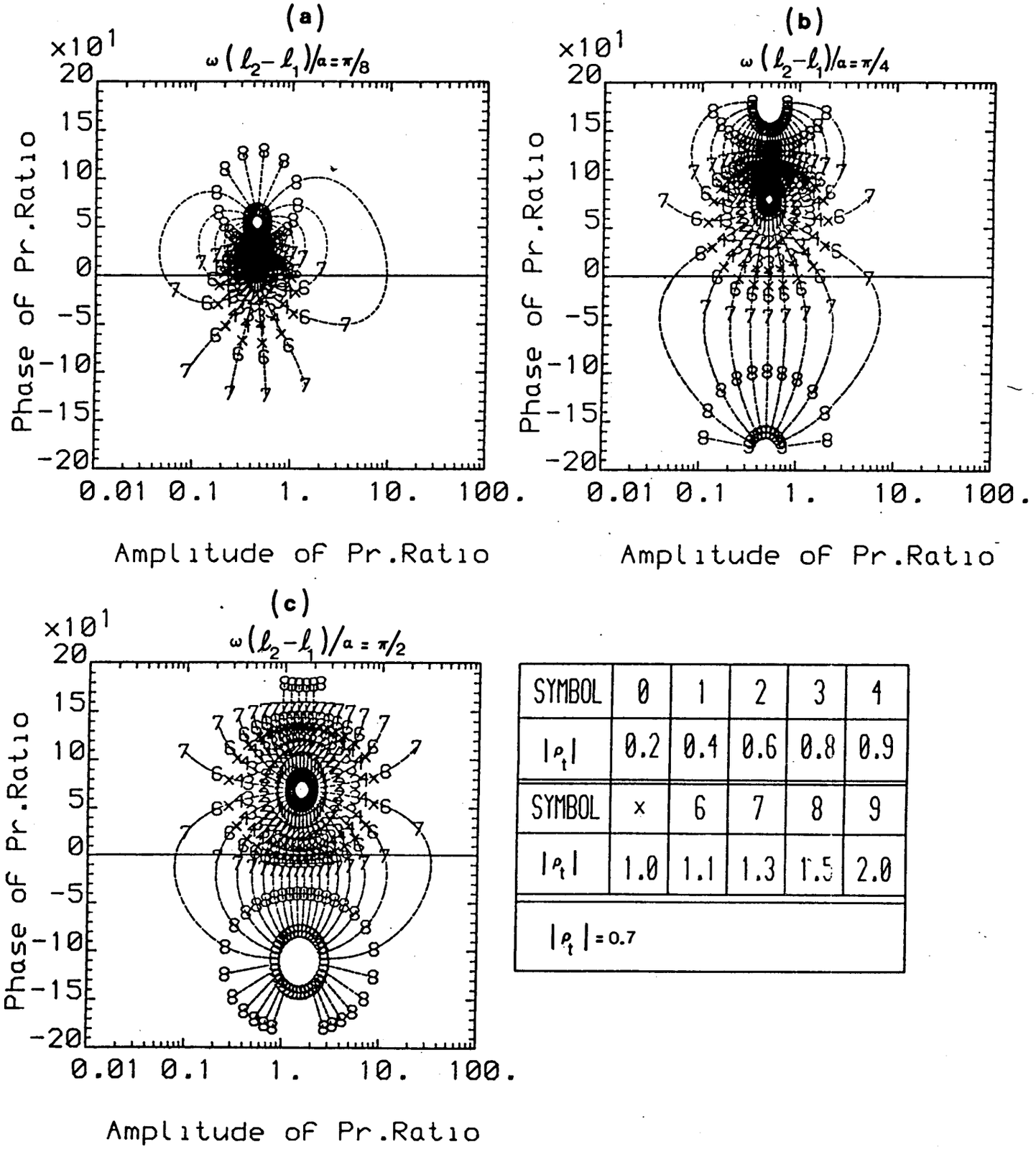

SYMBOL	0	1	2	3	4
$\lvert\rho_t\rvert$	0.2	0.4	0.6	0.8	0.9
SYMBOL	x	6	7	8	9
$\lvert\rho_t\rvert$	1.0	1.1	1.3	1.5	2.0

$\lvert\rho_t\rvert = 0.7$

Fig. 3.8 Relation between "Pressure Ratio and for different values of $\omega(\ell_2-\ell_1)/a$

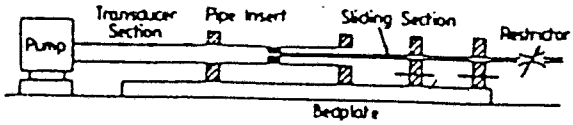

Fig. 3.9 'Hydraulic Trombone' lay-out

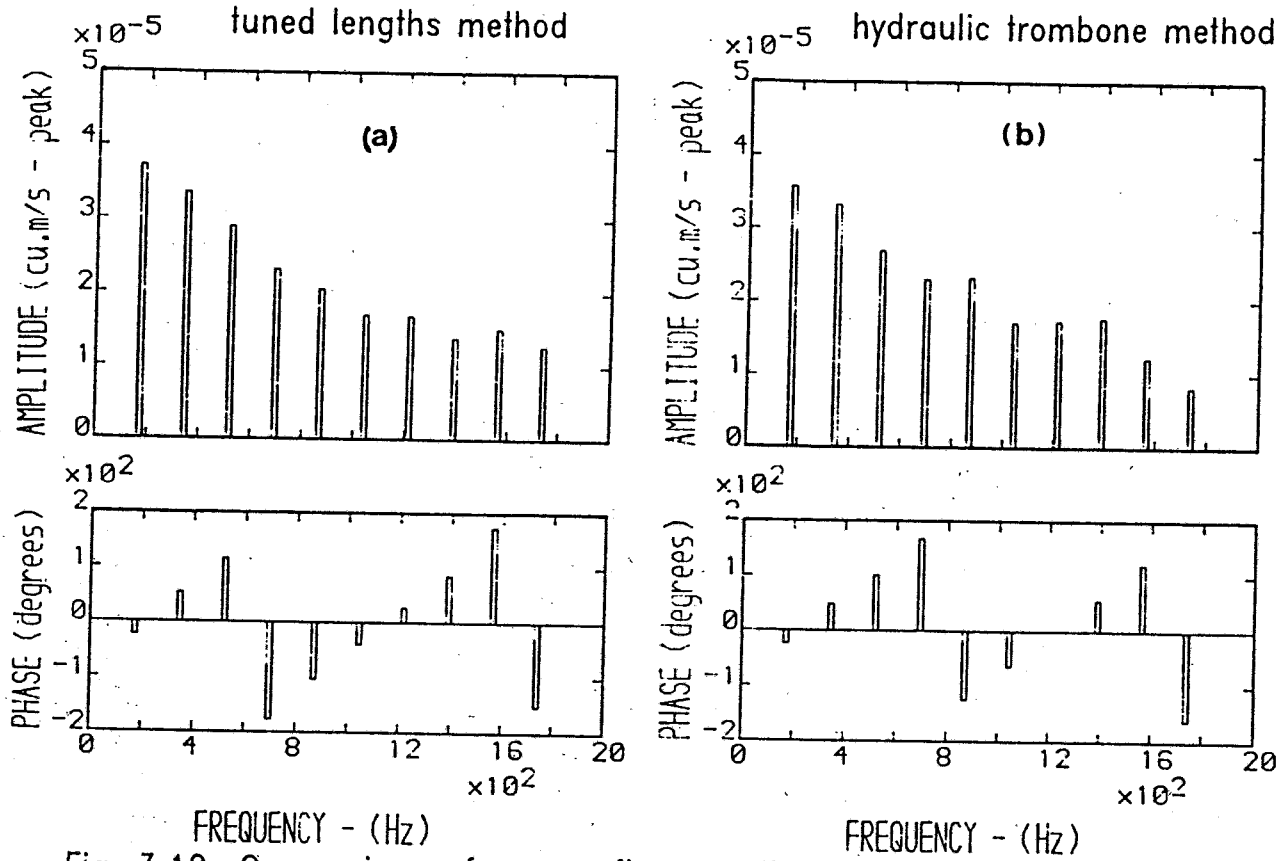

Fig. 3.10 Comparison of source flow results from 'tuned lengths' and 'hydraulic trombone' methods, in spectra form. (for pump A at 100 bar mean pressure)

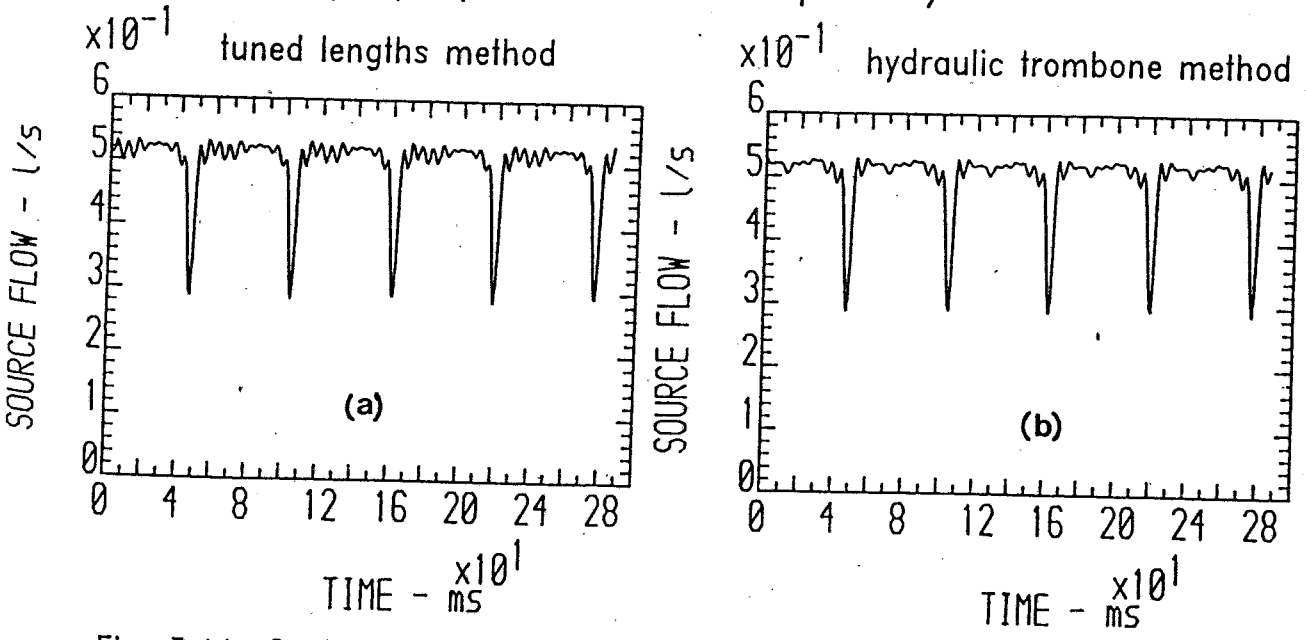

Fig. 3.11 Synthesized source flow comparison correspondent to results shown in fig.3.10

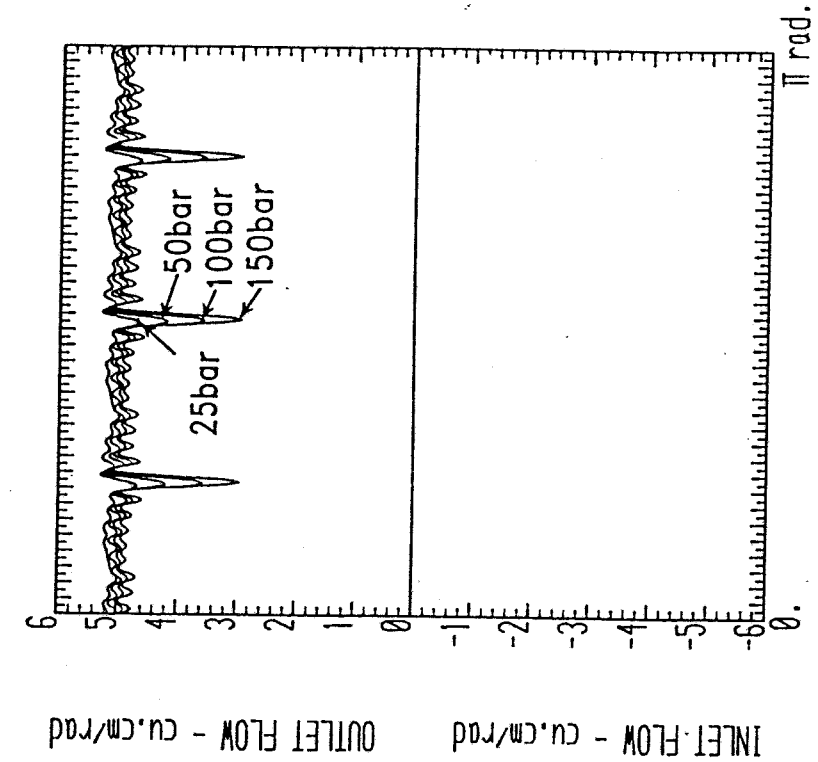

Fig. 3.13 Source flow of piston pump A at different outlet pressures (full swash)

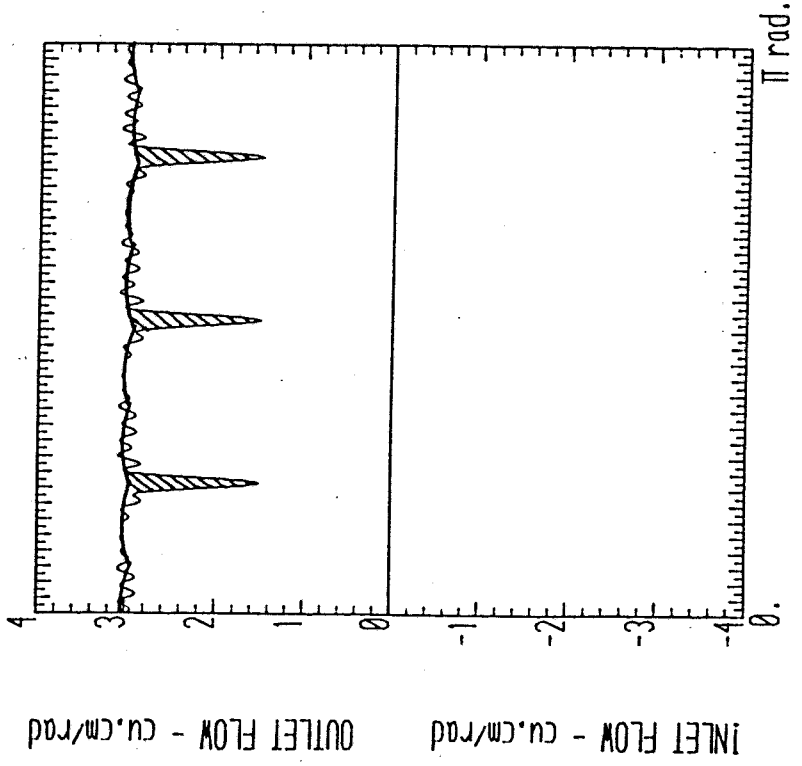

Fig. 3.12 Source flow of piston pump A showing compressed volumes (mean pressure = 100 bar)

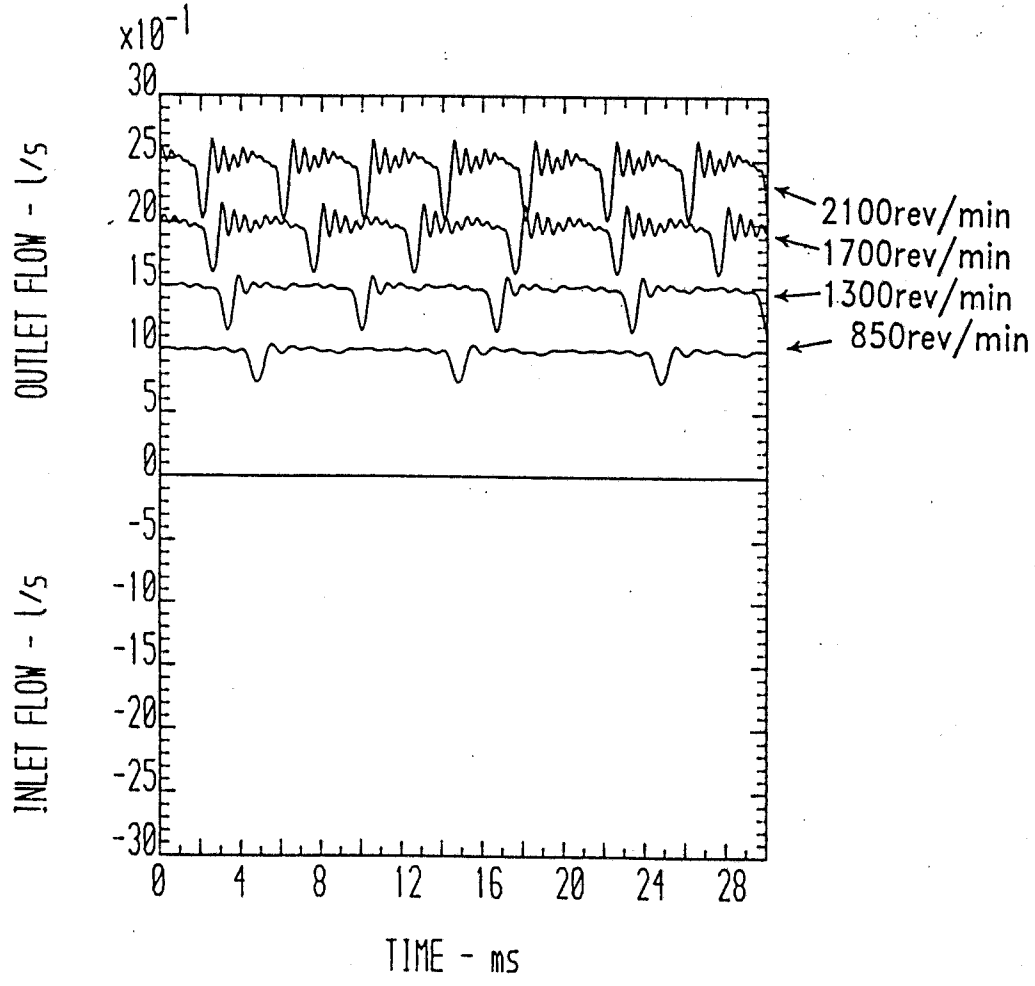

Fig. 3.14 Source flow of piston pump B at various shaft speeds (pressure=85 bar)

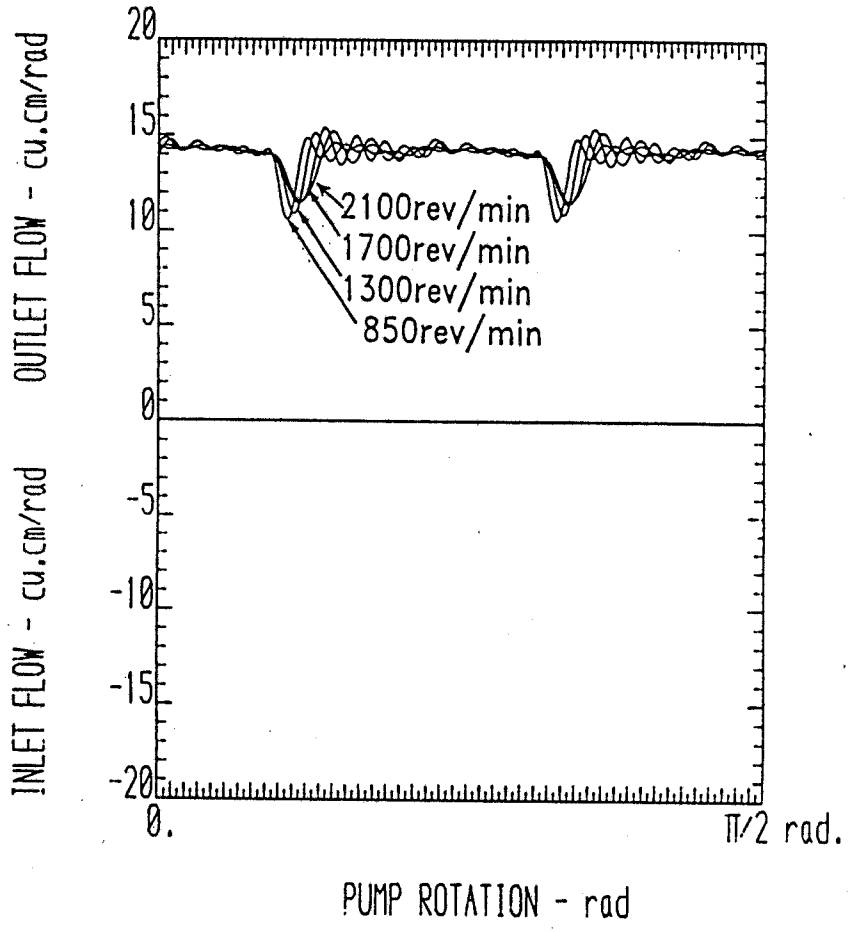

Fig. 3.15 Displacement ripple of piston pump B at different shaft speeds (pressure=85 bar)

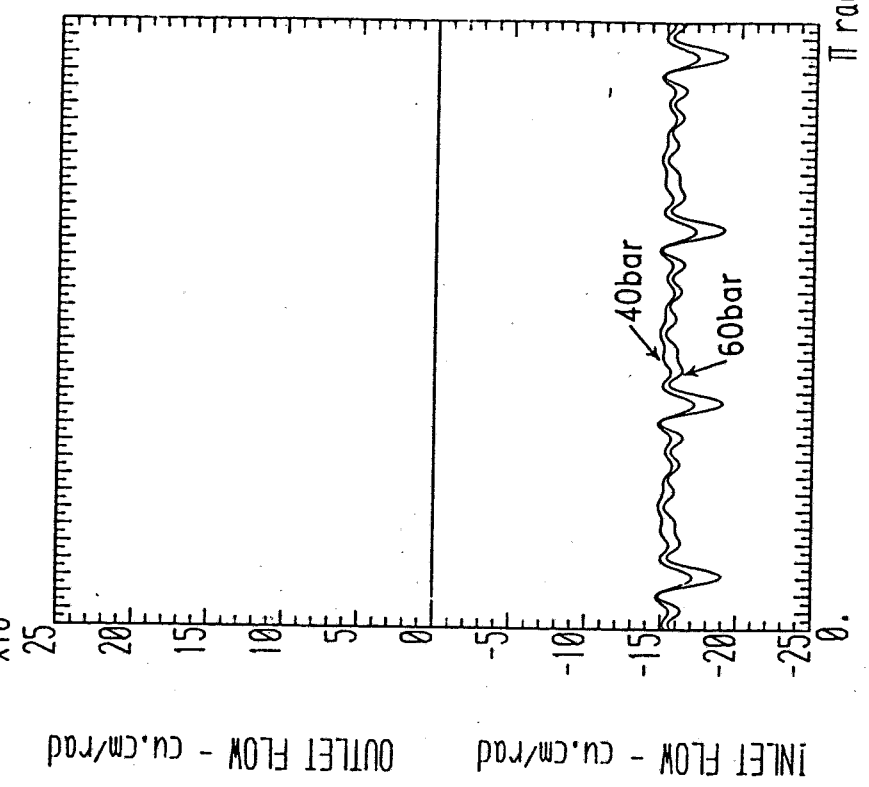

Fig. 3.17 Axial piston motor inlet displacement ripple at two mean pressures

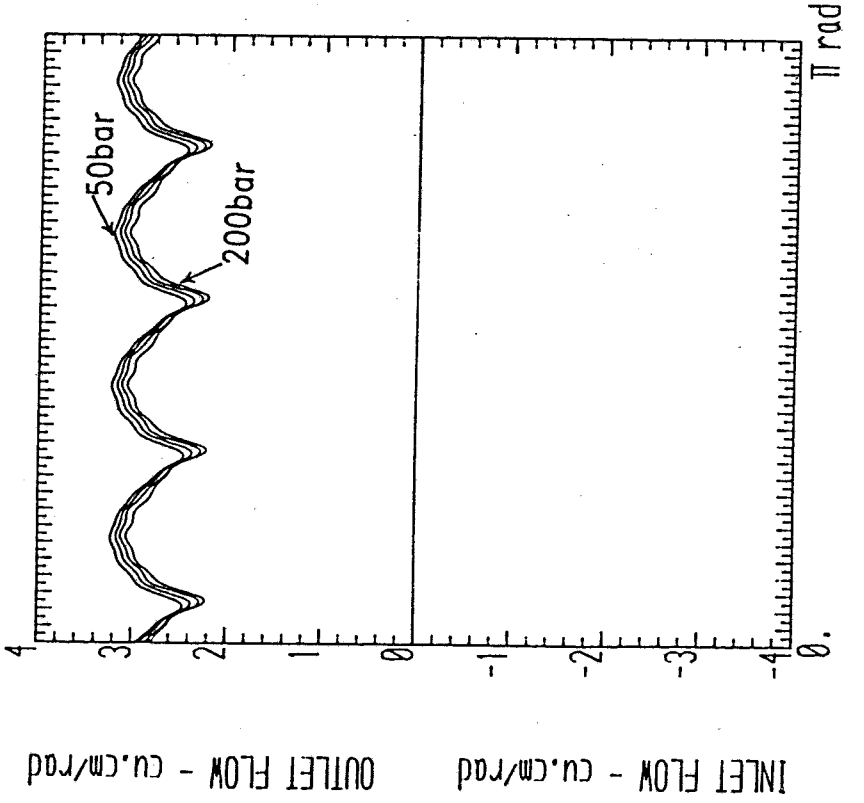

Fig. 3.16 Instantaneous displacement of gear pump C at 50, 100, 150 and 200 bar (mean displacements affected by leakage)

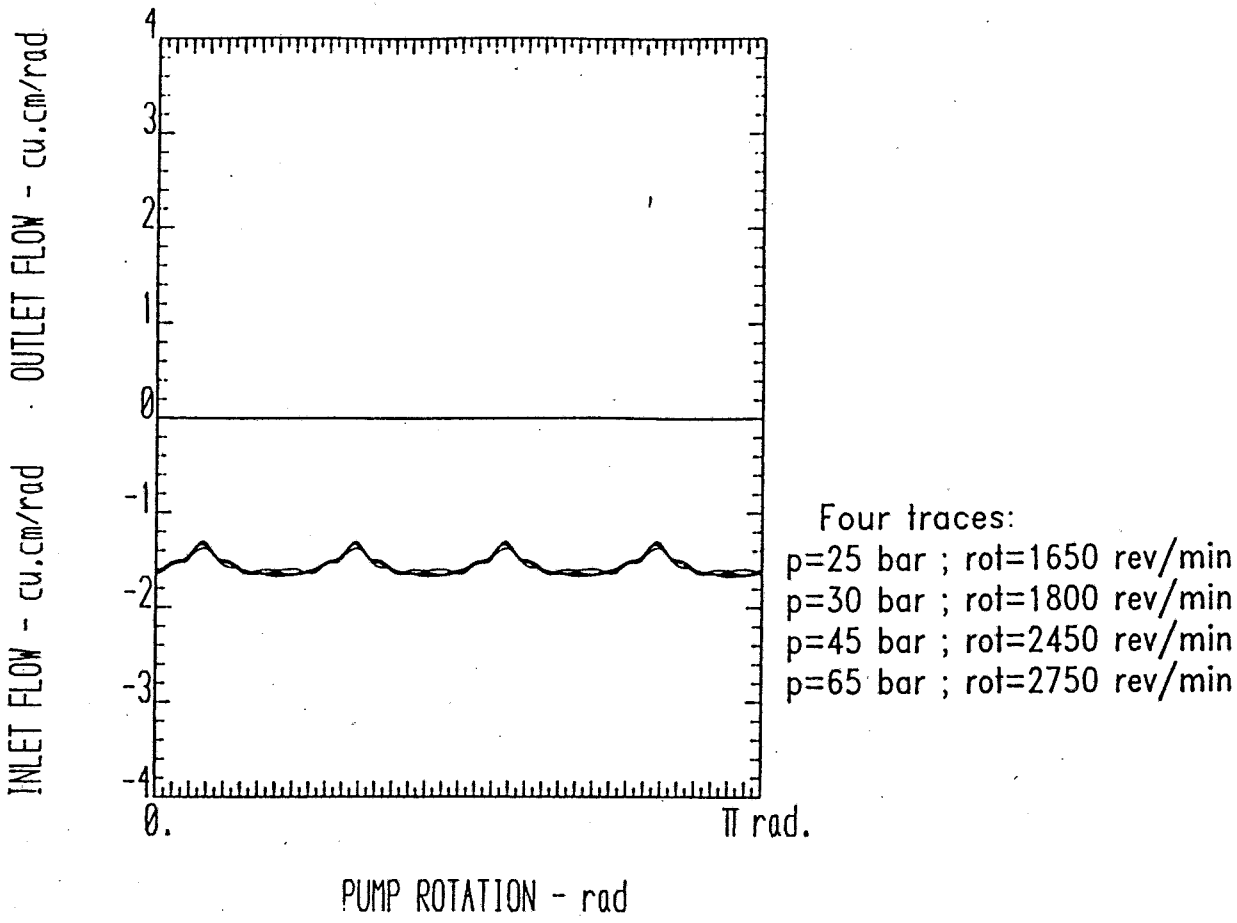

Fig. 3.18 External gear motor inlet displacement ripple at different mean pressures and speeds

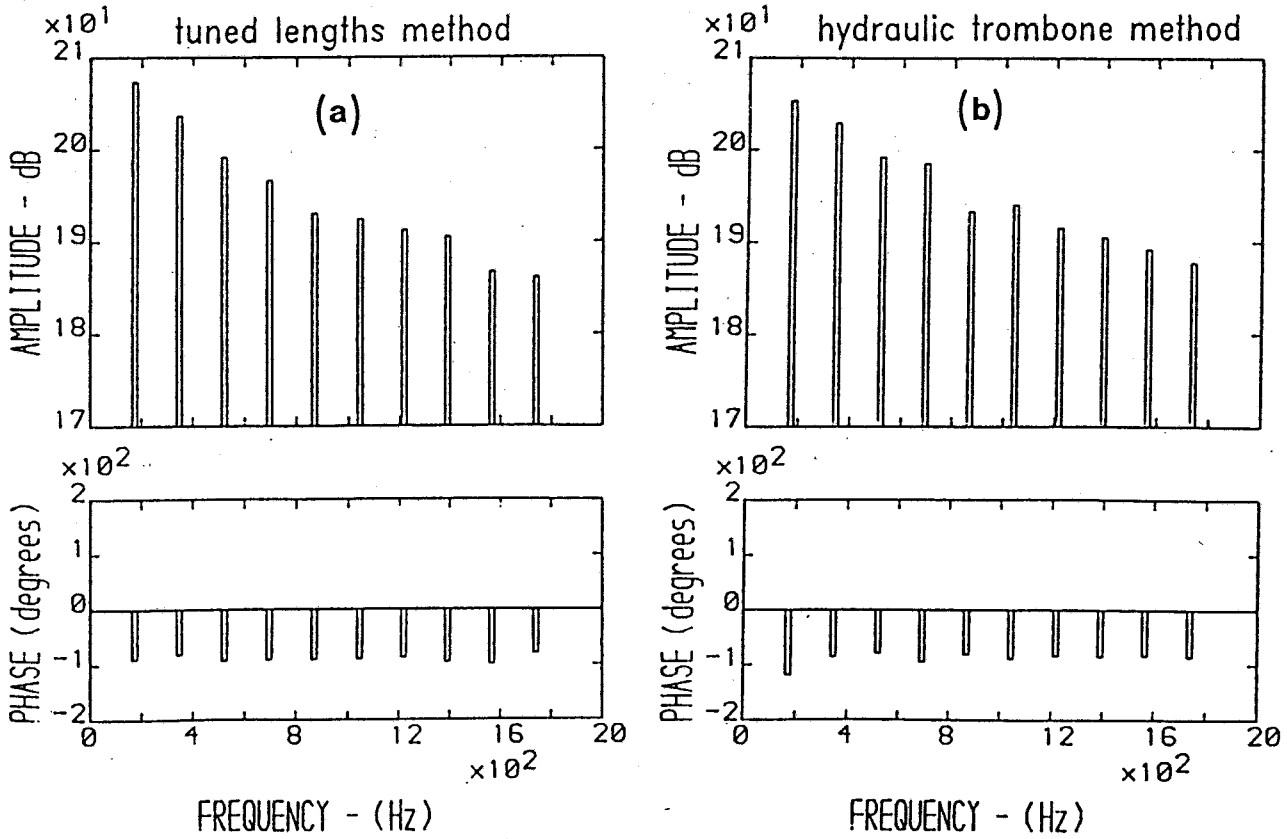

Fig. 3.19 Source impedance of pump A at 100 bar mean pressure Comparison of results from two test methods

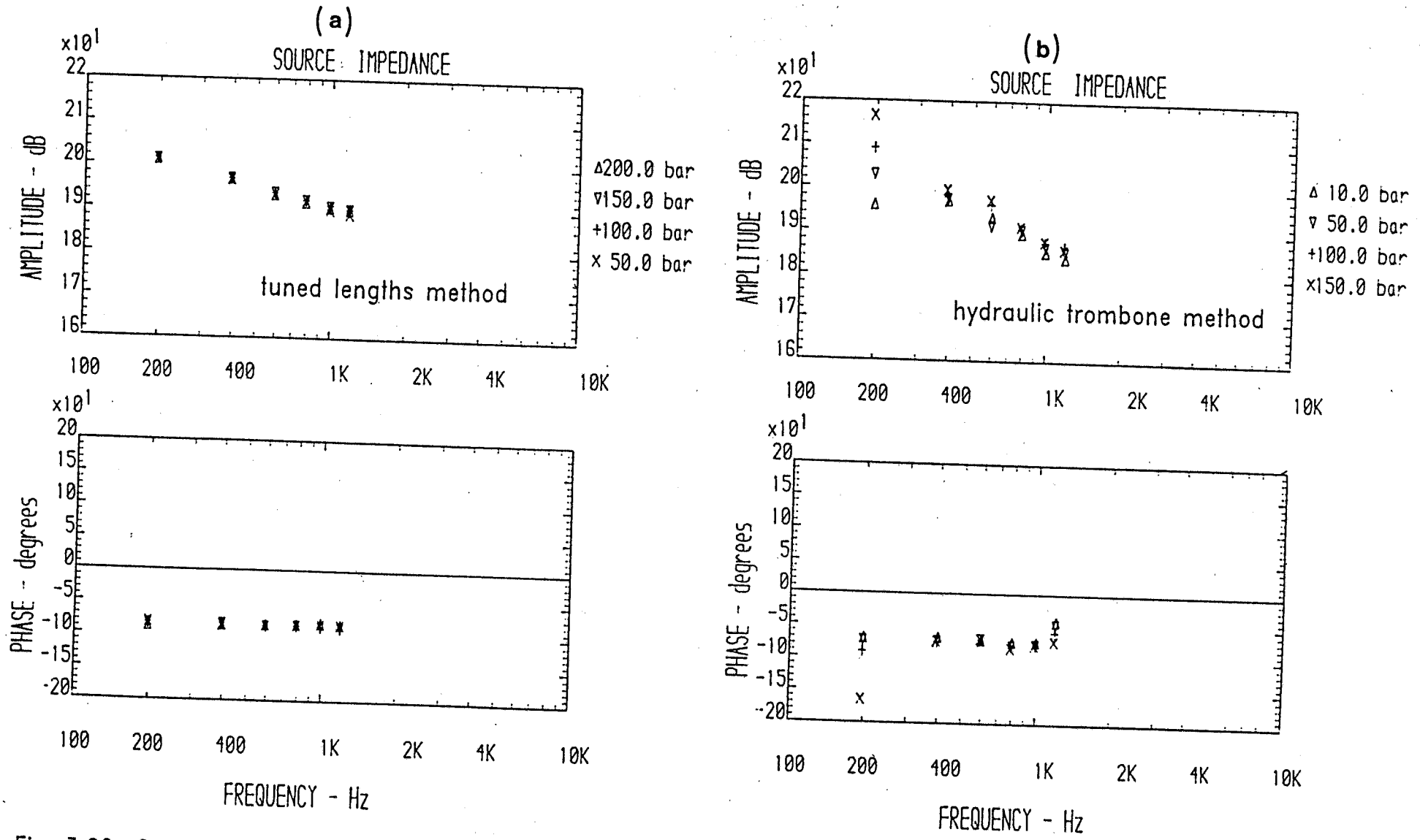

Fig. 3.20 Comparison of source impedance results of gear pump C from "tuned lengths" and "hydraulic trombone" methods for different mean outlet pressures

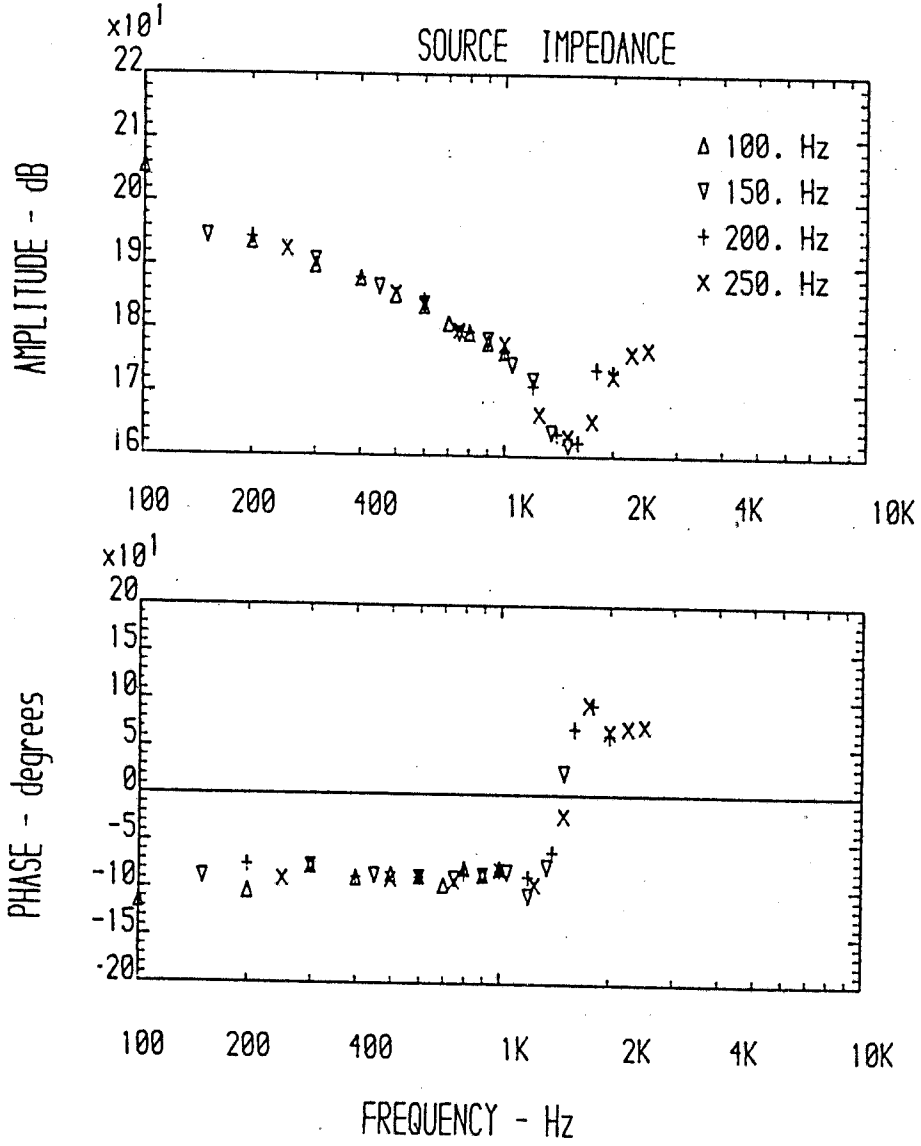

Fig. 3.21 Source impedance of axial piston pump B when tested at different fundamental frequencies (pressure=85 bar)

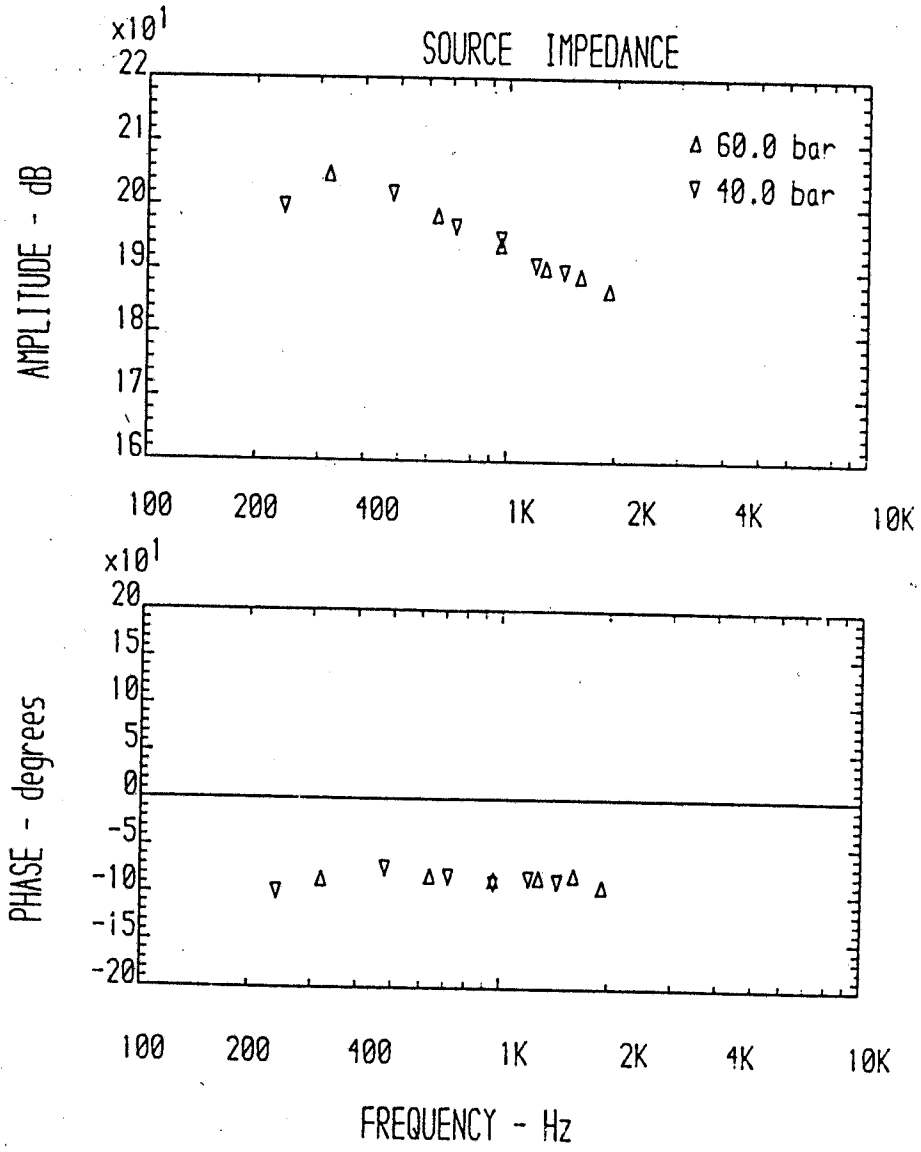

Fig. 3.22 Source impedance of axial piston motor A measured at two different system pressures

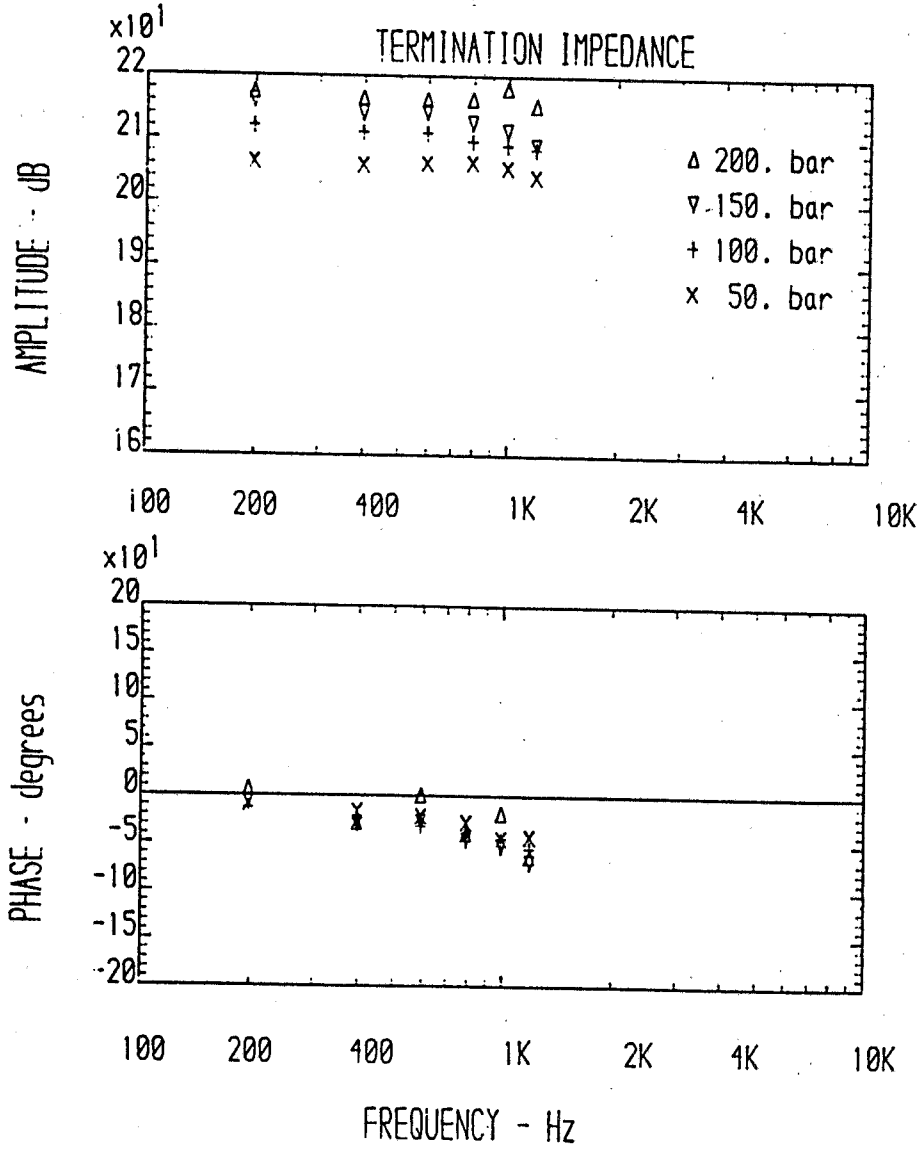

Fig. 3.23 Impedance of restrictor valve A at different mean pressures and a constant flow of 27 ℓ/min

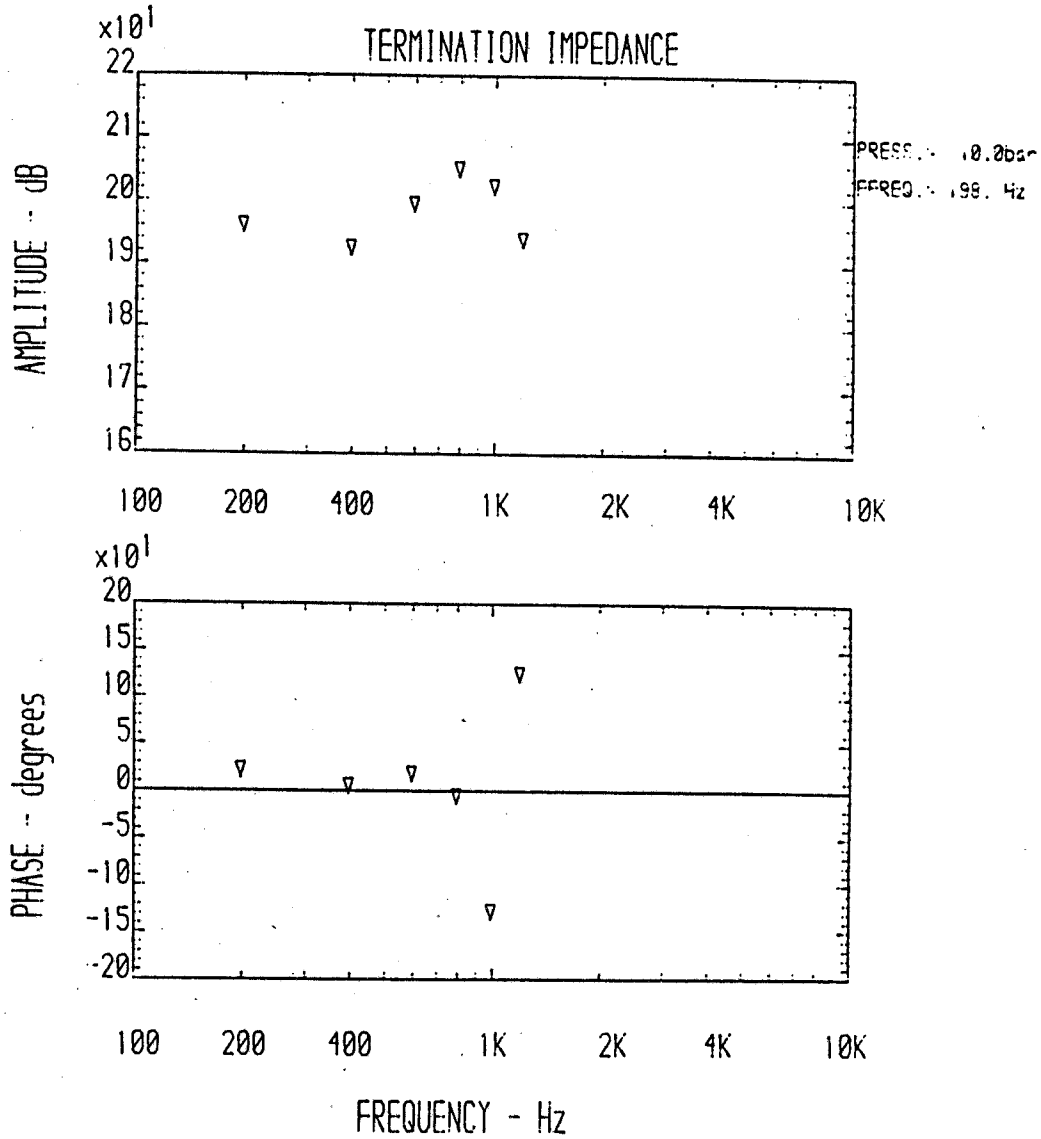

Fig. 3.24 Impedance of restrictor valve A at 10 bar mean pressure and 27 ℓ/min mean flow

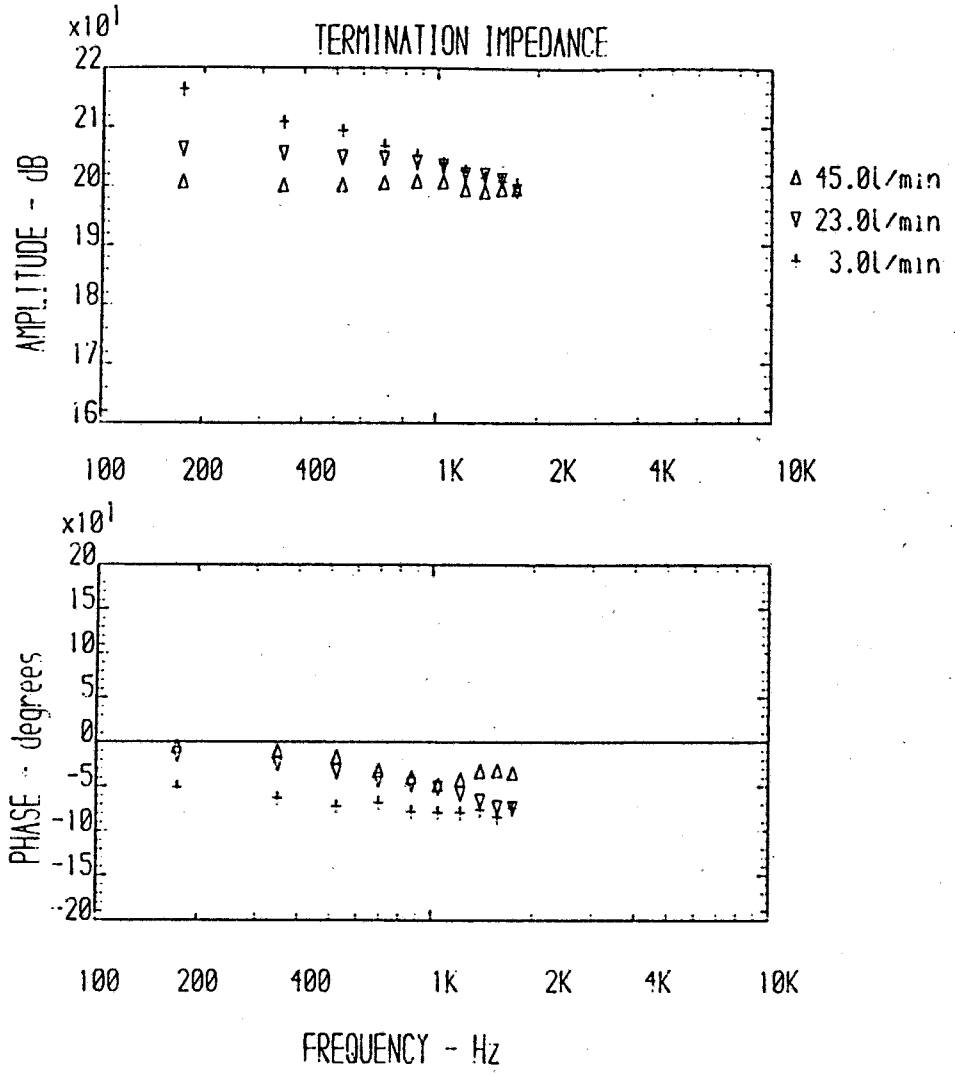

Fig. 3.25 Impedance of restrictor valve A at different mean flows and constant system pressure (50 bar)

CHAPTER IV

FLUID BORNE NOISE GENERATION IN PUMP SUCTION LINES

4.1 SUCTION PERFORMANCE OF HYDRAULIC PUMPS

The suction capability of a hydraulic pump is generally measured in terms of the minimum mean inlet pressure at which it will run without creating cavitation. This is very often presented graphically as a function of pump speed, as shown in fig.4.1a. This figure shows three regions, one for conditions at which no cavitation occurs, a second of severe cavitation and a third transitional region of incipient or 'micro-cavitation'. This information is acquired by testing a unit over a range of speeds and inlet pressures, and monitoring the mean output flow from the pump (see fig.4.1b). As the mean inlet pressure is reduced below a certain level the output flow falls, slowly at first but then more rapidly when the pressure reaches very low values, revealing the lack of fluid to fill the pumping elements of the unit.

One of the difficulties related to the detection of cavitation in a pump is the lack of an early warning of its occurrence. In fact, cavitation is mainly detected by its consequences in the loss of output performance of the pump and by the existence of typical cavitation wear (see section 5.3.4) when the pump is dismantled. There is, however, a non-intrusive technique of monitoring the existence of cavitation, which is by measuring the air borne noise emitted by the pump. Cavitation effects are associated with air borne noise at high frequencies (above 10 kHz [28]). Maroney, studying the effects of aeration and cavitation in before pump inlet lines, concluded that ultra sound measurements can detect cavitation

in its early stages, that is before damage is likely to occur or before pump and system performance is lowered. Furthermore, Maroney found that the pump-generated air borne noise decreases with decreasing mean inlet pressure, but below a certain pressure the air borne noise increases again as a result of cavitation effects. This is a very important conclusion as it means that when 'micro-cavitation' occurs in the inlet line, the pump generated noise is minimum, due to the attenuation provided by microscopic air bubbles (less than 0.1% in volume [29]), even though no noticeable pump performance degradation occurs [28]. This leads to Maroney's remark that "hydraulic system air/liquid volume ratios, like human blood sugar levels, should neither be too great or too small".

The fluid that enters a pump must be drawn from the reservoir by creating a pressure difference between the reservoir and the pump inlet. The flow taken in by a hydraulic pump is similar to that delivered by it in as much as both are composed of a fluctuating component superimposed on a mean flow. Due to the existence of this fluctuating flow transmission line effects occur in much the same way as in high pressure lines. Therefore, instantaneous variations of the fluid flow are translated into pressure variations which, in low mean pressure lines may assume very low instantaneous pressures indeed. Consequently, cavitation may occur on the inlet line to a pump, either as a result of the high fluid velocity (low mean pressure) or due to very low instantaneous values of pressure ripple. In addition, cavitation may occur in the suction port of the pump itself due to restricted passageways. If the inlet line is well dimensioned, however, the fluid velocity in the line is low and the possibility of cavitation effects is a function of the pump's own internal design and its fluid borne noise characteristics. Hence, in general, the steadier the flow drawn in by a pump, the better its

suction capabilities.

Axial piston and external gear pumps are the two most common types of hydraulic pump and a discussion of their suction characteristics is given below.

4.1.1 Axial piston pumps. Axial piston pumps are, perhaps, the most important type of pump used in hydraulic systems, due to their high efficiency, versatility, and ability to work at very high pressures. However, most have a poor suction performance and require boosting even at average running conditions.

Internal Design

The control of the fluid in the inlet of axial piston pumps is made through the use of a valve plate. In order to maintain a force balance at the sliding surface between the cylinder block and the valve plate (portplate), the area of each cylinder port is made much smaller than the piston area (up to four times), as shown in fig.4.2. This restriction creates inevitable pressure losses and very low pressures occur near the portplate, and inside the piston chamber. Furthermore, if cylinder port areas were large the axial forces acting on the cylinder barrel would be proportionally increased. Large bearings would be required in the pump to sustain such loads. This would mean an increase in the overall size of the pump. Indeed, the current need for small size units with high flows compels the use of small ports at the expense of a boosted suction line for all except very low speed operation. On piston motors, these restrictions are no longer an inconvenience, and smaller size units can be designed for the same capacity.

If the suction mechanism of a piston pump is examined in more detail, it is possible to define four effects which determine the

pressure losses when the fluid flows from the portplate to the piston chamber. One is dependent upon the axial velocity of the fluid, as referred above, the second is due to the tangential velocity of the fluid in the portplate, the third due to the centrifugal forces in the piston chamber and the fourth due to the fluid inertia.

For the loss of pressure due to the axial velocity of the fluid, the cylinder port may be considered as an orifice:

$$\Delta p_1 = c_1 \rho (v_1)^2 /2 \qquad (4.1)$$

This pressure drop not only varies with the movement of the piston but also with the shape and dimensions of the port. These dimensions are variable during the induction stroke. For most of the stroke the dimensions correspond to the whole port area. At the start and the end of the stroke, however, the area depends on the interference between the portplate area and the cylinder port and, in the case of the start of the stroke, depends in addition on the existence of relieving grooves. In order to determine the worst case for pressure drop, three conditions must be considered: at the start and end of the stroke, where the area is small (although the flow is small) and at mid-stroke when both the area and the flow are maximum. At the beginning of the induction stroke the dead volume, which is at pump discharge pressure, must be decompressed. This creates a reverse flow which will increase the pressure locally. Hence, cavitation is unlikely to occur. However, if relief grooves are not used to smooth the rate of change of area, the decompression will not be controlled and harsh fluctuations of pressure, will occur [30] creating, after the initial rise of local pressure, very low values due to the rapid reversal in the fluid velocity. This may give rise to local and instantaneous cavitation. Severe cavitation occurs when the pressure

loss around mid-stroke is very large and as a consequence oil vapour pressure is reached. At mid-stroke, when the mean fluid velocity is maximum, the pressure drop Δp_1 does not change its value sharply with time. Consequently, if Δp_1 gives rise to pressures as low as the oil vapour pressure, these will exist over a large angle of pump rotation and cavitation may not only occur near the portplate but inside the cylinders, as well. At the end of the stroke the conditions are geometrically similar to the beginning of the stroke. The fluid is, however, decreasing its velocity which gives origin to an increase in pressure and hence no likely danger of cavitation. Both at the beginning and end of the suction stroke one of the factors that must be considered is the rate of variation of area opening with pump angle of rotation against the rate of change of flow. One author has suggested that for both these conditions the instantaneous pressure must reach values very close to zero absolute [14]. This is simply because the existence of backflows, relieving grooves and inertia of the fluid in the piston chamber are not considered.

The loss of pressure due to the tangential velocity of the fluid is determined by the pitch diameter of the cylinder ports. When the fluid reaches the portplate it must enter a side branch (cylinder port) which is travelling at a speed (v_2), which is:

$$v_2 = r \cdot \omega \qquad (4.2)$$

The pressure drop is, hence, given by [14]:

$$\Delta p_2 = c_2 \cdot \rho \cdot v_1 \cdot v_2 / 2 \qquad (4.3)$$

The need to reduce this loss component led designers to reduce the cylinder port pitch diameter, without changing the distance between the pistons and the pump centre line, by drilling the port paths at

an angle, as shown in fig.4.3. This solution is also favourable from the centrifugal force point of view by helping drive the fluid into the cylinders. When the oil enters the cylinder it is forced towards the wall furthest from the centre line due to centrifugal effect. Hence, the wall closest to the pump centre line is last to fill. If the cylinder port is located at the cylinder centre line the fluid has to move against the centrifugal forces to fill the innermost wall. Consequently, positioning the cylinder port closer to the pump centre line helps filling the piston chamber and consequently avoids very low pressures.. The pressure drop due to the centrifugal force is then given by:

$$\Delta p_3 = [\ 1 - (r_1/r)^2\ ] \cdot \rho \cdot (v_2)^2 /2 \qquad (4.4)$$

where : r_1 - minimum distance between cylinder wall and pump centre line

Finally, the pressure lost to accelerate the fluid uniformly through the cylinder port, of length ℓ and area A_o, is given by:

$$\Delta p_4 = c_4 \frac{\rho\ \ell}{A_o} \frac{dQ}{dt} \qquad (4.5)$$

The equations given above were used by Hibi et al [14],[31] to evaluate the pressure losses in an axial piston. The pressure in the cylinder chamber during the stroke is given in fig.4.4. Although this was a very good theoretical exercise, the result has very little practical application as it does not take into consideration the existence of relief grooves, backflows (indeed the experimental tests were performed at an unrealistic delivery pressure of 11.5 bar [31]) and the effects of portplate timing mismatch [30]. Furthermore, if pressure were to fall to the levels shown in fig.4.4 air release and/or cavitation would occur which would invalidate the theory.

Flow Ripple

The theoretical fluctuating component of the flow taken in by an axial piston pump is determined by the geometry of the unit. Consequently, there is a direct relationship between the theoretical inlet displacement and the outlet displacement of the pump. However compressibility effects must also be considered. When a piston reaches T.D.C. the small dead volume delimited by the fully extended piston and the portplate is at mean discharge pressure. At the instant the inlet line is connected to the piston chamber an outflow will occur until pressures equalize. The fluid in the vicinity of the cylinder port first moves outwards after which it is forced back into the piston chamber. The pump instantaneous flow may, then, be represented as in fig.4.5. The timing effects shown in the figure were studied by Martin and Taylor [30] for different relief groove shapes and decompression zone angles. These effects depend, however, on the running conditions such as mean inlet and outlet pressures and on pump swash angle and speed of rotation. Unless the pump has constant running conditions timing mismatch effects will always occur.

4.1.2 External gear pumps. External gear pumps invariably have good suction performance. The inlet mechanism of these pumps is rather different from piston units due to the absence of a portplate. The suction cycle starts as two gear teeth come out of mesh and ends when the tips of the following teeth come into contact with the outer body wall (fig.4.6). The volumetric displacement on the inlet of the pump must be similar in shape to that on the outlet (see section 3.6.1), as the mechanism is identical, although the gears move in the reverse sense. Once again, the inlet flow is a mirror image of the outlet of the pump, as shown in fig.4.7.

The agreement between actual displacement and theoretical prediction depends upon whether the spaces in between teeth are completely filled with fluid or not. Due to centrifugal forces, the roots of the teeth are the zones of lowest pressure. In general, gear pumps have radially orientated suction inlets and therefore the direction of the fluid flow is opposite to the centrifugal force. In some cases, however, gear pumps have axially orientated inlet lines which are terminated near the roots of the teeth and hence have better chance of filling the spaces completely. The equation defining the pressure loss due to the centrifugal forces is [14]:

$$\Delta p = [1 - (r_d/r_a)^2] \rho . (v_a)^2 /2 \qquad (4.6)$$

where: r_a - radius of addendum

r_d - radius of dedendum

v_a - tang. veloc. measured at addendum diameter

ρ - fluid specific weight

This pressure loss increases with the size of the gear pitch diameter and the module.

When a pair of teeth come out of mesh and are ready for the induction of fluid, the space between the teeth and the following pair is in contact with the inlet line over a limited angle. This angle could be as little as 45 deg and for a pump speed of 3000 rev/min the corresponding time this space is open is less than 3ms, which may be insufficient for the complete filling. One of the important factors in the determination of this angle is the shape of the inlet chamber. Zalka et al [32] demonstrated that the inlet chamber of a gear pump could be changed (see fig.4.8) in order to extend the angle of entry which would improve the pump suction performance considerably. This modification of gear pump inlet

chamber was also proposed by Khaimovitch [33] as an example of a 'quiet' gear pump. However, such an approach seems to have been ignored by pump manufacturers because of production difficulties with pump bodies which are usually aluminium extrusions.

From this brief explanation it is easy to understand that the suction of a gear pump should have better performance than a piston pump both due to the internal design, which does not contain restricted passageways, and due to the smoother flow fluctuation generated.

4.2 METHODS OF DETERMINING PUMP INLET CHARACTERISTICS

Most of the experimental methods presented in chapter III for the determination of the outlet characteristics of pumps and the impedance of valves are not directly applicable to inlet lines. Some methods require the existence of high pressure in the line and others, if applied, would generate cavitation in the suction line of pumps.

It is therefore impossible to use a very high impedance pipe or a restrictor valve on the inlet side of a pump. The same applies to the reflectionless termination valve referred in section 3.3.2 which would cause turbulence and air release in the inlet line.

Only one single-transducer method is feasible for using on pump suction lines: this is the reflectionless termination method based on the use of a long hose. However, unless the tank static pressure is relatively large the losses in the line may be so great that cavitation will occur.

The most realistic approach to the experimental evaluation of pump inlet characteristics is through the use of two- and multi-transducer

methods. These are based on the existence of a standing wave in the line. If cavities exist in the fluid then a standing wave may not exist and the theory behind the methods is inapplicable. Such an could occurrence must be explored in detail. There are two possibilities: cavities could occur inside the pump, which is considered for all purposes a lumped element, or cavities could be formed in the line in the form of air bubbles. If cavities are formed inside the pump only, they will be swept to the discharge side of the pump and not propagated to the inlet line. In consequence the pump characteristics must be affected by this occurrence but whatever is produced inside the pump is propagated to the inlet line in the normal way. If cavitation is significant, however, the flow ripple generated by the pump may no longer be periodic, but be affected by the rate of formation of cavities. If air bubbles are formed in the line, however, there will be a two phase flow and the transmission line theory no longer applies.

The existence of air or cavities can be very effectively detected by monitoring the speed of propagation of sound in the fluid (i.e. by measuring the wavelength at a given frequency). If the pipe is filled with fluid, then the speed of sound should be around 1400 m/s, but if any amount of air is mixed with the fluid a sharp drop of speed of sound is experienced (around 93% drop in speed of sound for 1% volume air entrained in the fluid [29]). The most effective way of monitoring the speed of sound of the fluid in a hydraulic line by non-intrusive means is to measure the fluctuations of pressure at several points along the line, for different line lengths until a full wavelength at a particular frequency is described. This corresponds to the multi-transducer method (section 3.5). The tuned length method may also be used but it is less effective in determining the speed of sound as it relies on the information from

only two transducers. As the speed of sound may vary considerably, the information from only two transducers could lead to erroneous conclusions.

When using either of these methods for the evaluation of pump characteristics the amplitude of the termination reflection coefficient must be large (section 3.4.2). For a suction line the tank is the termination. If the tank behaves in the same manner as a volume, then Z_t will have a phase angle of -90 deg which results in a reflection coefficient, ($|\rho_t|$) of unity. This is ideal for the implementation of the test method.

Practical Difficulties

Previous authors researching into pump suction lines have controlled mean suction pressure through the use of a restrictor valve between overhead tank and pump [12] or by means of a restricted bleed line on a boosted suction line [31]. Both solutions are unsatisfactory as they can create conditions which produce the formation of air bubbles or cavities under low mean pressures. An apparently simple solution would be to use a tank that could have a variable head. However, this could result in long lines and a dependence between the length of line and the mean head pressure. The existence of inevitable bends in the pipe is, in addition, a disadvantage.

The solution adopted in the present work was to use a pressurized tank. Such a tank could provide the desired range of pump inlet pressures and flows without introducing any disturbing element in the suction line. Indeed, as discussed in a later section, it was also possible to perform tests at subatmospheric pressures.

Using the tank connected to the inlet of a pump through a straight and horizontal pipe line, it is possible to apply either the tuned length or the multi-transducer methods described in chapter III.

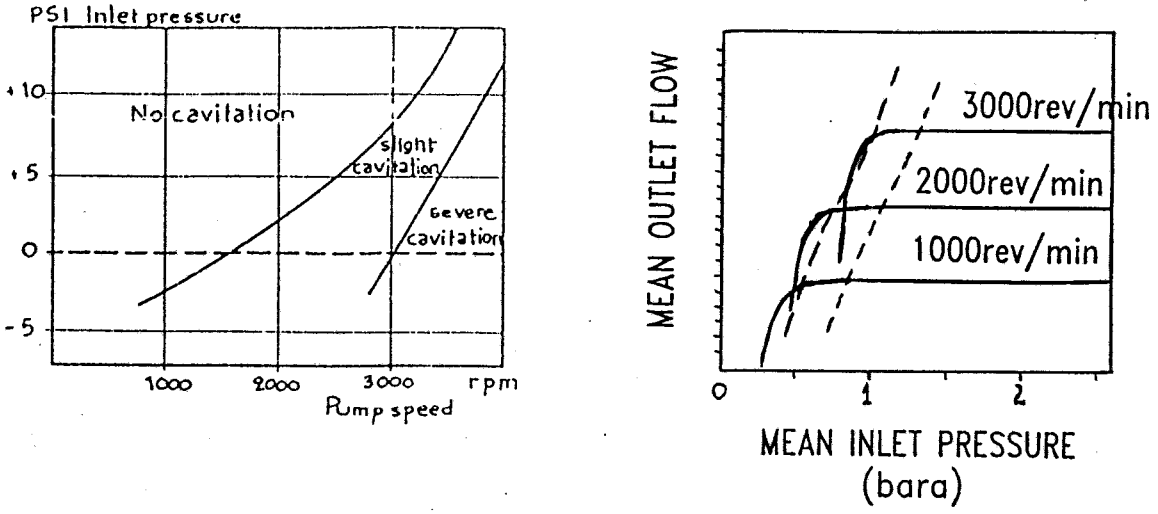

Fig. 4.1 Suction performance of a pump obtained from steady state analysis

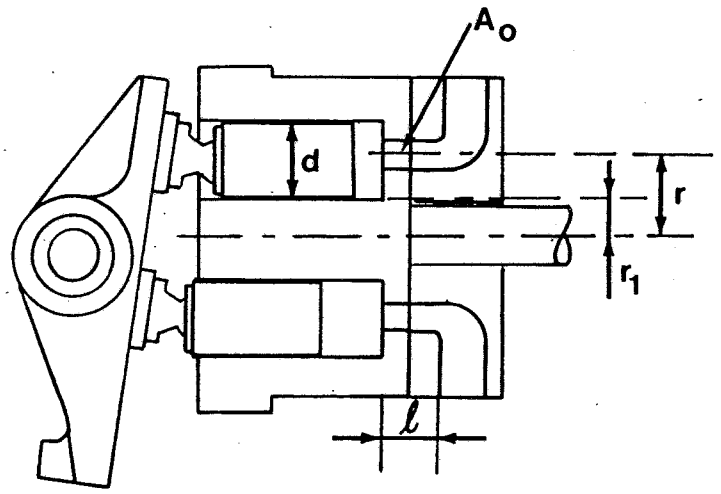

Fig. 4.2 Simple sketch of typical piston pump and fundamental dimensions

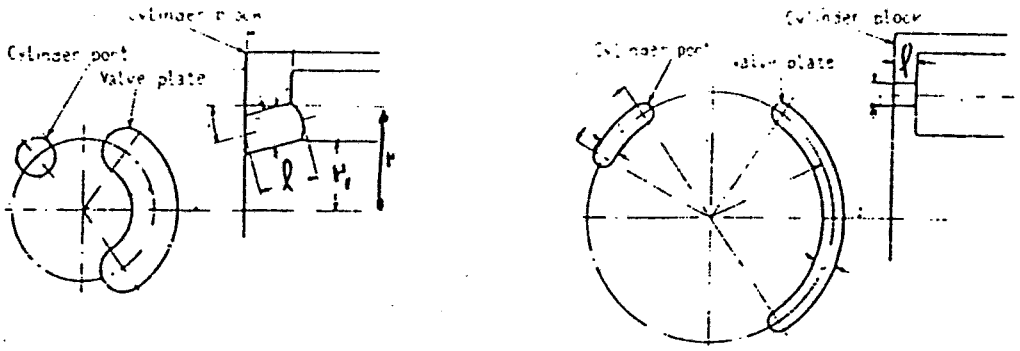

Fig. 4.3 Detail of piston pump porting arrangements (from ref.[14])

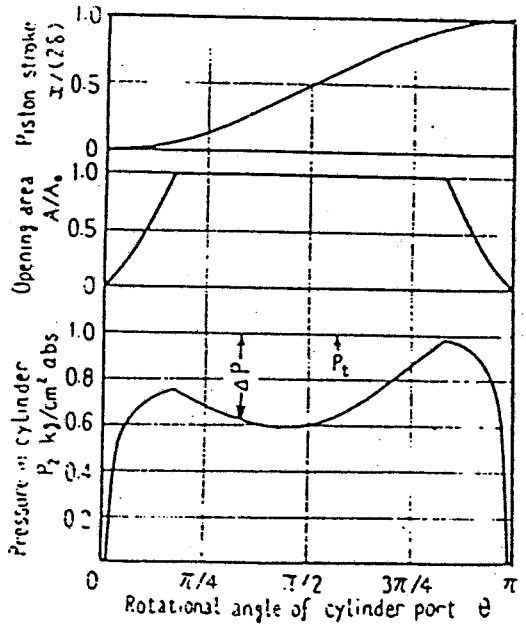

Fig. 4.4 Theoretical pressure inside piston chamber (from ref.[14])

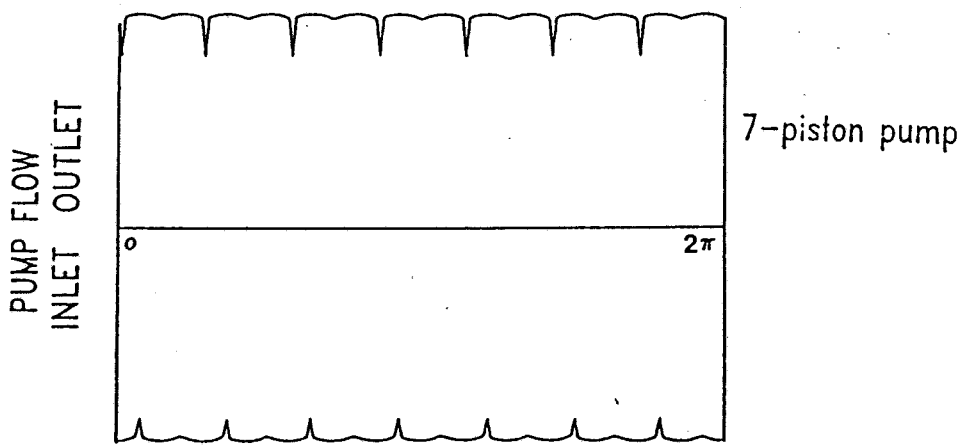

Fig. 4.5 Theoretical inlet and outlet displacement ripple of an axial piston pump showing port plate timing mismatch

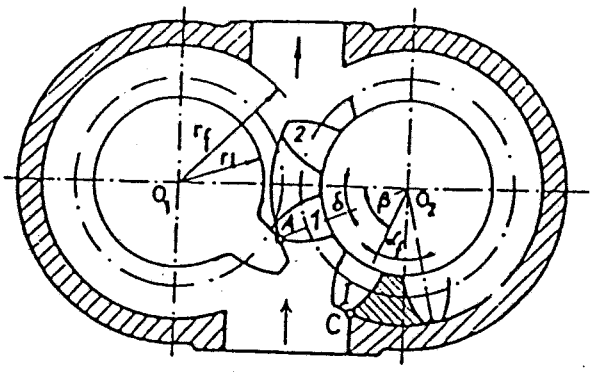

Fig. 4.6 Detail of external gear pump suction stage (from ref.[32])

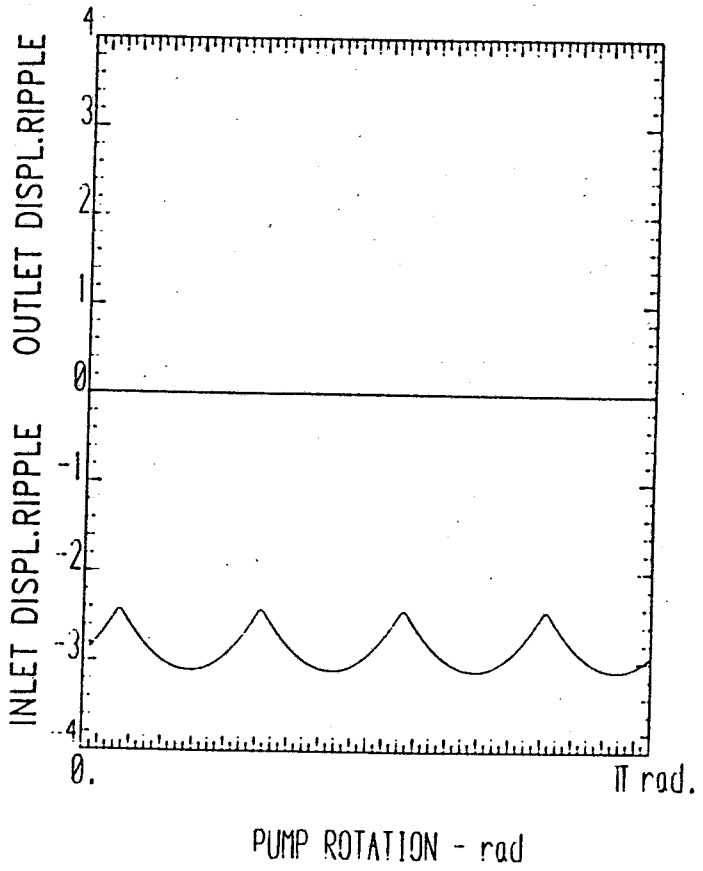

Fig. 4.7 Theoretical instantaneous flow admitted by an external gear pump

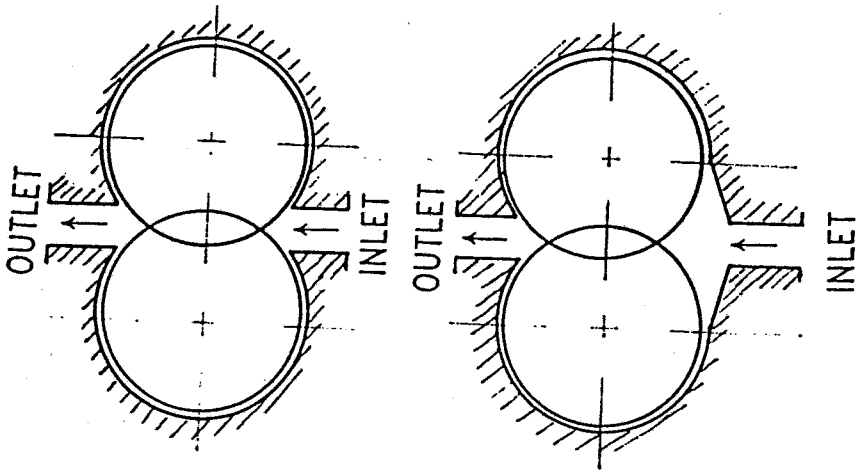

Fig. 4.8 Modification of inlet chamber of a gear pump

CHAPTER V

HYDRAULIC TANK AND SUCTION LINE DESIGN

5.1 INTRODUCTION

The hydraulic reservoir, an inherent component of all hydraulic systems, is generally not very highly regarded as it is very seldom mentioned in any detail in circuit diagrams. However, poor system performance and short component life can frequently be traced to improperly designed reservoirs [34].

The diversification of applications of hydraulics as well as the much higher demanded performance of the systems has seen improvements in all components in an orderly and objective way, but still the design of hydraulic tanks and suction lines is, apart from basic rules dictated by common sense and experience, as varied as it has ever been.

This chapter presents some aspects of the design of early reservoirs and the improvements that have been made and concludes with a description of some of the latest concepts in hydraulic tank design. This study was used as the basis for the design of the pressurized reservoir used during the experimental tests.

5.2 THE TRADITIONAL ROLE OF THE HYDRAULIC RESERVOIR

Until the early 1950's the hydraulic reservoir was considered the component where the fluid was 'stored', and was specifically designed to cool the oil and allow sufficient time for sedimentation of particulate matter to take place, before the oil was drawn into the pump suction line.

The flows and pressures involved in circuits were usually low which seldom caused problems in terms of the sizing and the shape of the reservoir. The shape would invariably be a box-like with large rectangular walls usually supported on a stand to increase its heat transfer capabilities; this would determine its capacity. More often than not, if the reservoir was to be part of a machine, its size and shape would be determined by the available space.

Some accessory components were common in reservoirs. For example a sight glass to read the oil level, a breather tube, draining plug and filler cap.

The position of the reservoir relative to the other components was varied depending upon the situation, but it was common practice to place the pump at a level above the oil in order to prevent leakages through the pump packings [35], when the system was stopped. Another advantage that could be drawn from this procedure was that the pump could be disconnected without having to drain the tank. For the same reason, return lines were very often vertically orientated.

Placing the electric motor and hydraulic pump on top of the reservoir, together with valves, was a common feature which would make the system neat and compact. Fig.5.1 shows a sketch of a simple reservoir of this type, which may as well be considered representative of today's available proprietary reservoirs.

5.3 THE FUNCTIONS OF AN HYDRAULIC RESERVOIR

From these early stages, hydraulic systems have found applications in many varied fields of engineering as main and vital components of ships, aircraft, heavy industrial machines (for example presses, guillotines, calenders, injection moulding machines), and mobile

equipment (earth moving vehicles, cranes, harvesters, etc.). In each of these fields hydraulics evolved in specific directions and the reservoir was one of the components which suffered most modifications depending on the type of application for which it was to be used.

In recent years there has been a trend towards increased use of hydraulics in mobile applications, and pumps have been developed to increase their power-to-weight ratio. This has lead to higher shaft speeds and pressures, closer tolerances and better materials to ensure reliability and long life.

However, as a pump manufacturer claimed in 1970 [34], "a high percentage of pump failures which occur during the first 500 hours can be directly traced to the reservoir". This statement had its origins in many pump failures and there has been great demand from pump manufacturers [34] and users [36] to reconsider the importance of the role of the hydraulic reservoir.

The two main functions of an hydraulic reservoir are: a) to work as an expansion chamber, in order to cope with the variations in volume of the oil and system; and b) to supply oil to the pump in a suitable condition to ensure a trouble-free functioning of the system. These conditions depend upon the pump suction characteristics. Hydraulic pumps are designed to work at very high efficiency levels, within a controlled range of mean inlet pressures, fluid viscosities and temperatures. It is a function of the reservoir to ensure that these conditions are met. Furthermore, the fluid must be free of air bubbles and must not contain solid particles greater than the clearances in the pump.

Each of these functions will be discussed in the following paragraphs.

5.3.1 The Reservoir as an Expansion Chamber. One of the main functions of the reservoir is to hold a variable quantity of fluid. This function is of vital importance in a system due to the variation of volume of the fluid with temperature and pressure, and due to the changes in the volume held by actuators and accumulators.

The thermal volumetric expansion of fluids can be given by:

$$\frac{\Delta V}{V} = c \cdot \Delta T \qquad (5.1)$$

where: ΔV - variation of fluid volume due to ΔT $[m^3]$

V - volume of fluid $[m^3]$

c - coefficient of thermal expansion $[K^{-1}]$

ΔT - variation of temperature $[K]$

The expansion of the system walls (pipe and hoses) due to variations in temperature is given by a similar equation, but the coefficients are different ($2.4*10^{-4}$ for oil and $1.6*10^{-5}$ for steel). This makes the wall expansion negligible compared with oil thermal expansion.

The inclusion of single rod actuators in a system, whether single or double-acting, involves changes in the overall capacity of the system and hence a change in the level of fluid in the tank.

The minimum level of a reservoir is obtained by considering the system at its lowest temperature, with the actuators fully extended and the accumulators completely filled with oil. The maximum level of the reservoir is obtained when the temperature is highest and the actuators and accumulators are holding minimum quantities of fluid.

5.3.2. The Reservoir as a Temperature Controller. The reservoir has traditionally been assigned the function of controlling the

temperature of the fluid. Indeed this practice is still favoured in the most recent recommendations on the manufacturing of hydraulic reservoirs [37] [38]. This practice results in the design of oversized reservoirs, in order to produce as large a surface area as possible. In turn, this results in a large volume of oil and a long time to reach the heat balance temperature. This means that the traditional approach does not achieve temperature control but simply sets a maximum temperature limit.

In general, most pumps are designed to run at 50C with the fluid at a specified viscosity. Any major deviation from the design specifications can only mean a loss of efficiency if the viscosity is too high, or lack of lubrication if the viscosity is too low. For instance, the viscosity of Shell Tellus 27 hydraulic oil decreases by a factor of 4 when the temperature changes from 20C to 50C, and for each 10C the temperature rises above 60C the rate of oxidation of the oil normally doubles. Hence, the reservoir must be designed to allow the oil to reach the design temperature rapidly and then maintain it at that level. This is best achieved in a system with low oil volume-to-heat generation ratio, and a suitably dimensioned cooler. This is the approach favoured by Fitch [15].

The capacity of a tank has traditionally been linked to the size of the pump. 'Rules of thumb' give guidelines which have in fact turned into standard recommendations. The NFPA Standards [38] for non-integral industrial fluid power hydraulic reservoir recommends: "the tank capacity (ℓ) must be a minimum of three times the pump operating capacity (ℓ/min)". However, common practice in mobile equipment is a ratio of pump flow (ℓ/min) to tank capacity (ℓ) of 5:1 [39]. However, these anomalies are small as can be seen by comparing the JIC (Joint Industry Conference) recommended practice [40], in

machine tool applications, of 10:1 (tank to pump flow) and the design of a D-9 bulldozer tractor [36] with a 700ℓ/min pump and a 65ℓ reservoir. The ratio between these two practices is over one hundred to one, which reflects the ad lib nature of these rules of thumb, and in fact to the principle of linking the sizing of the reservoir to the pump capacity. At least, these anomalies illustrate that small capacity reservoirs are feasible, and indeed this can mean great savings in oil.

At one time the use of a cooler in a hydraulic system was avoided, if at all possible, due to the relatively high price. However, if a small reservoir is used, the savings in oil are such that a cooler is no longer an unacceptable expensive item. This is, perhaps, only appreciated when oil has to be changed or when a major spillage occurs.

From this discussion it is apparent that the reservoir should not be used to control temperature. If a cooler is used on the return line prior to the reservoir the fluid temperature can be well controlled. This means that the temperature rises quickly during start-up conditions, due to the low system capacity, and when the normal temperature is reached the cooler will maintain it at that level.

Although the cooler is generally connected in series with the reservoir there are circumstances where anti-surge valves are introduced to by-pass the cooler when sudden surges of flow are returned to tank. These surges create pressure peaks that could damage the coolers [39]. If this occurs frequently in the operation of a machine, as in large presses for instance, there could be a case for considering the cooler to be run in parallel with the main system (see section 5.3.5).

The use of a proprietary electronic temperature controller, which switches the cooling fluid on and off, together with a thermocouple completes the fluid temperature control system.

5.3.3 Control of Pump Inlet Pressure. Improvements in the design of hydraulic pumps have always concentrated on higher pressures, higher efficiencies and reduced size. However, the suction capabilities of some pumps (mainly axial piston units) can only be referred to as poor. In fact, the fluid is invariably subjected to large, sometimes enormous, accelerations to fill each cylinder as it is suddenly opened to the inlet line. Recent improvements in pump design involving increased shaft speeds has only aggravated the problem.

Hence, modern pumps require oil to be supplied at a sufficiently high enough pressure to fill the pump inlet chamber (piston cylinder or gear tooth spaces) completely without air release or cavitation.

Supplying oil at the correct pressure to a pump is not the usual role of the reservoir. Very often pumps are boosted by other pumps which, due to their construction or size, have better suction characteristics. Indeed, a piston pump is the most difficult to fill and it is common practice to use a gear pump as a boost pump. Very often the two units are built in one body only, resulting in a compact arrangement. When using two positive displacement pumps in series, a relief valve is introduced to relieve excess flow. This, however, is not required if a centrifugal pump is used for boosting, because the excess flow is returned to the suction line as leakage. Such a solution can be found, for instance, in a Dowty Vardis axial piston pump [41]. However, the increased fluid turbulence at pump inlet is a disadvantage of this solution.

The boost pump can sometimes be omitted by elevating the tank to give a large positive head. In hydraulic presses, for example, this is the usual practice. Some presses are over 10 m high and positioning the hydraulic tank at the top provides a pressure of around 1 bar. Furthermore the reservoir is suitably positioned to fill the very large triple-acting actuators rapidly.

As an alternative, pressurized reservoirs may be employed. This is not a new idea, but in most cases the applications have been rather specialized as in aircraft hydraulic systems, for example. The most basic type of pressurized reservoir is almost identical to a conventional unpressurized tank, except that the breather is substituted by a pressurized air supply line, and the filler cap is properly sealed. These reservoirs normally operate at pressures up to 1 or 2 barg.

The use of pressurized reservoirs has also been linked to the need of having an air-free system. This can be achieved by fitting a rubber bag inside a sealed reservoir, and pressurizing it internally (fig.5.2). Although this solution is similar to a bladder-type accumulator, the rubber bag is thin, and the pressures involved are generally low (up to 1.5 bar). Perforated plates must be provided to limit the maximum expansion of the membrane an hence to protect the membrane from being damaged against rigid pipes or other components inside the tank.

Other designs of pressurized reservoirs include diaphragm and the piston types, being the latter widely used in aircraft for safety (as there is no danger of rupture of the membrane).

Fig.5.3 shows details of the pressurized tank used in the Concorde supersonic passenger airplane. In this design the interface between

air and oil is a metal bellows which can contract and expand with the variation of fluid in the tank. These reservoirs are pressurized to 3 bar by bleed air from the aircraft engines [42].

5.3.4 Aeration and Cavitation in Systems. Aeration is one of the main problems associated with badly designed reservoirs. Such effects can cause the oil to foam which causes the fluid compressibility to drop considerably resulting in sluggish system response accompanied by high frequency noise and the eventual loss of power and failure of main components, such as pumps.

Air can be present in a hydraulic system in three different forms: dissolved, entrained and free.

At normal conditions of temperature, and pressure, hydraulic mineral oil contains approximately 10% dissolved air (by volume). It cannot be visually detected and does not alter the properties of the oil (e.g. bulk modulus, viscosity, density). Under equilibrium conditions the oil is said to be saturated.

If the temperature or the pressure of the oil is changed, the amount of air dissolved varies. A similar phenomenon occurs when a bottle of champagne is opened and bubbles of carbon dioxide are formed as the pressure of the fluid suddenly drops.

The volume of air dissolved under equilibrium conditions is governed by Henry's law which states that the volume of air that can be dissolved under equilibrium conditions is proportional to the absolute pressure the fluid. If the fluid in the pump inlet line is saturated (10% air), when it enters the discharge line at a much higher pressure, it will become undersaturated and can dissolve considerably more air. Any air bubbles that may have been formed in the inlet line will tend to go back into solution.

The complex process of gas solution and evolution in liquids was studied by Schwietzer and Szebehely [43] for water, four fuel oils and thirteen lubricating oils. From this study it was clear that there are two main circumstances that can considerably influence the rate of evolution and solution of a gas in a liquid:

a) the level of agitation of the fluid;

b) the existence of nuclei, i.e. contamination.

Consider a quiescent (motionless) liquid in equilibrium with air at 2 bara, say. If the pressure is slowly reduced to atmospheric, no bubbles of air are likely to be formed although the pressure has been halved. The fluid is said to be supersaturated and is no longer in equilibrium. It could take a considerable time to get back to equilibrium conditions. However, if at this moment the container is shaken, bubbles will be formed instantaneously. The ratio between the rate of evolution under agitated and quiescent conditions is always of the order of several thousand to one [43]. If the pressure drop from equilibrium is sudden, however, then rapid release of air bubbles takes place (as when a bottle of champagne is opened).

In another study, Weyl and Marboe [44] examined the evolution of carbon dioxide from water, saturated at atmospheric pressure, in an ordinarily clean bottle. Reducing the pressure slowly from atmospheric to 0.06 bara readily produced bubbles. When the test was repeated with a thoroughly cleaned container no bubbles were produced. This phenomenum can also be noticed in a glass of champagne where the bubbles are only generated near the glass walls, particularly where there is an irregularity on the surface.

The major difference between the evolution and solution process is perhaps, its timing. Evolution is far quicker than solution, which means that if the pressure momentarily changes recovering its

initial value quickly, some air is more likely to come out of solution than go into solution. This can be exploited as a means of removing air from oil, by deliberatly causing turbulence in the fluid and allowing the air bubbles to be released to atmosphere.

Entrained air occurs as a result of dissolved air that has come out of solution as bubbles, or atmospheric air that is mixed with oil. Such occurrences must be avoided at all cost because the presence of entrained air in a hydraulic system causes a reduction in the bulk modulus and viscosity of the fluid and can also result in an increase in the temperature of the system.

The bulk modulus of a liquid-gas mixture is given by:

$$\frac{1}{\beta} = \frac{1}{\beta_\ell} + \frac{V_a \; p_a}{V \; p^2} \qquad (5.2)$$

where:

V	-	volume of mixture (≈volume of liquid)	$[m^3]$
V_a	-	volume of entrained air (at atmos. pressure)	$[m^3]$
β	-	bulk modulus of mixture	$[N/m^2]$
β_ℓ	-	bulk modulus of liquid	$[N/m^2]$
p	-	absolute pressure of mixture	$[N/m^2]$
p_a	-	atmospheric pressure	$[N/m^2]$

As the bulk modulus of air at atmospheric pressure is about 15000 times smaller than that of oil, even less than 0.1% of entrained air at atmospheric pressure will reduce the bulk modulus of the fluid by a factor of 10, if the pressure of the fluid is atmospheric. This reduction will result in sluggish response and in some instances lead to system instability.

As the viscosity of air is much less than that of oil, the presence of aerated oil in a pump results in the destruction of the

lubricating film and metal to metal contact is established in the bearings, vanes, gears or pistons. As the air passes from the low to the high pressure side of a pump the bubbles of air are compressed, which causes heat to be generated. This overheating, associated with the lack of lubrication, causes considerable wear to pumps. In fig.5.4(a) three stages of the wear of vanes are shown, taken from a vane pump run on aerated oil [34]. Fig.5.4(b) shows the eroded port plate of an axial piston pump that ran under aerated conditions [34].

Air is prevented from being released from solution if the pressure at any point in the system does not fall below tank pressure. The lowest values of pressure in a system occurs particularly at the inlet to a pump, downstream of valves (relief valves and non-return valves) and in general whenever jets and vortices occur. In particular any turbulence in the inlet line of a pump is likely to generate air release if there is pressure drop relative to the tank.

Atmospheric air is mixed with the oil by two mechanisms: the tank air-oil interface and ineffective (non air-tight) joints on the pump suction side. The tank is usually the only component where air and oil are in contact. Air is drawn into the oil either by the high turbulence or due to the formation of vortices at the surface. Large turbulence at the oil surface is the result of the high velocity of the oil from the return line being deflected to the surface or vibration of the tank itself (as in mobile equipment). Vortices are due to the inlet of a suction line being too close to the air-oil interface (less than 1.5 times the diameter of the line) [38].

One of the most common solutions to remove entrained air from the oil is to use a diffuser inside the tank. A diffuser (see fig.5.5) is designed to reduce the velocity of the oil returning to tank to

about 0.5 to 1m/s. This decreases the agitation of the oil surface considerably [34] and controls the size of the air bubbles returned to tank. If the diffuser has a large number of small holes (from 0.1 to 0.5mm diameter [45]), the numerous small air-bubbles in suspension in the oil are forced to combine and form larger bubbles, which rise rapidly to the surface where they are liberated.

As there are no standard deaerators suitable for hydraulic systems, the removal of entrained air must depend upon correct design of the reservoir. This should allow the slip velocity of the bubbles to be greater than the mean velocity of the oil in the tank. This has encouraged the use of baffles in early reservoir designs (as shown in fig.5.6) in order to increase the path between the return and the inlet lines, allowing sufficient time for air to be released and particulate to sediment. In some constructions (fig.5.6.c) the oil is forced to go over a baffle driving the bubbles close to the surface. In addition, screens have been used instead of diffusers to trap bubbles in a tank. This is particularly true in the case of larger tanks.

The slip velocity of air bubbles in oil can be evaluated from Stokes's equation:

$$v = \frac{(\rho_\ell - \rho_g)\ g}{18\ \mu}\ d^2 \qquad (5.3)$$

where: v - slip velocity of air bubble [m/s]

ρ_ℓ - liquid weight density [Kg/m^3]

ρ_g - gas weight density [Kg/m^3]

g - acceleration constant of gravity [m/s^2]

d - diameter of air bubble [m]

μ - dynamic viscosity of fluid [Ns/m^2]

Table 5.1 gives some values of slip velocities for different diameter air bubbles.

If a bubble of air is swept into the pump suction line, this is readily revealed by the change in the noise generated in the system. If the outlet pressure of the pump is, say, 100 bar the bubble will be reduced in volume by 100 times and be readily adsorbed in the oil.

In special applications, such as submarines, the agitation of the oil in the tank, and consequent noise, is defeated by the use of a balsa wood float. Fig.5.7 shows the arrangement used in a Polaris submarine [46].

Free air in an hydraulic system is the air that is trapped in pockets. In a properly designed system, free air should not constitute a problem, as the pipes should be orientated to allow all the air to be removed during the filling stage and, where appropriate, bleeding valves should be introduced and used whenever air enters the system. Even if purging is not performed, free air will, eventually, disappear because it will be dissolved. Until complete solution takes place the response of a system may be sluggish due to the reduction in stiffness.

There are circumstances where an "air-less" system is necessary. This is particularly the case when using hydrocarbon hydraulic oil at elevated temperatures (above 80C). The existence of a mixture of air and oil vapour at high temperatures is an explosion hazard. The two common solutions to this problem are to use a diaphragm or piston type pressurized reservoir or use a sealed reservoir pressurized by an inert gas such as nitrogen, argon or helium [47].

Cavitation can be distinguished from aeration as the rupture of the fluid due to a very low pressure. It is difficult to create conditions for testing a liquid under tension in a laboratory. If a force is applied at both ends of a container filled with liquid, in order to create a negative pressure, it is likely that air bubbles may be formed before the liquid tears apart. Harvey [48] subjected water to a negative pressure of 50 bar without visible failure. This shows that pure cavitation is not readily achieved and in most cases when the pressure falls to the vapour pressure of the fluid ($\approx$0.02 bara for water and $\approx 2 \times 10^{-6}$ bara for oil at 50C) it is the presence of air nuclei that provide the starting points of real cavitation. These cavities, filled with air, start being filled with oil vapor or, in more drastic cases, a vacuum may even instantaneously exist. When these cavities collapse next to a metal boundary, wear occurs due to the fatigue of the surface.

5.3.5 Contamination Control in a Reservoir. The role of the reservoir in the sedimentation of particulate matter is no longer acceptable. Only filters can perform this function efficiently.

The level of filtration required by hydraulic systems ranges from 10μm to 50μm on the inlet of a pump. In order to prevent larger particles from entering the suction line some system designers use filters on the inlet to a pump. This is, generally, considered bad practice unless the tank is pressurized, as the pressure drop in the filter may create aeration in the line. Another solution is to install a strainer or coarse filter which does not create an appreciable loss of pressure. Provided the fluid returned to the reservoir is clean, there is no need to filter the tank outlet.

The presence of contamination in a tank can only result from the following sources:

a) Improper cleaning of tank at the time of installation;

b) Return line fluid;

c) Breather intake;

d) Filling and topping-up of reservoir.

Before installation, the reservoir must be thoroughly cleaned. After connecting to the rest of the system, a comprehensive flushing program must be followed.

A filter must always be fitted on the return line. Filter elements are rather fragile and can be damaged by the pressure peaks. In some systems, an anti-surge valve is used to by-pass the filter allowing unfiltered oil to enter the reservoir. This solution may prove tempting but can lead to drastic consequences, such as the rapid wear of a pump. A better approach is to return the oil to a secondary reservoir which is used as a surge tank. The oil is, then, transferred to the main reservoir by a full-flow pump and filter arrangement.

The decision to position the filter either inside or outside the tank, is very important as in-tank filters are considered as an invitation to lack of maintenance due to their poor accessibility. When positioned outside the tank, some designers tend to fit two filters in parallel, each one capable of passing full system flow, so that one can be removed, for element replacement, whilst the system can be kept running.

The air breather is a serious source of contamination. An appreciable proportion of the particulate matter found in oil is dust which can be traced to the working environment of the system. Due to the changes in fluid level of the reservoir, atmospheric air is constantly drawn in or expelled from it. To prevent dust from

entering the reservoir, most air breathers today are equiped with a fine filter (2μm). However, in very hostile environments, such as earth moving machinery these breathers are quite easily blocked. This problem can be dealt with in two different ways. Some manufacturers employ rubber-bag type reservoirs (see fig.5.2.a) without pressurization, using the bag as a separator, and avoid the need for an filter. Others (for example, the Caterpillar Tractor Co.) use sealed reservoirs [36].

Some reservoirs are, in a way, pressurized reservoirs as they are designed to hold the air to approximately atmospheric pressure when the oil is cool and jacks fully extended (the condition of minimum oil in the tank) and be less than 1 bar when the fluid level in the tank is maximum. With this solution, the lack of breathing is compensated by a variable pressure in the tank. If the system is changed and the variations of pressure prove to be excessive, an additional volume of air may be necessary to lower the maximum pressure possible in the tank.

The last source of contamination is the filling and topping up of the system. According to the manufacturers, hydraulic oil cannot be guaranteed to be within the contamination requirements of modern hydraulic systems. Furthermore if the oil is introduced into the tank through the usual filler opening, this tends to increase the contamination levels as dust is drawn in from the atmosphere. The correct procedure is to provide a filling point upstream of the return filter using a quick release coupling for the purpose. A flushing rig should then be used to fill the system. In this way any new oil entering the system would pass through two filters: one in the flushing rig and one in the system. A filling point can be made available, in a non-pressurized reservoir, to be used only as a last

resort.

To illustrate the application of these concepts, a detailed example of the sizing of a reservoir is given in Appendix V.

5.4 DESCRIPTION OF PRESSURIZED TANK USED FOR SUCTION LINE STUDIES

The test rig used during the unboosted pump studies was basically a purpose built pressurized tank. In addition to the features discussed above, the design had to meet the special requirements of the suction line test method.

These requirements imposed a number of constraints which may be summarized as follows:

a) mean pressure in the tank must range from 0.4 to 11 bara

b) tank outlet must be at same height as pump inlet

c) it must be possible to use a variable length of line between pump and tank

d) mean temperature of fluid must be controllable to within ±2C

e) effective means of removing entrained air must be provided

f) it must be possible to deliberately dissolve air in the oil

g) in cases where the pump has a casing drain, which cannot be pressurized, means of recovering the lost fluid must be provided

Fortunately, the system under test does not contain any actuators or accumulators and the thermal expansion of the system walls is negligible. Consequently, the only variation in fluid level is due to the thermal expansion of the fluid in the reservoir.

Thus, the main feature of the tank is the ability to control air release in the fluid under different mean pressures. This is achieved through the use of two tanks instead of one (fig.5.8). The first tank consists of a horizontal cylindrical vessel and has the

duty of allowing the air bubbles to be released and is named the "stabilizing tank". The second is again a cylindrical vessel but is mounted vertically. This is the "delivery tank". Both tanks are completely filled with fluid and the air-to-oil interface occurs in a small tertiary reservoir, named the "interface tank", situated above the two main reservoirs. The duty of the tertiary reservoir is to maintain a perfectly steady interface at all times, i.e. no surface turbulence, in order to minimize the solution of air even under large mean pressures. The small interface area is of considerable assistance in this respect. Even if the fluid close to the surface is saturated, it will not be mixed with the fluid in circulation.

Any air bubbles entering the "stabilizing tank" are forced upwards into the "interface tank" whilst the oil is transferred to the "delivery tank". If any bubbles find their way into the "delivery tank", the inlet and outlet are positioned to ensure that the bubbles are forced upwards to the "interface tank" and liberated.

The laboratory air supply is used to pressurize the tank via a filter and a fine pressure regulator. The fluid level in the tank is controlled using two level detectors which switch a small top-up gear pump on and off as required. The detectors are situated on the side of the "interface tank". Should the fluid level rise above the top detector for more than 15 sec, as a result of thermal expansion of the fluid, for example, then the bleed valve is operated until the detector is cleared. Each level detector consists of a light sensitive switch and a bulb mounted either side of a sight glass. The difference in transparency due to the presence or absence of fluid is detected by the sensor and used to provide a logic signal. Details of the electronic circuit are given in Appendix VI. The top-up pump is connected to the "stabilizing tank" via a very fine

filter and a non-return valve which stops the pump from motoring when the tank is pressurized.

The cooling is performed by two air-oil coolers positioned underneath the "stabilizing tank" with an electrically operated fan between them. Oil temperature was measured using a thermocouple attached to the pump inlet and an electronic temperature controller was used to control the fan. The coolers were connected in parallel.

A large full-flow filter was connected upstream of the coolers preceeded by a turbine flowmeter and a non-return valve. This makes the tank unit self contained and sealed. On the "delivery tank" outlet line a bellmouth was machined to reduce the possibility of vortices when the fluid entered the suction line. A ball valve of exactly the same dimension as the internal diameter of the line was connected to facilitate changes in the length of line between the tank and pump. Fig.5.11 shows a photograph of the pressurized tank and of a pump under test.

TABLE 5.1

diameter of bubble (mm)	slip velocity (mm/s)	diameter of bubble (mm)	slip velocity (mm/s)
0.1	0.2	0.6	6.2
0.2	0.7	0.7	8.8
0.3	1.5	0.8	11.0
0.4	2.8	0.9	12.0
0.5	4.3	1.0	17.0

Table 5.1 Slip velocity of air bubbles in hydraulic oil
(ν= 28 cSt)

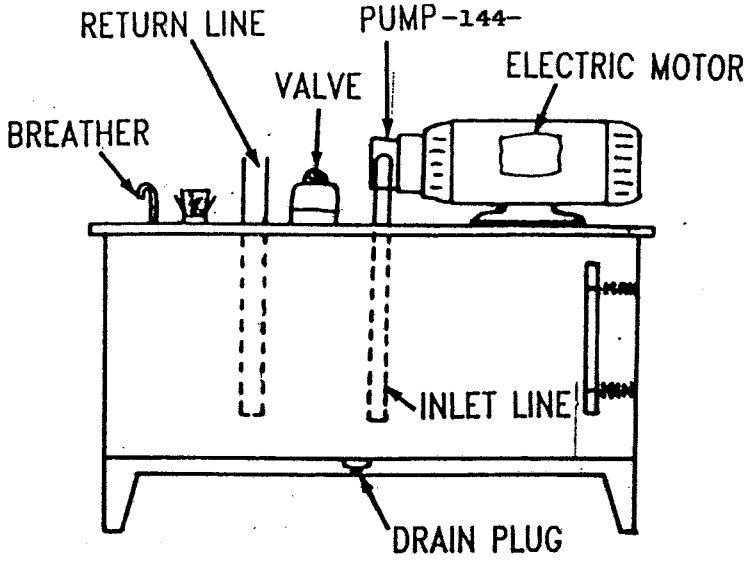

Fig. 5.1 Typical power pack

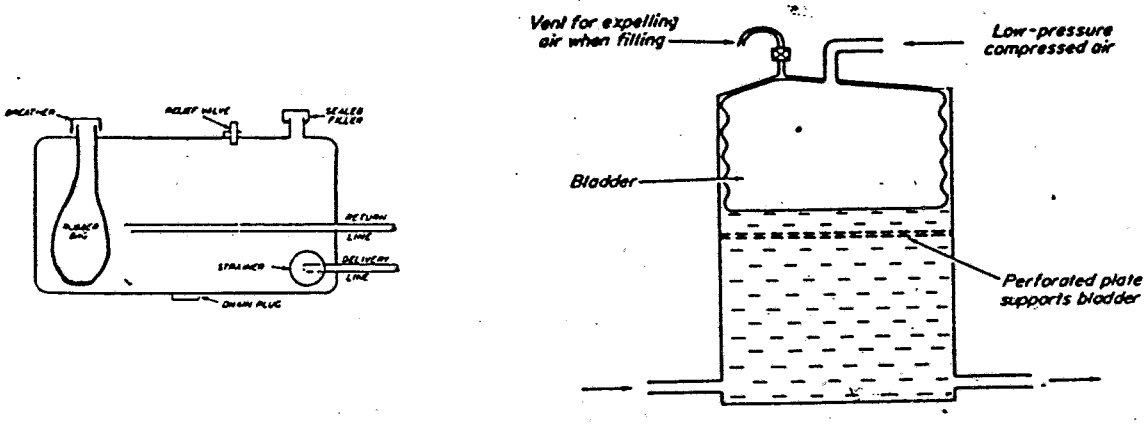

Fig. 5.2 Pressurized reservoirs with rubber bags

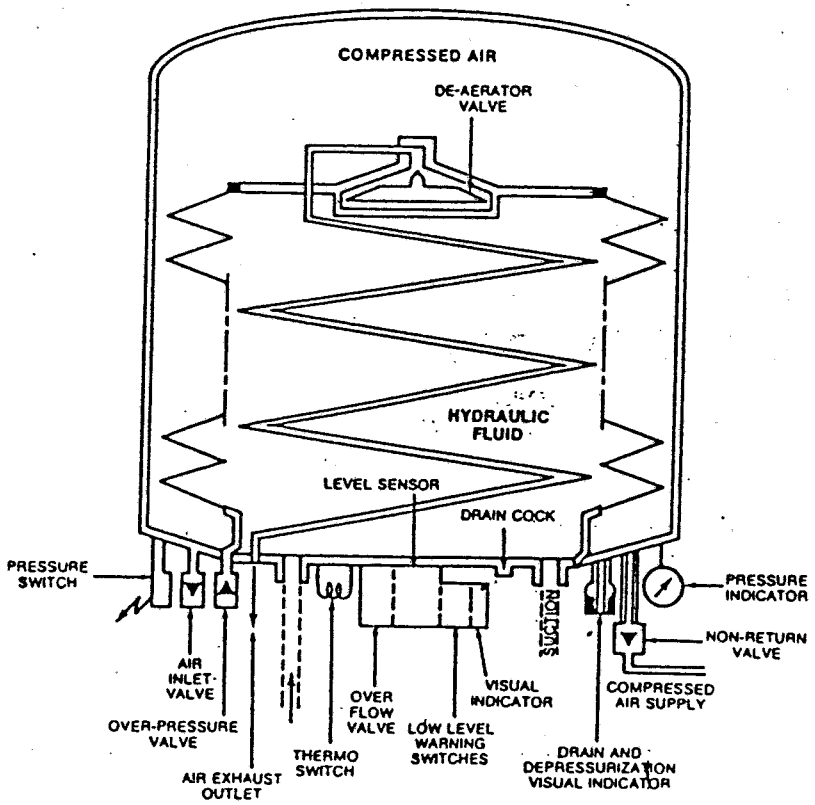

Fig. 5.3 Hydraulic reservoir of Concorde Supersonic plane

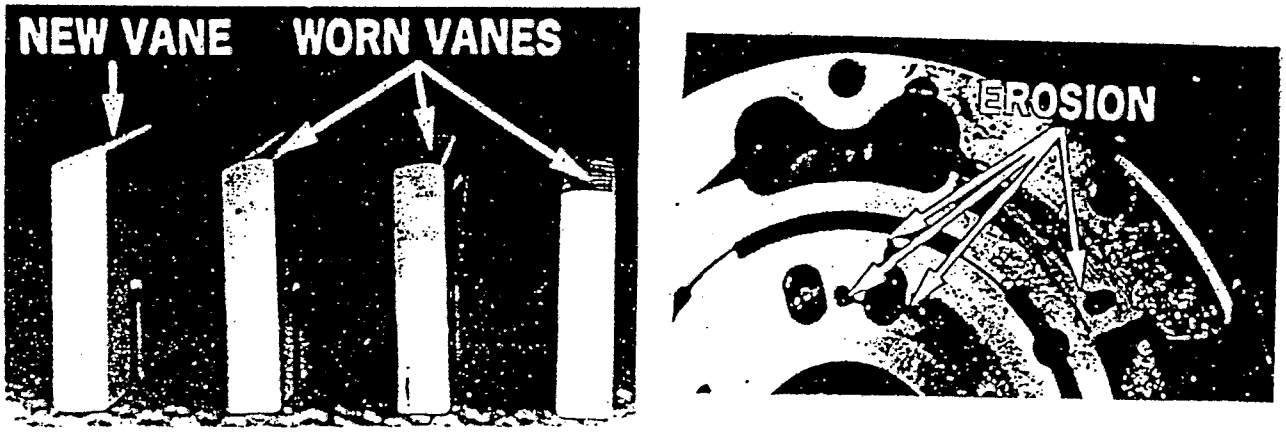

Fig. 5.4 Damage caused by aeration in pump components (from ref.[34])

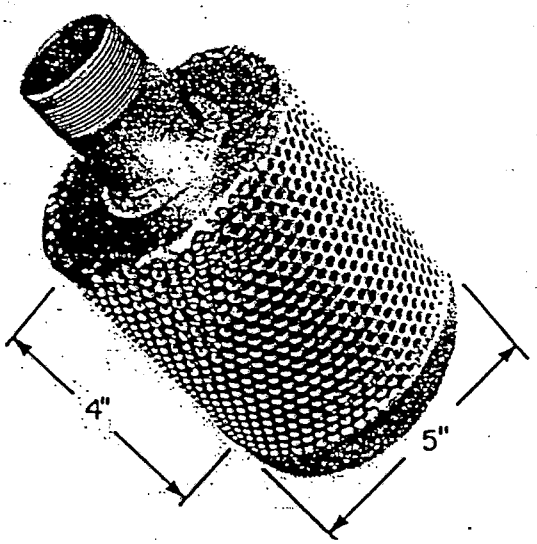

Fig. 5.5 Example of a diffuser (from ref.[34])

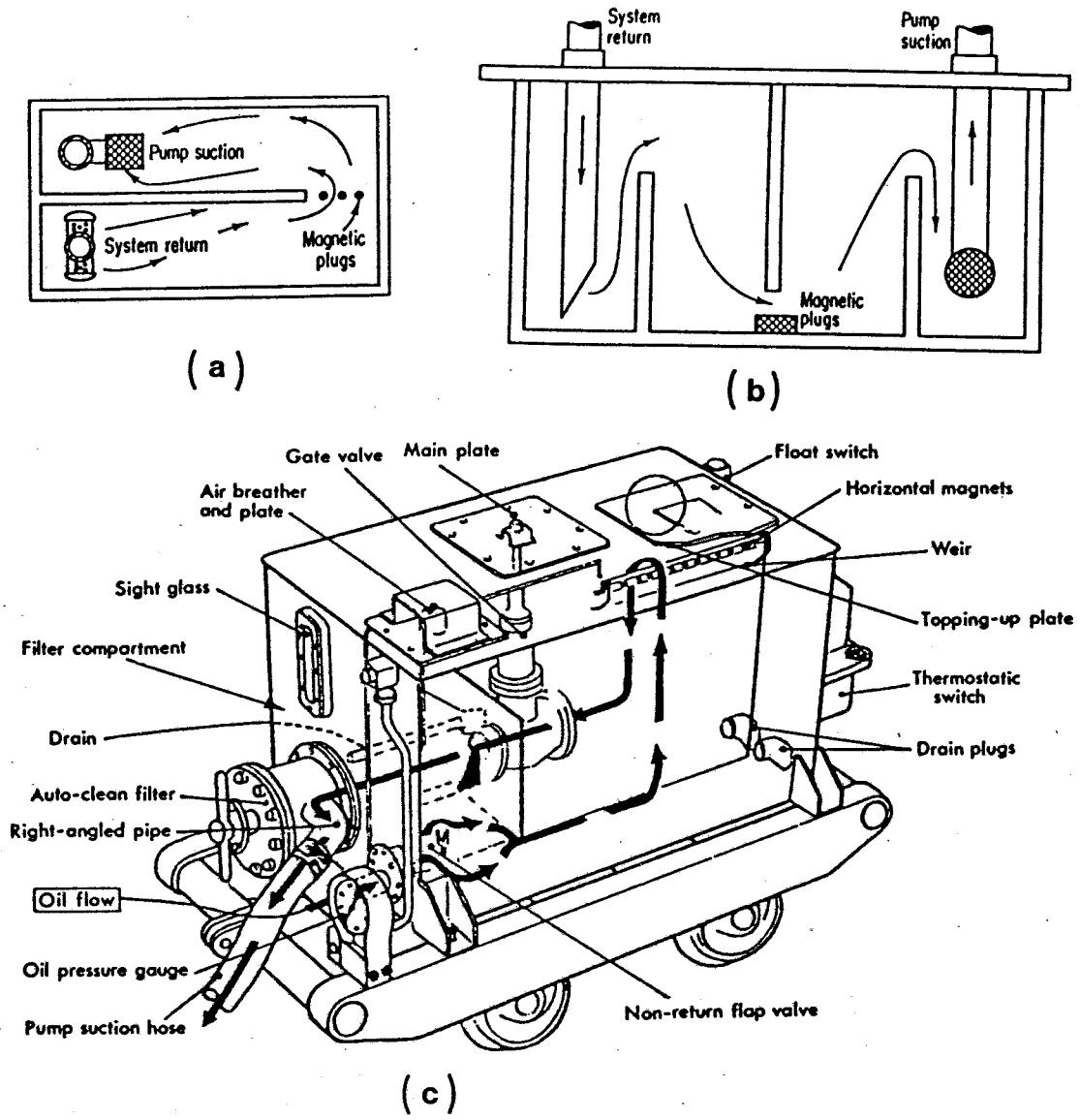

Fig. 5.6 Example of baffled reservoirs

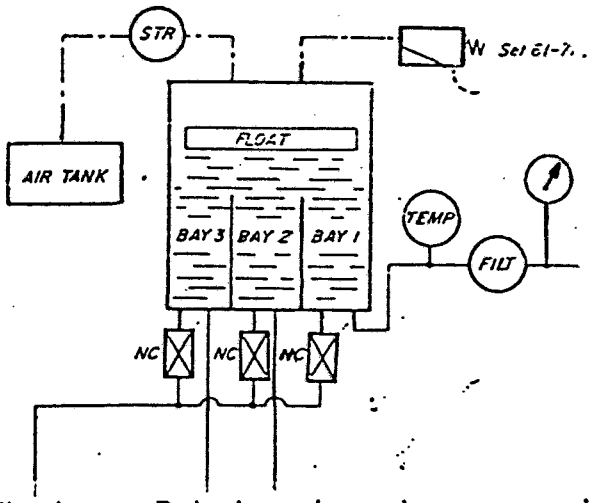

Fig. 5.7 Use of floats on Polaris submarine reservoirs (from ref.[46])

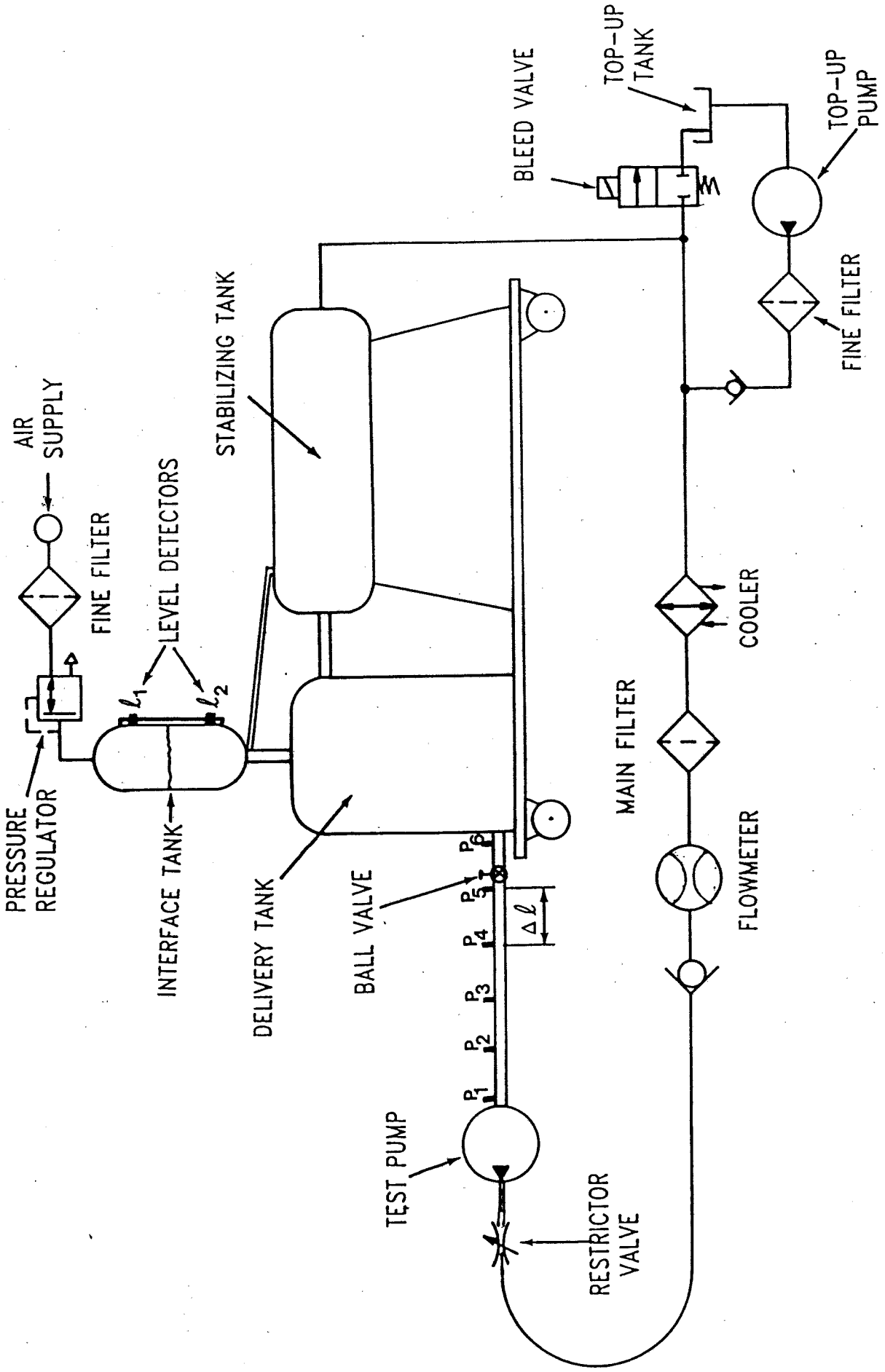

Fig. 5.8 Diagram of pressurized tank test rig

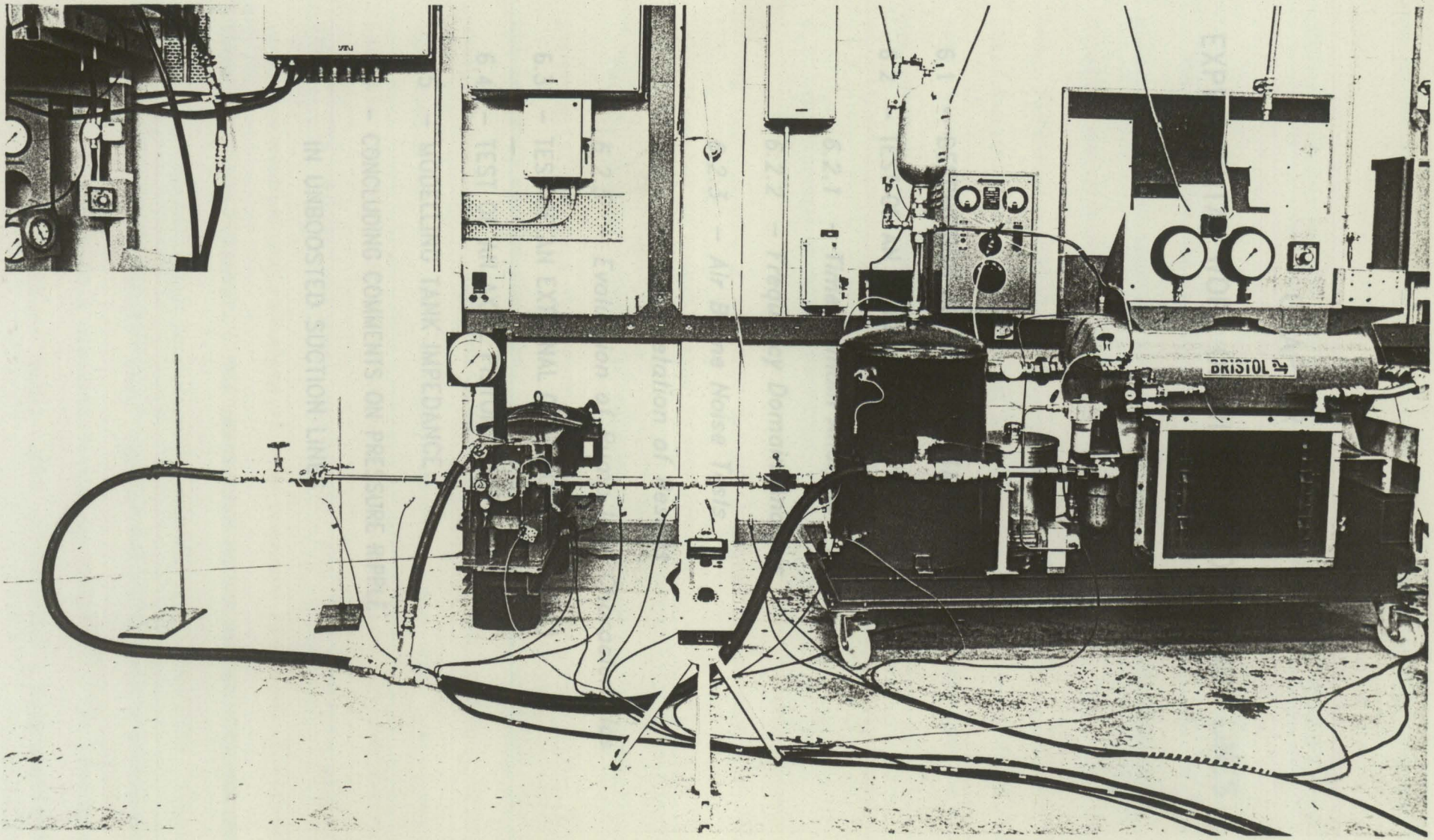
BRISTOL

CHAPTER VI

EXPERIMENTAL WORK ON UNBOOSTED SUCTION LINES

The work presented in this chapter describes the use of the pressurized tank test rig to evaluate pump inlet characteristics. A detailed analysis of pressure ripple is given both in the time and the frequency domain for four different pumps. The inlet characteristics of the pumps and the impedance of the pressurized tank were evaluated under different conditions and the results are presented and discussed.

6.1 DESCRIPTION OF INSTRUMENTATION

The instrumentation required for fluid borne noise analysis has been discussed in general terms in section 3.2.

For the studies reported in this chapter, up to six piezoelectric pressure transducers were mounted on the pump inlet line, flush with the internal wall of the pipe. Each transducer was connected to a charge amplifier. The pressure signals were analysed both in the time domain and in the frequency domain. For the time domain analysis a two-channel Gould-Advance digital storage oscilloscope was used. Its digital storage capability and the use of a plotter interface enabled the recording of some pressure waveforms presented later in this chapter. The resolution of the output plot was 500 points per channel which proved very satisfactory. Frequency domain analysis of the signals were carried out using both a continuous frequency analyser and a discrete frequency analyser. The spectrum analyser (Hewlett-Packard model 3582 A) provided a full amplitude spectrum of each signal. The Fourier Harmonic Analyser (Solartron

FRA 1170) was used to calculate the first ten harmonic components of each signal in terms of both amplitude and phase. Due to the large amount of data required for theoretical analysis of pressure ripple, the harmonic analyser was connected to an on-line computer (PDP-8) for fast acquisition and storage of data.

Two extra piezoelectric transducers were used, one mounted in the delivery tank and another at the test pump outlet.

The mean inlet line pressure was monitored by two diaphragm transducers (S.E. Lab type), one connected close to the pump inlet and the other close to the tank outlet. A turbine flowmeter measured the full flow through the system.

Fig.6.1 shows a full lay-out of instrumentation used during the tests whilst fig.6.2 shows a schematic diagram of the instrumentation.

A full description of details of instrumentation is presented in appendix VI.

6.2 TEST OF AN EXTERNAL GEAR PUMP (pump E)

An external gear pump (pump E, appendix VI) was mounted on a variable speed rig, using a hydraulic gear motor as the prime mover. The inlet of the pump was connected to the pressurized tank using a 25mm internal diameter pipe and the outlet of the pump was loaded by a restrictor valve.

6.2.1 Time Domain Analysis. An example of pressure fluctuations measured in the inlet line is shown in fig.6.3. These results were obtained with the pump at 900 rev/min and the mean pressure (measured close to the pump inlet) at atmospheric (1.0 bara). P_1 refers to the

pressure ripple measured close to the pump inlet flange, P_3 refers to the pressure ripple at a position close to the tank and P_2 is the pressure ripple measured at 0.8m from the pump. The length of line used was 1.85m. The pressure signals shown in the figure reveal relatively large values of peak-to-peak variation (1.2 bar for P_2) around the mean level which is represented by the straight line. The pressure ripple both at P_1 and P_2 falls to values close to 0.5 bara and rises to values of around 1.5 bara at regular intervals of about 10 ms. These traces show that when the pressure is low the shape of the signal is relatively smooth whereas when the pressure reaches a maximum it assumes sharp peaked forms. For this particular test the variation of pressure close to the tank is very much reduced compared with the other fluctuations.

Effects of mean inlet pressure

The effect of variation of mean pump inlet pressure on the pressure ripple is shown in fig.6.4. The waveforms presented correspond to position P_1 in the line. The mean pressure was varied from 0.9 to 2.0 bara with intermediate settings of 1.0 and 1.5 bara. The variation of mean inlet pressure produced very large changes in the pressure ripple. The pressure fluctuations not only changed significantly in peak-to-peak amplitude but also in shape. The pressure signal at 0.9 bara had a peak-to-peak amplitude of about 0.5 bar and a rather smooth shape. This signal was not very steady, however. At non-periodic intervals (typically several seconds) the signal momentarily changed showing a sudden collapse of pressure fluctuations followed by a recovery. The pressure ripple at mean pressures lower than 0.9 bara are not shown in the figure, but were found to be very unstable and aperiodic, with a very low amplitude. When the pressure was increased to atmospheric (2nd signal in fig.6.4) the pressure fluctuations became quite stable. The

amplitude ripple virtually doubled but the rather smooth shape remained. This signal shows a much clearer definition than that obtained at 0.9 bara, revealing a very strong 2nd harmonic component. At 1.5 bara mean pressure the signal exhibited very sharp variations of pressure which are associated with high frequency components. The amplitude of the signal was again almost doubled. When the pressure was raised to 2 bara the peak-to-peak pressure variation reached values of around 1.5 bar.

As the mean pressure was increased, it was found that the corresponding large fluctuations that occurred resulted in very low instantaneous pressures. This is illustrated in fig.6.5 which shows the pressure fluctuation for two different test conditions. Fig.6.5a, which shows the results at a mean pressure of 1.5 bara and a pump speed of 900 rev/min, clearly shows pressures as low as 0.2 bara. Even lower instantaneous pressures (0.1 bara) are shown in fig.6.5b. This signal was obtained at mean pressure of 2.0 bara and a speed of 1500 rev/min. Both signals were found to be periodic and quite repeatable. At mean pressures of about 0.8 and 0.9 bara the pressure ripple never fell below 0.5 bara.

Effects of pump speed

Fig.6.6 presents the behaviour of the pressure ripple in the pump suction line for pump shaft speeds of 900, 1500 and 1800 rev/min. For each running speed the mean pressure measured at the pump flange was adjusted to 2 bara. The traces demonstrate that peak-to-peak pressure fluctuations larger than the mean pressure in the line are quite common not only close to the pump inlet but even close to the tank (pressure P_3 at 1500 rev/min). At 1500 rev/min some pump frequency components appear to have assumed resonating values and hence the ripple is larger.

At a speed of 900 rev/min there is a strong 2nd harmonic component which is anti phase with the first harmonic. This reduces the amplitude of the first harmonic preventing very large excursions of the pressure signal from taking place. At twice this speed (1800 rev/min), and for that matter at 1500 rev/min as well, the 2nd harmonic reinforces the first and very high level sharp peaks in the pressure ripple occur.

Repeatability of waveform

In order to obtain repeatable results it is absolutely essential to regulate mean pressure accurately, which demands a fine control of tank pressure. Furthermore, because of the pressure drop along the pipe, it is necessary that the mean pressure is always measured at the same position (the pump inlet flange was considered throughout all the tests). Accurate means of measuring the mean pressure must be provided for this purpose (accurate pressure transducers). Fig.6.7 shows a comparison of three pressure signals measured on different days for near identical running conditions. Although the lack of repeatability of the results on the left hand side of the figure would be expected, given the instability of the waveform at low pressures, the results on the right hand side which correspond to a mean pressure of one bar above atmospheric shows the sensitivity of the pressure ripple to minor changes in running conditions.

6.2.2 Frequency Domain Analysis. The pressure signals shown in fig.6.4 were analysed in terms of their frequency components, as presented in fig.6.8. The results are shown on a dB-scale (10dB steps) for a range of frequencies from 0 to 2.5kHz. All four spectra reveal very well defined harmonic components, the 2nd harmonic (300 Hz) being the largest in most cases. This was due to the line length and speed combination used which amplified this particular harmonic.

As the mean pressure increased all harmonic components assumed larger values. The higher harmonics, however, exhibited larger increases than the lower harmonics.

The results shown in fig.6.8 refer to the pressure measured close to the pump inlet. When the pressure ripple measured close to the tank was analysed in the frequency domain the results were as shown in fig.6.9. From this figure the dependence of the ripple on the mean pressure is even more apparent. Furthermore, at the low mean pressures the higher harmonics generated by the pump do not reach the termination with any degree of strength. One possible hypothesis is that air is appearing somewhere in the suction line. This is a particularly important point and will be discussed in detail later. It is also important to note that in the cases of 1.5 and 2.0 bar mean pressure all harmonics up to the 13th are of the same order of magnitude (within 10dB). This gives some idea of the difficulty in fully characterizing the inlet pressure waveform by Fourier harmonic components.

For a theoretical analysis of the pressure ripple it is important to assess the repeatability of pressure signals in the frequency domain. Fig.6.10a shows the values of one harmonic of the pressure signal measured at a fixed position relative to the pump inlet at a mean pressure of 2 bara. The results correspond to successive tests of the system with different line lengths between pump and tank. The amount of scatter associated with the measurements gives an estimate of the repeatability of results. It must be emphasized that the system was disconnected between changes of line lengths and was reset to the same working conditions afterwards. The solid line represents a least squares fit of the transmission line equation to the experimental values. The results shown in fig.6.10a correspond to a

mean pressure of 2.0 bara in the inlet line. For comparison purposes, fig.6.10c gives an example of the repeatability that exists in the pressure ripple generated on the outlet line of the same pump, at a mean pressure of 50 bar. The results for the inlet line when the mean pressure was 1.5 bara are presented in fig.6.10b. This figure shows a rather more scatter of the data, although still follows a distinct wave pattern. However, at atmospheric pressure the results were much less consistent.

The existence of cavitation in suction lines is generally associated with high frequencies. Consequently, the pressure ripple measured close to the pump was analysed over a 25kHz frequency span at low mean pressures to search for very high frequency components (≈10 to 20 kHz) of the pressure ripple. Fig.6.11 shows the spectrum of the pressure ripple when the mean inlet pressure was 0.8 bara. No significant high frequency components were found.

6.2.3 Air Borne Noise Tests. In all experimental tests performed, one fact was perfect clear: the change in inlet pressure had a significant effect on air borne noise levels. When the mean inlet pressure was low (0.8 to 1.0 bara) the system was noticeably quieter than when the mean inlet pressure was above atmospheric.

In order to quantify this effect, a sound level meter (B&K type 2204) was positioned 1m away from the pump inlet flange. The values of air borne noise recorded are shown graphically in fig.6.12 on a A-weighted scale. Measurements at sub-atmospheric pressures were not possible due to the increased background noise produced by the vacuum pump employed. However the tests at pressures from atmospheric to 1.0 barg, and at different running speeds, clearly identify the relationship between the fluid borne noise in the line and the air borne noise. With the outlet pressure constant, an increase of 1.0

bar in the mean inlet line pressure (at 1500 rev/min) lead to an increase of 4dB in the overall noise levels radiated from the system (this is an increase of about 60%). At all running speeds the variation in system air borne noise with mean inlet pressure was significant. These results indicate that the use of flexible hoses in suction lines will assist in the design of quiet systems; not only from the structural isolation point of view, but also as a means of damping pressure fluctuations.

6.2.4 Interpretation of Results. The most striking observation from the results previously described is the remarkable difference between the pressure ripple characteristic of a gear pump inlet line and the outlet line. In chapter II it was stated that the pressure ripple on the outlet of a gear pump had a rather smooth shape and could be represented mathematically by six Fourier harmonic components. This is not the case for the inlet line where high frequencies are as important as the low frequency components. The distribution of the pressure ripple about the mean pressure level, is such that it is possible to have peak-to-peak pressure variations of more than twice the value of the mean pressure in the line (fig.6.5). Although the existence of large pressure ripples in the inlet line of a pump were expected (chapter IV), the strong sensitivity to small variations in mean pressure is rather surprising. There are two possible explanations for such an effect: changes in the tank reflection coefficient with mean pressure or changes in the pump characteristics with mean pressure. These possibilities will now be examined in detail.

6.2.5 Evaluation of Pump Inlet Characteristics. All the methods of determining the characteristics of hydraulic components in pressurized lines, as studied in chapter III, assumed that the

pressure ripple measured in the system was repeatable and that the speed of sound in the fluid was accurately known. From the above considerations it is unclear if these assumptions would apply to conditions in pump suction lines. Consequently great care had to be exercised at all stages to ascertain that no spurious results were wrongly considered. This was the reason why a large amount of experimental data had to be acquired to define the pressure standing wave in the line at each running condition. Six transducers were connected in the pump suction line to measure the pressure ripple. The results were analysed according to the multitransducer method described in chapter III. However, no trombone-like apparatus was used in the line due to the adverse effects that a sharp change in pipe section might cause in the flow pattern and pressure ripple. Therefore the line between the tank and the pump had an uniform internal diameter, with a small bellmouth at the tank end to prevent vortex effects from occurring. The variation of line lengths between tank and pump was achieved by actually changing the pipe.

Four transducers were positioned at fixed distances from the pump and only two fixed in relation to the tank. The distances between the first four transducers were chosen such that the shortest wavelength considered during tests was well defined (the highest frequency being the 10th harmonic). Consequently, the distance between the first and fourth transducers was kept below 0.5m. The pipe lengths were increased in steps until the difference between the shortest and the longest lengths of line was at least half a wavelength of the fundamental (lowest) frequency. In this way all harmonics of interest were obtained.

In order to obtain representative data, mean pressure was controlled to within 0.05 bar. In addition the Fourier analysis of

each signal was performed over ten successive periods of the waveform. The average of five successive analyses was taken as one result.

TESTS AT A SHAFT SPEED OF 900 rev/min

Pump E was firstly tested at a speed of rotation of 900 rev/min and mean inlet pressures of 1.5 and 2.0 bara. The results of pump source flow are shown in fig.6.13, where they are compared with the outlet flow produced by the pump at 50 bar (the inlet flows are deliberately displaced for clarity). The results show that the inlet and outlet source flows of the pump are of the same order of magnitude. Furthermore, the inlet results are very similar in terms of the waveform shape, apart from the backflow which occurs at the centre of each cycle. In fact, the same effect can be noticed on the outlet flow of the pump, although of much smaller amplitude. This shows that there is some volume that is transferred from the pump outlet back to the inlet.

The inlet source impedance of the pump (fig.6.14) was evaluated for the two mean pressure conditions. The two results, although well defined, are quite different from what could be expected, particularly when compared to the pump outlet impedance shown on the same figure. Over most of the frequency range the inlet impedance is much lower than the outlet impedance, even though the volume of oil in both the inlet and discharge passageways is virtually the same. This suggests that a low impedance element is present which dominates the capacitive effect. It will be shown later that air release in the pump body is responsible for this phenomenon.

The tank impedance is shown in fig.6.15. Initially, the large volume of oil contained in the tank was expected to result in a very low amplitude impedance at the termination and a phase close to -90

deg (section 4.2). However, the results consistently show an almost inductive type characteristic with an amplitude spectrum increasing with frequency, and a relatively constant positive phase spectrum. The tank impedance clearly decreases in amplitude with mean pressure, with a corresponding increase in phase. As the 25mm diameter pipe used in the test has a value of $|Z_o|$=187dB, a decreasing value of $|Z_t|$ (below 187dB) corresponds to an increase in $|\rho_t|$. This partially explains the larger pressure ripple values in the line at 2.0 bara mean pressure. Indeed, in terms of the experimental approach, this is favourable. From the theory of the tuned lengths method, large values of $|\rho_t|$ are desirable for an accurate assessment of the pump characteristics.

Some of the difficulties experienced in the interpretation of these results was at first attributed to the assumption that the speed of sound in the fluid was the same as in high pressure lines. If entrained air was present in the suction line, the speed of sound would fall considerably [29] and the predicted pump and tank characteristics would be incorrect. However, careful analysis of the results revealed that consistent and sensible characteristics could only be obtained by assuming that the speed of sound remained unchanged.

TEST OVER A RANGE OF SHAFT SPEEDS

Pump E was tested at different shaft speeds for the largest mean pressure possible in the suction line (2.0 bara). The aim here was to maintain as stable a waveform as possible. Indeed, in view of the difficulties in obtaining satisfactory repeatability at low speeds, an increase in pump speed will increase the amplitude of the flow fluctuation which could well lead to a decrease in waveform stability. The pump was tested at 900, 1200, 1500 and 1800 rev/min

with the same 25mm diameter pipe. Although this procedure of maintaining a common diameter pipe for different mean flows is open to criticism, the practical difficulties involved in testing , say, two diameter pipes would be enormous. Consequently, it must be understood that the pressure drop in the pump suction line will be different for each running speed. For example, in the tests performed at 900 rev/min the tank outlet pressure was very similar to pump inlet pressure regardless of the line length. The same cannot be stated for the case of 1800 rev/min where the tank pressure was 0.15 bar above the pump inlet pressure when the line length was 1.8m.

Fig.6.16 shows the results of source flow evaluated for pump E when running at different shaft speeds. These results are compared with the flow delivered by the unit at 50 bar when running at 1500 rev/min. In the case of the pump outlet, an increase in frequency (speed of rotation) results in an increase in the flow ripple amplitude. Fig.6.16, however, shows that this is not the case for the pump inlet.

The source impedances obtained at different speeds (fig.6.17) all follow the same trend. However, the variation with frequency is very different to the outlet in terms of both amplitude and phase. The amplitude spectrum is virtually constant and the phase changes from -60 deg at low frequencies to +60 deg at the higher frequencies. The impedance of the tank at different mean flows (fig.6.18) shows an inductive characteristic, as in the low speed test in fig.6.15.

To summarize, the pump characteristics obtained were completely different to those for the pump outlet and the tank impedance was found to be inductive rather than capacitive. In order to gain a better understanding of these effects, further tests were performed on two other external gear pumps and an axial piston pump. The

results of these tests will now be discussed.

6.3 TEST OF AN EXTERNAL GEAR PUMP (pump C)

The tests presented for external gear pump E give an impression of pressure ripples to be expected in gear pump suction lines. There were, however, some constraints in those tests which limited conclusions, such as the range of mean pressures tested (up to 2.0 bara) and the difficulties inherent to testing a large sized unit (large velocities in the suction line). Consequently, a smaller size unit of modern design was tested. This pump could be tested at a maximum continuous inlet pressure of 3.0 bara.

The pressure ripple generated in the suction line by this pump followed the same pattern as pump E, although in general the higher harmonic components were not as pronounced. The pressure fluctuations were, again, very dependent upon mean inlet pressure as shown in fig.6.19.

The inlet characteristics of this pump were evaluated for 1.5, 2.0 and 3.0 bara mean inlet pressures. The source flow generated on the inlet of the pump under these conditions is shown in fig.6.21. These results show that the three source flow traces are well defined. Both inlet and outlet source flows for this pump show no evidence of a significant 2nd harmonic component as in the case of pump E. The results of the source flow for different mean pressures are again deliberately displaced in mean flow for clarity. A comparison of the inlet and outlet flows show that the minimum flow drawn in and delivered by the pump occur at almost the same pump angular position. The main difference between the inlet flow traces occurs when the flow is a maximum. It appears from the figure that when the mean inlet pressure is reduced the fluid flow does not follow the

geometric displacement of the pump. When the mean pressure is large (3.0 bara) the pump displacement is closely followed. In order to examine this effect further, the pump was tested at atmospheric pressure (1.0 bara). The source flow corresponding to this condition (fig.6.22) is virtually non-existent. It is unlikely that this is the true flow ripple for the pump inlet. The results indicate that air is being released inside the pump, which damps most of the pressure ripple and this is reflected by the reduction in the predicted flow fluctuations. It is extremely unlikely that cavitation is occurring in this case as this would almost certainly have been accompanied by an increase in air borne noise and a loss of output flow. Neither of these occurred.

The mean inlet pressure was raised up to 5 bara for short periods of time for air borne noise measurements. The results presented in fig.6.20 correspond to the air borne noise levels measured at a distance of 1m from the pump (on the inlet side), when the pump was running at 1500 rev/min. Several combinations of mean inlet and outlet pressures were tested and the results demonstrate clearly that the increases in air borne noise levels due to variation in mean outlet pressure are as significant as the increases due to mean inlet pressure. In fact, when the mean inlet pressure was increased by 2 bar the air borne noise levels increased by as much as when the mean outlet pressure was increased by 150 bar. Another interesting point is that increasing the mean pressure above 3 bara produced virtually no further increase in the air borne noise levels (fig.6.20).

Assuming that air release does not occur above this pressure, the source flow fluctuation would be maintained at a constant level (as on the outlet line). Since the amplitude of the reflection coefficient at the tank has a value very close to unity, then the

pressure fluctuations in the line would remain virtually constant.

Further tests were carried out using a pump of the same batch as pump C (designated as pump C'). It was decided that as air release appeared to be the cause of the reduction of inlet source flow in pump C, the fluid should be partially deaerated before testing commenced. Under these conditions the fluid would at all times be undersaturated, reducing the possibility of air release. The partial deaeration was performed by running the pump for 30 mins at a mean inlet pressure of 0.5 bara (well below the lowest mean test pressure). Obviously, it was necessary to run the pump at this condition after each pipe change. For each pipe length selected the pressure was then raised to 1.0, 1.2 and 1.5 bara respectively. In order to prevent significant ingression of air into the system the time for each test was kept as short as possible. The mean pressure was not raised above 1.5 bara for the same reason. The results of these tests, are shown in fig.6.23. Previous tests on the delivery of this pump had shown that the outlet flow ripple exhibited a distinct backflow which varied with mean outlet pressure (in much the same manner as pump E). This effect also appears on the pump inlet, again in much the same way as occurred with pump E. It is clear that for pump E and pump C', a volume of oil passes from the outlet side of the pump back to the inlet independent of the geometrical displacement of the pump. In addition to this phenomenon, there was a considerable difference in the amplitude of the fluctuations compared to those obtained with pump C (see fig.6.22 and the results at 1 bara in fig.6.23, for an example).

These two effects can be examined quite separately. Clearly, there is a basic difference in the two pump flows irrespective of the air content or the mean pressure setting, even though the pumps are

from the same batch. This may be explained by a detailed study of the tolerances on the relief grooves machined in the pump bushes. The relief grooves are machined to relieve the pressure from the meshing teeth towards the outlet line. The grooves are positioned to leave this process until as late as possible. The size and position of the grooves is limited by the need to prevent direct leakage from the outlet line to the inlet (fig.6.24). In general, pump relief grooves are machined to achieve a certain amount of underlapping (25 μm). This prevents sharp pressure peaks occurring in the outlet line. Even if the bushes on different pumps are machined within the same tolerances, together with the gears, it is always feasible that the bushes might be positioned at a slightly different position (bushes are manufactured in two halves) creating a different sealing length. Furthermore, pressure relief occurs twice every pumping cycle and the same transfer of flow to the inlet can be observed at the point of minimum flow taken in by the pump. This can be seen in fig.6.25 where the actual inlet flow at 1.5 bara mean pressure is compared with the pump geometric displacement.

Consider now the behaviour of pump C' when tested at low mean inlet pressures with partially deaerated oil. It was found that under such conditions, the pressure ripple in the line was much more stable than for pump C. In addition, the flow ripple was much larger when the oil was deaerated. This is a further argument for the existence of air release in the pump inlet passageway of pump C, although of course in microscopic proportions as no decrease in mean outlet flow was observed.

The source impedance results for pump C (fig.6.26) are similar to those evaluated for pump E although of slightly higher magnitude. This is to be expected since pump C is much more compact than pump E

and therefore has a smaller dead volume. For pump C', however, the amplitude spectrum (fig.6.27) decreases with frequency (excluding 5th harmonic). This is closer to the characteristic associated with the outlet of the pump and should be expected if air release effects are less pronounced. The phase still shows quite unexpected values, probably due to small quantities of air still being released.

6.4 TEST OF AN AXIAL PISTON PUMP (pump A)

The axial piston pump (pump A) whose outlet characteristics were presented in chapter III, was tested in order to evaluate the source flow fluctuation and source impedance at the inlet. As the unit had variable swash setting, and could be run as a pump as well as a motor, it offered considerable potential for an investigation of inlet line behaviour. Indeed, it was possible to test the suction line under different flow conditions and different mean pressures without tight limitations.

TIME DOMAIN ANALYSIS

The time domain signals recorded on the inlet line to the piston pump (fig.6.29) show that there is a marked similarity to the time signals recorded on the outlet of the pump (fig.2.1). In fact, if the inlet pressure fluctuations are inverted it is virtually impossible to distinguish inlet pressure ripple from outlet pressure ripple. Indeed even the peak-to-peak amplitudes are similar. The pressure peaks which occur in the suction line are due to the decompression of the dead volume of oil in the cylinder as the piston passes from outlet to inlet. Consequently, the pressure ripple in the suction line is not only dependent upon mean inlet pressure, as shown in fig.6.29, but on mean outlet pressure, as well. Apart from these two facts, the pressure signals presented a similar behaviour

to that experienced with pump E, such as loss of stability of the waveform at low mean pressures accompanied by loss of definition of the high frequency components. There is little change in the shape of the waveform for pressure above 3 bara.

PISTON PUMP INLET CHARACTERISTICS

Pump A was tested using the tuned lengths method at two swash settings and five mean inlet pressures (1.0, 1.5, 2.0, 3.0, 4.0 and 5.0 bara). The results of source flow fluctuations for a range of inlet pressures were evaluated and are shown in fig.6.30. The results for both full and half swash settings are mainly characterized by the sudden reduction in flow being taken in by the pump. This is due to the decompression of the volume of oil in the cylinder and, as expected from the discussions in chapter IV, the backflow is larger at half swash setting. As the backflow is also dependent upon the difference between mean outlet and inlet pressures the results at different inlet pressures show very small but definite reductions in backflows.

This can be seen more clearly in fig.6.31 which shows the magnitude of the backflow as a function of the mean inlet pressure. The size of backflow for the half swash setting is larger than for the full swash. As the mean inlet pressure is reduced, the backflow increases until a maximum is reached. This strongly suggests that at inlet pressures below this, air release tends to damp out the flow fluctuations. Furthermore, the inlet pressure at which this occurs is different for the two swash settings. This seems to indicate a greater possibility of air release occurring at the lower of the two mean flows. This is somewhat surprising and means that the existence of air release is more likely caused by the magnitude of the flow ripple rather than by the mean magnitude of the flow level.

The results of pump inlet source impedance at full swash are shown in fig.6.32). For low pressures (1.0 bar test) the spectrum is very close to the characteristics presented for pumps C and E. However, at the higher pressures, 5 bara for example, the spectrum is very similar to the pump outlet characteristic (fig.3.19), and is typical of a lumped volume. Similar spectra were obtained from the results at half swash, although these exhibited considerably more scatter for the lower mean pressure tests. In this respect, the behaviour was similar to the source flow results. The results of impedance at the larger mean pressures again have amplitude and phase values, corresponding to a capacitive impedance.

The spectra of the tank impedance (fig.6.34), for the tests at half swash (24ℓ/min), are very similar to the results from the other pumps tests. This indicates that in all cases air release did not occur in the suction line, otherwise the calculation of the termination impedance would be affected. In addition, the results in fig.6.34 show that there is a variation of impedance with pressure in much the same manner as in the gear pump tests. Furthermore, the results of the tank impedance obtained from tests at full swash (47ℓ/min) were very similar to those at half swash (24ℓ/min), but of a slightly lower amplitude.

AIR BORNE NOISE

Air borne noise tests performed on the system when pump A was running at different mean inlet pressures produced results quite different from those obtained in gear pump tests. It was noticed that when the inlet pressure was reduced the system became quieter. Decreasing the mean pressure to very low values, however, increased again the air borne noise levels so that at 0.3 bara the system was 20 dBA noisier than at atmospheric pressure. When the pressure was

increased above 2.0 bara the air borne noise measurements did not change appreciably. This behaviour can be explained from the consideration of pump inlet characteristics. When the mean pressure in the inlet line is increased the pump inlet flow ripple decreases, tending to lower pressure ripple levels. However, the increase in mean pressure also results in a small decrease in the amplitude of the tank impedance, which in turn increases the termination reflection coefficient. These two effects tend to cancel each other, keeping the fluid borne noise level at a fairly constant value. When air is being released inside the pump, however, both source flow and the tank reflection coefficient are reduced and the fluid pressure ripple in the line is lowered considerably.

6.5 MODELLING TANK IMPEDANCE

The large volume of the fluid present in the tank was initially expected to produce a capacitive impedance, given by the equation,

$$Z_t = \frac{\beta}{j\ \omega\ V_T} \qquad (6.1)$$

where: V_T - tank volume $[m^3]$

For the very large volume of oil present this equation gives very low values of impedance amplitude with a corresponding phase of -90 degrees at all frequencies. The amplitude decreases with frequency at 20 dB/decade. As at these low values, $|Z_t|$ is smaller than $|Z_o|$, the corresponding reflection coefficient assumes a magnitude close to unity and a phase between 170 and 180 degrees. The tank impedance evaluated from the tests, however, corresponds to a tank reflection coefficient with of unity magnitude but with a phase of around -170 to -180 degrees. At first sight there appears to be a considerable difference between the two reflection coefficients. This is simply

because of the convention employed for defining phase angles (i.e. -180. to +180 deg). If a phase range of 0 to 360 degrees was employed, for example, it becomes clear that there is only a small difference between the two coefficients.

In order to account for the differences between theory and experiment it is necessary to refer to the work of Rayleigh [49], concerning open ended pipes. Rayleigh found that the actual reflection does not occur at the physical end of the pipe, but a short distance beyond the end of the line. This is due to the impossibility of achieving zero pressure fluctuation conditions within the limits of the pipe. Such an occurrence would imply the flow fluctuation at that point would be infinite.

This effect can be incorporated in the theory by assuming that the reflection occurs a short distance inside the tank, and that this can be represented by a pipe of length ℓ.

Using eq.2.11, which gives the entry impedance to a line terminated by a component of impedance Z_t,

$$Z_E = Z_o \frac{Z_t + Z_o\, j \tan(\omega\ell/a)}{Z_t\, j \tan(\omega\ell/a) + Z_o} \qquad (6.2)$$

assuming that the length of line is very short, $\tan(\omega\ell/a) \simeq \omega\ell/a$ and,

$$Z_E \simeq Z_o \frac{Z_t + Z_o\, j\, (\omega\ell/a)}{Z_t\, j\, (\omega\ell/a) + Z_o} \qquad (6.3)$$

and if the termination is a volume (eq.6.1), then

$$Z_E \simeq Z_o \frac{(\beta/(j\omega V)) + Z_o\, j\, (\omega\ell/a)}{(\beta\ell/(Va)) + Z_o} \qquad (6.4)$$

For large volumes, the capacitive term is very small, and it was found that a length of about 0.1m was necessary to change the impedance of the termination from inductive to capacitive for all harmonics. The highest harmonics became capacitive in nature with even shorter lengths. Hence, the reflection does indeed occur a

short distance inside the tank.

6.6 CONCLUDING COMMENTS ON PRESSURE RIPPLE IN UNBOOSTED SUCTION LINES

The results presented in this chapter have shown that pressure ripple exists in suction lines in the same form as in the discharge line of positive displacement pumps. In fact very large pressure fluctuations were recorded in the suction line of both external gear and axial piston pumps, with peak-to-peak values of up to 5 bar and instantaneous values as low as 0.1 bara. These fluctuations of pressure occurred at mean pressures above atmospheric and, although very low instantaneous pressures were recorded, no evidence of air release was encountered. The air borne noise radiated from a system was significantly affected by the mean pressure in the inlet line. It was found that when the mean pressure in the suction line was increased the air borne noise also increased. Consequently, the need to increase pump inlet pressures to prevent cavitation has an adverse effect on the noise generated by the system.

In general, the suction line of a pump can be described in fluid borne noise terms as having a very large reflection coefficient (+1) at the source and a -1 reflection coefficient at the termination. A typical example of the resultant standing wave pattern created in the line is shown in fig.6.35. This figure shows the standing wave generated by the second harmonic component of pump A when the mean inlet pressure is 5.0 bara. For the lower harmonics, the pressure fluctuations close to the tank are always small. This implies that if the tank is positioned close to the pump, the pressure fluctuations at all points in the line will be low. At the higher harmonics, there will almost certainly be a resonance in the line,

even when the line is short. However, for a given inlet pressure this is the best configuration to minimise air borne noise.

When testing the inlet characteristics of two gear pumps of the same batch, considerably different results were obtained, showing that the instantaneous flow admitted by the pump is very sensitive to small differences in the machining of relief grooves. Furthermore, the air content of the fluid at low mean pressures can determine the level of fluctuations present in the suction line. When one pump was tested with partially deaerated fluid at low mean pressures it was found that the source flow of the pump was not significantly affected by mean pressure. When another similar pump was tested under the same mean pressures without deaerating the fluid the pump source flow was very dependent upon mean pressure. This was also reflected in reduced pressure ripple levels. Consequently, it is important from the fluid borne noise point of view to run pumps at the lowest mean inlet pressure possible without running into cavitation problems. For this purpose a pressurized tank seems to be an ideal solution due to the ease with which suction line pressure can be controlled.

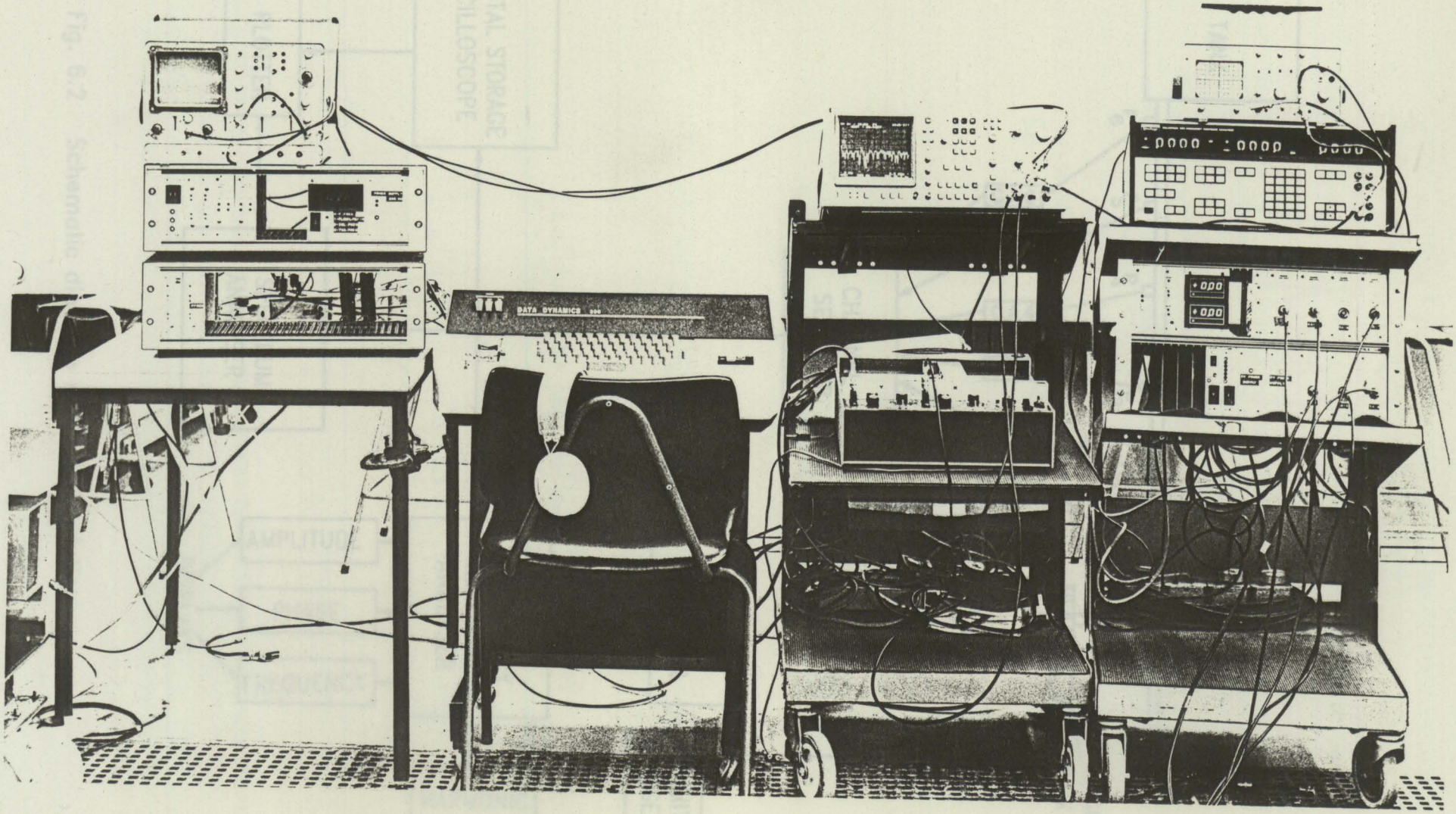
DATA DYNAMICS

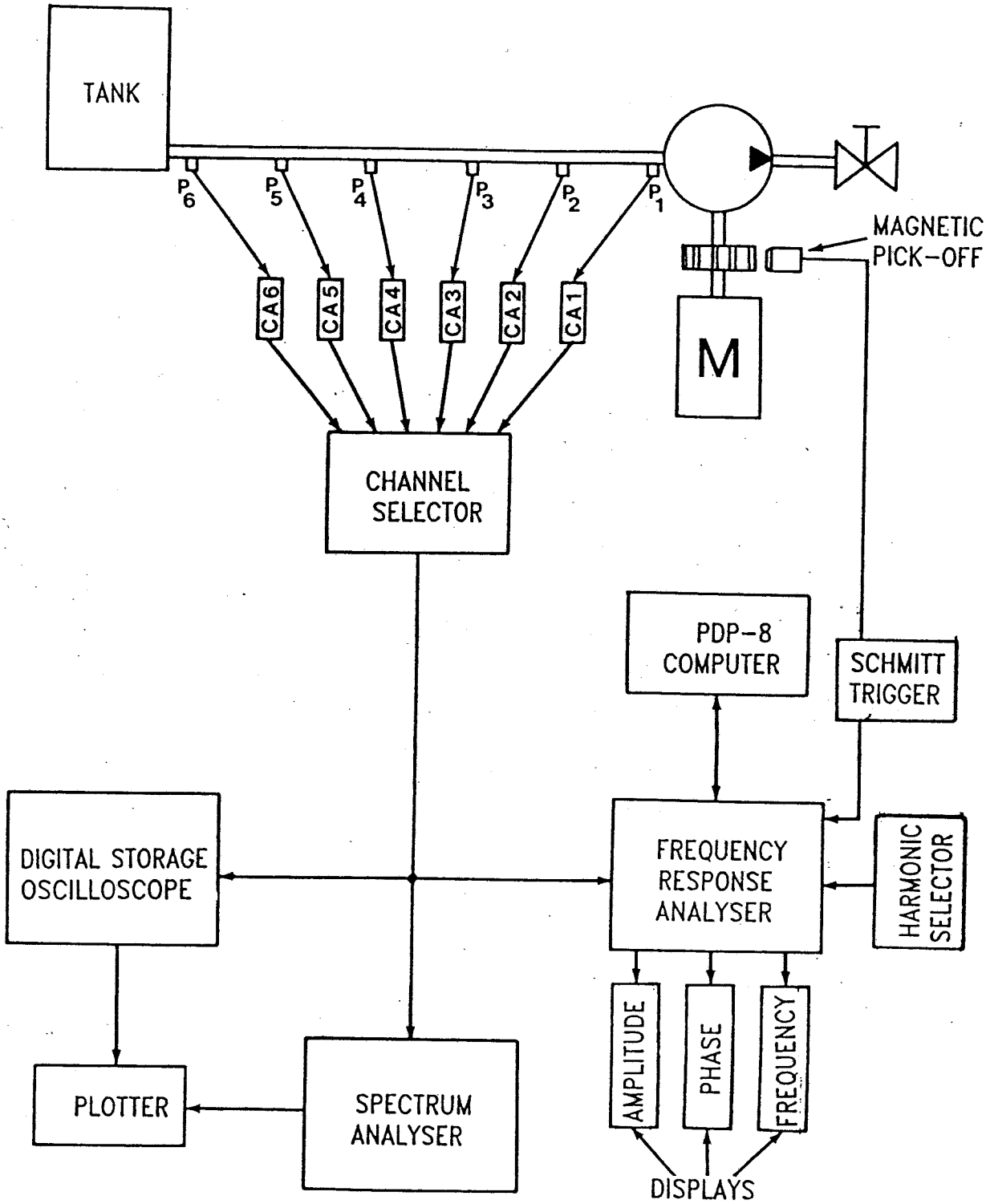

Fig. 6.2 Schematic diagram of instrumentation

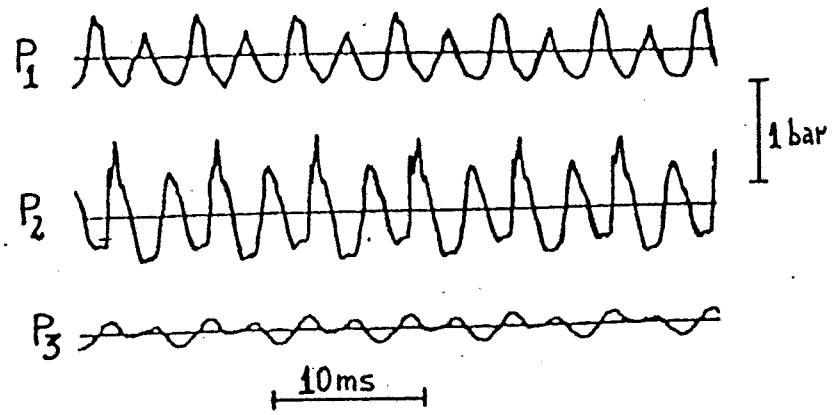

Fig. 6.3 Pressure signals measured at three points on the suction line of pump E, at atmospheric pressure (n=900 rev/min)

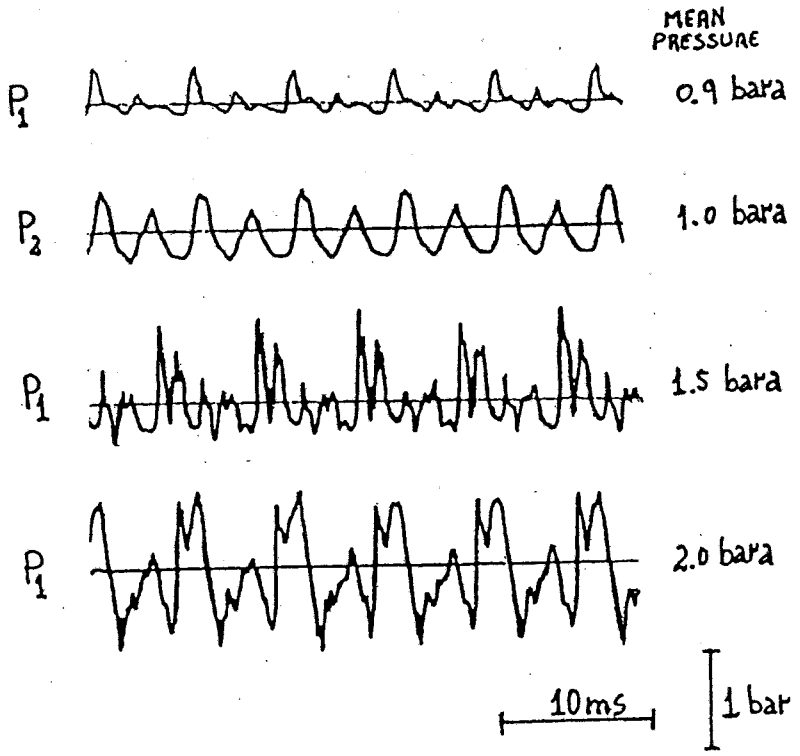

Fig. 6.4 Pressure signals measured near inlet flange of pump E, for different mean suction pressures.

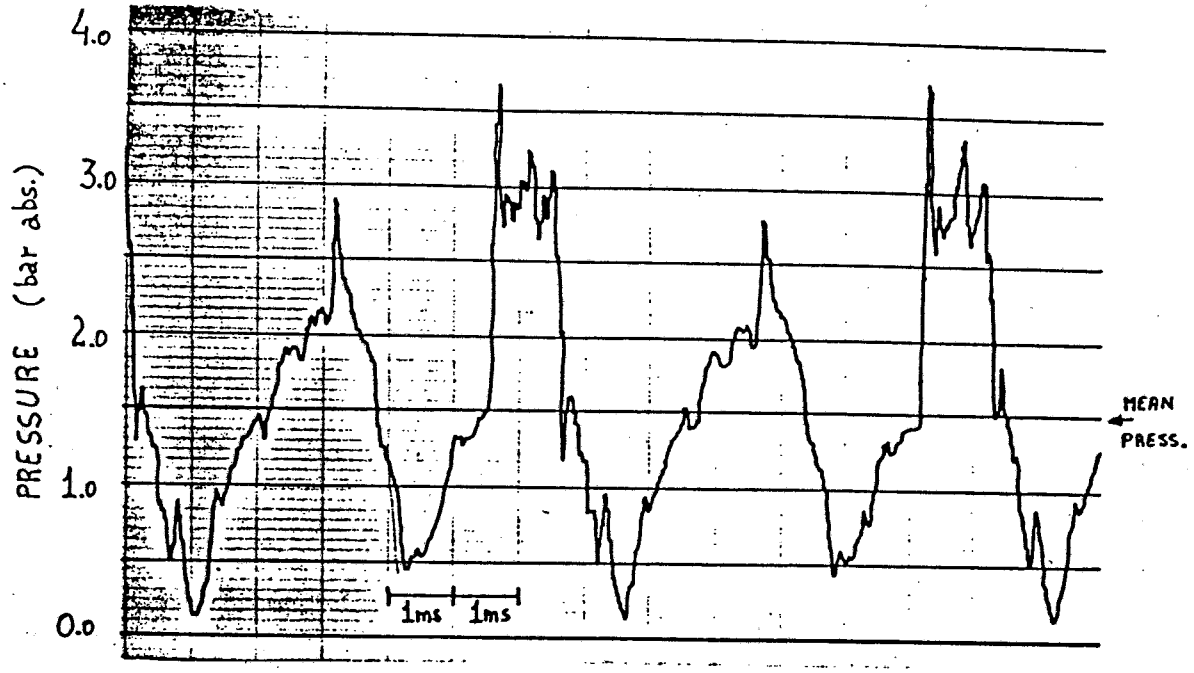

a) p = 1.5 bara ; n = 900 rev/min ; X = 1.42 m ; ℓ = 1.85 m

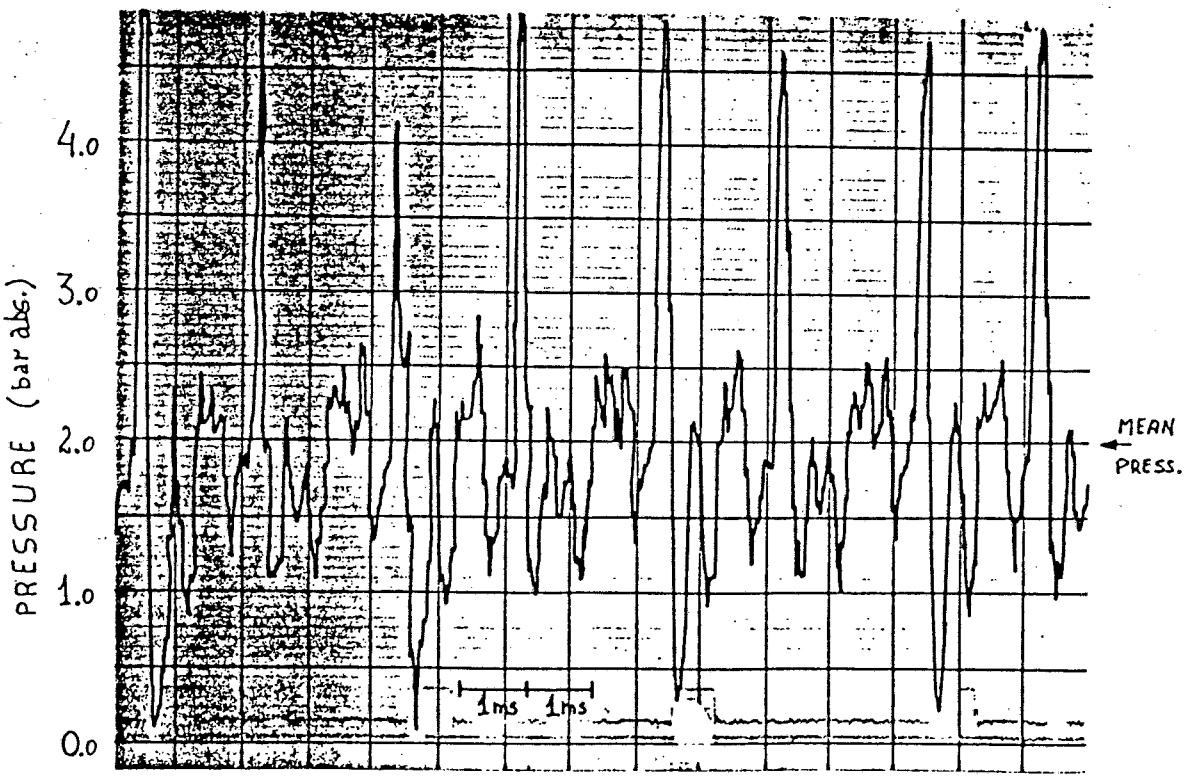

b) p = 2.0 bara ; n = 1500 rev/min ; X = 1.83 m ; ℓ = 1.85 m

Fig. 6.5 Some extreme cases of pressure fluctuation showing very low instantaneous pressures

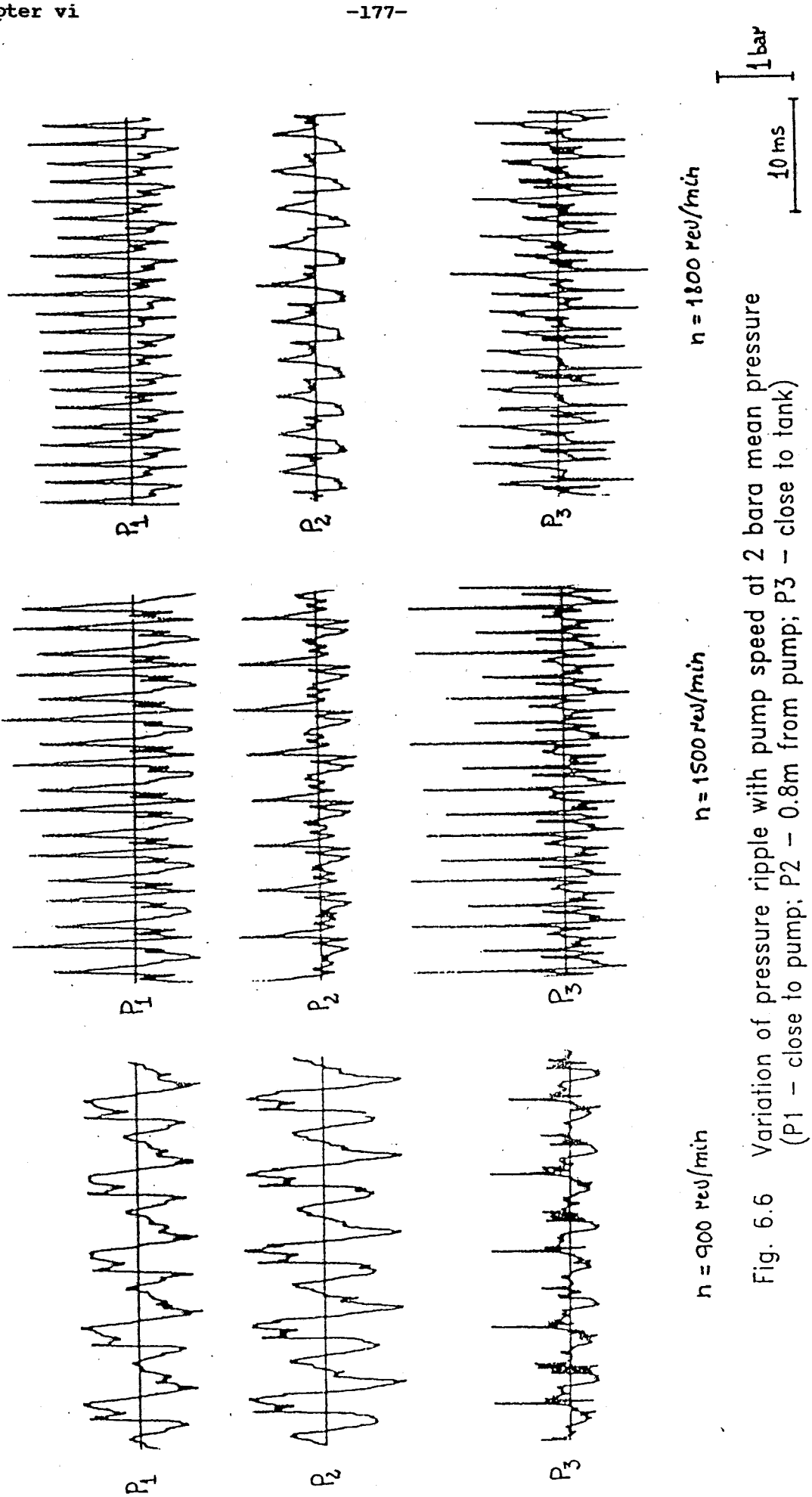

Fig. 6.6 Variation of pressure ripple with pump speed at 2 bara mean pressure
(P1 – close to pump; P2 – 0.8m from pump; P3 – close to tank)

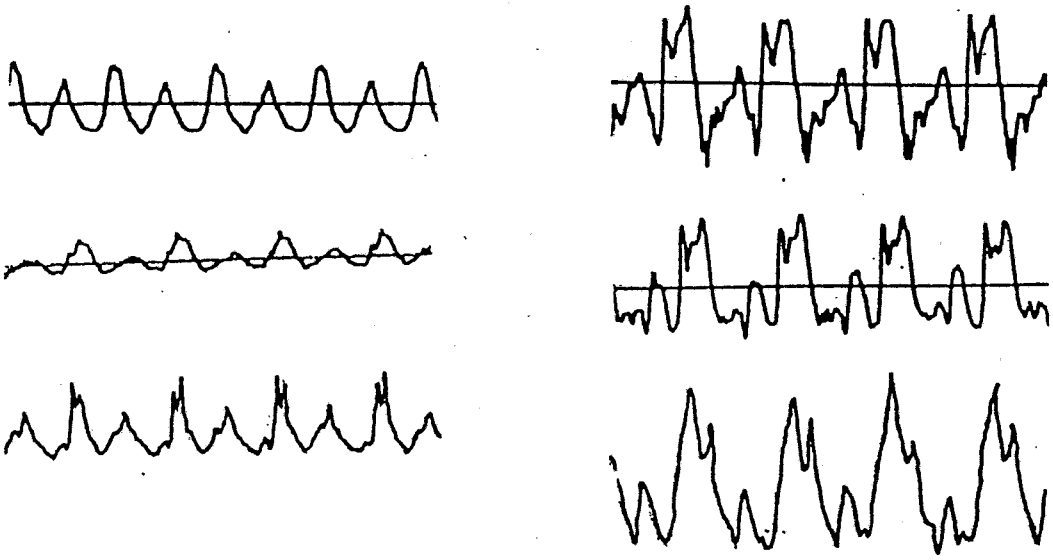

(a) 1 bara mean pressure (b) 2 bara mean pressure

Fig. 6.7 Repeatability of time domain pressure signals in the suction line of pump E (n=900 rev/min)

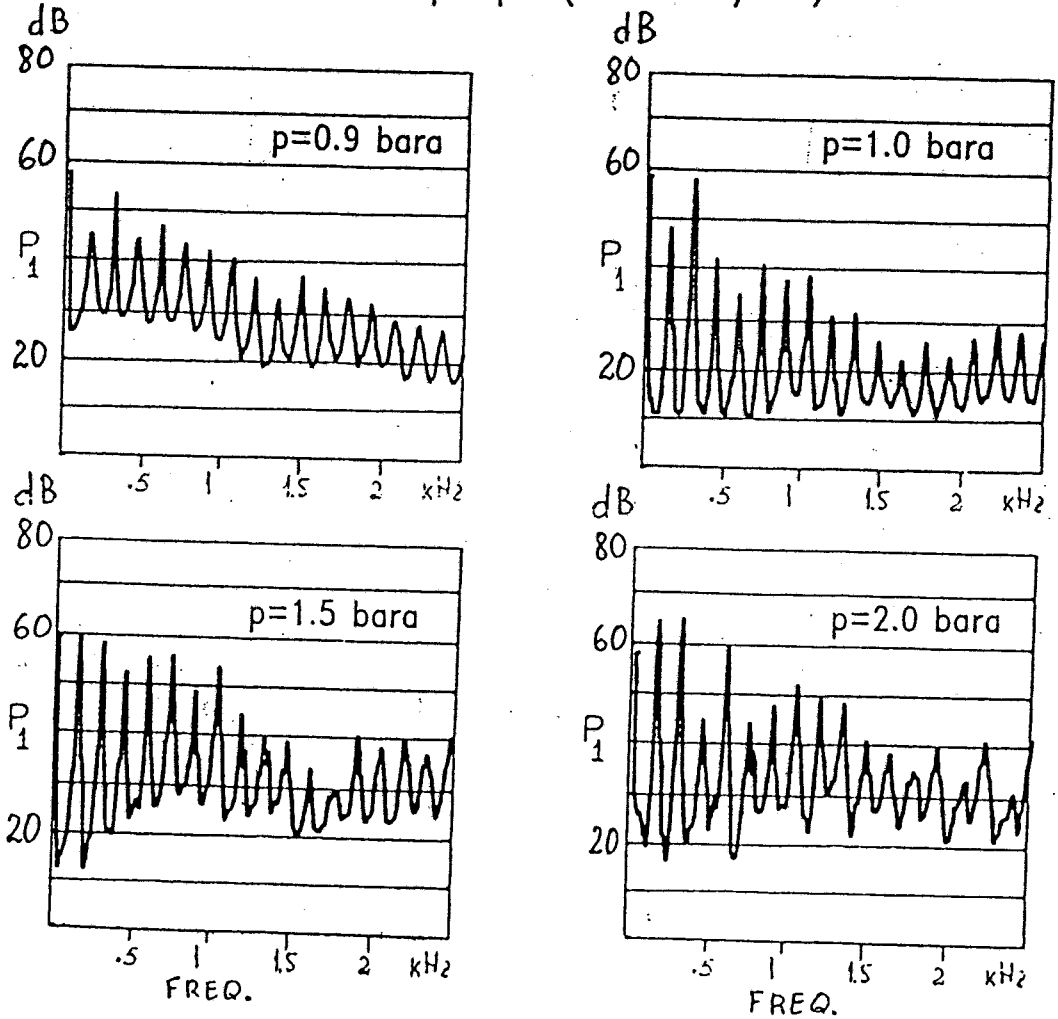

Fig. 6.8 Frequency spectra of pressure signals generated by pump E for different mean pressures (measured close to pump)

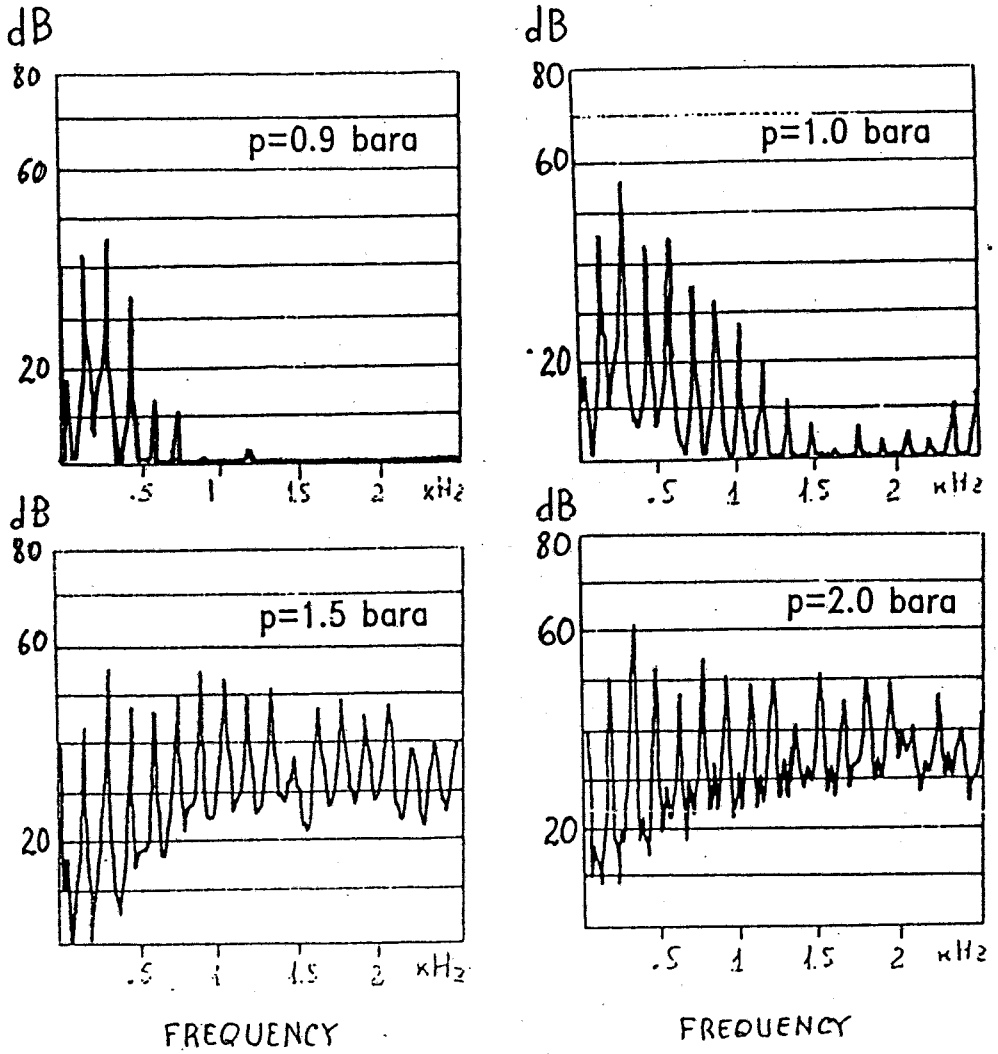

Fig. 6.9 Frequency spectra of pressure signals generated by pump E for different mean pressures (measured close to tank)

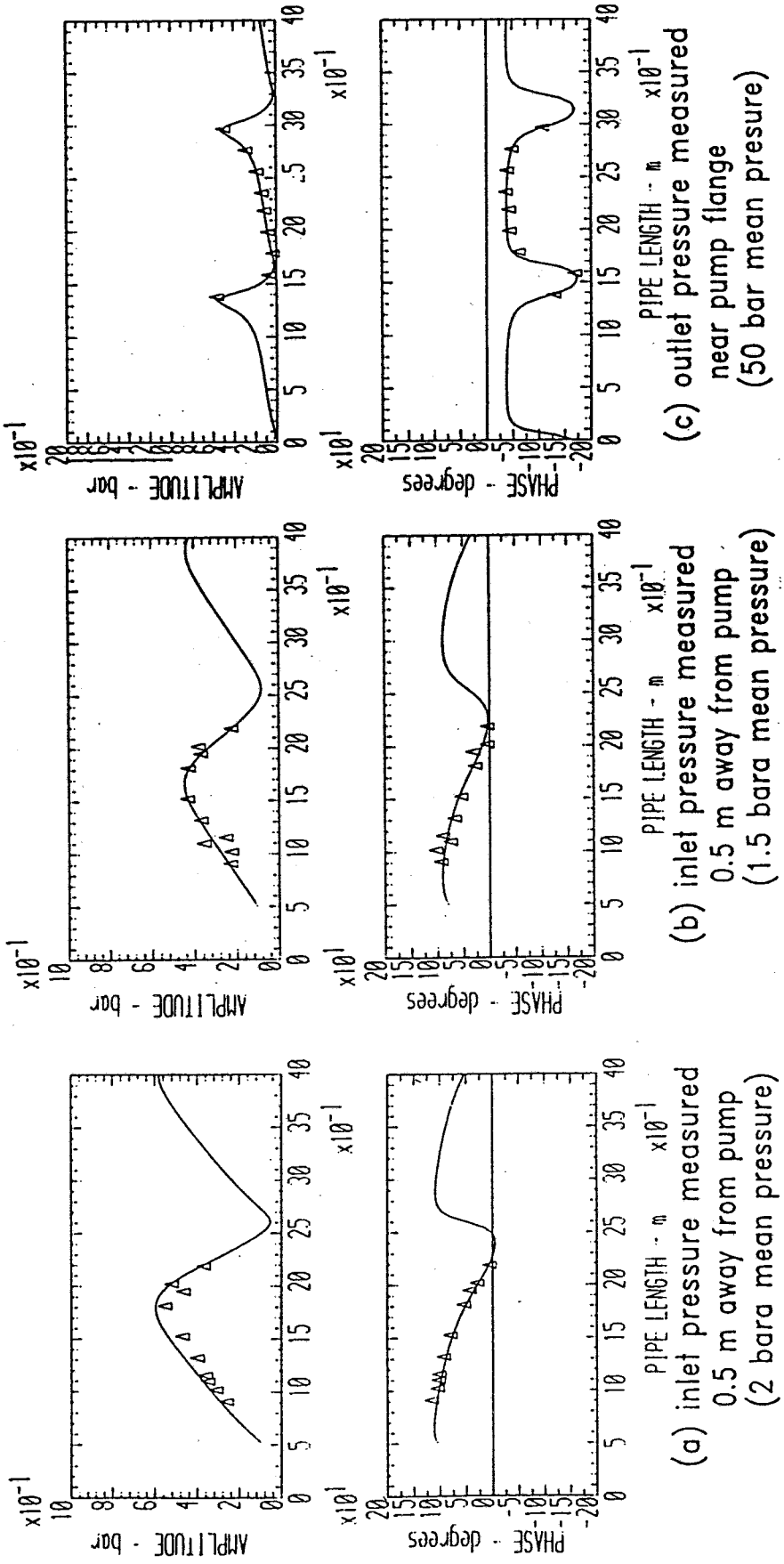

Fig. 6.10 Pressure ripple results for different lengths of line (solid line shows theoretical prediction)

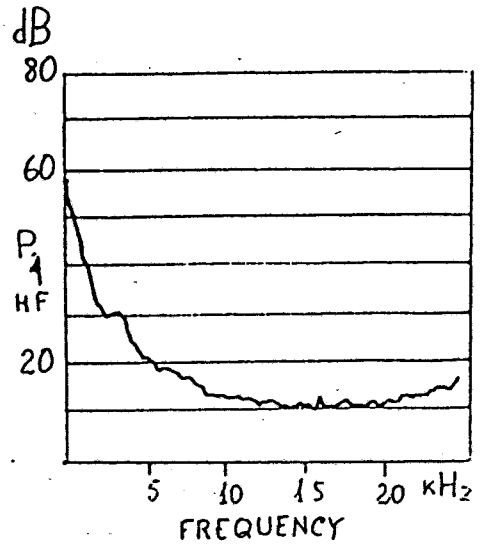

Fig. 6.11 25 kHz frequency spectrum of pressure signal

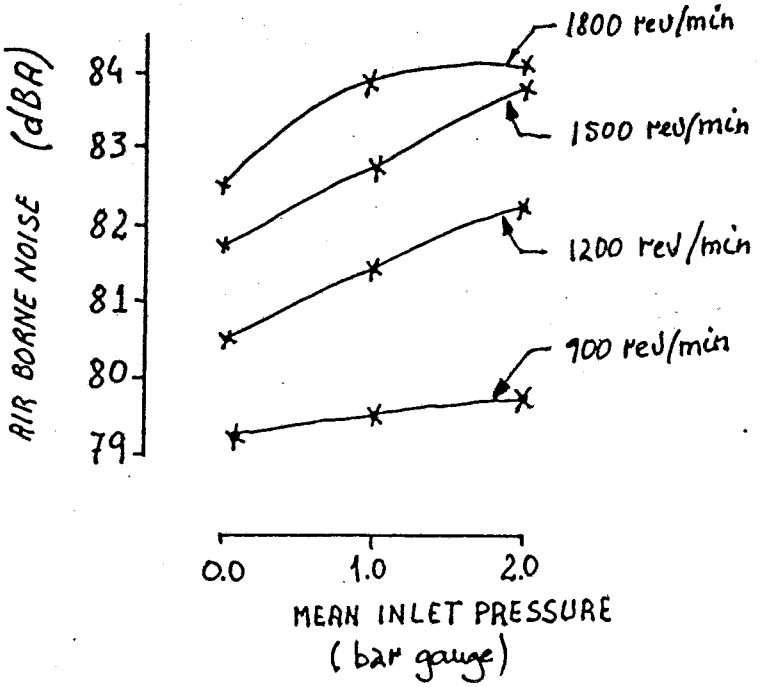

Fig. 6.12 Air borne noise results for pump E measured at 1 m away from pump

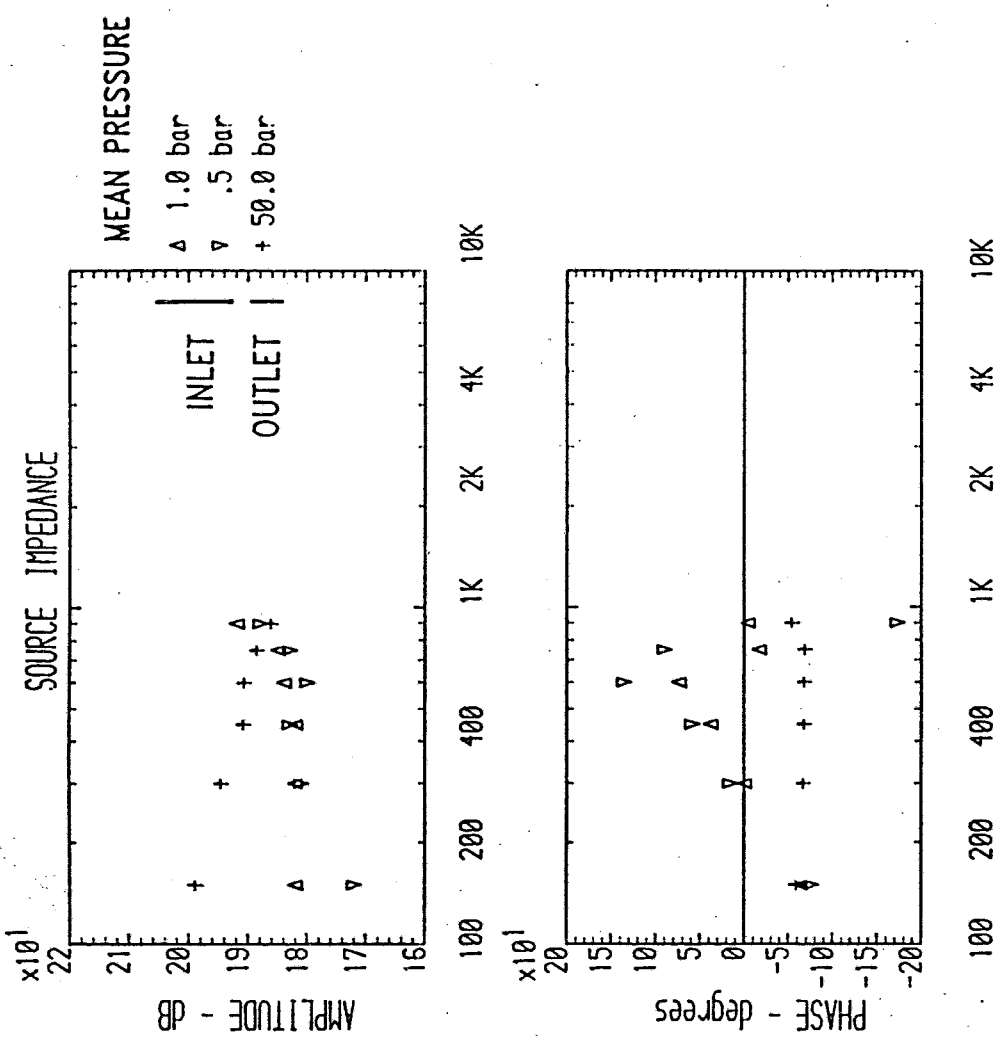

Fig. 6.14 Inlet and outlet source impedance of pump E at different mean pressures

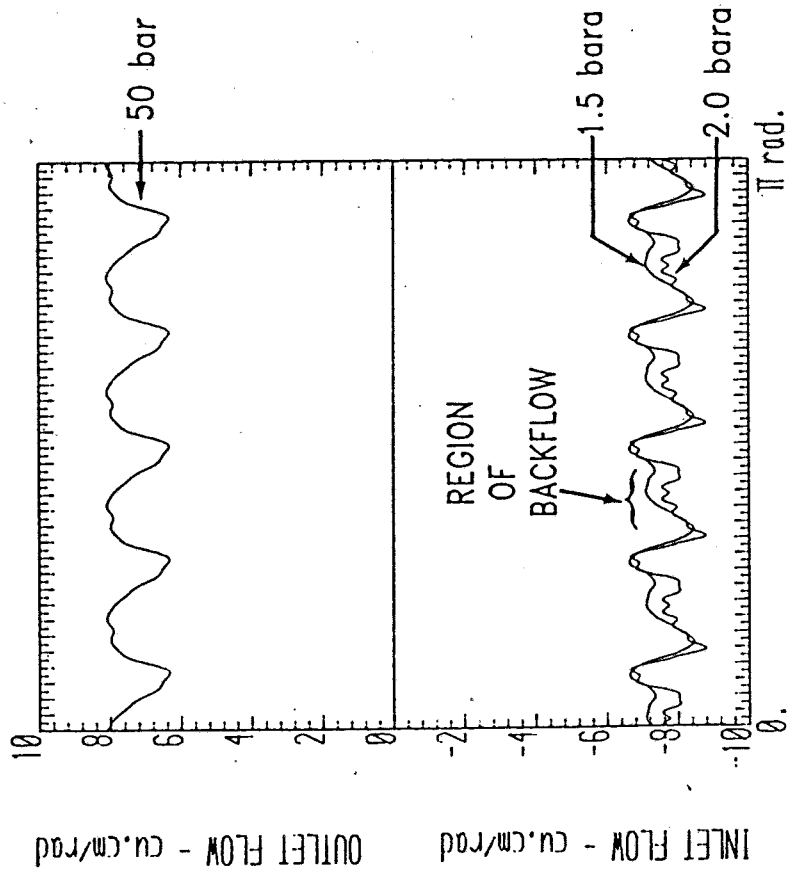

Fig. 6.13 Inlet and outlet source flows of pump E at different mean pressures

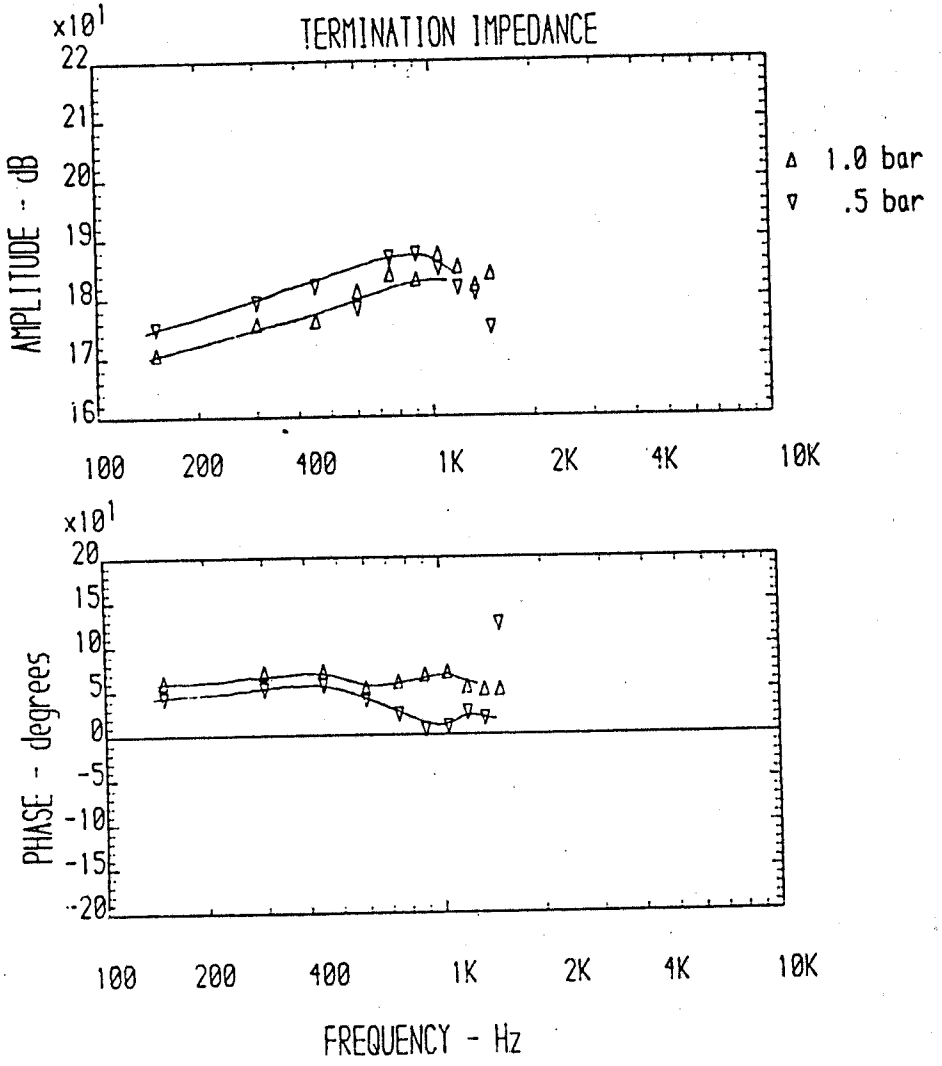

Fig. 6.15 Variation of tank impedance with mean pressure for a mean flow of 42 ℓ/min.

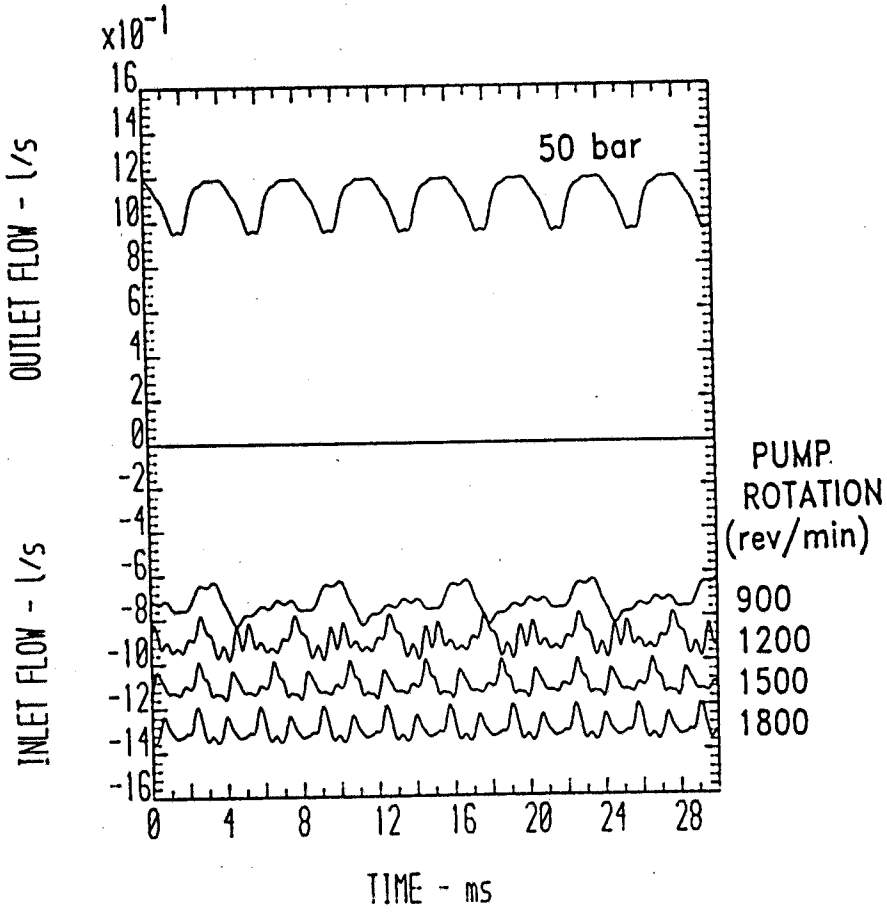

Fig. 6.16 Source flow of pump E at 2 bara mean inlet pressure, for different running speeds

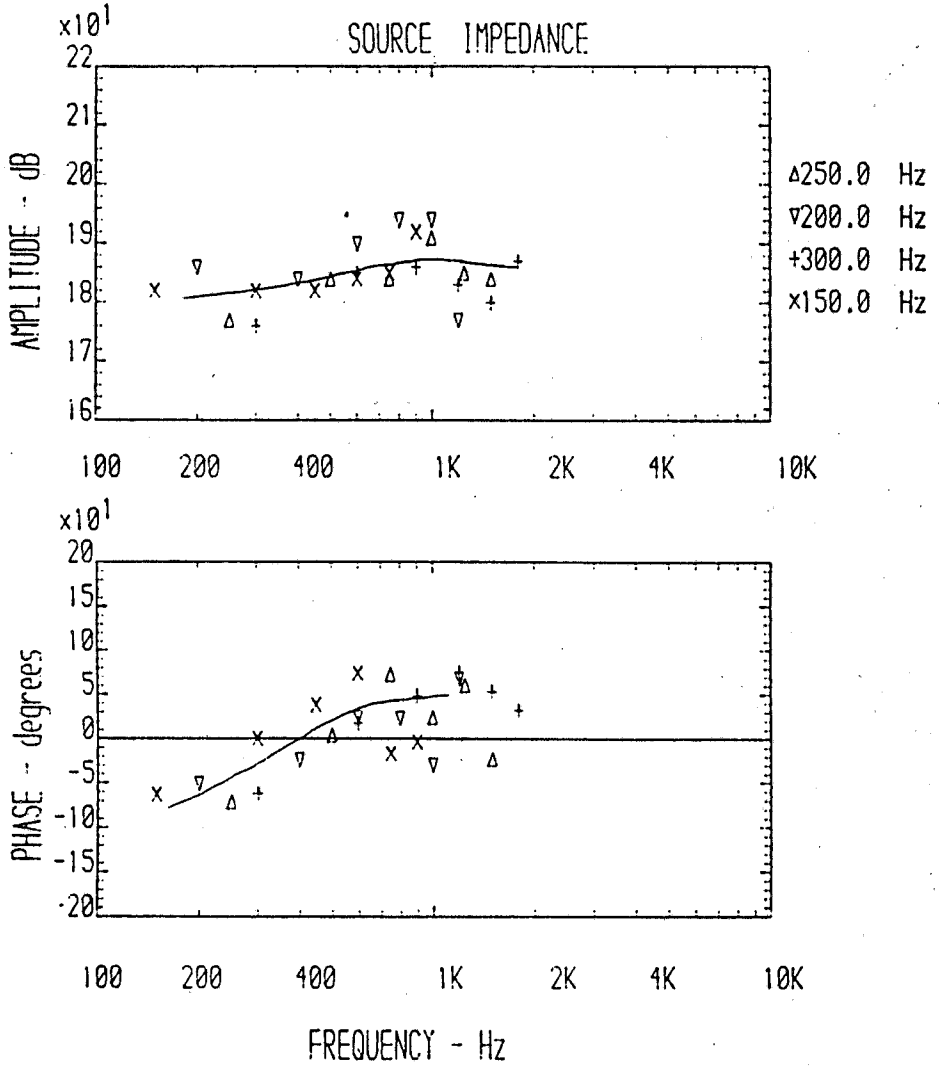

Fig. 6.17 Inlet source impedance of pump E at 2 bara mean inlet pressure, for different running speeds

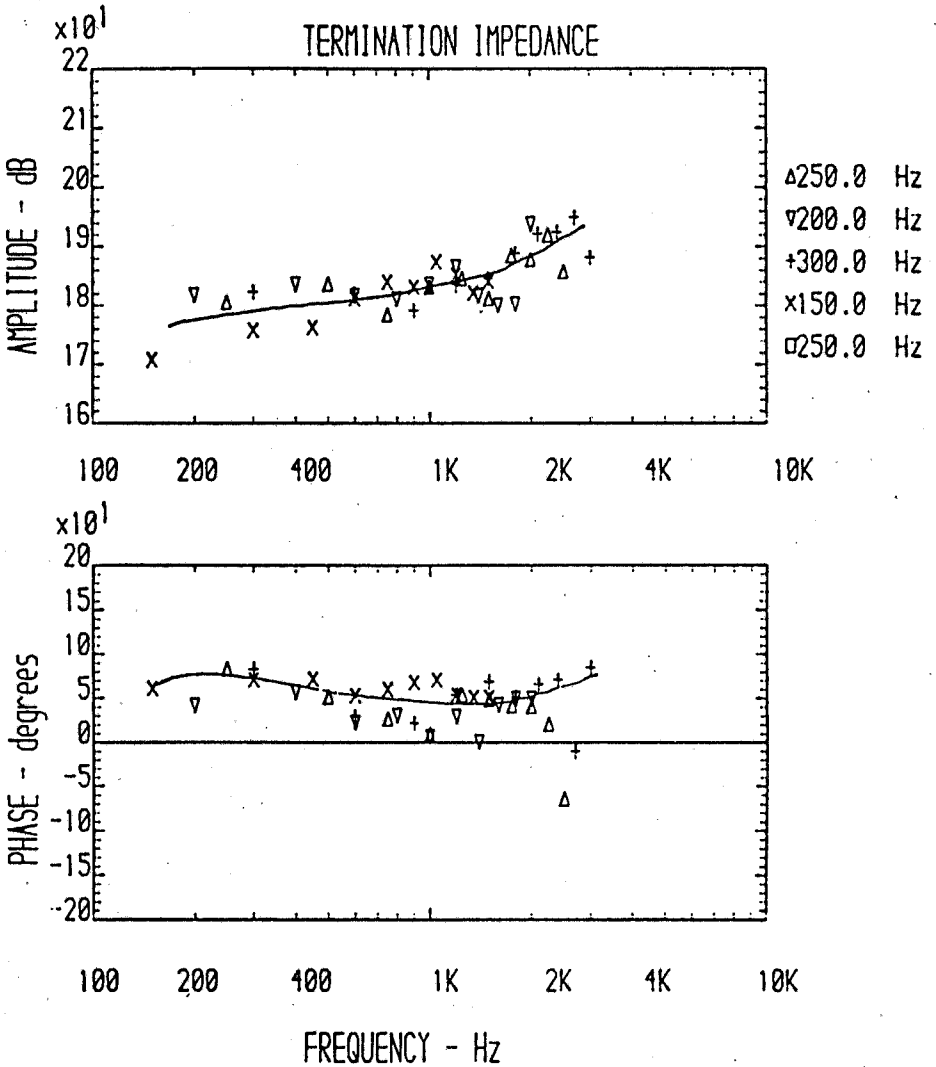

Fig. 6.18 Variation of tank impedance with pump rotating speed (different flows) for constant mean inlet pressure (2 bara)

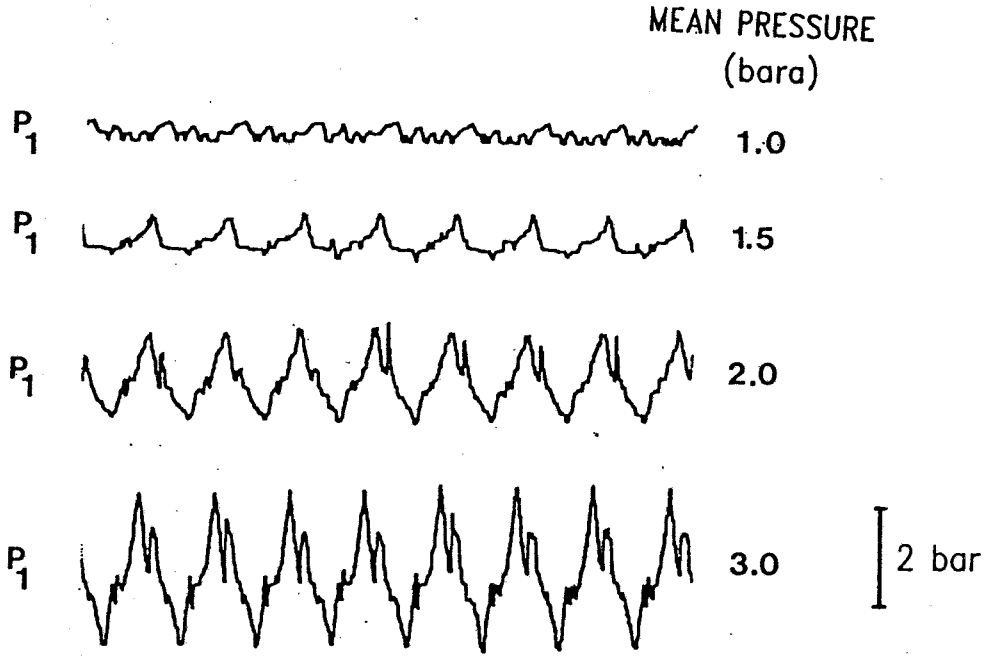

Fig. 6.19 Pressure ripple variation with mean inlet pressure, for pump C (measured close to the pump inlet flange)

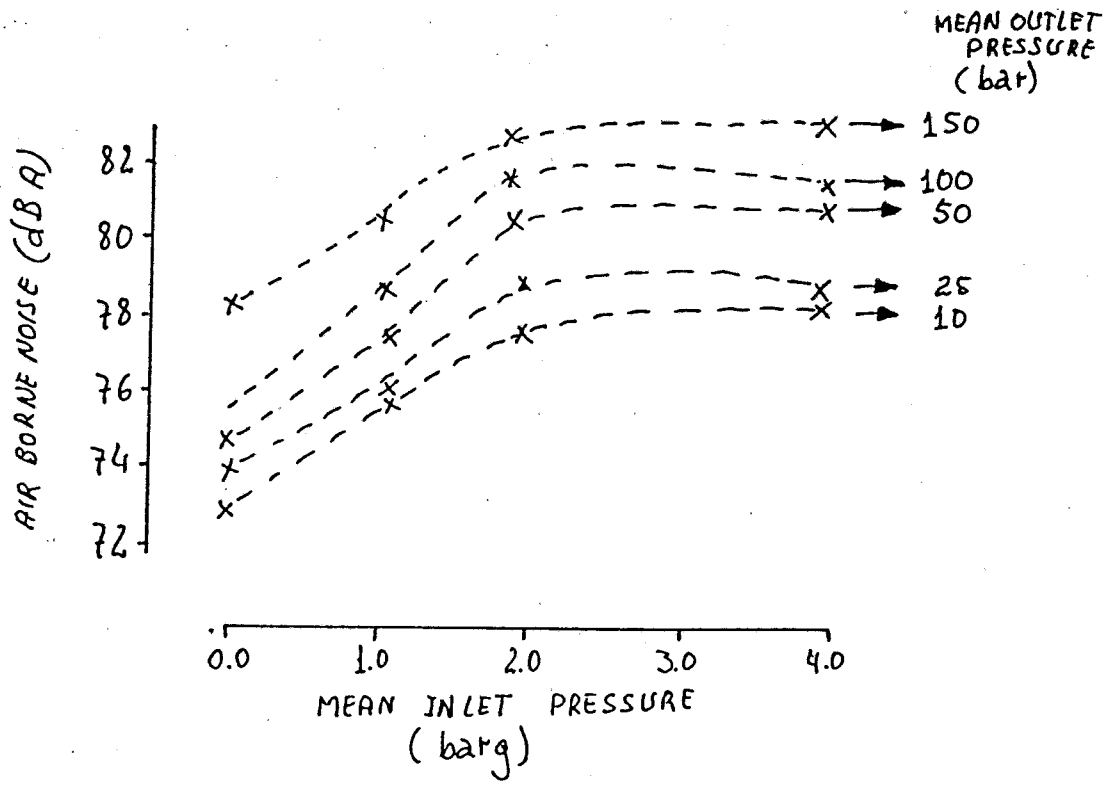

Fig. 6.20 Air borne noise results for pump C

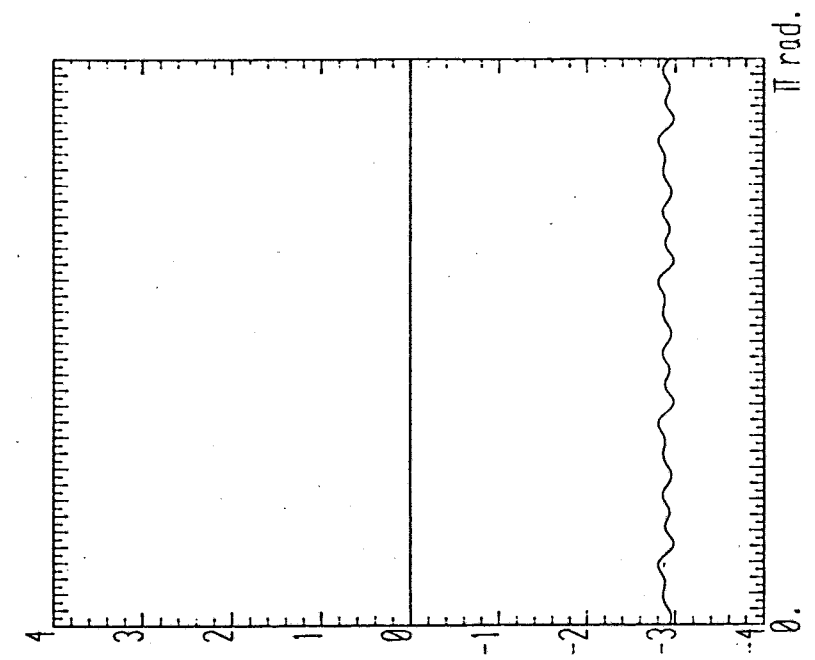

Fig. 6.22 Inlet source flow of pump C at atmospheric mean inlet pressures (n=1500 rev/min)

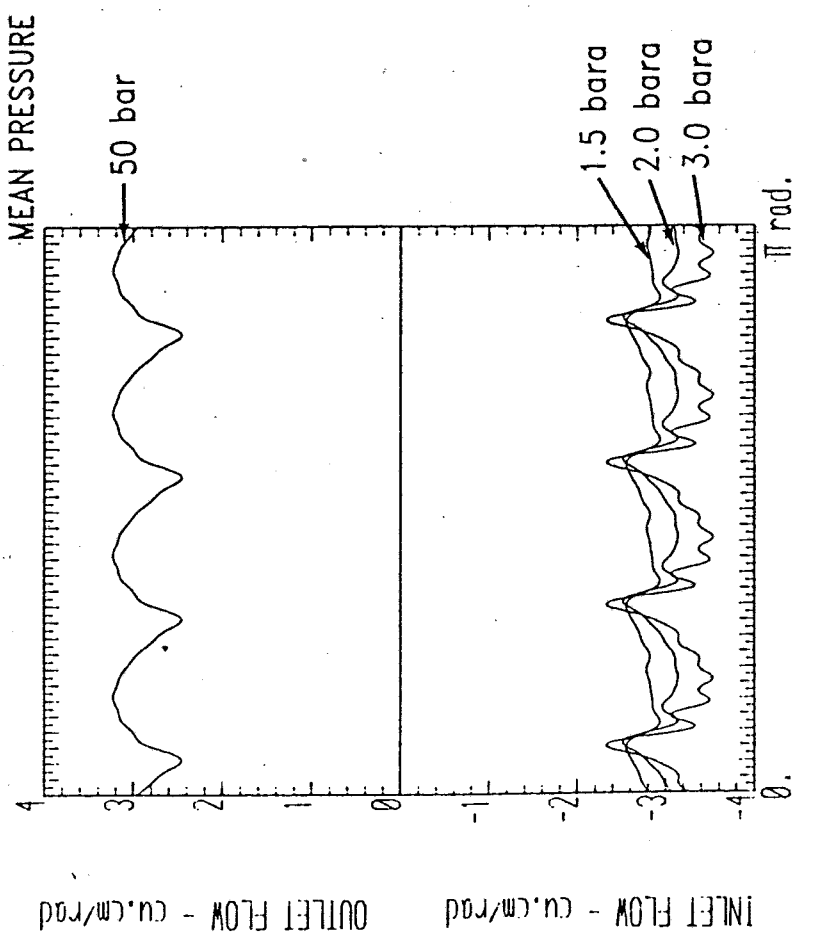

Fig. 6.21 Source flow of pump C for different mean inlet pressures (n=1500 rev/min)

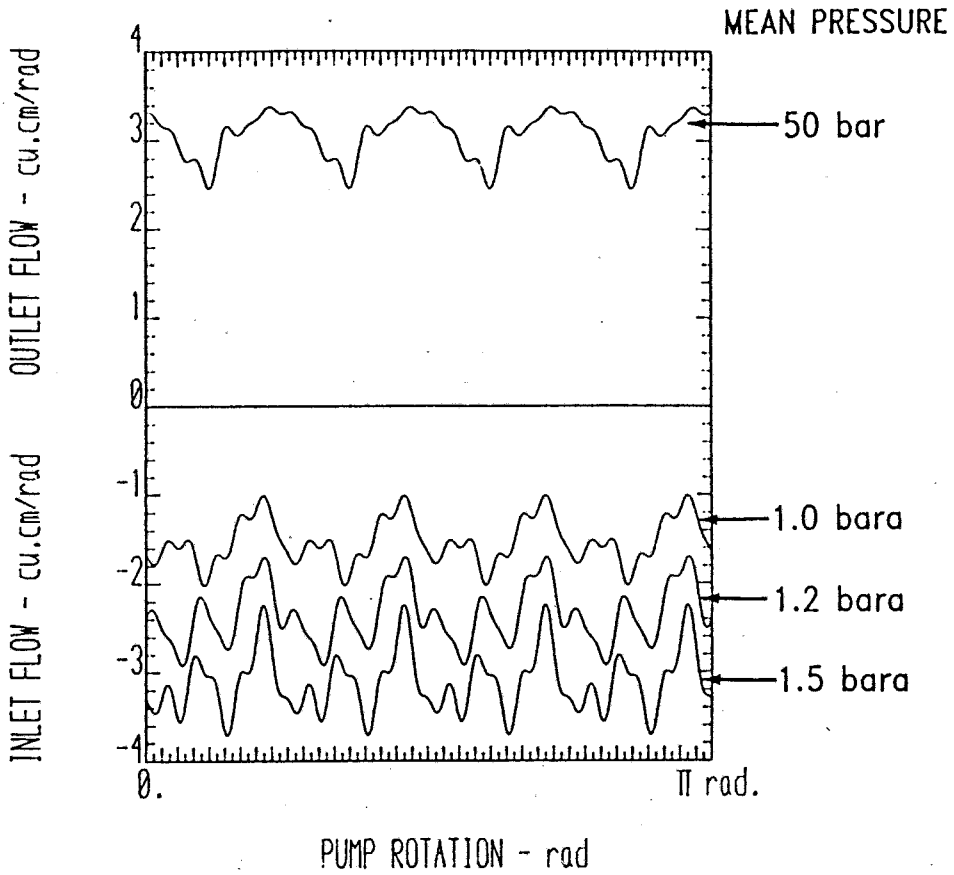

Fig. 6.23 Inlet and outlet source flows of pump C'

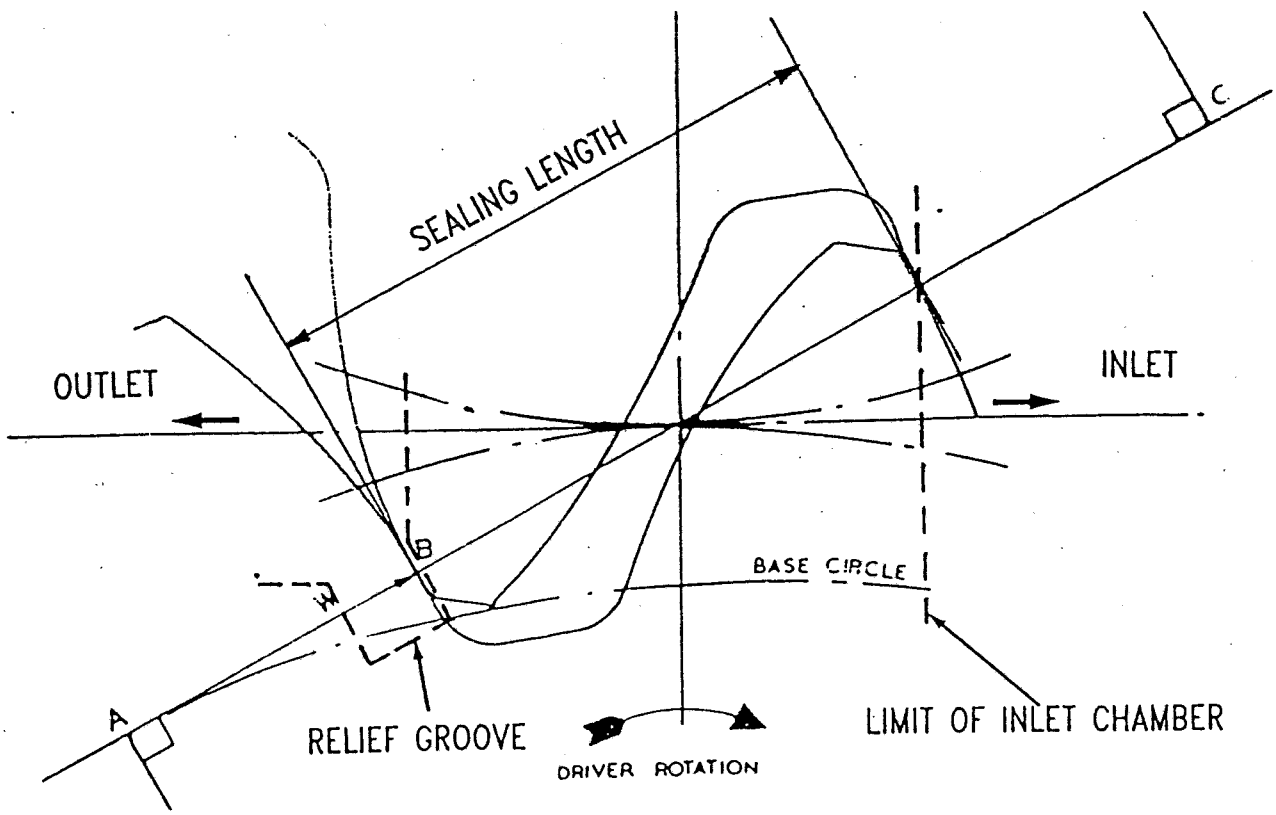

Fig. 6.24 Detail of gear pump relief groove arrangement

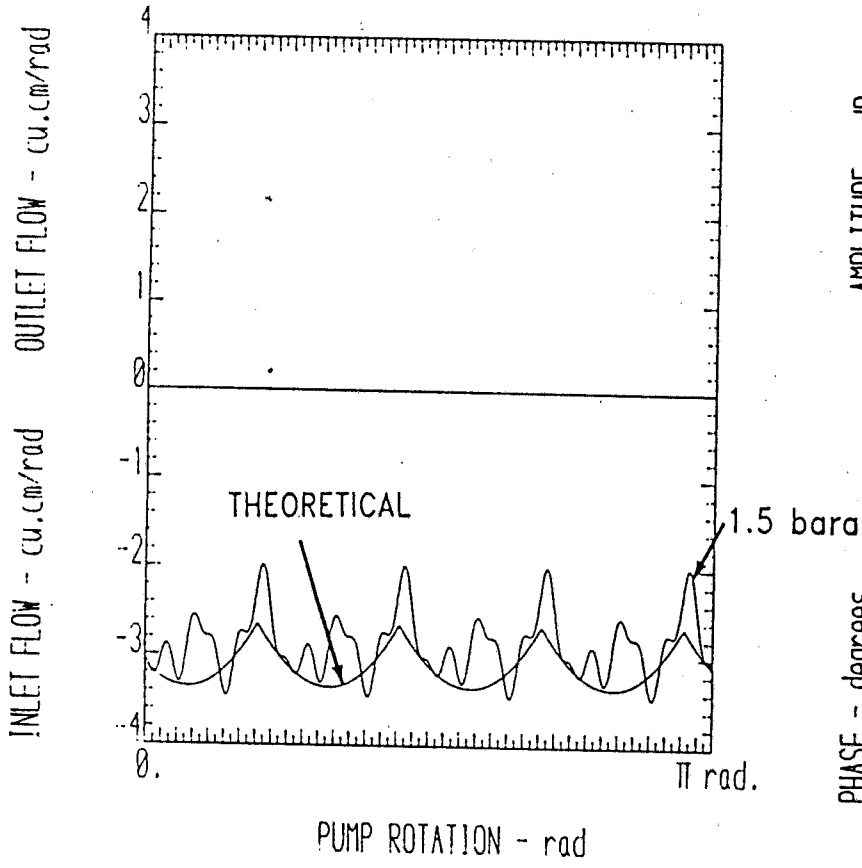

Fig. 6.25 Comparison between actual source flow of pump C' and theoretical pump displacement

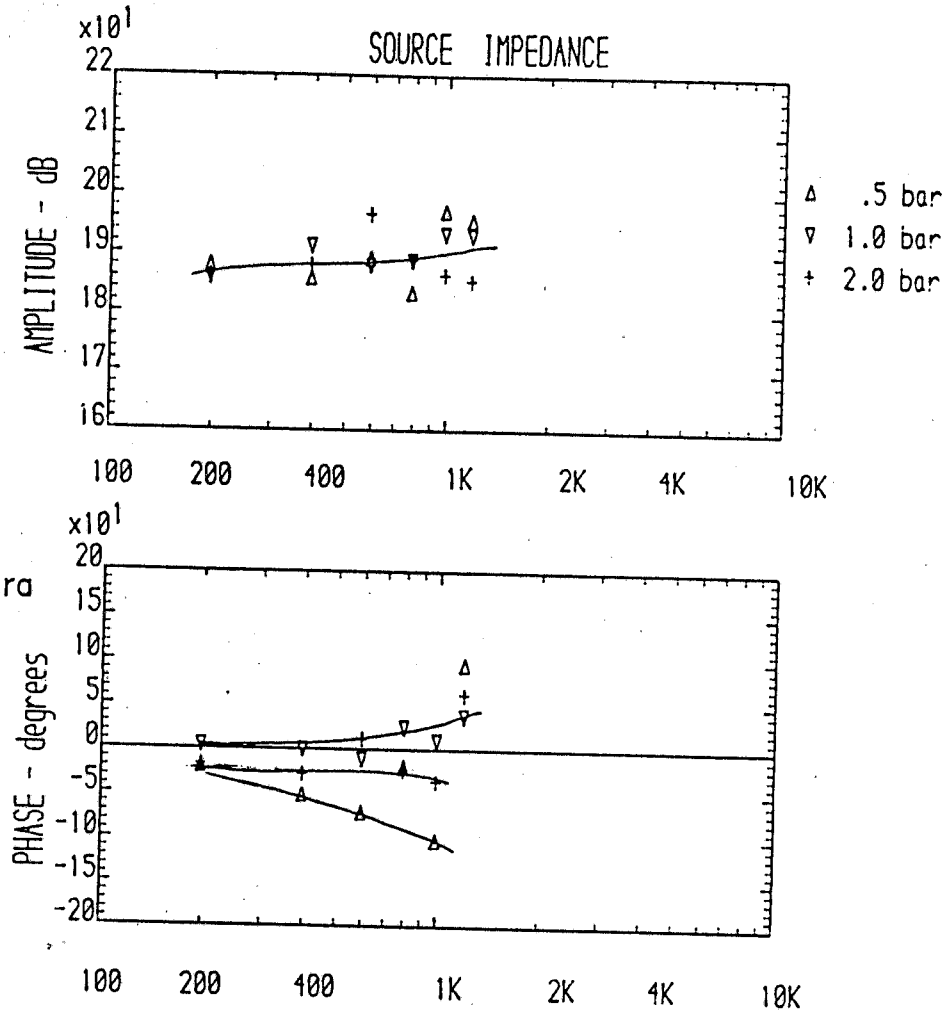

Fig. 6.26 Inlet impedance of pump C (n=1500 rev/min)

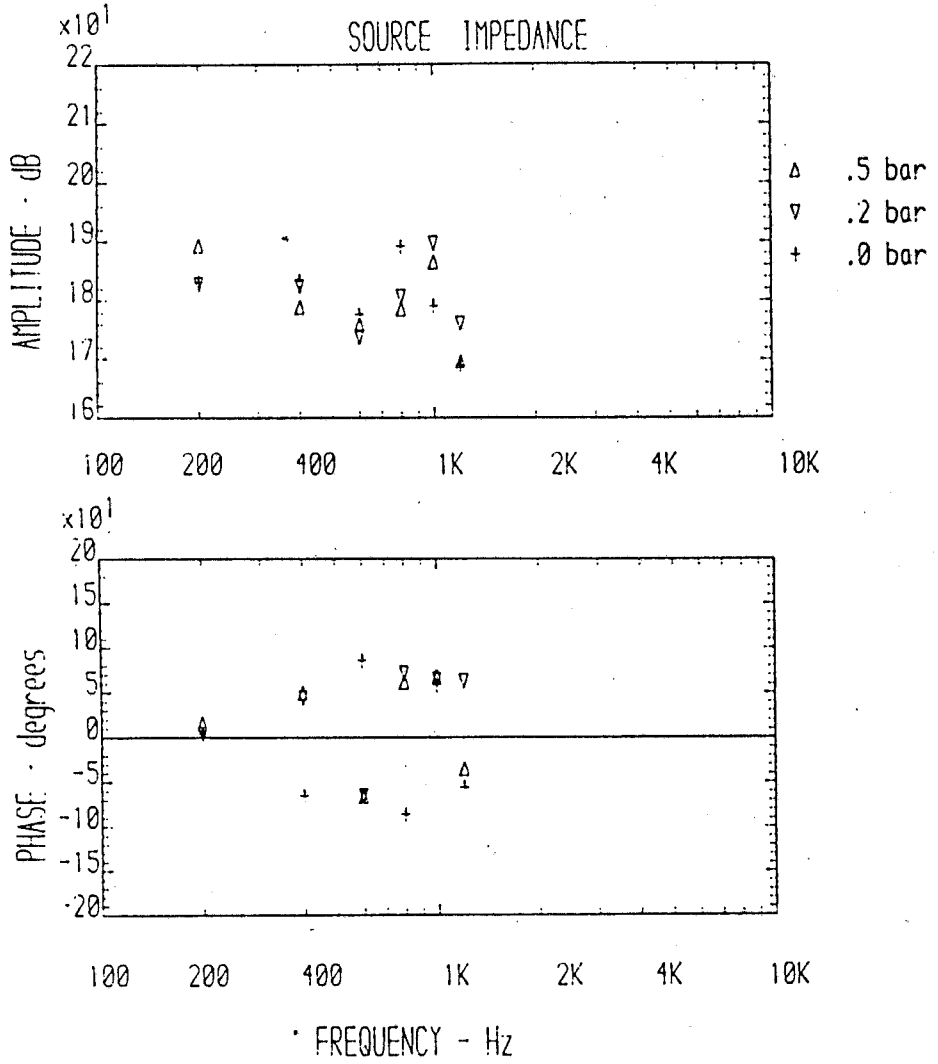

Fig. 6.27 Inlet source impedance of pump C'

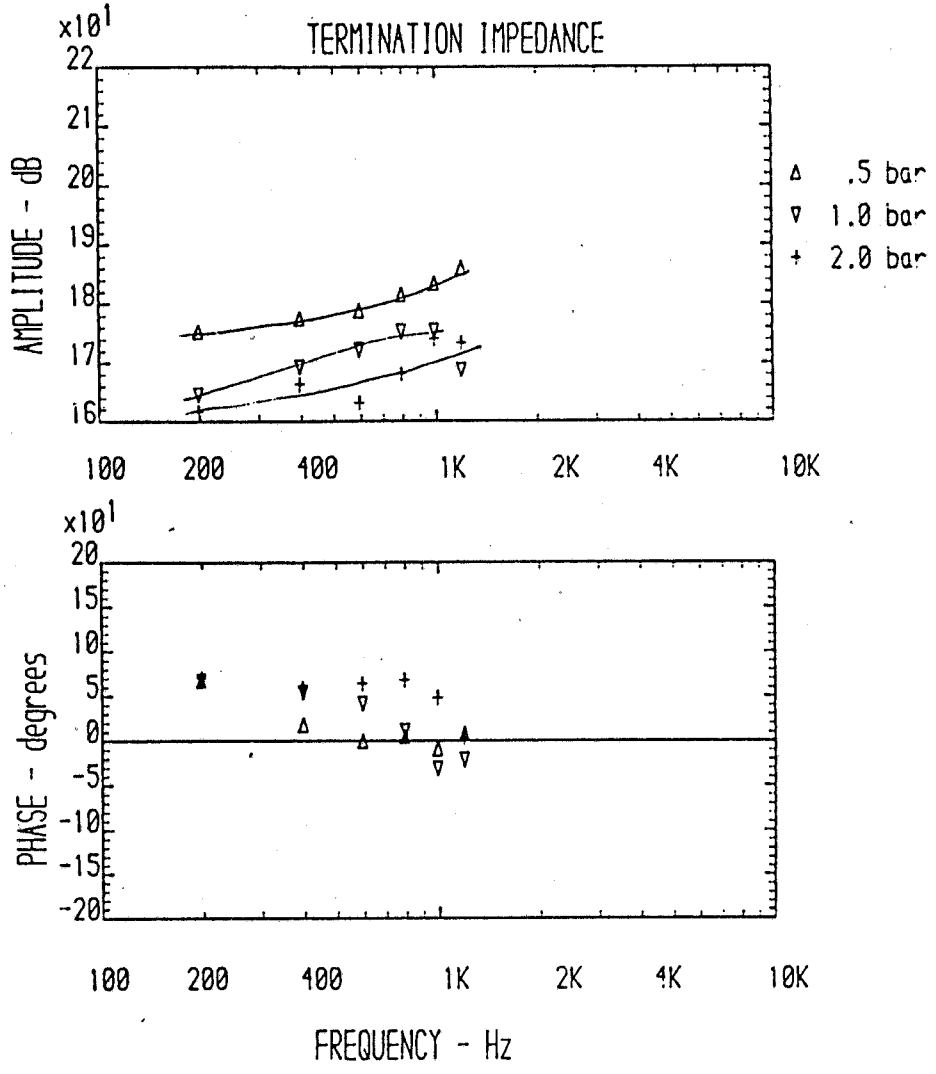

Fig. 6.28 Tank impedance evaluated from tests of pump C

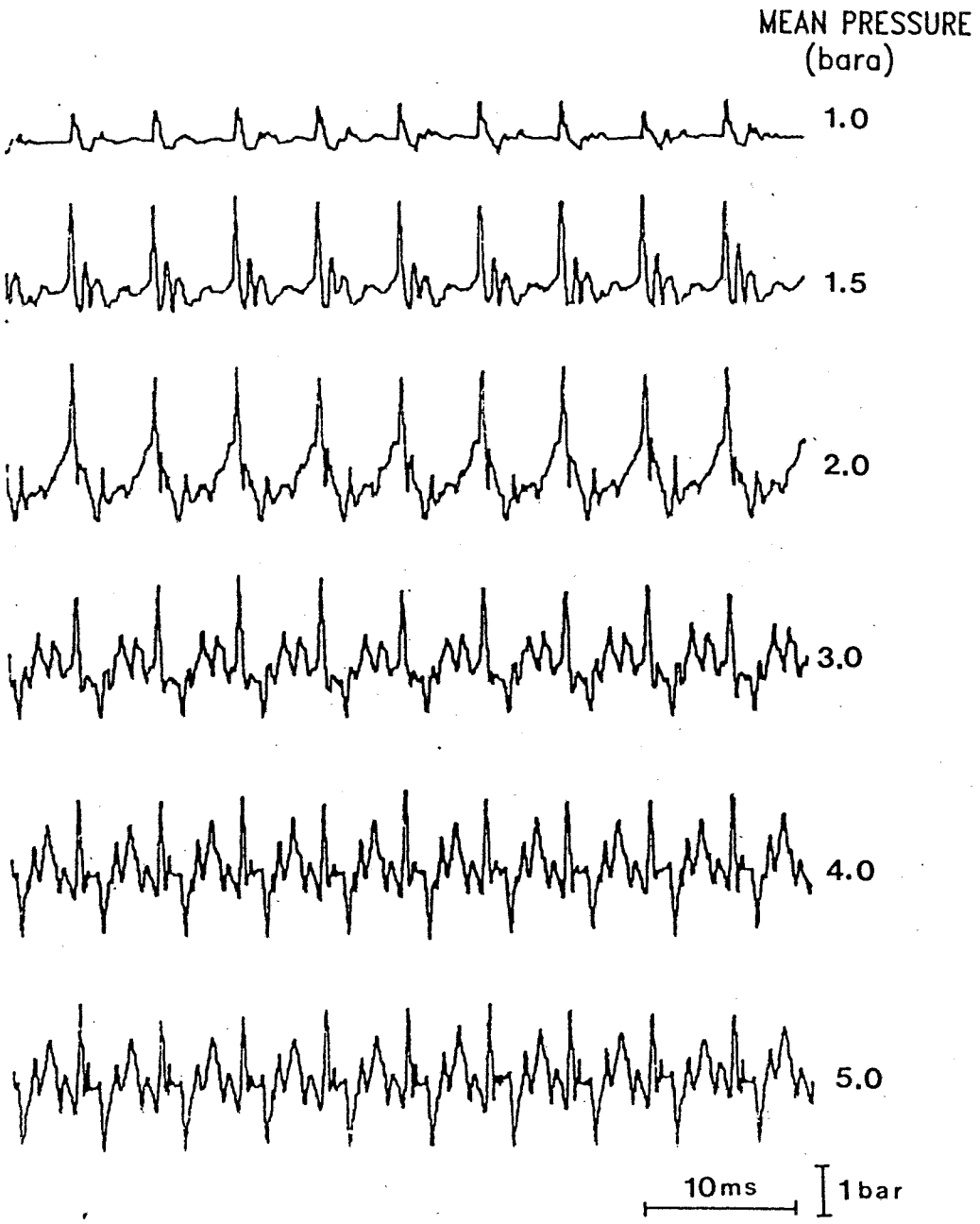

Fig. 6.29 Pressure ripple generated at a point in the suction line of axial piston pump A for varying mean pressures
(n=1500 rev/min ; outlet press= 100 bar)

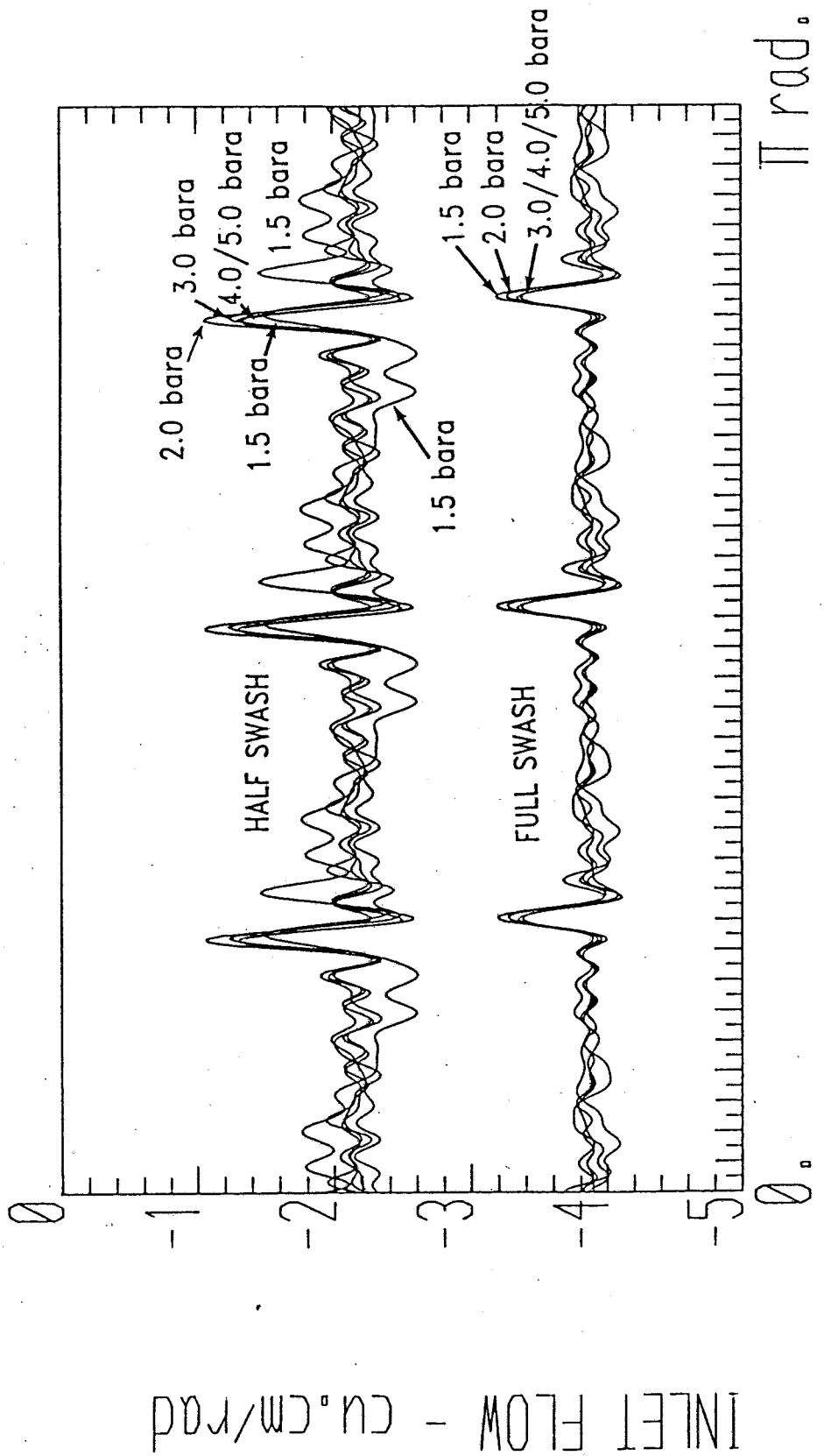

Fig. 6.30 Variation of source flow of pump A for different swash setting and mean inlet pressure
(n=1500 rev/min ; outlet press= 100 bar)

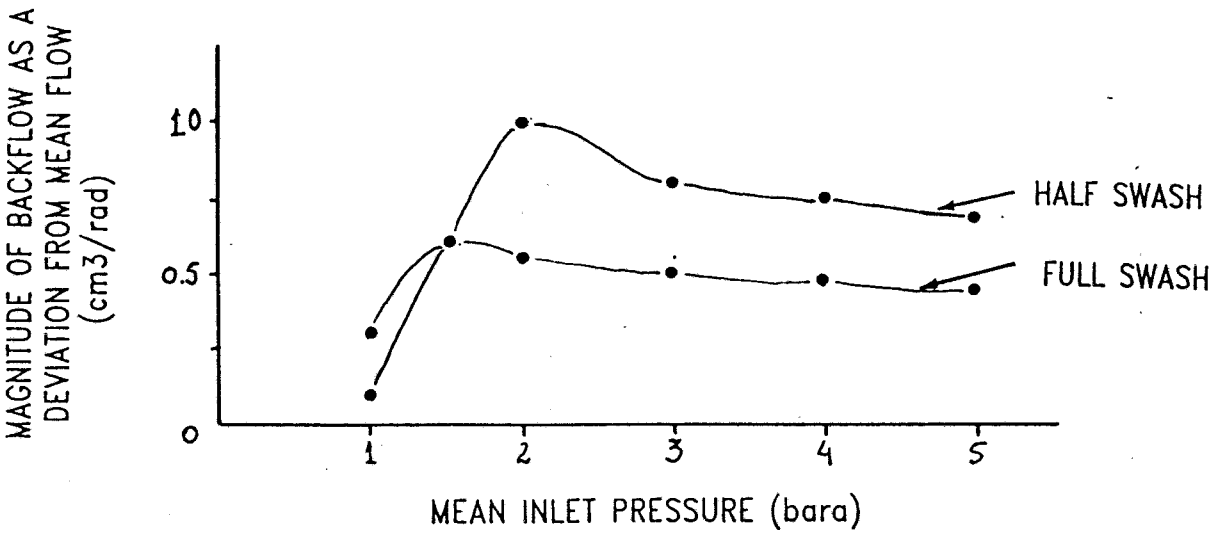

Fig. 6.31 Variation of backflow generated by pump A with mean pressure

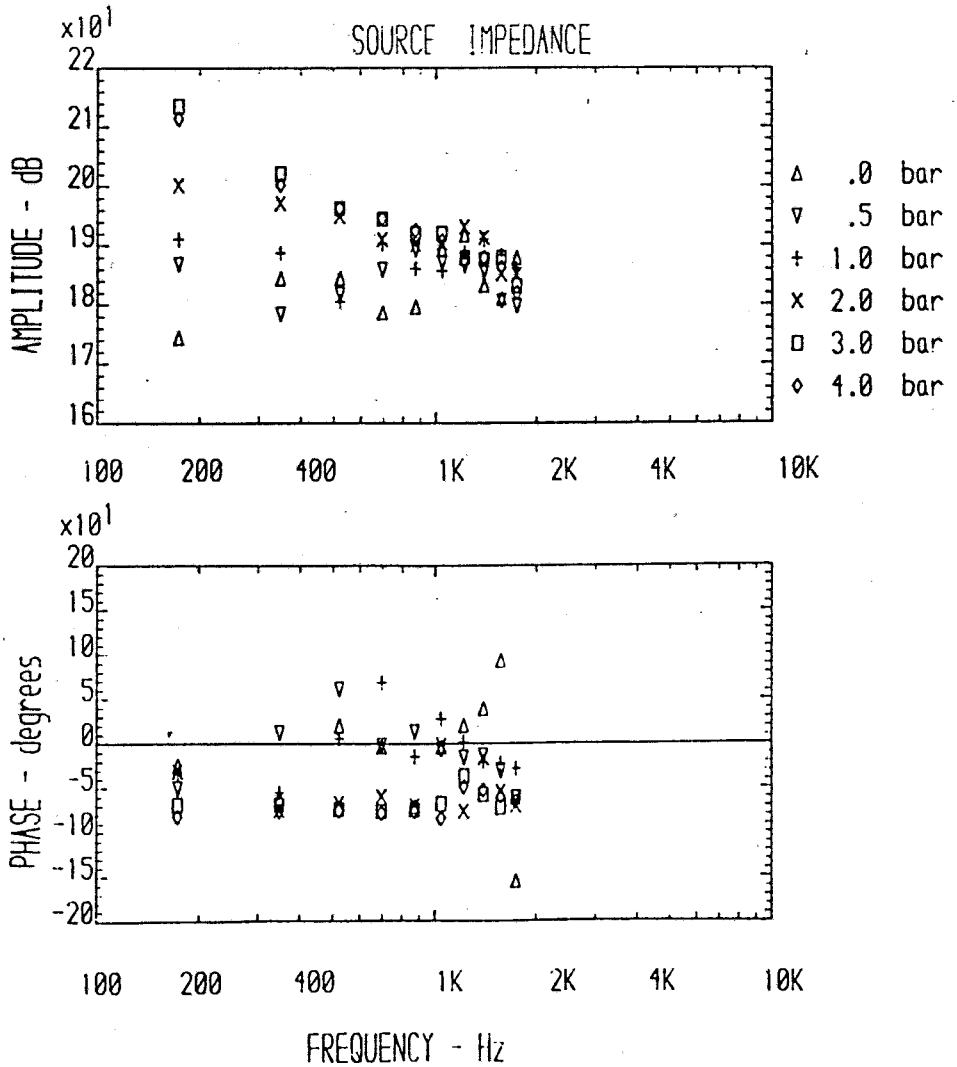

Fig. 6.32 Inlet impedance of pump A at full swash setting

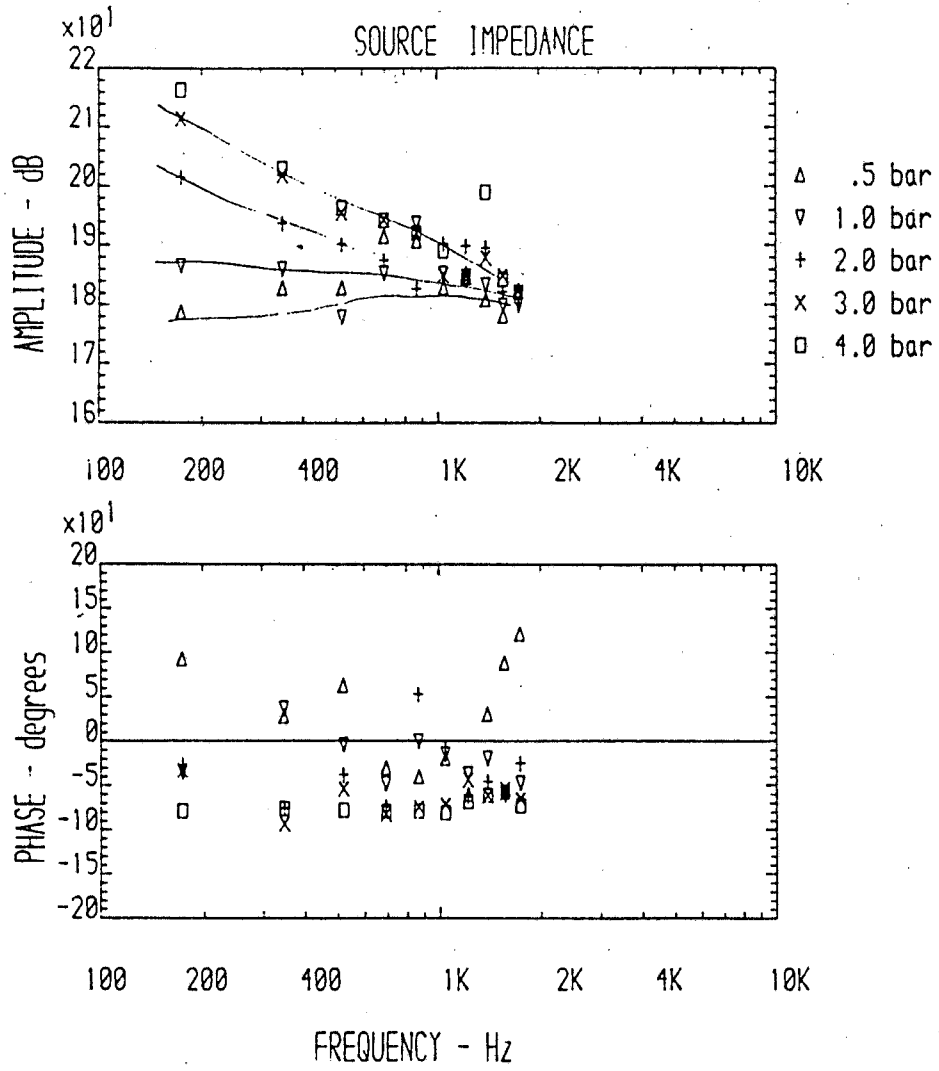

Fig. 6.33 Impedance of pump A at half swash setting

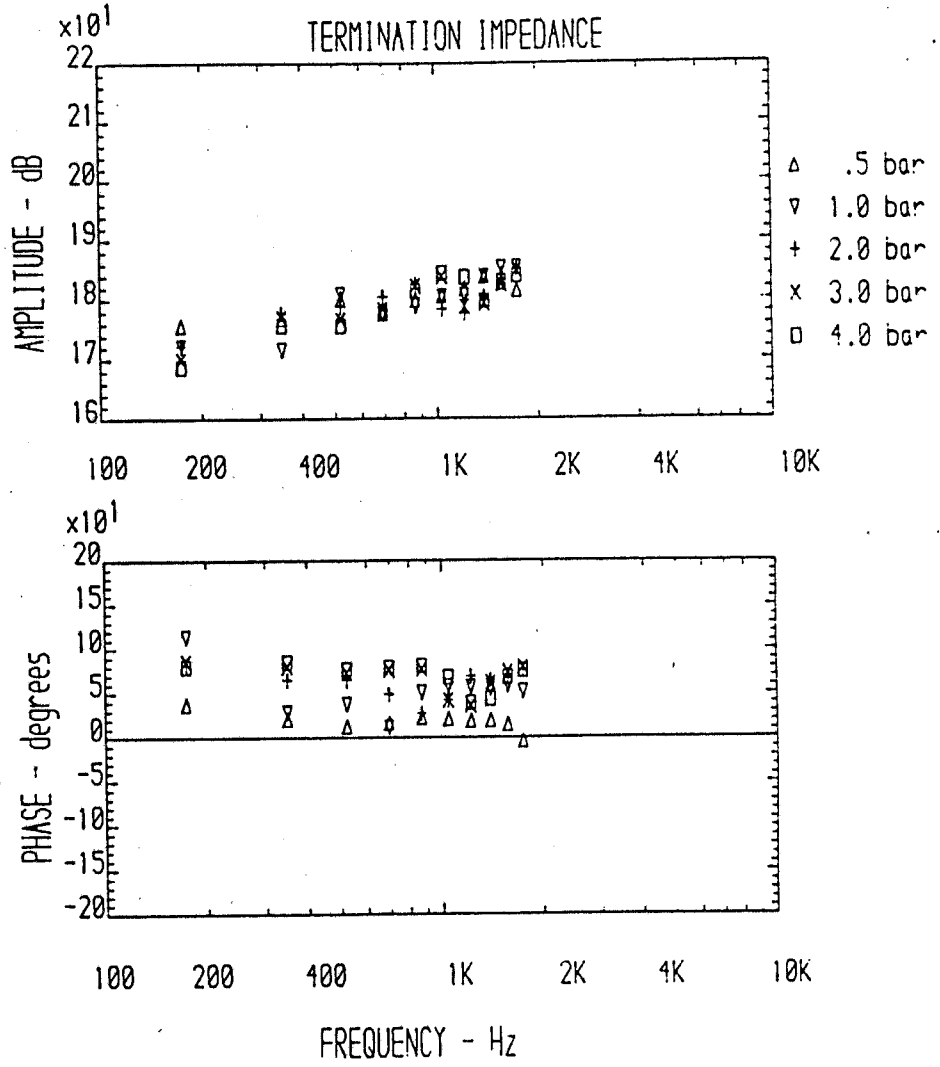

Fig. 6.34 Impedance of tank evaluated from test of pump A at half swash setting

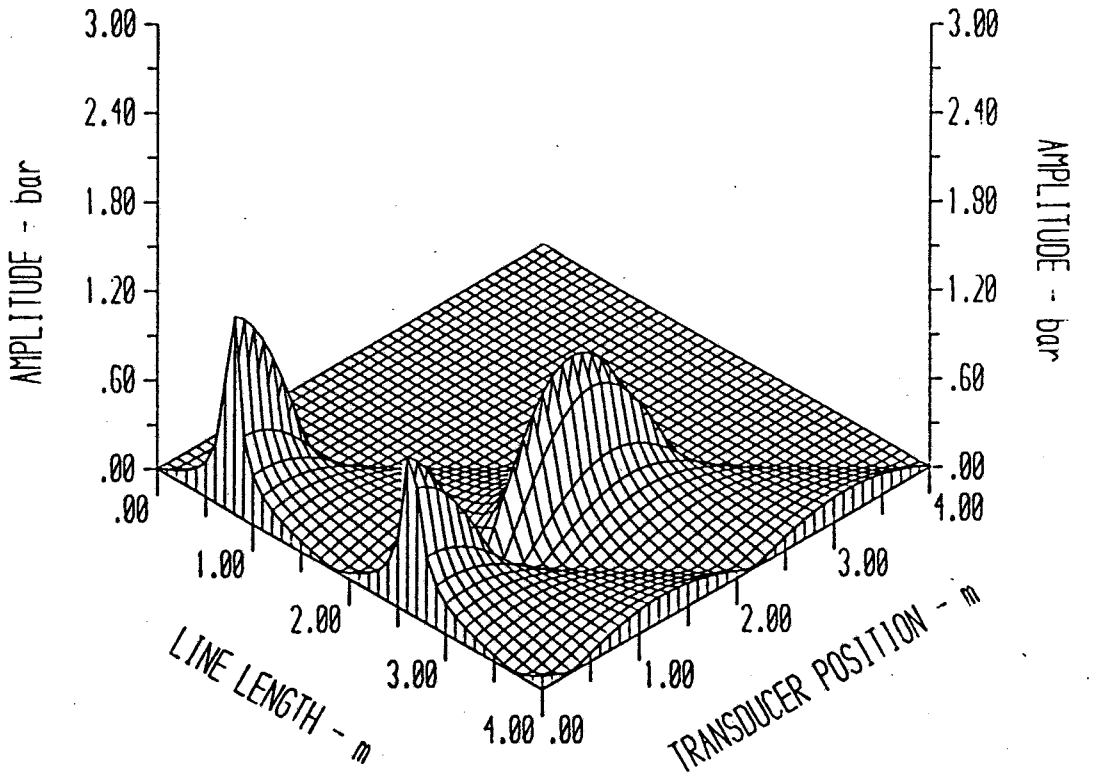

Fig. 6.35 Typical standing wave pattern in a pressurized pump suction line

CHAPTER VII

EXPERIMENTAL WORK ON BOOSTED SUCTION LINES

7.1 REVIEW OF PREVIOUS WORK

In an earlier work, the author presented the results on tests on the suction line of an axial piston pump when boosted by an external gear pump [11]. This work provided considerable information about the behaviour of pressure ripple in the boost line of a piston pump. It was found that two waveforms were present in the line, one generated by the boost pump outlet (external gear pump G) and another produced by the boosted pump inlet (axial piston pump A). Under most conditions the gear pump generated waveform was found to be dominant in determining the overall pressure signal. The piston pump generated waveform was mainly characterized by 'spikes' occurring at piston frequency intervals. Fig.7.1 shows an example of pressure signal measured at a point in the boost line (designated 'both'), when the mean pressure was 4 bar. The two waveforms designated 'pump A' and 'pump G' are the two waveforms generated each pump alone at that point. The third signal results from the sum of the first two. In general, the levels of the amplitude of the waveform increased considerably with mean boost pressure and peak-to-peak values of over 20 bar were recorded when the mean boost pressure was 19 bar. The piston pump generated waveform was found to be dependent upon both mean boost and mean piston pump outlet pressures.

In this work, considerable difficulty was found when attempting to measure the characteristics of the two pumps. This was mainly due to the problems involved in applying the extended pipe length method (section 3.4.1) to a system containing two flow ripple generators and

a branch line (for the relief valve). The method required the use of many different pipe lengths between boost and boosted pumps. As each pump was driven by a separate electric motor the use of rigid pipe connecting the two structures resulted in mechanical vibration of the pipe. Furthermore, each new line length connected involved moving one of the pumps away from the other. Due to the extensive work involved in this process only a limited number of line lengths could be tested. When the theoretical analysis was performed the predicted pump characteristics showed scatter. This was particularly true when determining the characteristics of the piston pump at the higher harmonics. This was attributed to the use of the gear pump generated ripple as the 'excitation' for the determination of the piston pump characteristics (as in 'pump-motor' systems, section 2.5.2). As the high frequency content of gear pump generated waves is very small, it is easy to conclude that very large errors can be incurred when predicting component characteristics under these circumstances.

The work presented below is aimed at solving the theoretical and practical difficulties experienced when studying pressure ripple in boosted suction lines.

7.2 TEST RIG

The rig used for testing the boost line of axial piston pump A was fundamentally different from that of early work. Both boost and boosted pumps were mounted on the same drive shaft, either side of an electric motor (fig.7.2). With this solution the whole test rig was assembled on a single structure. This does have the disadvantage of requiring a 'U' shaped boost line. However, from previous experience (section 2.5.3) this should not constitute a problem if the bends used have reasonably large radii. In this study, the bends used were

of about 0.3m radii, which was considered to be sufficiently large.

An axial piston pump (pump F) was used as a boost pump to avoid the difficulties associated to the use of gear pumps, as mentioned above.

The relief valve was mounted close to the boost pump at all times and the length of line was varied by increasing the 'depth' of the 'U' shape (fig.7.2).

Four piezoelectric transducers were attached to the boost line, as shown in fig.7.2. The mean pressure in the boost line was varied by the setting of the relief valve, which exhausted the excess flow delivered by the boost pump.

7.3 THEORETICAL MODEL

A boost system can be modelled by considering the existence of two flow ripple generators and a branch line (fig.7.3a). If the purpose of a test is to evaluate the characteristics of one of the sources only (boosted pump in this case), the model can be simplified by arranging for the branch line to be very close to the other source. This enables the source and the branch line to be considered as one lumped element with characteristics Q_s" & Z_s" evaluated at the junction (fig.7.3b). In this manner the system is reduced to the equivalent of a 'pump-motor' system. If the harmonic frequencies of both sources are not coincident, the frequency components of the pressure signal in the boost line can be found at the harmonics of each source pumping frequency. The boost system can, therefore, be considered to be constituted by two independent simple sub-systems A and B (fig.7.3c). The source impedance (Z_s) in sub-system A can be determined either as the source impedance of that sub-system or as

the termination of sub-system B. Obviously the two spectra results should be identical.

7.4 EXPERIMENTAL TESTS

The two pumps used in the boost system had different numbers of pumping elements. As they were driven at the same shaft speed, the different number of elements assured different frequencies for most harmonic components. Pump A had 7 pistons and pump F had 9. This means that the frequency of the 7th harmonic component of the boost pump (pump F) coincided with the 9th harmonic of the boosted pump (pump A).

The system was tested at different mean boost pressures (4,10,20 bar) and two mean discharge pressures (100 and 150 bar). An example of a pressure signal in the boost line is shown in fig.7.4 when the boost pressure was 10 bar and the discharge pressure was 150 bar. This signal was measured close to the boosted pump inlet when the length of line between the two pumps was 1.8 m. In contrast to the studies reported in [11], it was found that the boost pump generated waveform was not, in general, the main component of the overall pressure waveform. This is to be expected; unlike an external gear pump a piston pump outlet flow ripple is very dependent on mean pressure. As for this study the boost pump works at very low mean pressures its source flow fluctuation is very small compared to its behaviour at higher mean pressures. The flow fluctuation is also small compared to an external gear pump of the same capacity.

As in the previous studies [11], the pressure ripple in the boost line was found to be quite dependent upon mean boost and discharge pressures. At lowest mean pressure (4 bar), however, it was found that the relief valve was exhibiting some instability, due to the

combination of very low flow passing through it and the low pressure conditions. Hence, the pressure ripple was not as repeatable as at the higher mean pressure settings.

7.5 EVALUATION OF BOOSTED PUMP CHARACTERISTICS

The inlet characteristics of pump A were evaluated for all combinations of the following conditions: 10 and 20 bar mean boost pressure and 100 bar and 150 bar mean discharge pressure.

The inlet source flow evaluated when the discharge pressure was 100 bar is shown in fig.7.5. The results presented for 10 and 20 bar mean boost pressure follow exactly the same pattern but for the amount of backflow, which increases at the lower mean boost pressure. This was, in fact, also found when pump A was tested under unboosted conditions (fig.6.30). Fig.7.5 shows, however, a further very important detail: in Chapter IV it was shown that for a piston pump with an odd number of pumping elements there was an underlying ripple at twice pumping frequency (fig.4.5). This can be seen in fig.7.5 as a minimum in between each pair of backflows. When the pump was tested at 150 bar mean discharge pressure the source flow results obtained (fig.7.6) were still very similar to the previously shown in fig.7.5, apart from the expected increase in backflow due to the larger decompression of the dead volume as each piston opens to the inlet line.

It was stated earlier that the pressure waveform in the boost line was very dependent upon mean boost pressure. This was true for both the boost and boosted pump generated waves. Although it is obvious that the boost pump generated waveform should increase with mean pressure, due to the larger boost pump source flow, the same cannot be said about the boosted pump. The boosted pump source flow

actually reduces its amplitude with increased mean boost pressure but, in fact, the pressure waveform is increased due to the larger increase in the relief valve impedance with mean pressure. This point is very important to consider because under ideal conditions the flow through the relief valve is low (to save power) and hence the impedance is high. This results in large pressures ripple in the line.

The inlet impedance results of pump A were obtained in two different ways, as explained above. When the boosted pump was considered as a flow generator, its source impedance was as presented in figs.7.7 and 7.8, respectively for 100 and 150 bar outlet pressure. Both results are virtually identical, although show a certain amount of scatter. Nevertheless, the amplitude spectrum is very similar to that of fig.6.32 when pump A was tested unboosted at 5 bara mean pressure. The inlet impedance of the boosted pump was evaluated as the termination of the sub-system which has as flow generator the boost pump, and the results are shown in fig.7.9. These results show considerably less scatter than figs.7.7 and 7.8 for the very same pump characteristic. This is not surprising as it is known that the evaluation of termination impedance is always more accurate than the determination of source impedance (section 3.6.3).

7.6 MODELLING INLET SOURCE IMPEDANCE

In chapter VI it was stated that the inlet impedance of piston pump A showed a mainly capacitive characteristic. In fact, pump impedances are more accurately modelled if inductive effects are also included. In this case, the impedance of a pump (Z_s) is represented by:

$$Z_s = \frac{\beta}{j\,\omega\,V_p} + j\,\rho\,\frac{\omega\,\ell}{A} \qquad (7.1)$$

where: A - cross sectional area of pump discharge passageway [m^2]

j - complex number operator

V_p - internal volume of pump [m^3]

ℓ - length of pump discharge passageway [m]

β - bulk modulus of fluid [Ns/m^2]

ρ - density of fluid [kg/m^3]

ω - frequency [rad/s]

The internal volume of the inlet and outlet chambers of pump A were measured by filling each chamber completely with fluid and measuring its volume. The results for both the inlet and outlet were 38 cm^3. Assuming that the pump inlet passageway can be represented by a length of line ℓ of cross sectional area equal to the pump port size (17.5 mm diameter), eq.7.1 was used to to plot the prediction of Z_s on fig.7.9 (solid line). The corresponding length of passageway was 6 cm. The agreement experienced in fig.7.9 is quite remarkable, particularly because such agreement could not be found when predicting the outlet impedance of the same pump. Knowing that the volumes of both inlet and outlet chambers are equal, the inlet and outlet impedances should be identical apart from considerations of bulk modulus variations with mean pressure. In fact, this would result in marginally increased impedance on the pump outlet, in relation to the inlet. The outlet impedance that was evaluated for pump A (fig.7.10) was in reality lower than the inlet impedance, and the volume to which the outlet impedance corresponds is 52 cm^3 and the length of passageway is 2 cm. This is represented by the solid in fig.7.10. Even when pump A was tested as a motor (fig.3.22) the impedance at the lower harmonics did not reach values as large as those presented in fig.7.9. However, at the higher harmonics the

values of impedance were virtually the same. The odd behaviour of the impedance values on the pump outlet could not be explained. From the results it appears that the outlet chamber has a volume larger than that measured.

In conclusion, the inlet source impedance of pump A was found to be very close to that predicted from the passageway geometry.

7.7 PREDICTION OF PRESSURE RIPPLE IN A BOOST SYSTEM

Having found that the experimental tests performed on the boost system provided satisfactory results for the characteristics of the boosted pump, a computer model of the system was developed in order to predict the pressure ripple at any point in a boost line. The boost line was characterized by two flow generators and a valve at the end of a branch line.

Since the boost pump and relief valve had not been tested as part of the boost line work, the tuned length method was used to test individually boost pump F and valve B under the exact conditions met in the boost system (same mean flow and mean pressure). The values of the characteristics of the boost pump, boosted pump and relief valve were, then, used as data in the computer program. An example of the results is shown in fig.7.11. This figure shows a comparison between the experimental results acquired when testing the boost line and the corresponding computer prediction. In both cases, the traces presented are a synthesis, combining the first six harmonic components of each flow generator. Although the experimental and predicted traces are not identical in shape there is a strong similarity and a definite agreement in terms of peak-to-peak amplitude of the waveform. It must be emphasized that perfect agreement of the experimental and predicted waveforms would mean an

accurate reproduction of the amplitude and phase of all six harmonics of both pumps. Bearing this in mind, the prediction must be regarded as quite satisfactory.

Of course, in fig.7.11 two waveforms are summed to produce the results. For completeness, fig.7.12 gives a comparison of the experimental and predicted traces of only one of the waveforms (the boosted pump generated waveform). Again, the shapes are not identical but the prediction of the amplitude of the waveform is accurate. A comparison of figs.7.11 and 7.12 shows that, from the pressure ripple point of view, it is much better to have only one generator in a pump suction line rather than two. This again strengthens the case for the use of a pressurized reservoir whenever possible.

It was stated in chapter VI that if the fluid was saturated with air at the conditions present in the inlet line, then air release occurred in the pump. This in turn, reduced the pressure fluctuations in the line, but did not affect volumetric efficiency. This will not be the case in boosted systems because the fluid passing from the tank to the boost line becomes undersaturated due to the increase in pressure. Moreover, using a pressurized reservoir obviates the need for a relief valve in the line which further reduces the air borne noise generated by the system. In terms of power requirements, particularly in variable swash pump inlet lines, the use of a pressurized tank is also far better than a boost pump, as no power is wasted at any time.

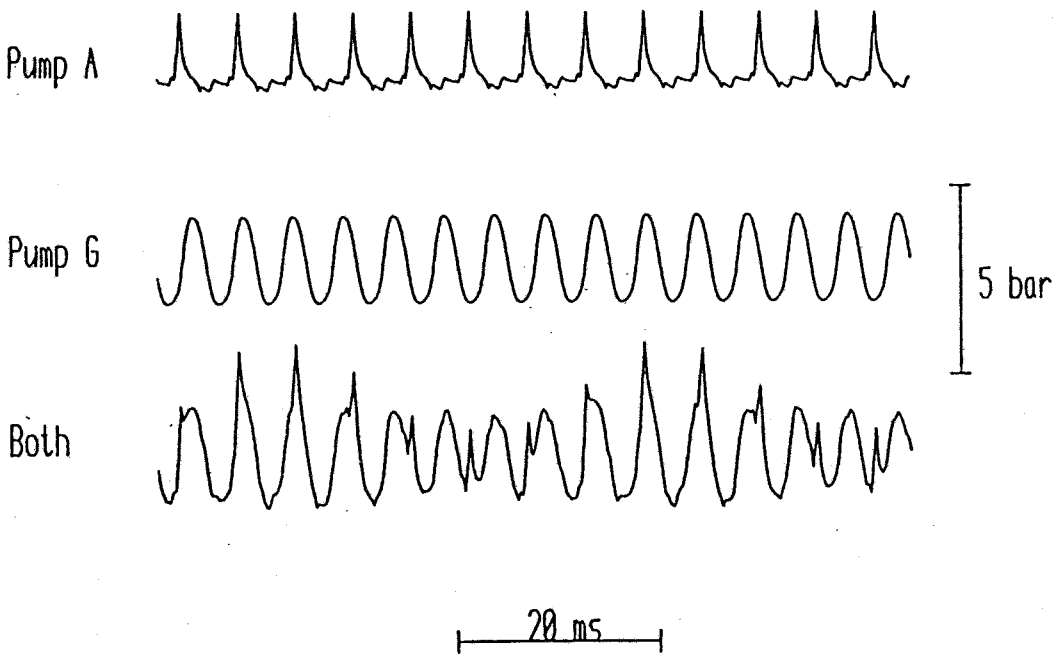

Fig. 7.1 Example of pressure waveform in a boost line composed of a gear pump boosting a piston pump. The two top traces show waveforms generated by each pump individually (boost press.=4 bar)

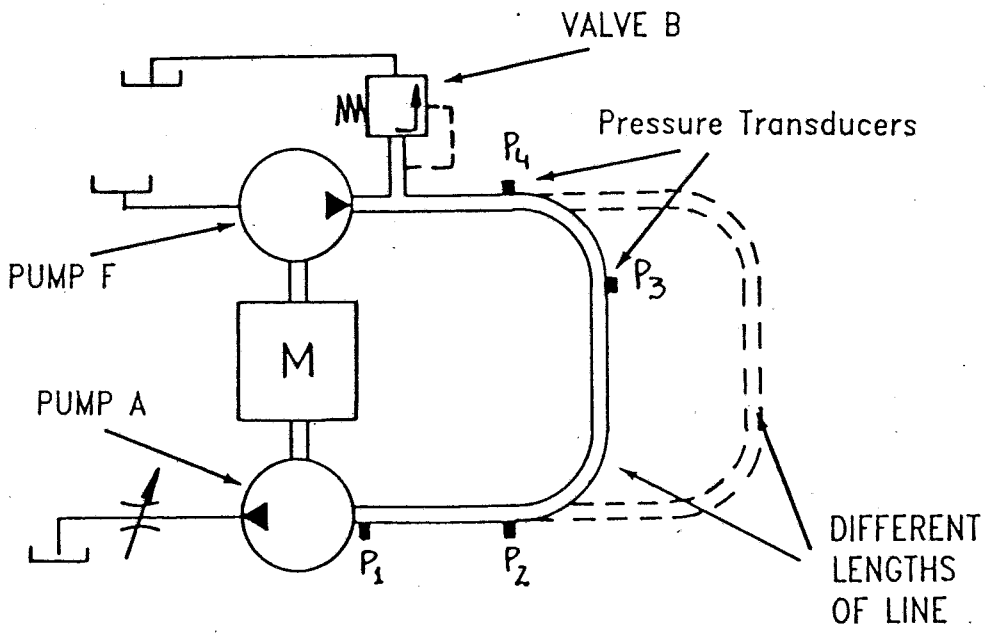

Fig. 7.2 Test rig used for boost system analysis

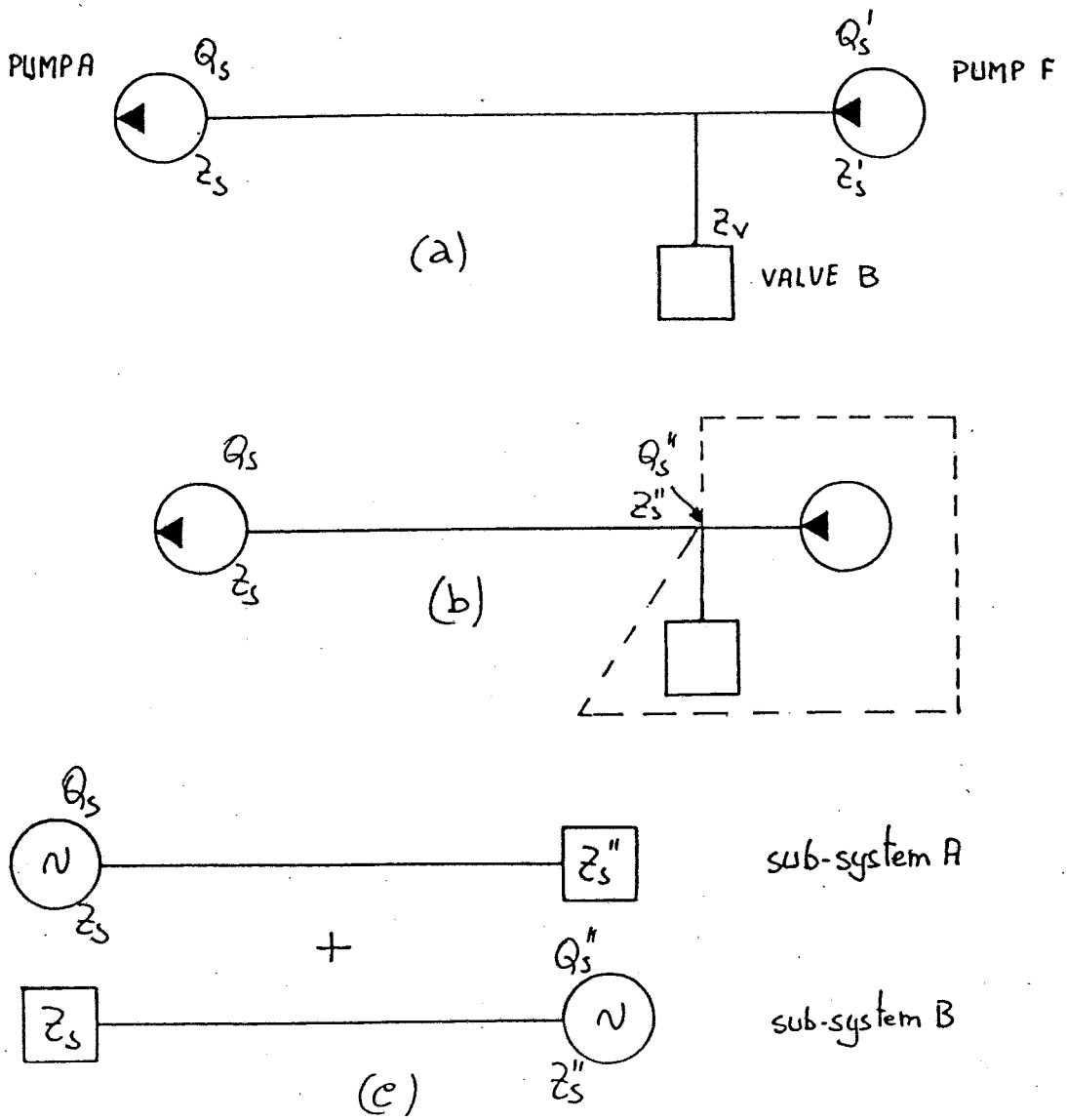

Fig. 7.3 Theoretical model of boost system

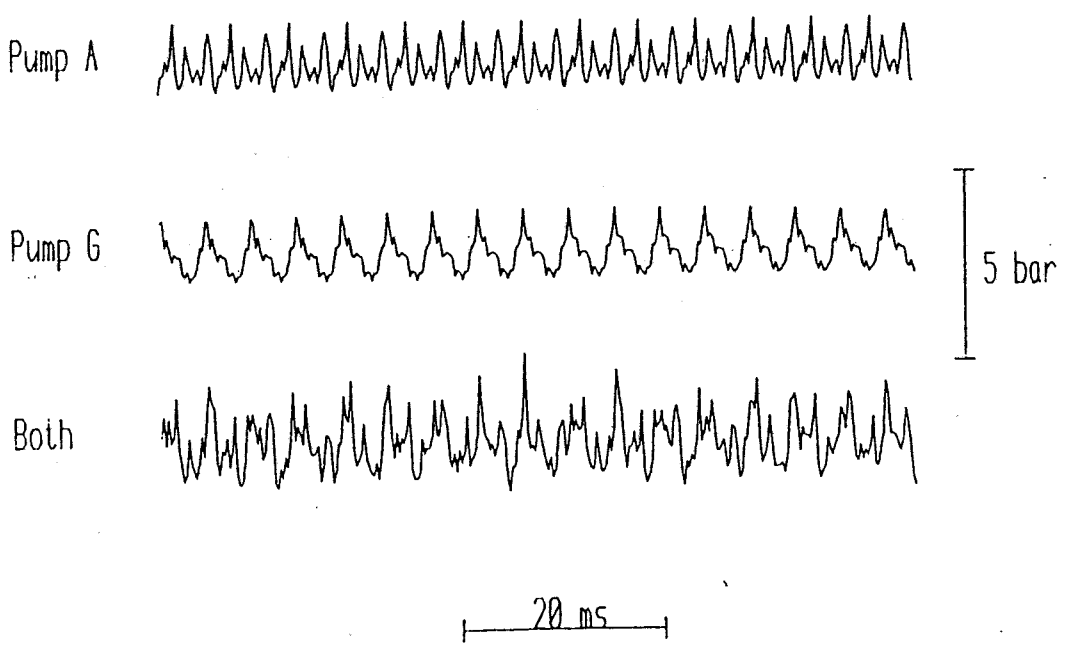

Fig. 7.4 Example of pressure waveform in a boost line composed of a piston pump boosting another piston pump. The two top traces show waveforms generated by each pump individually (boost press.=10 bar)

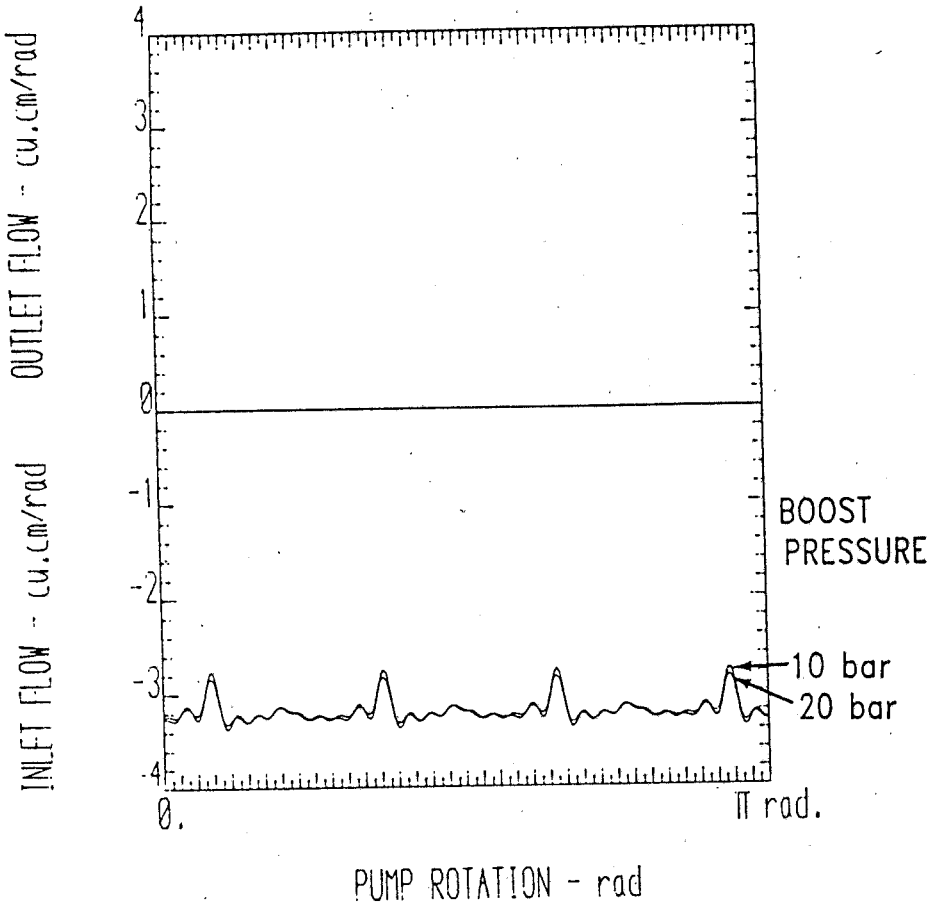

Fig. 7.5 Inlet source flow of pump A for 100 bar discharge and 10 and 20 bar boost pressure

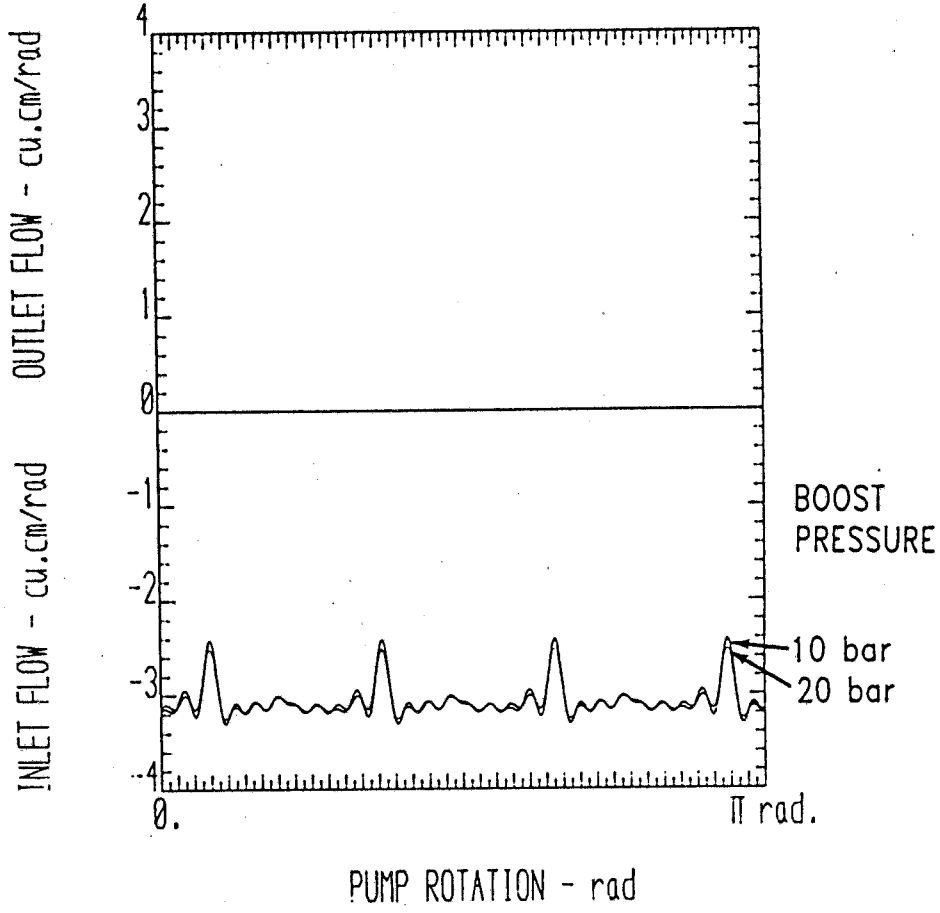

Fig. 7.6 Inlet source flow of pump A for 150 bar discharge and 10 and 20 bar boost pressure

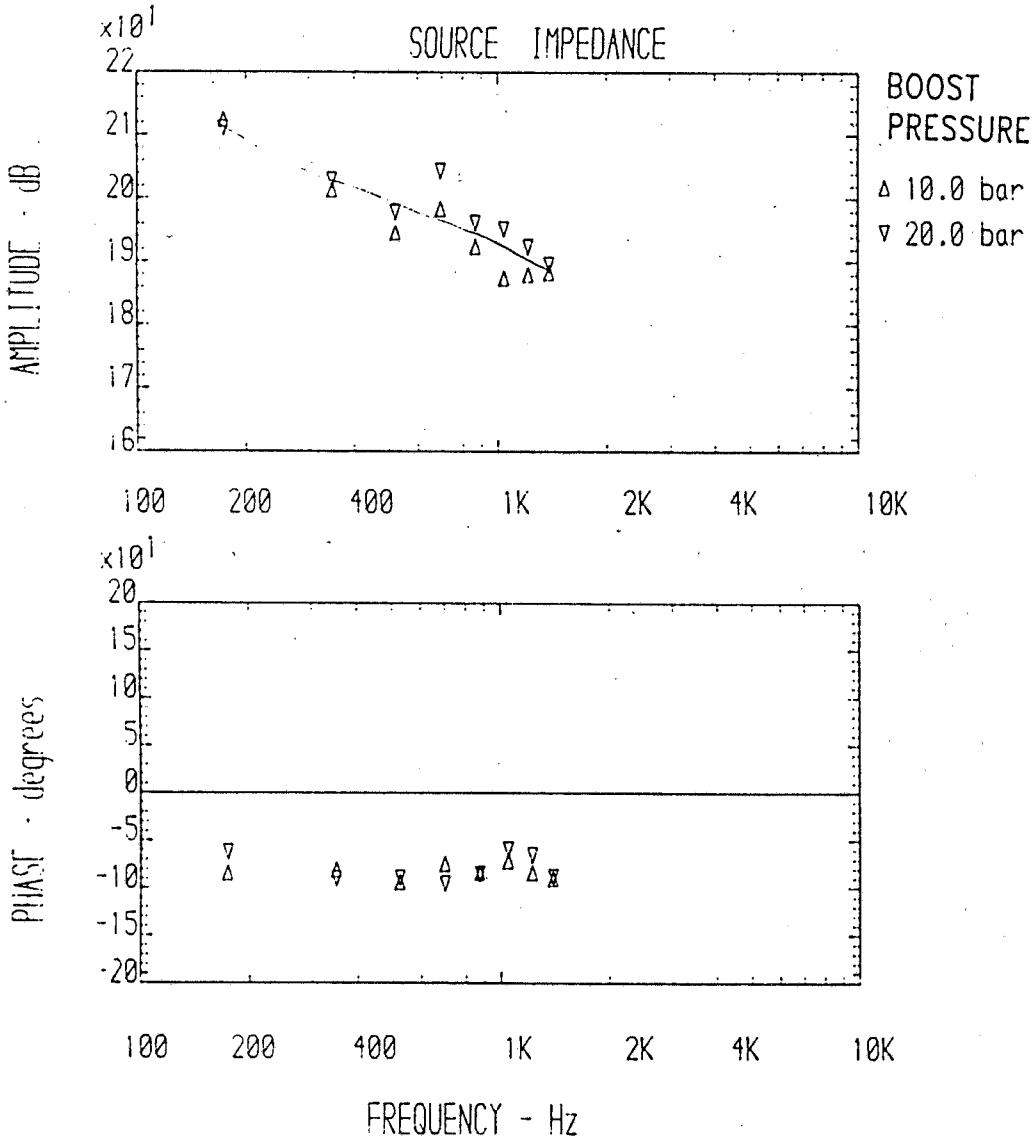

Fig. ..7 Inlet source impedance of pump A for 100 bar disch. (calculated from data of sub-system A)

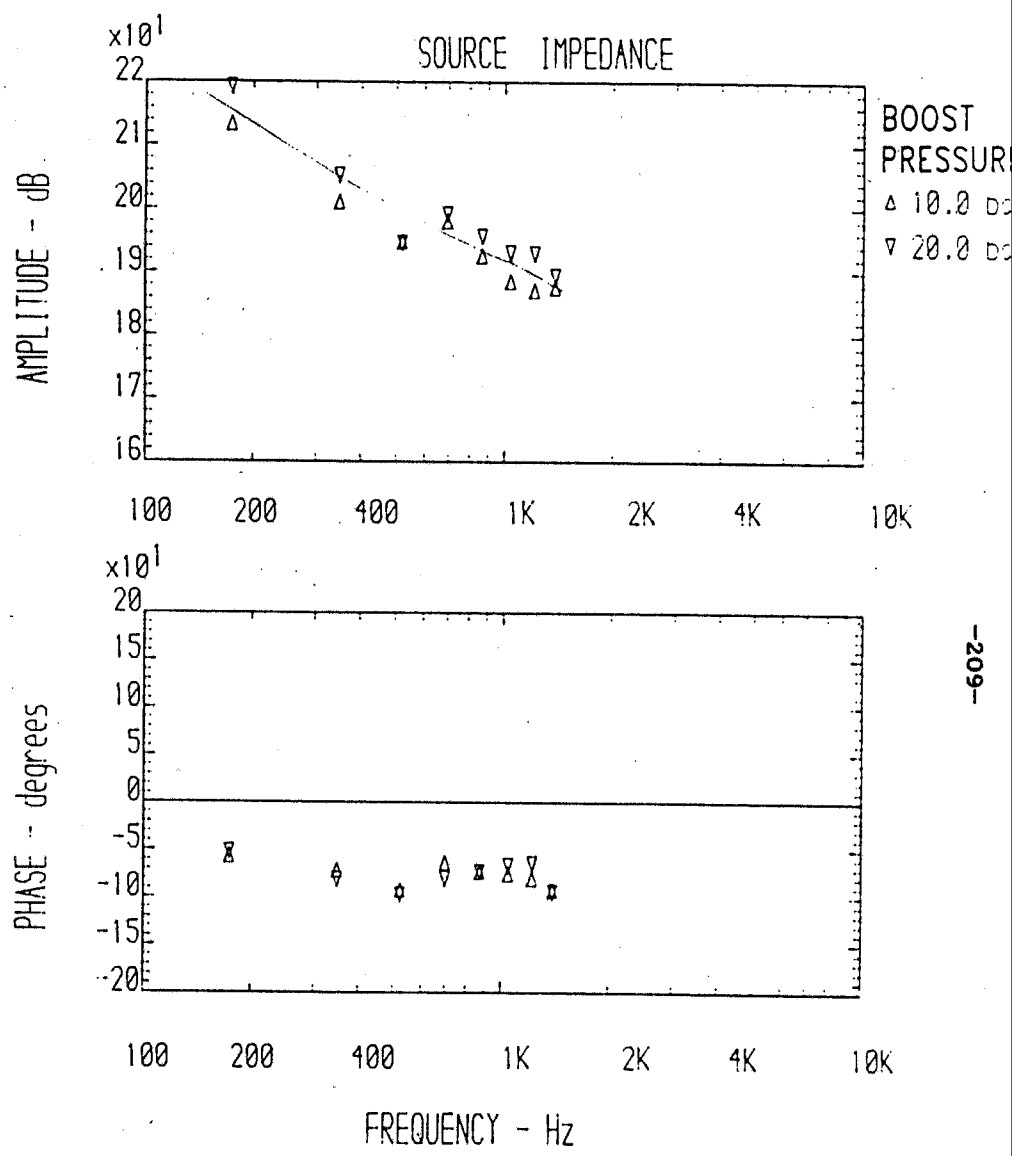

Fig. 7.8 Inlet source impedance of pump A for 150 bar disch. (calculated from data of sub-system A)

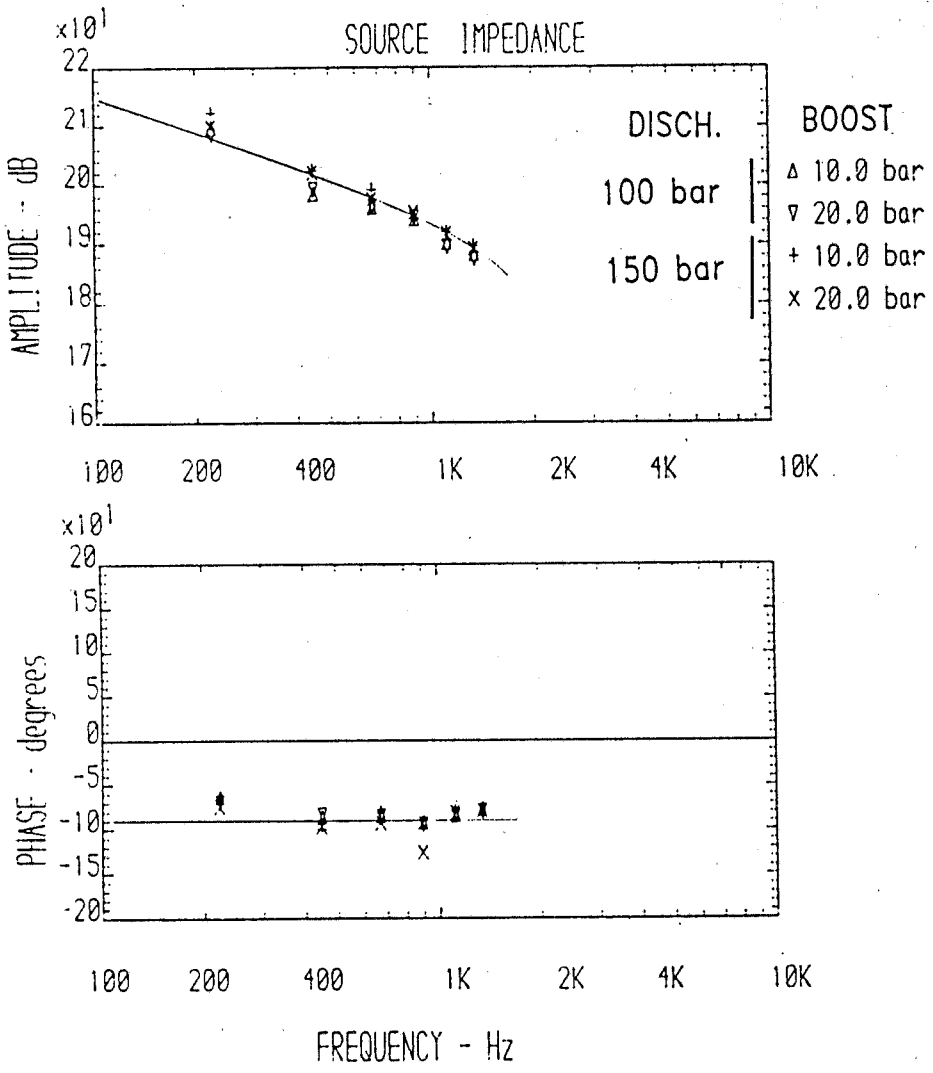

Fig 7.9 Inlet source impedance of pump A (calculated as termination of sub-system B) and comparison with predicted impedance (Vp= 38 cm3 : = 6 cm)

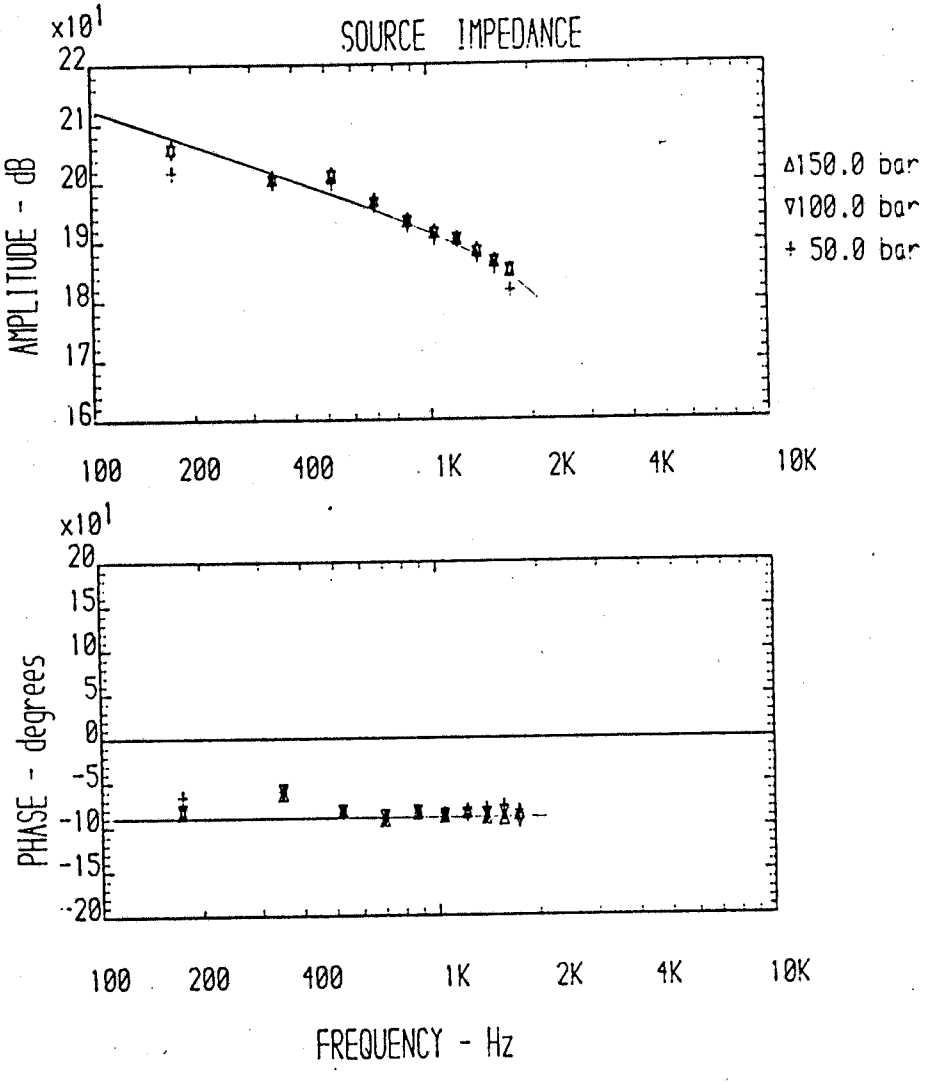

Fig. 7.10 Outlet impedance of pump A and comparison with predicted impedance (Vp= 52 cm3 , = 2 cm)

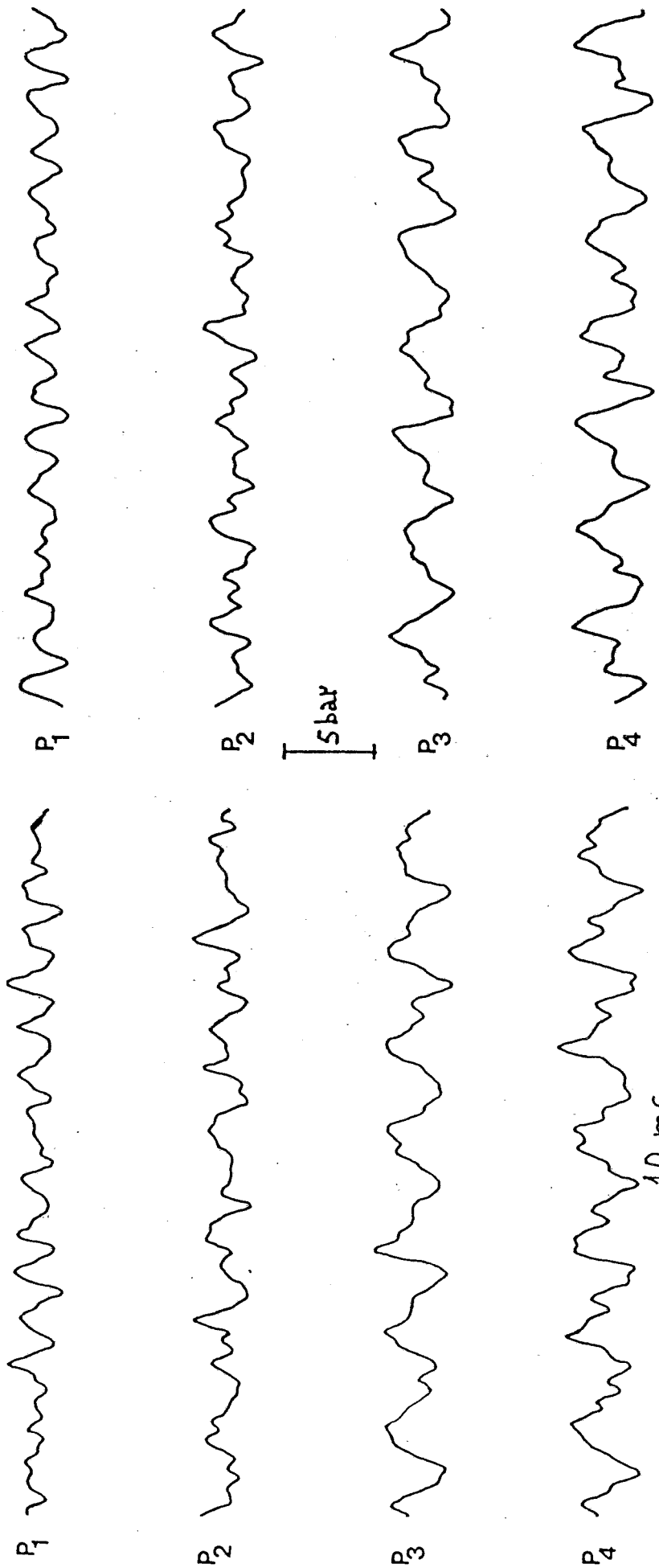

Fig. 7.11 Comparison of experimental and predicted pressure waveform in a boost line, at four positions in the line (boost= 10 bar ; disch= 100 bar ; ℓ = 2.33 m)

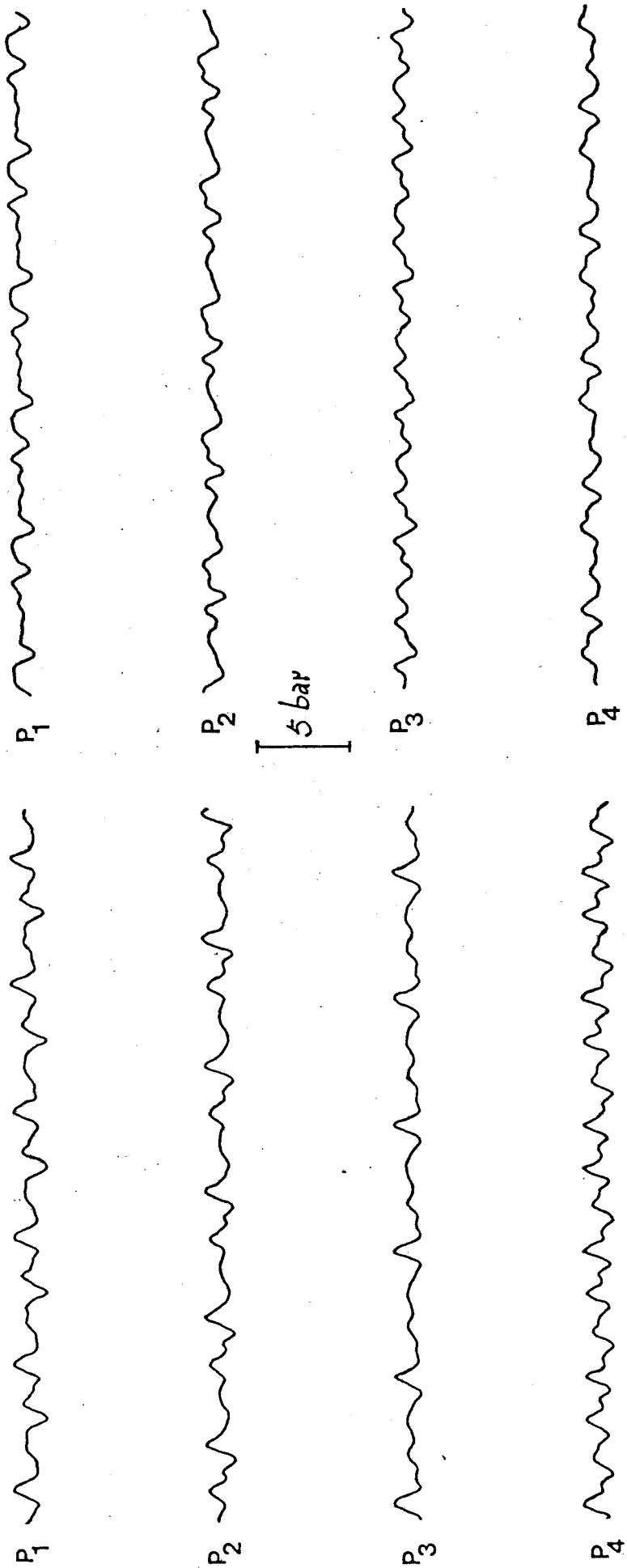

(a) experimental (b) predicted

Fig. 7.12 Comparison of experimental and predicted boosted pump generated pressure waveform, at four positions in the boost line (boost= 10 bar; disch= 100 bar; ℓ= 2.33 m)

CHAPTER VIII

CONCLUSIONS

8.1 - THE TEST METHOD

8.2 - PUMP INLET TESTS

8.1 THE TEST METHOD

An experimental test method has been developed to enable the fluid borne noise characteristics of hydraulic components to be evaluated. The technique, named the 'tuned length method', was applied to high pressure and low pressure hydraulic lines.

The implementation of the method was carried out with the assistance of an interactive digital computer program which provides advice on suitable conditions under which components can be tested. The method was used to evaluate the characteristics of both active components (pumps and motors) and passive components (valves and a hydraulic tank).

Due to the intrinsic theoretical basis of the test method, the evaluation of the characteristics of the components terminating the system is bound to be more accurate than the evaluation of the source impedance. The prediction of the source flow was always found to be very consistent with the results obtained from other test method and also with theoretical models. Provided that the mean pressure in the system was above atmospheric the method still proved to be valid, showing that plane wave propagation theory could be applied.

The tuned length method has, nevertheless, an inherent practical difficulty, which is the need to test a system several times, using a number of different lengths of line. This makes the method laborious and prevents it from being regarded, in its present form, as a Standard Method of testing fluid borne noise characteristics of

hydraulic components (active and passive). However, in view of the potency of the technique, it is recommended that further work should be devoted to find means of simplifying the test procedure.

8.2 PUMP INLET TESTS

Tests have been performed on the suction lines of external gear pumps and axial piston pumps. These tests have shown that the unsteady flow taken in by the pump creates a pressure standing wave in the inlet line in much the same manner as in high pressure lines. The pressure standing wave is extremely sensitive to the mean pressure level. As the pressure in the suction line was reduced below atmospheric, the pressure fluctuations became quite small and unstable. Increasing the pressure, restored waveform stability and also increased pressure ripple amplitudes considerably. These variations in pressure ripple levels with mean pressure are completely different to those observed in outlet lines. For instance, in the case of an external gear pump, the fluid borne noise characteristics of its outlet do not vary significantly with system pressure. Consequently, any changes in pressure ripple levels with mean pressure are almost entirely due to change in loading valve characteristics, rather than changes in pump characteristics. This is not the case with the suction line of an external gear pump. It was found that at atmospheric pressure the flow ripple produced by the pump on its inlet was very much reduced compared to that produced at higher mean pressures. This suggested that air release occurred at some instant in the induction stroke of the pump. No evidence of air being released in the suction line (before reaching the pump inlet) exists, since wave propagation theory was shown to be still valid under these conditions. This appears to be true despite the fact that instantaneous pressures near absolute zero were recorded at

several points in the line with mean pressures well above atmospheric. No damping of the pressure waveform occurred as a consequence. It appears that the pressure transients are too rapid for air release to occur (less than 0.1 ms). Further confirmation of air release occurring inside the pump inlet passageway was obtained by carrying out tests on a pump using partially deaerated oil. The instantaneous flow taken in by the pump did not show the same strong dependence on suction pressure as in the case of previous tests. This implies that under normal suction conditions the spaces between teeth are not totally filled with oil. Although this has a considerable effect on fluid borne noise levels, the volumetric efficiency of the pump is virtually unaffected.

The results obtained for external gear pumps were obtained at inlet pressures up to 2 bar. Tests at pressures above this level were not possible due to pump design limitations. However, the same limitations did not apply when performing tests on an axial piston pump. Tests on the inlet of an axial piston pump presented a similar pressure ripple behaviour as observed in the tests on external gear pumps. At low mean pressures the predicted flow fluctuation generated by the pump did not follow the same pattern as at higher mean pressures. It was in fact damped. This, again, indicated the existence of air release inside the pump. The amplitude of flow fluctuations was found, as expected, to increase with decreasing swash plate angle. An important point emerging from the results is that the possibility of air release in the inlet of the piston pump is more dependent upon the flow fluctuation generated by the pump rather than the mean flow taken in.

Levels of air borne noise generated by the system increased with increasing pressure ripple levels in the inlet line, which in turn

were dependent on mean inlet pressure. In the case of an external gear pump, for instance, the increase in air borne noise caused by a 2 bar increase of mean inlet pressure was as large as that caused by a variation of 100 bar in the pump discharge line. This is particularly important and calls for effective means of reducing pressure ripple in pump suction lines, especially at a time when in many applications pressurized reservoirs are becoming more and more popular.

REFERENCES

[1] Heron, R.A. and Hansford I.

'Air borne due to structure borne vibration transmitted through pump mountiungs and along circuits'

I.Mech.E.Conference - Quiet Oil Hydraulics - Where are we now? London, Nov. , 1977.

[2] Henderson, A.R.

'Measuring the performance of fluid borne noise attenuators'

I.Mech.E.Conference - Quiet Oil Hydraulics - Where are we now? London, Nov. , 1977.

[3] Tuc, B.

'The use of flexible hoses for reducing pressure ripple in hydraulic systems'

PhD. Degree Thesis of the University of Bath, 1981.

[4] McCandlish, D., Edge, K. and Tilley, D.G.

'Fluid borne noise generated by positive displacement pumps'

I.Mech.E.Conference - Quiet Oil Hydraulics - Where are we now? London, Nov. , 1977.

[5] Bowns, D.E. and McCandlish, D.

'Pressure ripple propagation'

I.Mech.E.Conference - Quiet Oil Hydraulics - Where are we now? London, Nov. , 1977.

[6] Foster, K. and Hannan, D.M.

'Fundamental fluidborne and airborne noise generation of axial piston pumps'

I.Mech.E.Conference - Quiet Oil Hydraulics - Where are we now? London, Nov. , 1977.

[7] Fielding, D., Foster, K., Hooke, C.J. and Martin M.J.
'Sources of pressure pulsation from a gear pump'
I.Mech.E.Conference - Quiet Oil Hydraulics - Where are we now? London, Nov. , 1977.

[8] Crook, A. and Heron, R.A.
'Airborne noise from hydraulic lines due to liquid borne noise'
I.Mech.E.Conference - Quiet Oil Hydraulics - Where are we now? London, Nov. , 1977.

[9] Tilley, D.G. and Butler, M.D.
'The generation and transmission of fluid borne pressure ripple in hydraulic systems'
I.Mech.E.Conference - Quiet Oil Hydraulics - Where are we now? London, Nov. , 1977.

[10] Bowns, D.E., Edge, K.A. and McCandlish, D.
'Factors affecting the choice of a standard method for the determination of pump pressure ripple'
I.Mech.E.Conference - Quiet Oil Hydraulics - Where are we now? London, October, 1980.

[11] Freitas, F.J.T.
'A study of pressure fluctuations in the boost line of a piston pump'
MSc thesis, University of Bath, 1980.

[12] Lindsay, I.
'The reduction of fluid borne noise in gear pump suction lines'
MSc. thesis, University of Bath, 1981.

[13] Ascroft, J. and Newman, P.

'A study of air-release and cavitation in the suction line to a positive displacement pump'

Project Report for the B.Sc. Degree in Engineering

University of Bath, 1980.

[14] Hibi, A.,Ibuki, T., Ichikawa, T. and Yokote, H.

'Suction Performance of Axial Piston Pump (1st report)'

Bulletin of the JSME, vol.20, no.139, Jan.1977

[15] Fitch. E.C.

'The Basic Hydraulic Reservoir'

The BFPR Journal, 1978, 11, 1, 19-25

Oklahoma State University, Oklahoma.

[16] McCandlish, D., Edge, K.A. and Tilley, D.G.

'Fluid borne noise generated by positive displacement pumps'

I.Mech.E.Conference - Quiet Oil Hydraulics - Where are we now?

London, November 1977.

[17] Bath University Report

'Noise in Hydraulic Systems'

(MEMTRB Contract at the Fluid Power Centre)

Contract No. RD/1112/01, Report No. BaU4, April 1978.

[18] Longmore, D.K. and Tuc, B.

'Reduction of Fluid Borne Noise in Hydraulic Circuits by means of Flexible Hoses'

I.Mech.E.Conference - Quiet Oil Hydraulics - Where are we now?

London, October 1980

[19] Longmore, D.K.

'The Transmission and Attenuation of Fluid Borne Noise in

Hydraulic Hoses'

I.Mech.E.Conf. -Quiet Oil Hydraulic Systems-Where are we now?

London, Nov.1977

[20] Duke, K. and Dransfield, P.

'Improving Gear Pump Relief Groove Design'

32nd Nat. Conf. on Fluid Power

Ceveland, Ohio 1976.

[21] Bowns, D.E., Edge, K.A. and Tilley, D.G.

'The Assessment of Pump Fluid Borne Noise'

I.Mech.E. Conference - Quiet Oil Hydraulics - Where are we now?

London, November 1977.

[22] Unruh, D.R.

'Outlet Pressure Ripple Measurement of Positive Displacement Hydraulic Pumps'

National Conference on Fluid Power, Cleveland

October 26-28, 1976.

[23] Szerlag, S.F.

'Rating Pump Fluid Borne Noise'

SAE Paper 750830, September 8-11 1975.

[24] Theissen, H.

'Volumenstrompulsation von Kolbenpumpen'

Oilhydraulik und Pneumatik, 588-591, Sept.1980.

[25] AHEM Publication

'Revised Draft British Standard for the Measurement of Pressure Ripple Levels Generated in Hydraulic Fluid Power Systems and Components'

London, 1981.

[26] Wing, T.

'The Fluid-borne Noise Characteristics of Hydraulics Components and their Measurement'

PhD Degree Thesis, University of Bath, 1982.

[27] Edge, K. A.

'The Theoretical Prediction of the Impedance of Positive Displacement Pumps'

6th Int. Fluid Power Symposium

Cambridge, England , April 1981.

[28] Maroney, G.E.

'The effect of air/liquid volume ratios on pump noise emission'

Paper No.P76-55, Fluid Power Resaerch Conference

Oklahoma State University, October, 1976.

[29] Pearsall, I. S.

'The velocity of water hammer waves'

Symposium on Surges in Pipelines

Inst. Mech. Eng., 180 (1965-1966).

[30] Martin, M. J. and Taylor, R.

'Optimised Port Plate Timing of Axial Piston Pumps'

5th Int. Fluid Power Symposium, vol.1

Durham, England, Sept.1978.

[31] Ibuki, T., Hibi, A., Ichikawa, T., Yokote, H.

'Suction performance of Axial Piston Pump'

(2nd report, Experimental Results)

Bulletin of the J.S.M.E., vol.20, no.145, July 1977.

[32] Zalka, A. and Latranyi, J.

'Suction capability and cavitation of gear pumps'

2nd Fluid Power Symposium. Paper H3.
Guildford, England, 4-7 Jan 1971

[33] Khaimovitch, E.M.
'Hydraulic Control of Machine Tools'
Pergamon Press, 1965, pag.156.

[34] Eley, James M.
'Reservoir Design as viewed by a Pump Manufacturer'
S.A.E. paper 700721, (Sept.1970)

[35] Editors of "Hydraulic Pneumatic Power"
'Principles of Hydraulics'
Trade & Technical Press,Ltd. England, 1972.

[36] Junck, J.A.
'Sealed Hydraulic System for a Track-type Tractor'
Hydraulics and Pneumatics, pp.96-100, Oct.1962

[37] AHEM Publication
'Design Construction and Selection of Hydraulic Reservoirs'
Recommended Manufacturing Practice 4/81.

[38] ANSI-B93.18-1973
'Non-integral Industrial Fluid Power Hydraulic Reservoirs'
National Fluid Power Association, Milwaukee, Wisconsin 53222

[39] Wirtz, Edward A.
'Reservoir Design for Mobile Equipment Hydraulic Circuits'
Society of Automotive Engineers, Paper 700722, (Sept.1970)
Milwaukee, Wisconsin

[40] Pippenger, J.J. and Richard M.K.
'Fluid Power Controls'

McGraw-Hill Book Company, New York, 1959.

[41] Dowty Hydraulic Units Limited
Catalogue DHU/240/1/1500/TY
Cheltenham, GL510TP. Jan. 1973.

[42] Schefer, L.J.
'Concorde has designed-in reliability'
Hydraulics and Pneumatics, pp.51-55, Dec.1976

[43] Schweitzer, P.H. and Szebehely, V.G.
'Gas evolution in liquids and cavitation'
Journal of Applied Physics, Vol.21, pp.1218-1224, Dec. 1950

[44] Weyl, W.A. and Marboe, E.C.
Research, Vol. 2 , 1949

[45] Fitch, E.C.
'Designing Mobile Equipment Type Hydraulic Reservoirs'
BFPR Journal, 12, pp.23-27, 1979
Oklahoma State University, Stillwater, Oklahoma

[46] Tisdale, W. and Behney, E.
'Submarine hydraulics ... designing for safety and silence'
Hydraulics and Pneumatics, Feb. 1960

[47] Lewis, E. and Stern, H.
'Design of Hydraulic Control Systems'
McGraw-Hill Book Company, Inc. - 1962

[48] Harvey, E.N.
'On cavity formation in water'
Journal of Applied Physics, 18, 161 (1947)

[49] Rayleigh, J.

'The theory of sound'

Dover Publications, 1896, vol.II, sec.306,307, & appx.A

[50] Eirich

'Rheology Volume I'.

Academic Press.

[51] Pearsall, I.S. & Kane, J.

'Viscosity and specific gravity of five hydraulic fluids'

National Engineering Laboratory.

[52] Hayward, A.T.J.

'How to estimate the bulk modulus of hydraulic fluids'

Hydraulic Pneumatic Power, January 1970.

[53] Foster,K. and Parker, G.A.

'Transmission of power by sinusoidal wave motion through hydraulic oil in a uniform pipe.'

Proc. I. Mech. E.,vol.179, part 1,no.19, 1964-65

APPENDICES

APPENDIX I – COMPUTER PROGRAM DOCUMENTATION OF SUBROUTINE "fluid_prop.fortran"

APPENDIX II – COMPUTER PROGRAM DOCUMENTATION OF SUBROUTINE "gamma_zo.fortran"

APPENDIX III – COMPUTER PROGRAM DOCUMENTATION OF PROGRAM "tunemeth.fortran"

APPENDIX IV – COMPUTER PROGRAM DOCUMENTATION OF SUB-PROGRAM "tune_sub.fortran"

APPENDIX V – SIZING OF A HYDRAULIC RESERVOIR

APPENDIX VI – DESCRIPTION OF COMPONENTS

COMPUTER PROGRAM DOCUMENTATION

FOR SUBROUTINE "fluid_prop.fortran"

Library Classification

BENGF fluid_prop.221.01

TITLE- EVALUATION OF PROPERTIES OF SHELL TELLUS OIL 27

New Fortran_5a Multics 25/2/80

No special hardware requirements

Author : F.Freitas

Purpose - To evaluate density, dynamic viscosity and effective bulk modulus of fluid in pipe at desired temperature and mean pressure.

Associated Subroutines - An inbuilt subroutine **daf** evaluates the **Dow and Fink** density factors [50].

When used in wave propagation programs the subroutine output is used as input information for subroutine **gamma_zo**, which evaluates the wave propagation constant and line characteristic impedance.

All variables transferred via argument list:

```
call fluid_prop(p,t,idia,th,denp,mup,beff)
```

All variables are real

Input Information(via argument list)

p - mean pressure [bar]

t - mean temperature [C]

idia - internal diameter of pipe [m]

th - thickness of pipe wall [m]

Output Information (via argument list)

denp - dens. of oil at press. 'p' and temp. 't' [Kg/m^3]

mup - dyn.visc.of oil at pres.'p' and temp.'t' [Ns/m^2]

beff - eff. bulk mod. of oil in pipe [N/m^2]

Limitations and Accuracy of Program - Single precision is used throughout

No Inbuilt Error Messages

Storage : 1 Record length

PROGRAM ACTION AND ALGORITHM

The program calculates the properties of Shell Tellus Oil 27 using general formulae appropriate to all mineral oils. The initial values and constants were evaluated to match the experimental results given in the manufacturers data charts. The results at atmospheric pressure and 352Kg/cm2 (345bar) were used throughout to check agreement between the general formulae and experimental results.

a) Evaluation of Density

i) Variation of density with temperature (Fig.A1.1):

The density of a mineral oil decreases linearly with temperature, according to the equation:

$$dent = den - C * (t - 20) \qquad (A1.1)$$

where: dent - density at temperature t [Kg/m^3]

den - density at 20 C [Kg/m^3]

t - temperature [C]

C - constant

From Fig.A1.1 : den = 870.0 Kg/m^3

(at atmos. press.) C = 0.625

ii) Variation of density with pressure (Fig.A1.1):

The variation of density of hydraulic oils with pressure is determined by the **DOW-FINK** equation [50] :

$$denp = dent * \left(1 + \frac{aa * p}{6.895*10^{-2}} - \frac{bb * p^2}{(6.895*10^{-2})^2}\right) \qquad (A1.2)$$

where: denp - density at temp. t and pressure p [Kg/m^3]

aa,bb- Dow-Fink density factors

p - pressure [bar]

The Dow-Fink density factors are a function of temperature, as shown in Fig.A1.2.

The density at 345 bar (denh) is calculated in order to evaluate, in the following section, the dynamic viscosity of the fluid at that pressure.

Fig.A1.3 presents the results of density produced by this routine for commonly used values of temperature and pressure.

b) Evaluation of Kinematic and Dynamic Viscosity

The variation of the kinematic viscosity of the fluid with temperature, shown in Fig.A1.4, follows the **MacCoull-Walther** equation [50]:

$$\log_{10}(nu-0.6) = 10^{(A-B*\log_{10}(t+273))} \qquad (A1.3)$$

where the constants A and B are evaluated in order to follow the experimental values (Fig.A1.4) at atmospheric pressure and 345 bar (352Kg/cm^2).

At atmos. press. A1 = 10.67 and B1 = 4.213

at 345 bar A2 = 8.245 and B2 = 3.218

The dynamic viscosity is given as the product:

mu = dent * nu (at temp. t and atmos. press)

or muh = denth * nuh (at temp. t and 345 bar)

The variation of dynamic viscosity with pressure is given by [51]:

$$(\log_{10} \mu_2)^2 = (\log_{10} \mu_1)^2 + m * p \qquad (A1.4)$$

where m is a function of oil temperature. As the dynamic viscosity is known at temperature t for atmos. pressure and 345 bar, m can be evaluated. However, for this oil it was found that the results of equation A1.4 coincide with the results of the following equation:

$$mup = mu + (mup - mu) * p / 345. \qquad (A1.5)$$

where: mup - dyn. viscosity at temp. t and press. p

In Fig.A1.5 a plot of the results of kinematic viscosity of the oil is presented for varying temperature and pressure. Fig.A1.6 shows, for the same conditions of temperature and pressure, the values of dynamic viscosity.

c) Evaluation of Bulk Modulus

The value of bulk modulus required for wave propagation studies is the isentropic tangent bulk modulus, as the pressure fluctuations are rapid, occurring around a constant mean level of pressure. However, the charts currently available refer only to values of isentropic secant bulk modulus, as shown in Fig.A1.7.

i) Variation of bulk modulus with temperature (Fig.A1.7):

The bulk modulus varies with temperature according to the following equation [52]:

$$bot = \frac{bo}{10^{0.024*(t-20)}} \qquad (A1.6)$$

where: bo - isent. secant bulk modulus at 20 C [bar]

bot- isent. secant bulk modulus at temp. t [bar]

ii) Variation of bulk modulus with pressure (Fig.A1.7):

The isentropic secant bulk modulus of the oil varies linearly with pressure:

$$bp = bot + 5.6 * p \qquad (A1.7)$$

where: bp - isentropic secant bulk modulus at temp. t and pressure p.

iii) Transformation of secant into tangent bulk modulus:

The secant bulk modulus can be evaluated from [33]:

$$bT = bp * \frac{bp - p}{bo} \qquad (A1.8)$$

where: bT - isentropic tangent bulk modulus at temp. t and press. p

iv) Effect of pipeline elasticity on bulk modulus

The effective bulk modulus of the oil is affected by the pipe, according to the following equation:

$$\frac{1}{beff} = \frac{1}{bT} + \frac{idia}{th * E} \qquad (A1.9)$$

where: idia - internal diameter of pipe [m]

th - thickness of pipe wall [m]

E - Young's Modulus of pipe material

=2.1 ell N/m^2 for steel

Fig.A1.8 presents the values of isentropic tangent bulk modulus evaluated by the subroutine for different values of temperature and pressure.

Experimental tests carried out to evaluate the speed of sound in the oil have shown some discrepancy with predicted values (evaluated as in Appendix II). A 3% reduction in bulk modulus had to be made to achieve accurate predictions.

```
      subroutine fluid_prop(p,t,idia,th,denp,mup,beff)
*
*     subprogram name - fluid_prop.fortran
*
*     library classification - BENGF fluid_prop.221.01
*
*     TITLE - Properties of SHELL TELLUS OIL 27
*
*     New Fortran 7a Multics                    25/2/80
*
*     No special hardware requirements
*
*     Author - F.Freitas
*
*     Purpose - Evaluate density, viscosity and bulk
*               modulus of fluid in pipe at mean pressure 'p'
*               and mean temperature 't'
*
*     Revisions -
*
*     ALL VARIABLES ARE  REAL
*
*     Input Information(via argument list)
*       p    - mean pressure                              [bar]
*       t    - mean temperature                           [C]
*       idia - internal diameter of pipe                  [m]
*       th   - thickness of pipe wall                     [m]
*
*     Output Information (via argument list)
*       denp - dens. of oil at press. 'p' and temp. 't'   [Kg/m3]
*       mup  - dyn.visc.of oil at pres.'p' and temp.'t'   [Ns/m2]
*       beff - eff. bulk mod. of oil in pipe              [N/m2]
*
*     Variables names (excluding input/output information)
*
*       bT   -tang. bulk mod. at press.'p' and temp.'t'   [N/m2]
*       bo   -sec. bulk mod. at atmos. press. and 20 C    [bar]
*       bot  -sec. bulk mod. at atmos. press. and temp.'t'[bar]
*       bp   -sec. bulk mod. at press.'p' and temp.'t'    [bar]
*       den  -density at atmos. press. and 20 C           [Kg/m3]
*       dent -density at atmos. press. and temp.'t'       [Kg/m3]
*       denth-density at 345 bar and temp.'t'             [Kg/m3]
*       mu   -dyn. visc. at atmos.press. and temp.'t'     [Ns/m2]
*       muh  -dyn. visc. at 345 bar and temp.'t'          [Ns/m2]
*       nu   -kinem. visc. at atmos. press. and temp.'t'  [cSt]
*       nuh  -kinem. visc. at 345 bar and temp.'t'        [cSt]
*
*       aa,bb,A1,B1,A2,B2,C -constants
*
*
*     Inbuilt Associated subroutine-  daf(t,aa,bb)   -
*                                   Evaluates the
*     'DOW-FINK' density factors. The results of this
*     subroutine can be used as input information for
*     subroutine  gamma_zo in wave propagation programs
*
*     NO inbuilt error messages
```

```
*
*       * * * * * * * * * * * * * * * * * * * * * * * * * * * *
*
        real idia,nu,nuh,mu,muh,mup
*
*       INITIAL VALUES
*       --------------
*
        bo    =1.85e04
        den   =870.0
*
        A1    =10.67
        B1    =4.213
        A2    =9.338
        B2    =3.646
        C     =0.625
*
*       GENERAL EQUATIONS
*       -----------------
*
        dent  =den-C*(t-20.0)
*
        nu    =0.6+10.0**(10.0**(A1-B1*alog10(t+273.0)))
        nuh   =0.6+10.0**(10.0**(A2-B2*alog10(t+273.0)))
*
        mu    =dent*nu*1.0e-06
*
*       Evaluation of 'Dow-Fink' density factors
        call daf(t,aa,bb)
*
        denth =dent*(1.0+aa*345.0*1.0e02/6.895
&       -bb*345.0*345.0*1.0e04/47.54)
        denp  =dent*(1.0+aa*p*1.0e2/6.895-bb*p*p*1.0e4/47.54)
*
        muh   =denth*nuh*1.0e-06
        mup   =mu+(muh-mu)*p/345.0
*
        bot   =bo/(10.0**(0.0024*(t-20.0)))
        bp    =bot+5.6*p
        bT    =bp*(bp-p)/bot
*       Change units from 'bar' to 'N/m2' and decrease
*       calculated value by 3% to agree with
*       experimental tests
        bT=bT*0.97e05
        beff  =bT/(1.0+bT*idia/(th*2.1ell))
*
        return
        end


        subroutine daf(t,aa,bb)
*
*       TITLE - Evaluation of 'DOW-FINK' density factors
*
*
        dimension a(10),b(10)
        data a/4.08,4.19,4.29,4.38,4.46,4.53,4.59,4.63,
&       4.66,4.68/
        data b/6.8,6.4,6.0,5.7,5.4,5.1,4.9,4.7,4.5,4.4/
        i=(t-4.5)/11.1+1
        if(i.lt.1)i=1
```

```
if(i.gt.9)i=9
dt=t-(4.5+11.1*(i-1))
j=i+1
aa=a(i)+(a(j)-a(i))*dt/11.1
bb=b(i)+(b(j)-b(i))*dt/11.1
aa=aa*1.0e-06
bb=bb*1.0e-11
return
end
```

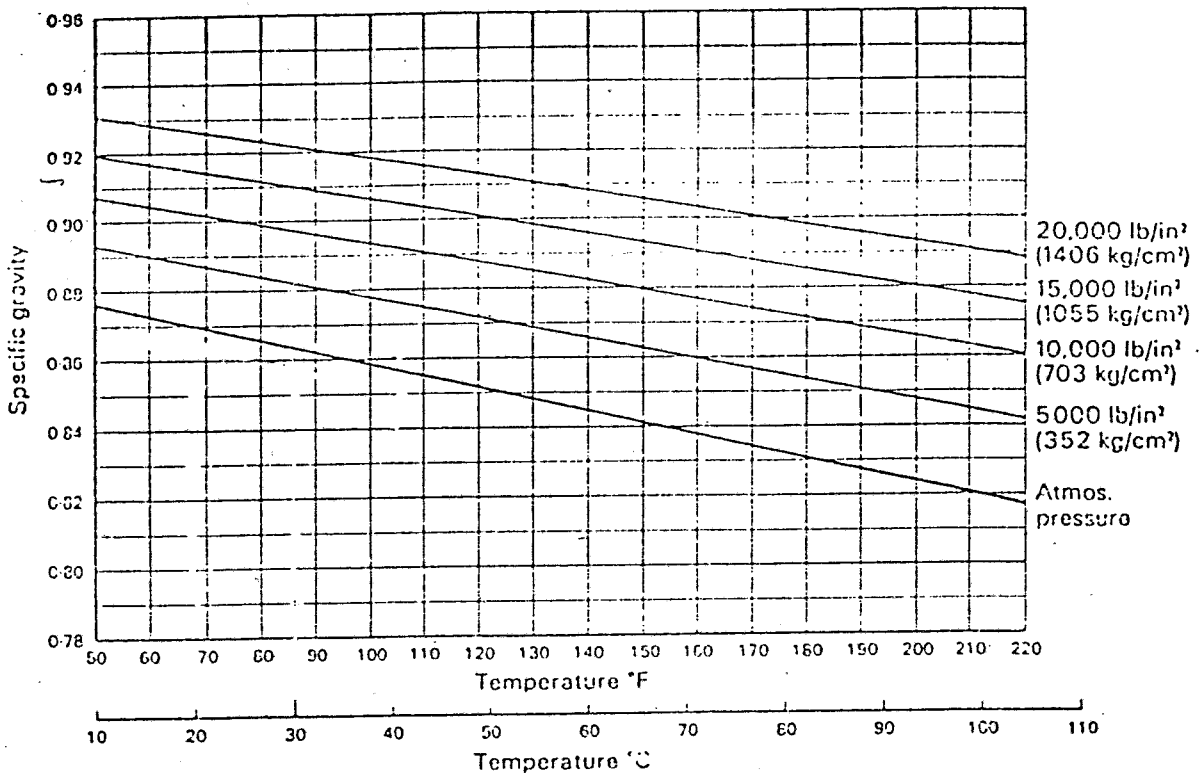

Fig.A1.1 Specific gravity against temperature and pressure for Shell Tellus Oil 27

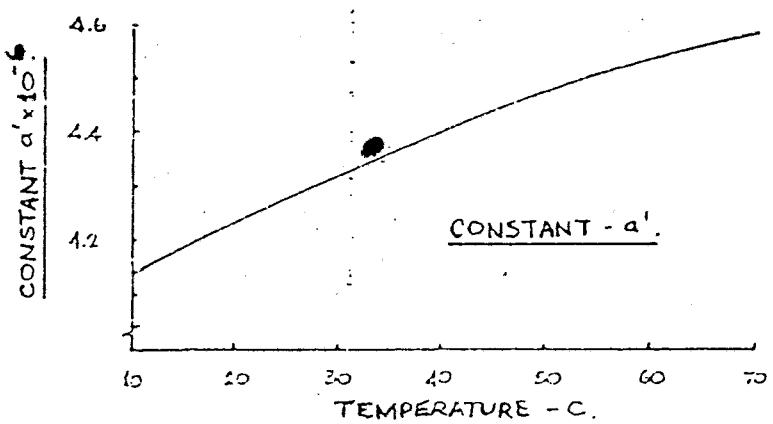

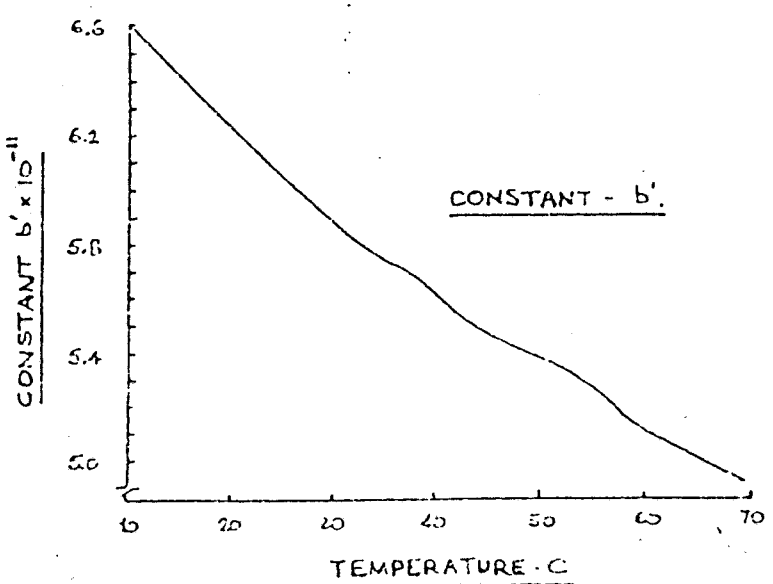

Fig.A1.2 'Dow-Fink' density equation constants a' and b'

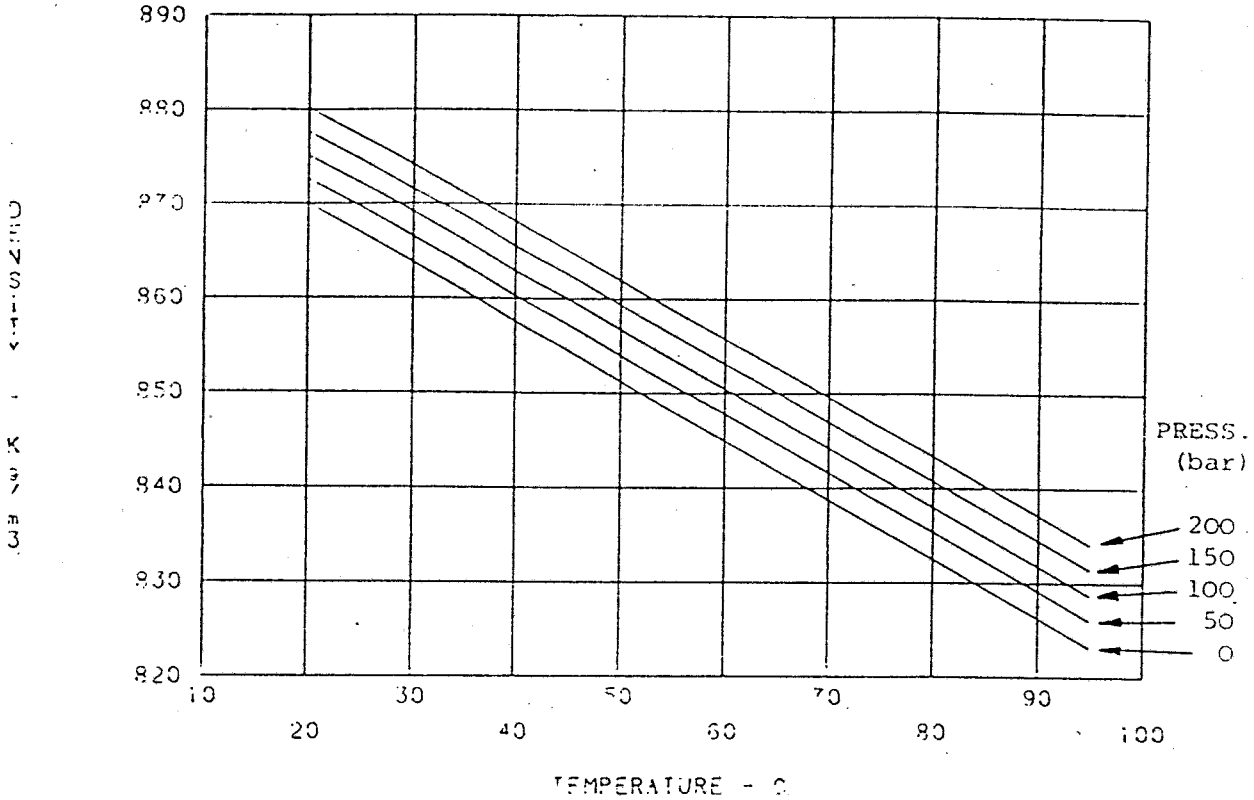

Fig.A1.3 Results of oil density from subroutine 'fluid_prop'

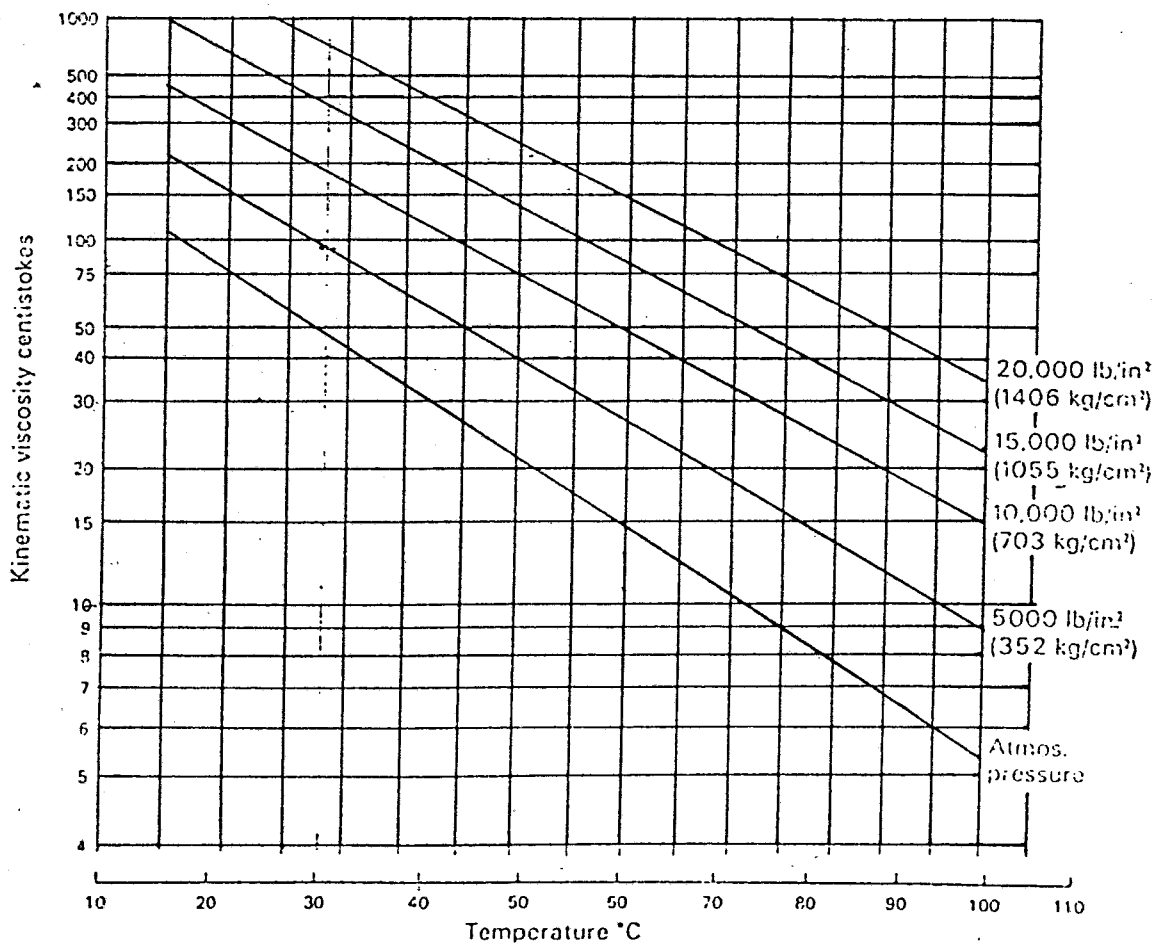

Fig.A1.4 Kinematic viscosity against temperature and pressure for Shell Tellus Oil 27

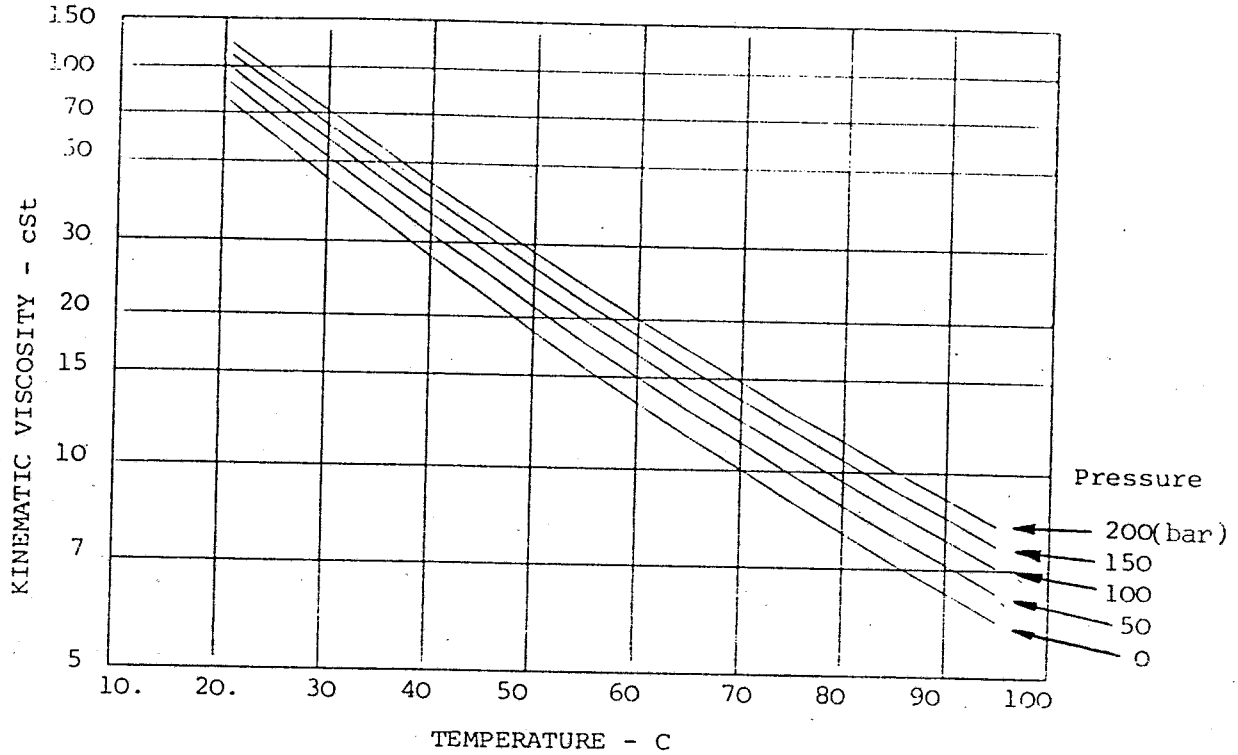

Fig.A1.5 Results of kinematic viscosity of oil from subroutine 'fluid_prop'

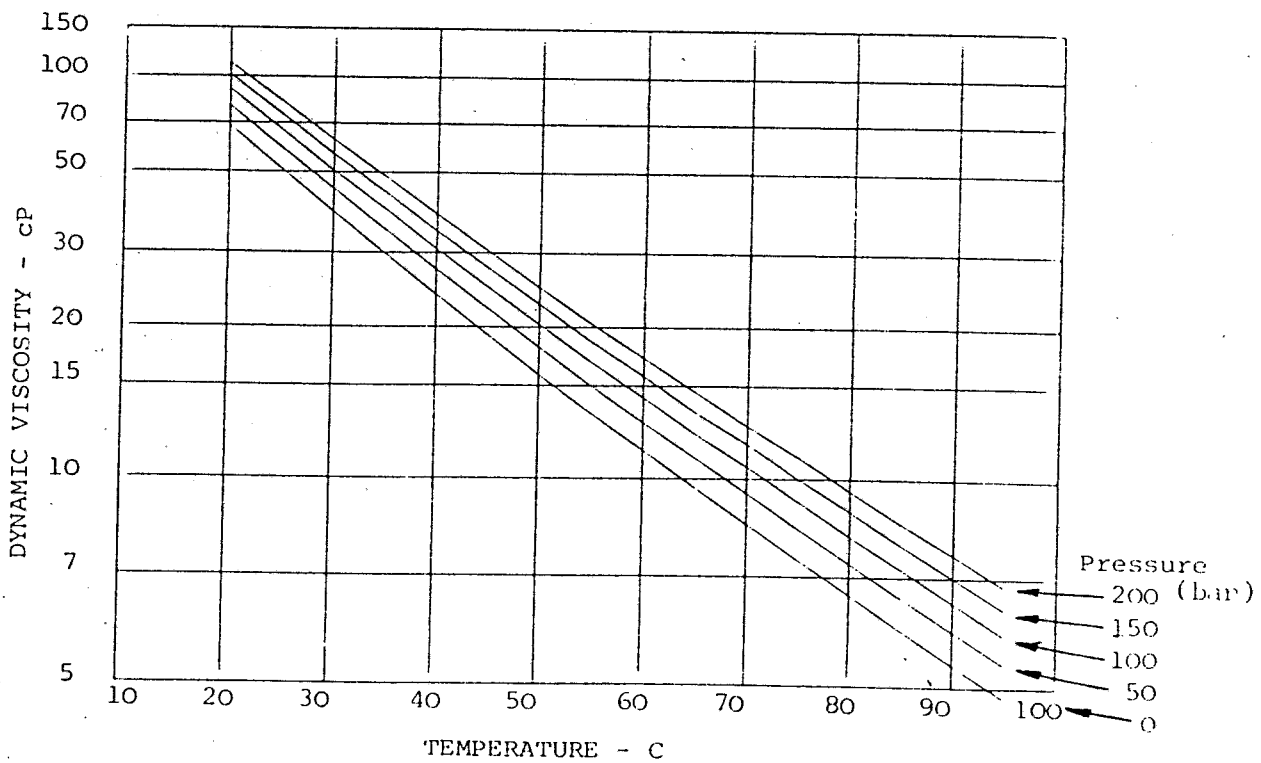

Fig.A1.6 Results of dynamic viscosity of oil from subroutine 'fluid_prop'

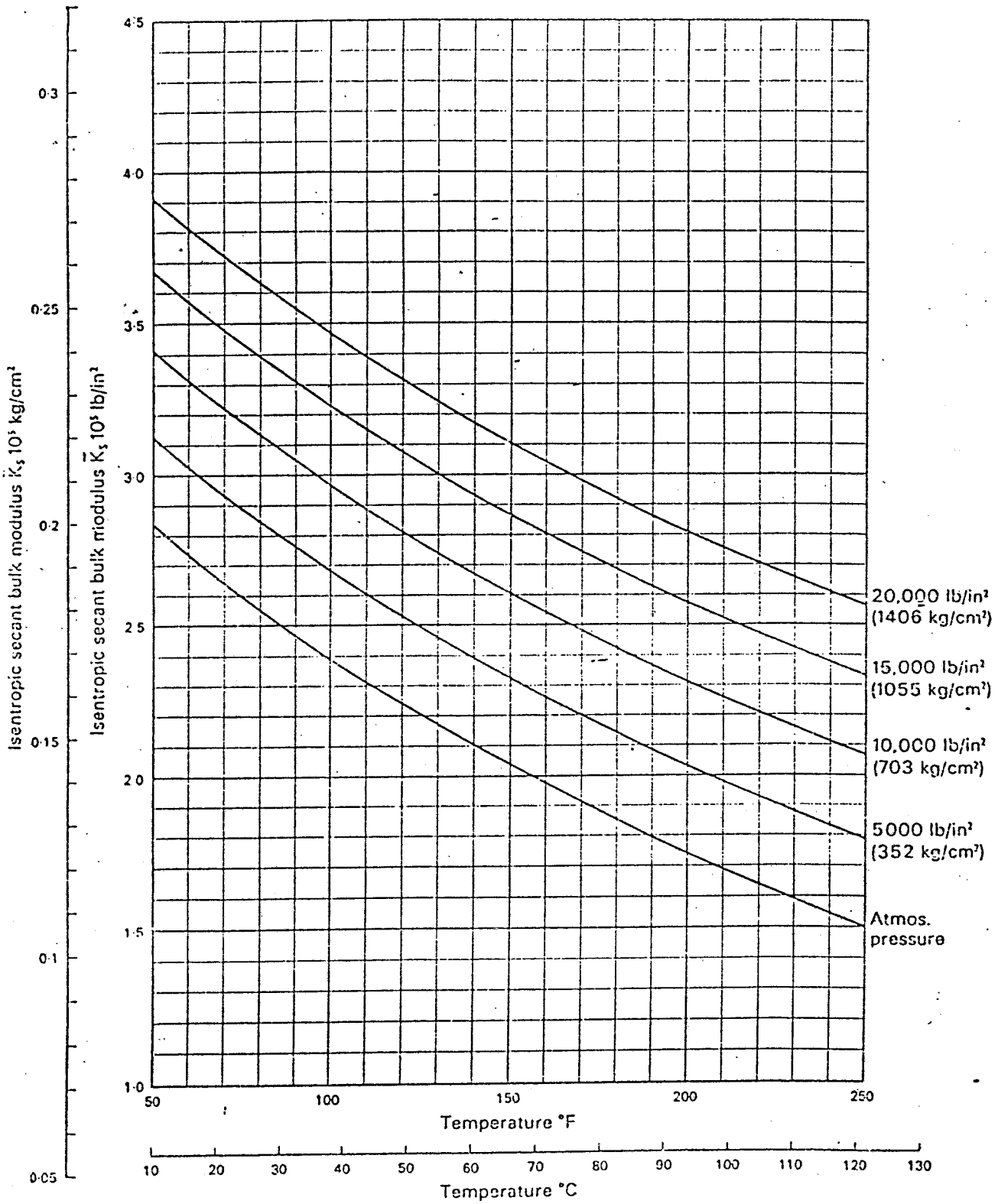

Fig.A1.7 Isentropic secant bulk modulus against temperature and pressure for Shell Tellus Oil 27

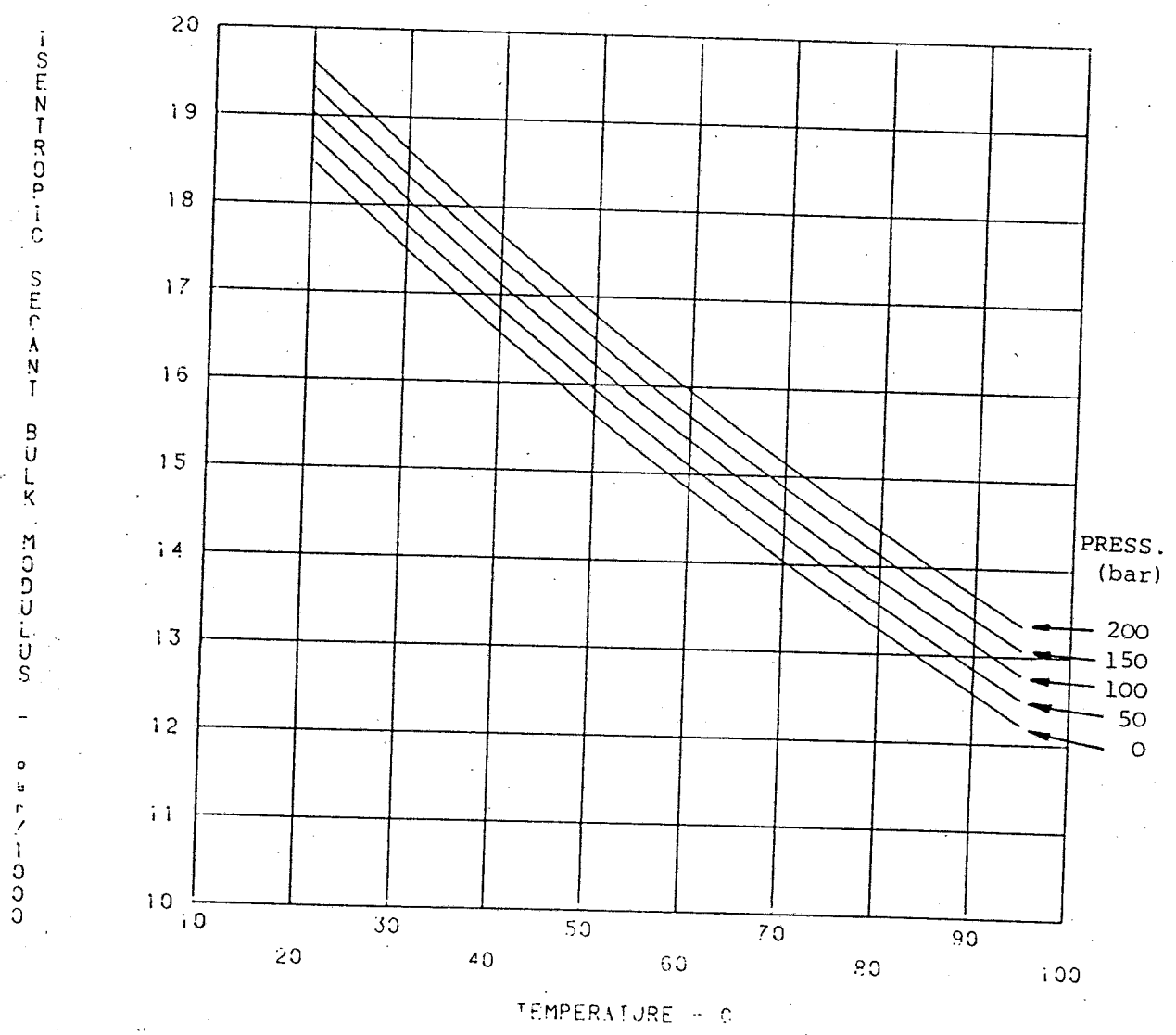

Fig.A1.8 Results of isentropic secant bulk modulus of oil from subroutine 'fluid_prop'

COMPUTER PROGRAM DOCUMENTATION

FOR SUBROUTINE "gamma_zo"

Library Classification

BENGF gamma_zo.222.01

TITLE- EVALUATION OF WAVE PROPAGATION CONSTANT AND PIPE CHARACTERISTIC IMPEDANCE

New Fortran_5a Multics 25/2/80

No Special hardware requirements

Author : F.Freitas

Purpose - To evaluate the wave propagation constant and the pipe line characteristic impedance

Associated Subroutines - The properties of the fluid, used as input information for this subroutine may be evaluated by using subroutine **fluid_prop** (BENGF.221.01).

All variables transferred via argument list:

call gamma_zo(freq,idia,den,mu,beff,gamma,zo)

All input variables are real. The output variables are complex.

Input Information

freq	- frequency	[Hz]
idia	- internal diameter of pipe	[m]
den	- density of oil at working conditions	[Kg/m^3]
mu	- dyn. visc. of oil at working conditions	[Ns/m^2]

beff - effective bulk mod. of oil in pipe [N/m^2]

Output Information (complex variables)

gamma - wave propagation constant

zo - pipe characteristic impedance

Limitations and Accuracy of Program - Single precision is used throughout. Values of frequency <100 Hz should be avoided or may lead to warning message.

Error Message - If conditions exist such that the transmission line equations are no longer applicable a warning message is displayed on the terminal. In general this only occurs when data is incorrect. The error message is given when the 'ha' factor (see below) is less than 10.

Storage : 1 Record length

PROGRAM ACTION AND ALGORITHM

The action of this program is based on the definition of γ (wave propagation constant) and zo (pipe characteristic impedance).

From plane wave propagation theory [5]:

$$\gamma = \left[\frac{R}{\beta} * A * s + \frac{\rho}{\beta} * s^2 \right]^{1/2} \qquad \text{(A2.1)}$$

and

$$Zo = \left[\frac{R + \frac{\rho}{A} * s}{\frac{A}{\beta} * s} \right]^{1/2} \qquad \text{(A2.2)}$$

where: A - area of pipe

R - press drop in pipe/unit flow/unit length

ρ - density of oil

β - effective bulk modulus

s - Laplace transform operator

The pipe resistance is evaluated assuming laminar flow conditions:

$$R = \frac{128.0 * \mu}{\pi * d^4} \qquad (A2.3)$$

In order to take into account of the influence of frequency on the wave front configuration a correction factor [53] must be applied to the fluid density and viscosity using a dimensionless quantity "ha", where:

$$ha = \left[\frac{d}{2} * \frac{\omega * \rho}{\mu} \right]^{1/2} \qquad \text{for } ha > 10 \qquad (A2.4)$$

The frequency dependent values of density and viscosity become:

$$denf = den * \left(1 + \frac{\sqrt{2}}{ha} \right) \qquad (A2.5)$$

$$muf = mu * (0.0425 + 0.175 * ha) \qquad (A2.6)$$

Substituting these values in equations (A2.1),(A2.2) and (A2.3) the values of γ and Zo are evaluated.

From the value of propagation constant it is possible to evaluate the speed of sound, for a loss less case:

$$a = \frac{j\omega}{\gamma} \qquad (A2.7)$$

In fig.A2.1 the values of the speed of sound are presented for different values of frequency and pressure, for a 20mm diameter steel pipe and 2mm thickness wall and with the fluid at 40 C.

```
      subroutine gamma_zo(freq,idia,den,mu,beff,gamma,zo)
*
*     subprogram name - gamma_zo.fortran
*
*     library classification - BENGF gamma_zo.223.01
*
*     TITLE - Evaluation of propagation constant
*             and pipe impedance
*
*     New Fortran 5a Multics          25/2/80
*
*     No special hardware requirements
*
*     Author -  F.Freitas
*
*     Purpose - Evaluate the wave propagation constant and
*               pipe characteristic impedance
*
*     Revisions -
*
*     ALL VARIABLES TRANSFERRED VIA ARGUMENT LIST
*
*     Input Information
*     -----------------
*       freq   - frequency                                  [hz]
*       idia   - internal diameter of pipe                  [m]
*       den    - density of oil at working conditions       [Kg/m3]
*       mu     - dyn. visc. of oil at working conditions    [Ns/m2]
*       beff   - effective bulk mod. of oil in pipe         [N/m2]
*
*     Output Information (complex variables)
*     --------------------
*
*       gamma  - wave propagation constant
*       zo     - pipe characteristic impedance
*
*     Variables names (excluding input/output information)
*       ap     - internal area of pipe                      [m2]
*       denf   - density of oil at frequency 'freq'         [Kg/m3]
*       ha     - correction factor
*       muf    - dyn. visc. of oil at frequency 'freq'      [Ns/m2]
*       r      - pipe resistance                            [N/m2]
*       w      - frequency                                  [rad/s]
*
*     Associated Subroutine - The properties of the oil used
*                             as input information for this
*     subroutine may be evaluated using subroutine 'fluid_prop'.
*
*     Error message : A warning is given when ha<=10.
*
*     * * * * * * * * * * * * * * * * * * * * * * * * * * * *
*
      real mu,idia,muf
      complex gamma,zo
*
      pi   =3.14159
*
```

```
      ap    =idia*idia*pi/4.0
      w     =2.0*pi*freq
      ha    =idia*sqrt(w*den/mu)/2.0
*
      if(ha.le.10.0)write(6,10)
      denf =den*(1.0+(sqrt(2.0)/ha))
      muf   =mu*(0.425+0.175*ha)
      r     =128.0*muf/(pi*(idia**4.0))
*
*
      gamma=csqrt(cmplx((w*w*denf/(-beff)),(ap*r*w/beff)))
*
      zo=csqrt(cmplx((denf*beff/ap**2.),((-r)*beff/(ap*w))))
*
10    format(1h ,"WARNING:    variable  ha <= 10.0 ")
      return
      end
```

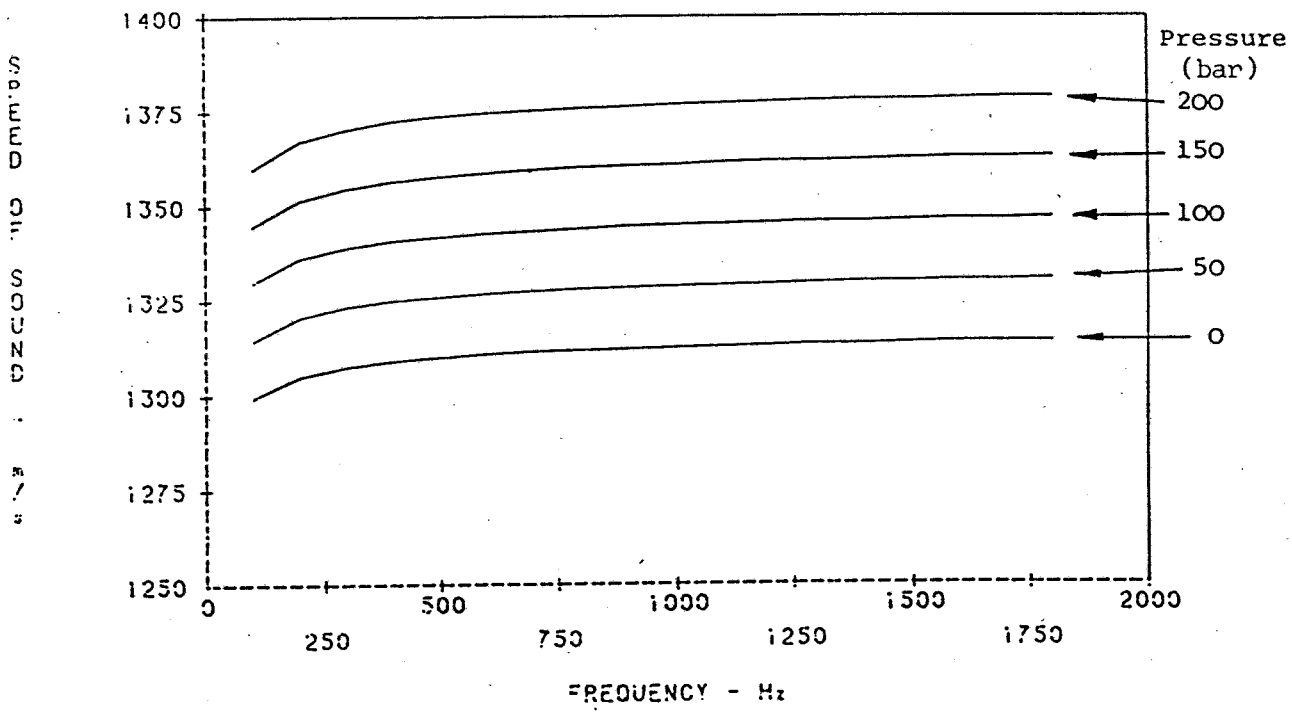

Fig.A2.1 Variation of speed of sound in a fluid with pressure and frequency

COMPUTER PROGRAM DOCUMENTATION

FOR PROGRAM "tunemeth.fortran"

Library Classification

BENGP tunemeth.223.01

TITLE - EVALUATION OF SOURCE FLOW, SOURCE IMPEDANCE AND TERMINATION IMPEDANCE USING TUNED LENGTHS METHOD

New Fortran 5a Multics 29/7/80

A graphics terminal or hard-copy plotter is required for plotted output.

Author : F. Freitas

Purpose - Evaluate source and termination characteristics in a pump/rigid pipe/termination system using the tuned length test technique. The system may be tested at several different frequencies or mean pressures.

Associated Subroutines

fluid_prop - evaluates oil properties (BENGF.221.01)

gamma_zo - evaluates wave propagation const. and pipe impedance (BENGF.222.01)

devend - gino library routine

piccle - gino library routine

vterm - gino library routine

units - gino library routine

tunesub - sub -program containing the following routines: (BENGF.224.01)

ginoflow - plots volume ripple vs pump rotation

ginotime - plots source flow vs time

insertion- prints on top right corner of each plot data details

quest1 - interactive questioning routine

quest2 - interactive questioning routine

quest3 - interactive quesioning routine

quest4 - interactive questioning routine

setgino - plots impedances (dB) vs frequency (log scale)

Input variables (from file01 or terminal if working interactively)

bb	- character string variable	-
calib	- calibration factor of pressure transducers	[bar/volt]
file	- array containing data file numbers	-
freq	- array containing fundamental frequencies	[Hz]
isca	- identifier of input data scale:Volts or dB	-
kpar	- identifier of parameter varied during tests	-
l	- line length array	[m]
mm(1)	- number of harmonics	-
mm(2)	- number of different values of parameter	-
mm(3)	- number of pipe lengths	-
mpres	- array containing values of mean pressure	[bar]
nn(1)	- mean temperature	[C]
nn(2)	- internal diameter of pipe	[mm*10]
nn(3)	- thickness of pipe wall	[mm*10]
scale	- identifier of type of output data scale	-
x	- position of 1st transducer in line	[m]
y	- position of 2nd transducer in line	[m]

Input variables (from terminal only)

aa - character string variable -

anal - identifier of type of output:printed or plotted-

flow - array containing mean pump flow [ℓ/s]

np - number of pumping elements -

Input variables (from user data files - exper. results)

apx - ampl of harm comp of pres fluct at point x [volt or dB]

apy - ampl of harm comp of pres fluct at point y [volt or dB]

ppx - phase of harm comp of pres fluct at point x [deg]

ppy - phase of harm comp of pres fluct at point y [deg]

Error Messages - a large number of error messages is built mainly in the interactive part of the program, to prevent the user from giving incorrect answers or supplying mistyped data.

Storage - 6 Records length

PROGRAM ACTION AND ALGORITHM

The program is constituted by three distinctive parts:

a) Interactive data aquisition

b) Processing of experimental data

c) Output of results

A basic flow diagram of the program is shown in fig.A3.1

a) Interactive data aquisition - the program was designed to suit the needs of a large variety of users, i.e. from the casual user, with little knowledge of computer matters, to the heavy user interested in quick and efficient response.

All the information necessary to define the test conditions is

stored in a data file named **file01**. This file contains a great deal of information which may not be easy to write for the casual user. Hence, the program itself will create the file for the user from answers given during the interactive part of the program. The file is stored afterwards and may be used for a second run or subsquent runs of the program without further interaction. The heavy user may create the data file himself and by-pass the lengthy process of interactive work.

The system may be tested either at different pump speeds (different fundamental frequencies) or different mean pressures (up to 10). This is named the **test parameter** throughout the program. The test parameter may have only one value if the system is tested at only one mean pressure and one fundamental frequency.

Up to 10 harmonics of the fundamental frequency may be processed and up to 20 line lengths may be tested.

If the user chooses interactive use and has no initial data file (file01), this will be created for him and initialized by setting all data variables to zero. If file01 already exists, it will be read as it is. The program will go through all the variables asking the user whether their values are correct or need to be modified.

When enough information has been gathered, the program advises on suitable lengths to be tested, assuming that the two transducers are close to the pump and close to the termination. If they are not, the lengths suggested by the program must be understood to be the distances between the transducers. After this, an escape has been introduced in case tests have not yet been performed. The program stops after having written **file01** with the new data (so far).

The experimental data files are named **fileXX**, where XX is a two-digit number between 20 and 99 in order to avoid possible selection of numbers such as 14 and 15 which are used by the program as output data files. A second escape exists after these numbers are given in case files are not written. File **file01** is updated if the escape is used.

The experimental values of pressure fluctuation must be in the form (amplitude,phase), where the amplitude is the R.M.S. value in volts or dB (relative to 10^{-5} volts) and the phase is the angle in advance of the reference signal in relation to each harmonic component.

Throughout the interactive part of the program the answers **yes** and **no** are accepted if typed only as **y** or **n**, but any other answer may give an error message.

b) Processing experimental data. The processing of results is contained in a large loop for successive tests at different values of the test parameter. This is characterized by the variable **tes**.

The fluid properties are evaluated using **fluid_prop**. The first test file is read and pressure ripple amplitudes and phases are converted to **bar** and **rad**, respectively.

The results of the line length tests are used for the evaluation of ρ_t and ρ_t. For each harmonic the lengths are checked for agreement with tuned conditions. Only the lengths that meet the required conditions are processed.

The value of ρ_t for each line length and each harmonic is obtained using the following equation:

$$\rho_t = \frac{e^{-\gamma x} - \frac{p_x}{p_y} e^{-\gamma y}}{e^{-\gamma(2\ell - x)} - \frac{p_x}{p_y} e^{\gamma(2\ell - y)}} \qquad \text{(A3.1)}$$

An average value, for each harmonic, of ρ_t is evaluated from all the tuned conditions encountered. If for any harmonic the number of tuned conditions is less than two, then a warning message is displayed. When the calculated value of $|\rho_t| < 0.3$, the subsequent evaluation of ρ_t may not be accurate and another warning message is issued. The calculations proceed only for the harmonics at which ρ_t was evaluated.

For the evaluation of ρ_t, pairs of line length tests must be considered. Each test contains two pressure readings (p_x and p_y) and hence, for each pair of lengths considered ρ_t can be evaluated either through p_x values or through p_y values. An average value of ρ_t is calculated from all accepted conditions.

For all the harmonics at which ρ_t and ρ_t were evaluated, Q_s is found by using both p_x and p_y, according to the following equation :

$$Q_s = \frac{p\,(Z_s + Z_o)}{Z_s\, Z_o} * \frac{1 - \rho_s\, \rho_t\, e^{-2\gamma\ell}}{e^{-\gamma x} + \rho_t\, e^{-\gamma(2\ell - x)}} \qquad \text{(A3.2)}$$

where: $p = p_x$
or $p = p_y$

The results of individual values of Q_s from all line length tests are averaged and transformed into S.I. units ($[m^3/s]$). The final value of Q_s is transformed into the peak-to-peak amplitude.

On three occasions in the program an averaging process of complex data must be carried out, corresponding to the evaluation of the reflection coefficients ρ_t and ρ_t and the source flow ripple, Q_s. Whilst the individual values of Q_s are usually very similar and consistent, the values of either ρ_t or ρ_t calculated from individual

tests may present scattered results, both in terms of amplitude and phase.

A simple way of finding the average of two complex numbers is to average both the real and imaginary components. However, although the operation is mathematically correct it may provide false answers, as shown in fig.A3.4. In the first example (a), it is shown how it is possible to obtain, from two numbers of similar amplitude but different phase, a result (OC) which is unrepresentative of the average. Although example (a) is over-pessimistic in terms of phase, it highlights one of the facts when evaluating ρ_t and ρ_t: The amplitude results are much more consistent than the phase results. The example presented in (b) shows that larger amplitude components have a dominating effect when averaging phase. Occasionally, values of $|\rho|$ much greater than 1. are evaluated (see section 2.4). As these values are definitely in error and impose their phase on to the results, the final value will be badly affected. Hence, when large values of $|\rho|$ are detected those data values are not processed. If in this context a large value is considered to be one where $|\rho|>1.$, then the final result has a high content of lower amplitude components which may be very erroneous. To counter-balance this, a large value of $|\rho|$ was considered to be one where $|\rho|>1.5$.

In fig.2.4 the result OC' is evaluated from averaging amplitudes and phases of complex data, independently. Although this does not provide a true mathematical average of two complex values it does give a more realistic representation of the components. However, this process is not as easy as averaging the real and imaginary parts, because of averaging phase around the limiting values. Consider, for example, the case where the phase ϵ [-180.,+180.] and two phase are to be averaged. Let $phase_1$=175. and $phase_2$=-160., the

average of these two values is NOT:

$$\text{phase} = \frac{175 + (-160)}{2} = 7.5$$

but,

$$\text{phase} = \frac{175 + (-160.+360.)}{2} = 187.5$$

but this value is not within [-180.,+180.] and has to be modified to:

$$\text{phase} = 187.5 - 360. = -172.5$$

this is the true mean value of the phases. If a third value is to be averaged to the former two, then the average of the first two must be weighed by a factor of 2.

A basic flow diagram of phase averaging is shown in fig.A3.5. This was the process used throughout the program providing very satisfactory results.

c) Output of results. The output results of termination and source impedances and source flow may be printed or plotted. Printed results of impedance may be in S.I. units (Ns/m^5) or dB (relative to 1 Ns/m^5), whereas source flow harmonics will always be printed in m^3/s. Graphical results of impedance are only plotted in dB vs a logarithmic scale of frequency ([Hz]), as in a Bode-plot. The graphical output of source flow is given either as a Fourier synthesis of its harmonic components (peak value) versus time, or in the form of a displacement ripple versus pump angle of rotation.

All graphics have fixed scales for ease of comparison of successive test results.

The results file (file14) contains a heading detailing values of fundamental frequency and mean pressure of the test, followed by

averaged values of amplitude and phase of ρ_t, Z_t, ρ_t, Z_s and Q_s. Whenever the values of a particular harmonic are not successfully evaluated a line of **hyphens** will appear.

The results presented in **file15** are only to be studied if a detailed analysis is desired and can only be of interest to the specialist user. The file contains the individual values of ρ_t and the line lengths used in their evaluation, in order to pin-point erroneous data values. The second part of the file gives similar details on the evaluation of **rhosx** and **rhosy**, and the pairs of line lengths which were considered.

The program finishes with the updating of file01, so that a second run of the program may be done without further interaction. This may be required, for example, when the output is to be plotted and only written output was demanded in the first run.

TYPICAL PROGRAM RUN

A typical run of the program is presented below. The example corresponds to a system composed of an external gear pump, rigid steel pipe and an adjustable restrictor as a load. The system was tested at 10, 50, 100 and 150 bar mean pressures. Ten different line lengths were connected between source and termination. For practical reasons neither transducer could be very close to the pump or restrictor valve. Pressure transducer P_1 was positioned 0.11 m away from the pump, and transducer P_2 was 0.075 m from the termination.

Typically only six harmonic components are considered when defining gear pump generated ripple (see section 2.1), although ten harmonics are presented in the example run. Results for the highest four harmonics (see file14) show less consistency than the first six.

All harmonics at 150, 100 and 50 bar tests were successful apart from the 9th harmonic for the 100 bar test due to scattered data. For the 10 bar test, the restrictor valve impedance is similar to the line impedance at the lower harmonics and the program warns of possible innacurate prediction of Z_s and Q_s.

Only part of file15 is presented below due to its extensive length but the results are representative.

Typical plotted output results are shown in fig.A3.3 for termination impedance, source impedance and source flow.

LISTING OF PROGRAM "tunemeth.fortran"

```
*     PROGRAM NAME  - tunemeth.fortran
*
*     LIBRARY CLASSIFICATION  -          BENGF tunemeth.223.01
*
*     TITLE - EVALUATION OF SOURCE FLOW,SOURCE IMPEDANCE AND
*             TERMINATION IMPEDANCE USING TUNED LENGTHS METHOD
*
*     New Fortran 5a Multics                                  27/3/80
*
*     A graphics terminal may be used to see plotted output
*
*     Author -  F.Freitas
*
*     Purpose - EVALUATE SOURCE AND TERMINATION CHARACTERISTICS OF A
*           PUMP/RIGID PIPE/TERMINATION SYSTEM WITH DIFFERENT PIPE
*           LENGTHS.  FUNDAMENTAL FREQUENCY OR MEAN PRESSURE CAN BE
*           VARIED FOR DIFFERENT SETS OF EXTENDED PIPE LENGTH TESTS.
*
*     REVISIONS  -
*
*     SOME COMMENTS ON " RUNNING PROCEDURE OF THE PROGRAM "
*
*      THE PROGRAM RUNS INTERACTIVELY WITH THE USER ASKING ALL
*      INFORMATION NECESSARY TO PERFORM THE TASK
*
*     HOW TO WRITE A DATA FILE COMPATIBLE WITH THE PROGRAM:
*
*     1 - create as many files as the number of different
*       fundamental frequencies or mean pressures tested
*       (file numbers must be >=20 and <=99).
*     2 - type data in each file as follows:(p-pipe;t-transd;h-harm)
*
*     amp(h1,t1,p1) pha(h1,t1,p1)    amp(h1,t2,p1) pha(h1,t2,p1)
*     amp(h2,t1,p1) pha(h2,t1,p2)    amp(h2,t2,p1) pha(h2,t2,p1)
*     . . . . . .                    . . . . . .
*     amp(h1,t1,p2) pha(h1,t1,p2)    amp(h1,t2,p2) pha(h1,t2,p2)
*     . . . . . .                    . . . . . .
*     amp(hn,t1,pn) pha(hn,t1,pn)    amp(hn,t2,pn) pha(hn,t2,pn)
*
*     AFTER RUNNING THE PROGRAM ONCE ALL THE NECESSARY INFORMATION
*     TO REPEAT THE RUN HAS BEEN STORED.
*
*     INBUILT ERROR MESSAGES - several error messages are built in
*                 the program in order to help the user avoiding
*                 mistakes when feeding data or answering questions.
*
*     Input variables (from file01 or terminal if interactive action)
*
*     bb      - character string variable                      -
*     calib   - calibration factor of pressure transducers     [bar/volt]
*     file    - array containing data file numbers             -
*     freq    - array containing fundamental frequencies       [Hz]
*     isca    - identifier of input data scale:Volts or dB     -
*     kpar    - identifier of parameter varied during tests    -
```

```
*     l       - line length array                                    [m]
*     mm(1)   - number of harmonics                                  -
*     mm(2)   - number of different values of parameter              -
*     mm(3)   - number of pipe lengths                               -
*     mpres   - array containing values of mean pressure             [bar]
*     nn(1)   - mean temperature                                     [C]
*     nn(2)   - internal diameter of pipe                            [mm*10]
*     nn(3)   - thickness of pipe wall                               [mm*10]
*     scale   - identifier of type of output data scale              -
*     x       - position of 1st transducer in line                   [m]
*     y       - position of 2nd transducer in line                   [m]
*
*     Input variables (from terminal only)
*
*     aa      - character string variable                            -
*     anal    - identifier of type of output:printed or plotted-
*     flow    - array containing mean pump flow                      [l/s]
*     np      - number of pumping elements                           -
*
*     Input variables (from user data files - exper. results)
*
*     apx     - ampl of harm comp of pres fluct at point x           [volt or dB]
*     apy     - ampl of harm comp of pres fluct at point y           [volt or dB]
*     ppx     - phase of harm comp of pres fluct at point x          [deg]
*     ppy     - phase of harm comp of pres fluct at point y          [deg]
*
*     Insource variables names (* denotes complex variable)
*
*     ab      - character string variable                            -
*     ac      - character string variable                            -
*     ad      - character string variable                            -
*     add     - character string variable                            -
*     ag      - character string variable                            -
*     beff    - effective bulk modulus of fluid in pipe              [N/m2]
*     counter- incremental variable of pairs of lengths tested-
*               when evaluating rhos
*     denp    - density of fluid                                     [Kg/m3]
*     factx   - factor used in calculation of rhosx                  *
*     facty   - factor used in calculation of rhosy                  *
*     gamma   - wave propagation constant                            *
*     i       - subscript; identifies harmonic in calculations       -
*     idia    - internal diameter of pipe                            [m]
*     jok     - incremental variable counting number of line         -
*               lengths rejected when evaluating rhot
*     joker   - incremental variable counting number of pairs of     -
*               line lengths rejected when evaluating rhos
*     lim     - constant used on printing stage to file15            -
*     l1      - identifies 1st pipe length when evaluating rhos-
*     l2      - identifies 2nd pipe length when evaluating rhos-
*     maqs    - mean value of |qs|                                   [m3/s]
*     marhos  - mean value of |rhos|                                 -
*     marhot  - mean value of |rhot|                                 -
*     mpqs    - mean value of phase of qs                            [deg]
*     mprhos  - mean value of phase of rhos                          [deg]
*     mprhot  - mean value of phase of rhot                          [deg]
*     mrhos   - mean value of rhos                                   *
*     mrhot   - mean value of rhot                                   *
*     mup     - dynamic viscosity of fluid                           [Ns/m2]
*     mzs     - mean value of zs                                     *
*     mzt     - mean value of zt                                     *
*     par     - array containing values of parameter varied          -
```

```
*     pha    - phase of rhot                                        [deg]
*     phaqx  - phase of qsx                                         [deg]
*     phaqy  - phase of qsy                                         [deg]
*     phax   - phase of rhosx                                       [deg]
*     phay   - phase of rhosy                                       [deg]
*     pi     - constant =3.14159                                    -
*     px     - pressure fluctuation at point x                      *
*     py     - pressure fluctuation at point y                      *
*     qsx    - pump source flow evaluated using px                  *
*     qsy    - pump source flow evaluated using py                  *
*     ratio  - ratio of pres. fluct. for evaluation of rhot         *
*     ratiox - ratio of pres. fluct. for evaluation of rhosx        *
*     ratioy - ratio of pres. fluct. for evaluation of rhosy        *
*     rhosx  - source reflection coefficient evaluated from         *
*              pressures at point x
*     rhosy  - source reflection coefficient evaluated from         *
*              pressures at point y
*     rhot   - termination reflection coefficient                   *
*     temp   - mean oil temperature                                 [C]
*     tes    - identifier of parameter value under calculation-
*     th     - thickness of pipe wall                               -
*     totaqs - totalizer value of |qs|                              -
*     totarhos- totalizer value of |rhos|                           -
*     totarhot- totalizer value of |rhot|                           -
*     totpqs - mean value of phase of qs                            [deg]
*     totprhos- mean value of phase of rhos                         [deg]
*     totprhot- mean value of phase of rhot                         [deg]
*     vec    - variable used to check tuned length condition        [rad]
*     z      - array holding values of harmonic frequency           [Hz]
*     zero   - constant =0                                          -
*     zo     - impedance characteristic of pipe                     [Ns/m5]
*
*    Associated Sub-programs
*
*     fluid_prop - evaluates oil properties (BENGF fluid_prop.221.01)
*     gamma_zo   - evaluates wave propagation constant and
*                  pipe impedance (BENGF gamma_zo.222.01)
*     tunesub    - this sub-program contains the following
*                  sub-routines (BENGF tunesub.224.01):
*         ginoflow  - plots pump source flow vs pump rotation
*         ginotime  - plots pump source flow vs time (ms)
*         insertion - writes at top right corner of plot
*                     data details
*         quest1    - questioning routine for interactive data input
*         quest2    - questioning routine for interactive data input
*         quest3    - questioning routine for interactive data input
*         quest4    - questioning routine for interactive data input
*         setgino   - plots impedances (dB) vs frequency (Hz-log)
*
*
*     * * * * * * * * * * * * * * * * * * * * * * * * * * * * * *
*
*     DECLARATIVE STATEMENTS
*
      dimension nn(3),mm(3),calib(2),x(20),y(20),
     &  joker(10,10),jok(10,10),freq(10),pha(20,10),z(10),
     &  totarhot(10),totprhot(10),totarhos(10),totprhos(10),flow(10),
     &  totaqs(10),totpqs(10),par(10),phay(20,20,10),phax(20,20,10)
      integer tes,scale,counter,file(10),test,anal
      real idia,l(20),mup,mpres(10),marhot,mprhot,marhos,mprhos,
     &  maqs(10),mpqs(10),mazt(10),mpzt(10),mazs(10),mpzs(10)
```

```
      complex px(20,10),py(20,10),zo(10),gamma(10),ratio,rhot(20,10),
&     ratiox,ratioy,factx,facty,qs(10),mrhot(10,10),mzt,mzs,
&     mrhos(10,10),rhosx(20,20,10),rhosy(20,20,10),qsx(20,10),qsy(20,10)
      character*26 ab(3),ad(3),add(2)
      character*17 ac(2),ag
      character*1 aa,bb
      external fluid_prop(descriptors),gamma_zo(descriptors),
&     quest1(descriptors),quest2(descriptors),quest3(descriptors),
&     ginoflow(descriptors),setgino(descriptors),insertion(descriptors)
      open(6,mode="out",form="formatted",carriage=.true.,defer=.true.)
      open(14,mode="out",form="formatted",carriage=.true.,defer=.true.)
      open(15,mode="out",form="formatted",carriage=.true.,defer=.true.)
*
*     INITIAL VALUES
*
      pi=3.14159
      ac(1)="FUNDAMENTAL FREQ."
      ac(2)=" MEAN PRESSURE "
      add(1)="file no.at fund.freq."
      add(2)="file no.at mean press"
      ab(1)=" NUMBER OF HARMONICS "
      ab(3)=" NUMBER OF PIPE LENG."
      ad(1)=" MEAN TEMPERATURE "
      ad(2)="INTERNAL DIAMETER  (mm*10)"
      ad(3)="THICK. OF PIPE WALL(mm*10)"
      ag="Pipe test"
      zero=0
*
*     INTERACTIVE PART OF PROGRAM
*
1     print,'Hello!  Do you want interactive program action?'
      input,bb
      if(bb.eq."n") go to 30
      if(bb.eq."y")go to 5
      print,' Please answer "yes" or "no"'
      go to 1
5     print,'Is the input data file (file01) already written?'
      input,aa
      if(aa.ne.'n')go to 30
10    do 20 i=1,120
      write(1,1000)zero
20    continue
      rewind 1
30    read(1,1000,err=40)mm,nn,kpar,scale,file,mpres,freq,isca
      read(1,1000,err=40)calib,(l(i),x(i),y(i),i=1,20)
      go to 50
40    print,"file01 contains some error; do you want to rewrite it?"
      input,aa
      if(aa.eq.'y')go to 10
      go to 990
50    if(kpar.eq.1)go to 70
      do 60 i=1,10
60    par(i)=mpres(i)
      go to 90
70    do 80 i=1,10
80    par(i)=freq(i)
*
90    if(bb.eq.'n')go to 420
      print,"THIS PROGRAM EVALUATES THE SOURCE FLOW AND THE SOURCE AND "
      print,"TERMINATION IMPEDANCES IN A SYSTEM AS REPRESENTED"
      print,"         IN THE FOLLOWING PICTURE"
```

```
      print
      print,"          **                                  ___"
      print,"    ------*  *-------------------------------| T |-------"
      print,"   |       **                                  ___         |"
      print,"   |      PUMP                                             |"
      print,"  |_|                                                     |_|"
      print
      print,"TESTS PERFORMED ON THIS SYSTEM ARE SUPPOSED TO VARY EITHER:"
      print,"         1 - Fundamental frequency"
      print,"         2 - Mean pressure"
      print
      print,"   For each pair of frequency and mean pressure"
      print,"   Several pipe length tests are allowed"
      print
      print,'   WHICH PARAMETER DO YOU VARY IN TESTS? "1" or "2"'
      call quest4(kpar)
      if(kpar.eq.2)go to 140
120   ab(2)="NUMBER OF FUND.FREQUENCIES"
      do 130 i=1,10
      par(i)=freq(i)
130   continue
      go to 160
140   ab(2)="NUMBER OF MEAN PRESSURES"
      do 150 i=1,10
      par(i)=mpres(i)
150   continue
160   print,"   THIS PROGRAM IS PREPARED TO ACCEPT UP TO:"
      print,"                    10 ",ab(2)
      print,"                    10 HARMONICS "
      print,"                    20 DIFFERENT PIPE LENGTHS "
      print
      call questl (ab,nn)
      call quest2(ac(kpar),nn(2),par)
      call questl(ad,mm)
      if(kpar.eq.2) go to 210
170   print,"    Which mean pressure did you use?[bar]"
      read(5,1000,err=190)mpres(1)
      do 180 i=1,10
      mpres(i)=mpres(1)
      freq(i)=par(i)
180   continue
      go to 230
190   write(6,1070)
      go to 170
200   write(6,1070)
210   print,"  Which fundamental frequency did you use?[Hz]"
      read(5,1000,err=200)freq(1)
      do 220 i=1,10
      freq(i)=freq(1)
      mpres(i)=par(i)
220   continue
230   print,"Do you need suggestions of suitable lengths to test?"
      input,aa
      if (aa.eq."n") go to 250
      do 240 i=1,nn(2)
      call fluid_prop(mpres(i),mm(1)/1.,mm(2)/10000.,mm(3)/10000.,
&     denp,mup,beff)
      call gamma_zo(freq(i),mm(2)/10000.,denp,mup,beff,
&     gamma(i),zo(i))
      write(6,1240)ac(kpar),i
      write(6,1250)0.4*pi/cabs(gamma(i)),0.6*pi/cabs(gamma(i))
```

```
      write(6,1250)0.2*pi/cabs(gamma(i)),0.3*pi/cabs(gamma(i))
      write(6,1250)0.13*pi/cabs(gamma(i)),0.2*pi/cabs(gamma(i))
      write(6,1250)0.1*pi/cabs(gamma(i)),0.15*pi/cabs(gamma(i))
      write(6,1260)
240   continue
250   print,'Have you performed tests already?'
      input,aa
      if(aa.eq.'n') go to 950
260   print,"  The length of pipes used and pressure points are:"
      write(6,1030)ag
      do 270 i=1,nn(3)
      write(6,1040)ag,i,l(i),x(i),y(i)
270   continue
      print,"  Do you want to change them?"
280   input,aa
      if(aa.eq."y")go to 290
      if(aa.eq."n") go to 320
      print,'  Please answer "yes" or "no"'
      go to 280
290   do 300 i=1,nn(3)
      write(6,1060)i
      read(5,1000,err=310)l(i),x(i),y(i)
300   continue
      go to 260
310   write(6,1070)
      go to 260
320   print
      print,"The pressure readings are given in individual files by"
      print,"AMPLITUDE and PHASE of all HARMONICS, for different"
      write(6,1080) ac(kpar)
340   print,"   (THE FILE NUMBERS MUST BE >=20 AND <=99)"
      print
      call quest3(add(kpar),nn(2),file)
      do 350 i=1,nn(2)
      if(file(i).lt.20.or.file(i).gt.99) go to 340
350   continue
      print,"  ARE EXPERIMENTAL DATA FILES ALREADY WRITTEN?"
      input,aa
      if(aa.eq."n") go to 950
      print," Which units did you use for input data amplitude?"
      print,"        1 - in VOLTS"
      print,"        2 - in dB"
      call quest4(isca)
380   print," Give overall calibration factors for pressure points
     & in 'bar/volt':"
      print," Calibration factor for pressure 1 ="
      read(5,1000,err=390)calib(1)
      print," Calibration factor for pressure 2="
      read(5,1000,err=390) calib(2)
      go to 400
390   write(6,1070)
      go to 380
*
400   print,"    Which scale do you want for Impedance Results?"
      print,'        1 - SI units (Ns/m**5)'
      print,'        2 - dB scale'
      call quest4(scale)
420   print,"   Do you want to have:"
      print,"        1- Results printed into a file (file14)"
      print,"        2- Plotted results (output to attached file)"
      print,"        3- Both"
```

```
430   read(5,1000,err=440)anal
      if(anal.eq.1.or.anal.eq.2.or.anal.eq.3)go to 450
      print,'        Please answer "1" or "2" or "3" only'
      go to 430
440   write(6,1070)
      go to 420
450   th=mm(3)/10000.0
      temp=mm(1)
      idia=mm(2)/10000.0
*
*
*     START CALCULATIONS LOOP FOR EACH TEST DATA
*
      do 880 tes=1,nn(2)
*
*     Fluid Properties
*
      call fluid_prop(mpres(tes),temp,idia,th,denp,mup,beff)
*
*     SET TOTALIZERS TO ZERO
*
      do 460 i=1,nn(1)
      totarhot(i)=0.0
      totprhot(i)=0.0
      totarhos(i)=0.0
      totprhos(i)=0.0
      totaqs(i)=0.0
      totpqs(i)=0.0
      joker(i,tes)=0
      jok(i,tes)=0
460   continue
*
*     READING EXPERIMENTAL DATA
*
      do 530 ll=1,nn(3)
      do 490 i=1,nn(1)
      read(file(tes),1000) apx,ppx,apy,ppy
      if(isca.eq.1)go to 470
      apx=calib(1)*10**((apx-100.0)/20.)
      apy=calib(2)*10**((apy-100.0)/20.)
      go to 480
470   apx=calib(1)*apx
      apy=calib(2)*apy
480   ppx=ppx*pi/180.0
      px(ll,i)=cmplx((apx*cos(-ppx)),(apx*sin(-ppx)))
      ppy=ppy*pi/180.
      py(ll,i)=cmplx((apy*cos(-ppy)),(apy*sin(-ppy)))
490   continue
*
*     EVALUATION OF TERMINATION REFLECTION COEFFICIENT AND IMPEDANCE
*
      do 520 i=1,nn(1)
      z(i)=i*freq(tes)
      call gamma_zo(z(i),idia,denp,mup,beff,gamma(i),zo(i))
      rhot(ll,i)=0.0
      pha(ll,i)=0.0
*     Select tuned conditions
      vec=cabs(gamma(i))*abs(y(ll)-x(ll))
      do 500 n=1,15
      if(vec.gt.0.65*pi+pi*(n-1))go to 500
      if(vec.gt.0.35*pi+pi*(n-1))go to 510
```

```
      jok(i,tes)=jok(i,tes)+1
      go to 520
500   continue
*     calculate rhot for accepted cases
510   ratio=px(ll,i)/py(ll,i)
      rhot(ll,i)=(cexp(-gamma(i)*x(ll))-ratio*cexp(-gamma(i)*y(ll)))
&     /(ratio*cexp(-gamma(i)*(2*l(ll)-y(ll)))
&     -cexp(-gamma(i)*(2*l(ll)-x(ll))))
*
      pha(ll,i)=atan2(aimag(rhot(ll,i)),real(rhot(ll,i)))
*     make phase additionable to mean value
      if(abs(totprhot(i)-pha(ll,i)).gt.pi.and.pha(ll,i).lt.0.0)
&     pha(ll,i)=pha(ll,i)+2.0*pi
      if(abs(totprhot(i)-pha(ll,i)).gt.pi.and.pha(ll,i).ge.0.0)
&     pha(ll,i)=pha(ll,i)-2.0*pi
*
      if(cabs(rhot(ll,i)).gt.1.5)go to 515
      go to 517
515   jok(i,tes)=jok(i,tes)+1
      if(cabs(rhot(ll,i)).gt.1.5)rhot(ll,i)=10.
      go to 520
517   totarhot(i)=totarhot(i)+cabs(rhot(ll,i))
*     evaluate mean value of phase
      totprhot(i)=(totprhot(i)*(ll-1-jok(i,tes))
&     +pha(ll,i))/(ll-jok(i,tes))
      if(totprhot(i).gt.pi)totprhot(i)=totprhot(i)-2*pi
      if(-totprhot(i).gt.pi)totprhot(i)=totprhot(i)+2*pi
520   continue
530   continue
*
*     write individual values of rhot for accepted values only
      write(15,1200)
      write(15,1090)ac(1),freq(tes),ac(2),mpres(tes)
      write(15,1110)
      write(15,1120)
      write(15,1100)
      if(nn(1).gt.5)go to 540
      lim=nn(1)
      go to 550
540   lim=5
550   do 580 ll=1,nn(3)
      do 560 i=1,lim
      if(cabs(rhot(ll,i)).ne.0.0)go to 570
560   continue
      go to 580
570   write(15,1130)ll,(cabs(rhot(ll,i)),pha(ll,i)*180./pi,i=1,lim)
580   continue
      if(nn(1).le.5)go to 590
      write(15,1300)
      write(15,1100)
      do 610 ll=1,nn(3)
      do 590 i=lim+1,nn(1)
      if(cabs(rhot(ll,i)).ne.0.0)go to 600
590   continue
      go to 610
600   write(15,1130)ll,(cabs(rhot(ll,i)),pha(ll,i)*180./pi,i=lim+1,nn(1))
610   continue
*     calculate mean value of rhot
620   do 630 i=1,nn(1)
      if(nn(3)-jok(i,tes).eq.0.0)go to 630
      marhot= totarhot(i)/(nn(3)-jok(i,tes))
```

```
      mprhot= totprhot(i)
      mrhot(i,tes)=cmplx((marhot*cos(mprhot)),(marhot*sin(mprhot)))
      if(marhot.le.0.3) write(6,1320)i,ac(kpar),par(tes)
      if(marhot.gt.1.1)write(6,1340)i,ac(kpar),par(tes)
      if(nn(3)-jok(i,tes).lt.2)write(6,1350)i,ac(kpar),par(tes)
630   continue
*
*     EVALUATION OF SOURCE REFLECTION COEFFICIENT AND IMPEDANCE
*
      counter=0
      l2=1
640   do 680 l1=l2+1,nn(3)
      counter=counter+1
      do 670 i=1,nn(1)
      rhosx(l1,l2,i)=0.0
      rhosy(l1,l2,i)=0.0
      phax(l1,l2,i)=0.0
      phay(l1,l2,i)=0.0
*     if rhot was not evaluated for this harmonic
*     rhos cannot be calculated
      if(cabs(mrhot(i,tes)).eq.0.0)go to 670
*     select tuned conditions
      vec=cabs(gamma(i))*abs(l(l1)-l(l2))
      do 650 n=1,15
      if(vec.gt.0.65*pi+pi*(n-1))go to 650
      if(vec.gt.0.35*pi+pi*(n-1))go to 660
      joker(i,tes)=joker(i,tes)+1
      go to 670
650   continue
*     calculate rhos for accepted cases
660   ratiox=px(l1,i)/px(l2,i)
      ratioy=py(l1,i)/py(l2,i)
*
      factx=cexp(-gamma(i)*x(l1))
      factx=(factx+mrhot(i,tes)*cexp(-gamma(i)*(2.0*l(l1)-x(l1))))
&     /(cexp(-gamma(i)*x(l2))+mrhot(i,tes)*cexp(-gamma(i)*(2.0*
&     l(l2)-x(l2))))
      rhosx(l1,l2,i)=(ratiox-factx)/(mrhot(i,tes)*((ratiox*cexp(-2.0*
&     gamma(i)*l(l1)))-(cexp(-2.0*gamma(i)*l(l2))*factx)))
      facty=(cexp(-gamma(i)*y(l1))+mrhot(i,tes)*cexp(-gamma(i)*(2.0*
&     l(l1)-y(l1))))/(cexp(-gamma(i)*y(l2))+mrhot(i,tes)
&     *cexp(-gamma(i)*(2.0*l(l2)-y(l2))))
      rhosy(l1,l2,i)=(ratioy-facty)/(mrhot(i,tes)*(ratioy*cexp(-2.0*
&     gamma(i)*l(l1))-cexp(-2.0*gamma(i)*l(l2))*facty))
*
      if(cabs(rhosx(l1,l2,i)).gt.1.5.or.cabs(rhosy(l1,l2,i).gt.1.5)go to 665
      go to 667
665   joker(i,tes)=joker(i,tes)+1
      if(cabs(rhosx(l1,l2,i)).gt.1.5)rhosx(l1,l2,i)=10.
      if(cabs(rhosy(l1,l2,i)).gt.1.5)rhosy(l1,l2,i)=10.
      go to 670
667   totarhos(i)=totarhos(i)+cabs(rhosx(l1,l2,i))
*     make phasex additionable to mean value
      phax(l1,l2,i)=atan2(aimag(rhosx(l1,l2,i)),real(rhosx(l1,l2,i)))
      if(abs(totprhos(i)-phax(l1,l2,i)).gt.pi.and.phax(l1,l2,i).lt.0.0)
&     phax(l1,l2,i)=phax(l1,l2,i)+2.0*pi
      if(abs(totprhos(i)-phax(l1,l2,i)).gt.pi.and.phax(l1,l2,i).ge.0.0)
&     phax(l1,l2,i)=phax(l1,l2,i)-2.0*pi
*
*     evaluate mean value of phase
      totprhos(i)=(totprhos(i)*(2.0*counter-2-2*joker(i,tes))
```

```
&     +phax(l1,l2,i))/(2*counter-1-2*joker(i,tes))
      if(totprhos(i).gt.pi)totprhos(i)=totprhos(i)-2*pi
      if(-totprhos(i).gt.pi)totprhos(i)=totprhos(i)+2*pi
*
      totarhos(i)=totarhos(i)+cabs(rhosy(l1,l2,i))
*     make phasey additionable to mean value
      phay(l1,l2,i)=atan2(aimag(rhosy(l1,l2,i)),real(rhosy(l1,l2,i)))
      if(abs(totprhos(i)-phay(l1,l2,i)).gt.pi.and.phay(l1,l2,i).lt.0.0)
&     phay(l1,l2,i)=phay(l1,l2,i)+2.0*pi
      if(abs(totprhos(i)-phay(l1,l2,i)).gt.pi.and.phay(l1,l2,i).ge.0.0)
&     phay(l1,l2,i)=phay(l1,l2,i)-2.0*pi
*
*     evaluate mean value of phase
      totprhos(i)=(totprhos(i)*(2.0*counter-1-2*joker(i,tes))
&     +phay(l1,l2,i))/(2.0*counter-2.0*joker(i,tes))
      if(totprhos(i).gt.pi)totprhos(i)=totprhos(i)-2*pi
      if(-totprhos(i).gt.pi)totprhos(i)=totprhos(i)+2*pi
670   continue
680   continue
      l2=l2+1
      if(l2.eq.nn(3))go to 685
      go to 640
*     write individual values of rhos
685   write(15,1140)
      write(15,1150)
      write(15,1100)
      do 720 l2=1,nn(3)
      do 710 l1=l2+1,nn(3)
      do 690 i=1,lim
      if(cabs(rhosx(l1,l2,i)).ne.0.0)go to 700
690   continue
      go to 710
700   write(15,1160)l1,l2,(cabs(rhosx(l1,l2,i)),
&     phax(l1,l2,i)*180.0/pi,i=1,lim)
      write(15,1160)l1,l2,(cabs(rhosy(l1,l2,i)),
&     phay(l1,l2,i)*180.0/pi,i=1,lim)
710   continue
720   continue
      if(nn(1).le.5)go to 770
      write(15,1280)
      write(15,1100)
      do 760 l2=1,nn(3)
      do 750 l1=l2+1,nn(3)
      do 730 i=lim+1,nn(1)
      if(cabs(rhosx(l1,l2,i)).ne.0.0)go to 740
730   continue
      go to 750
740   write(15,1160)l1,l2,(cabs(rhosx(l1,l2,i)),
&     phax(l1,l2,i)*180.0/pi,i=lim+1,nn(1))
      write(15,1160)l1,l2,(cabs(rhosy(l1,l2,i)),
&     phay(l1,l2,i)*180.0/pi,i=lim+1,nn(1))
750   continue
760 continue
770   do 780 i=1,nn(1)
      if(counter-joker(i,tes).lt.2)write(6,1360)i,ac(kpar),par(tes)
      if(totarhos(i).eq.0.0)go to 780
      marhos=totarhos(i)/(2*counter-2*joker(i,tes))
      mprhos=totprhos(i)
      mrhos(i,tes)=cmplx((marhos*cos(mprhos)),(marhos*sin(mprhos)))
780   continue
*
```

```
*     EVALUATION OF SOURCE FLOW
*
      do 800 ll=2,nn(3)
      do 790 i=1,nn(1)
      if(cabs(mrhos(i,tes)).eq.0.or.cabs(mrhot(i,tes)).eq.0)go to 790
      qsx(ll,i)=((px(ll,i)*1.0e05/(zo(i)*(1.0+mrhos(i,tes))/2.0))
&     /(cexp(-gamma(i)*x(ll))+mrhot(i,tes)*cexp(-gamma(i)*(2.0*l(ll)-
&     x(ll)))))*(1.0-mrhot(i,tes)*mrhos(i,tes)*cexp(-2.0*gamma(i)*l(ll)))
      qsy(ll,i)=((py(ll,i)*1.0e+05/(zo(i)*(1.0+mrhos(i,tes))/2.0))/(cexp
&     (-gamma(i)*y(ll))+mrhot(i,tes)*cexp(-gamma(i)*(2.0*l(ll)-y(ll)))))
&     *(1.0-mrhot(i,tes)*mrhos(i,tes)*cexp(-2.0*gamma(i)*l(ll)))
*
      totaqs(i)=totaqs(i)+cabs(qsx(ll,i))+cabs(qsy(ll,i))
*
      phaqx=180.0*atan2(aimag(qsx(ll,i)),real(qsx(ll,i)))/pi
      phaqy=180.0*atan2(aimag(qsy(ll,i)),real(qsy(ll,i)))/pi
*     make phaqx additionable to mean phase of qs
      if(abs(totpqs(i)-phaqx).gt.180.and.phaqx.lt.0)phaqx=phaqx+360
      if(abs(totpqs(i)-phaqx).gt.180.and.phaqx.ge.0)phaqx=phaqx-360
      totpqs(i)=(totpqs(i)*(2*ll-4)+phaqx)/(2*ll-3)
      if(totpqs(i).gt.180.0)totpqs(i)=totpqs(i)-360.0
      if(totpqs(i).lt.-180.0)totpqs(i)=totpqs(i)+360.0
*     make phaqy additionable to mean phase of qs
      if(abs(totpqs(i)-phaqy).gt.180.and.phaqy.lt.0)phaqy=phaqy+360
      if(abs(totpqs(i)-phaqy).gt.180.and.phaqy.ge.0)phaqy=phaqy-360
      totpqs(i)=(totpqs(i)*(2*ll-3)+phaqy)/(2*ll-2)
      if(totpqs(i).gt.180.0)totpqs(i)=totpqs(i)-360.0
      if(totpqs(i).lt.-180.0)totpqs(i)=totpqs(i)+360.0
*
790   continue
800   continue
*
*     evaluate mean value of qs
      do 810 i=1,nn(1)
      if(cabs(mrhos(i,tes)).eq.0.0.or.cabs(mrhot(i,tes)).eq.0.0)go to 810
      maqs(i)=1.414*totaqs(i)/(2*(nn(3)-1))
      mpqs(i)=totpqs(i)
810   continue
*
*     PRINTED RESULTS OUTPUT
*
      if(anal.eq.2) go to 820
*
      write(14,1230)
      write(14,1090)ac(1),freq(tes),ac(2),mpres(tes)
      write(14,1180)
      write(14,1190)
      write(14,1170)
820   do 850 i=1,nn(1)
      if(cabs(mrhos(i,tes)).eq.0.0)go to 840
      marhot=cabs(mrhot(i,tes))
      mprhot=180.0*atan2(aimag(mrhot(i,tes)),real(mrhot(i,tes)))/pi
      mzt=zo(i)*(1.0+mrhot(i,tes))/(1.0-mrhot(i,tes))
      mazt(i)=cabs(mzt)
      mpzt(i)=180.0*atan2(aimag(mzt),real(mzt))/pi
      marhos=cabs(mrhos(i,tes))
      mprhos=180.0*atan2(aimag(mrhos(i,tes)),real(mrhos(i,tes)))/pi
      mzs=zo(i)*(1.0+mrhos(i,tes))/(1.0-mrhos(i,tes))
      mazs(i)=cabs(mzs)
      mpzs(i)=180.0*atan2(aimag(mzs),real(mzs))/pi
      if(anal.eq.2)go to 850
```

```
      if(scale.eq.2)go to 830
      write(14,1210)i,marhot,mprhot,mazt(i),mpzt(i),marhos,mprhos,
&     mazs(i),mpzs(i),maqs(i),mpqs(i)
      go to 850
830   write(14,1220)i,marhot,mprhot,20.0*alog10(mazt(i)),mpzt(i),
&     marhos,mprhos,20.*alog10(mazs(i)),mpzs(i),maqs(i),mpqs(i)
      go to 850
840   write(14,1290)
850   continue
*
*     PLOTTED RESULTS OUTPUT
*
      if(anal.eq.1) go to 880
      if(tes.gt.1)go to 855
      call vterm
      call units(6.4)
      print,' Do you want the flow plot to be:'
      print,'    1 - vs time'
      print,'    2 - vs pump angle of rotation'
      call quest4(iplot)
      if(iplot.eq.2)go to 855
      print,'  Give plotting time (in ms)'
      input, time
855   write(6,1310)ac(kpar),par(tes)
      read(5,1000,err=865)flow(tes)
      if(tes.gt.1)go to 857
      write(6,1330)
      read(5,1000,err=865)np
857   do 860 i=1,nn(1)
      if(cabs(mrhos(i,tes)).eq.0.0) z(i)=10.0
*     unobtained results are plotted as very low values of amplitude
      if(maqs(i).eq.0.0)maqs(i)=1.0e-08
      if(mazt(i).eq.0.0)mazt(i)=1.0e+08
      if(mazs(i).eq.0.0)mazs(i)=1.0e+08
      mazs(i)=20.0*alog10(mazs(i))
      mazt(i)=20*alog10(mazt(i))
860   continue
      go to 870
865   write(6,1070)
      go to 855
870   call setgino(z,mazt,mpzt,nn(1),2)
      call insertion(freq(tes),mpres(tes))
      call piccle
      call setgino(z,mazs,mpzs,nn(1),1)
      call insertion(freq(tes),mpres(tes))
      call piccle
      if(iplot.eq.2)call ginoflow(flow(tes),z,nn(1),maqs,mpqs,np)
      if(iplot.eq.1)call ginotime(flow(tes),z,nn(1),maqs,mpqs,time)
      call insertion(freq(tes),mpres(tes))
      call piccle
880   continue
      if(anal.eq.1)go to 940
      call devend
940   print," The analysis is complete"
950   rewind 1
      write(1,1020)mm
      write(1,1020)nn
      write(1,1020)kpar,scale
      write(1,1020)file
      write(1,1010) mpres
      write(1,1010) freq
```

```
      write(1,1020)isca
      write(1,1010)calib
      write(1,1010)(l(i),x(i),y(i),i=1,20)
990 close(1)
      close(5)
      close(6)
      close(14)
      stop
1000 format(v)
1010 format(10f8.3)
1020 format(10i5)
1030 format(1h ,a9,6x,"L",6x,"X",6x,"Y")
1040 format(1h ,a9,i2,2x,f5.3,2x,f5.3,2x,f5.3)
1050 format(1h ,a23)
1060 format(1h ,"Type the values of L,X,Y for test",i2,"-  ")
1070 format(1h ," Wrong value. TRY AGAIN")
1080 format(1h ,9x,a23)
1090 format(1h0,5x,a19,"-",f6.1,3x,a17,"-",f6.1)
1100 format(1h0,67("*"))
1110 format(1h0,10x,"  TERMINATION REFLECTION COEFFICIENTS")
1120 format(1h0,"PIPE   1",12x,"2",12x,"3",12x,"4",12x,"5")
1130 format(1h ,i2,2x,10(f5.2,1x,f5.0,2x))
1140 format(1h0,10x,"  SOURCE REFLECTION COEFFICIENTS")
1150 format(1h0,"ll l2",5x,"1",11x,"2",11x,"3",11x,"4",11x,"5")
1160 format(1h ,i2,2x,i2,2x,10(f4.2,1x,f5.0,2x))
1170 format(1h0,69("*"))
1180 format(1h0,6x,"RHOT",11x,"ZT",11x,"RHOS",11x,"ZS",14x,"QS")
1190 format(1h0," H",2x,"AMP",2x,"PHA",4x,"AMP",6x,"PHA",4x,"AMP",2x,
&    "PHA",4x,"AMP",6x,"PHA",4x,"AMP",6x,"PHA")
1200 format(1h0,10x,"  RESULTS OF COMPONENTS CHARACTERISTICS")
1210 format(1h ,i2,1x,2(f4.2,1x,f5.0,1x,e9.3,1x,f5.0,1x),e9.3,1x,f5.0)
1220 format(1h ,i2,1x,2(f4.2,1x,f5.0,1x,f9.3,1x,f5.0,1x),e9.3,1x,f5.0)
1230 format(1h0,25x," AVERAGED RESULTS ")
1240 format (1h ,"Lengths for tests at ",a17,"-",i2,":")
1250 format(1h ,"Two/three lengths between ",f5.2," and ",f5.2,"metres")
1260 format(1h ,"One/two very short lengths are necessary")
1270 format(1h ,i4,"  gamma(",i2,") -  ",f5.2)
1280 format(1h0,"ll l2",5x,"6",11x,"7",11x,"8",11x,"9",10x,"10")
1290 format(1h ,65("-"))
1300 format(1h0,"PIPE    6",12x,"7",12x,"8",12x,"9",11x,"10")
1310 format(1h ,"Give mean pump flow in l/s;(- for inlet;+for outlet)",
&     /1h ," for ",a17,"=",f5.1," :  ")
1320 format(1h0,"WARNING: The value of |rhot|<0.3 for harmonic number"
&    ,i2,/1h ," for ",a17,"=",f5.1)
1330 format(1h ,"Type number of pumping elements :  ")
1340 format(1h0,"WARNING: The value of |rhot|>1.0 for harmonic number"
&    ,i2,/1h ," for ",a17,"=",f5.1)
1350 format(1h0,"WARNING: Insufficient number of lengths to define 'rhot'"
&    ,/1h ," for harmonic number",i2,/1h ," for ",a17,"=",f5.1)
1360 format(1h0,"WARNING: Insufficient number of lengths to define 'rhos'"
&    ,/1h ," for harmonic number",i2,/1h ," for ",a17,"=",f5.1)
      end
```

TYPICAL RUN OF PROGRAM "tunemeth"

with file01 already written but not correct

(user inputs are preceded by "(IN)")

```
(IN) tunemeth
Hello!  Do you want interactive program action?
(IN) yes
Is the input data file (file01) already written?
(IN) y
THIS PROGRAM EVALUATES THE SOURCE FLOW AND THE SOURCE AND
TERMINATION IMPEDANCES IN A SYSTEM AS REPRESENTED
          IN THE FOLLOWING PICTURE

          **                                ___
   -------*  *-------------------------------| T |--------
   |       **                                ---          |
   |      PUMP                                            |
   |_|                                                   |_|

TESTS PERFORMED ON THIS SYSTEM ARE SUPPOSED TO VARY EITHER:
          1 - Fundamental frequency
          2 - Mean pressure

   For each pair of frequency and mean pressure
   Several pipe length tests are allowed

   WHICH PARAMETER DO YOU VARY IN TESTS? "1" or "2"
(IN) 2
   THIS PROGRAM IS PREPARED TO ACCEPT UP TO:
                  10 NUMBER OF MEAN PRESSURES
                  10 HARMONICS
                  20 DIFFERENT PIPE LENGTHS

The values of the following variables are:
1 -  NUMBER OF HARMONICS        =   10
2 - NUMBER OF MEAN PRESSURES    =    3
3 -  NUMBER OF PIPE LENG.       =   10
Do you want to change any?
(IN) 2                              <---(deliberate typing mistake)
Please answer "yes" or "no"
(IN) yes
Which parameter do you want to change? "1","2" or "3"
(IN) 2
Type the new value of NUMBER OF MEAN PRESSURES
(IN) 4
The values of the following variables are:
1 -  NUMBER OF HARMONICS        =   10
2 - NUMBER OF MEAN PRESSURES    =    4
3 -  NUMBER OF PIPE LENG.       =   10
Do you want to change any?
(IN) no
The actual value of each  MEAN PRESSURE   is:
  MEAN PRESSURE    1 is =   150.0
  MEAN PRESSURE    2 is =   100.0
```

```
  MEAN PRESSURE    3 is =    50.0
  MEAN PRESSURE    4 is =    10.0
DO YOU WANT TO CHANGE THEM?
(IN) y
TYPE THE NEW VALUE OF   MEAN PRESSURE    - 1  : (IN) 150.
TYPE THE NEW VALUE OF   MEAN PRESSURE    - 2  : (IN) 100.
TYPE THE NEW VALUE OF   MEAN PRESSURE    - 3  : (IN) 50.
TYPE THE NEW VALUE OF   MEAN PRESSURE    - 4  : (IN) 10.
The actual value of each  MEAN PRESSURE   is:
  MEAN PRESSURE    1 is =   150.0
  MEAN PRESSURE    2 is =   100.0
  MEAN PRESSURE    3 is =    50.0
  MEAN PRESSURE    4 is =    10.0
DO YOU WANT TO CHANGE THEM?
(IN) no
The values of the following variables are:
1 -  MEAN TEMPERATURE          =   40
2 - INTERNAL DIAMETER  (mm*10) =  150
3 - THICK. OF PIPE WALL(mm*10) =   20
Do you want to change any?
(IN) y
Which parameter do you want to change? "1","2" or "3"
(IN) 1
Type the new value of  MEAN TEMPERATURE
(IN) 50
The values of the following variables are:
1 -  MEAN TEMPERATURE          =   50
2 - INTERNAL DIAMETER  (mm*10) =  150
3 - THICK. OF PIPE WALL(mm*10) =   20
Do you want to change any?
(IN) no
  Which fundamental frequency did you use?[Hz]
(IN) 198.
Do you need suggestions of suitable lengths to test?
(IN) yes
Lengths for tests at  MEAN PRESSURE   - 1:
Two/three lengths between  1.32 and  1.98metres
Two/three lengths between  0.66 and  0.99metres
Two/three lengths between  0.43 and  0.66metres
Two/three lengths between  0.33 and  0.50metres
One/two very short lengths are necessary
Lengths for tests at  MEAN PRESSURE   - 2:
Two/three lengths between  1.31 and  1.96metres
Two/three lengths between  0.65 and  0.98metres
Two/three lengths between  0.42 and  0.65metres
Two/three lengths between  0.33 and  0.49metres
One/two very short lengths are necessary
Lengths for tests at  MEAN PRESSURE   - 3:
Two/three lengths between  1.29 and  1.94metres
Two/three lengths between  0.65 and  0.97metres
Two/three lengths between  0.42 and  0.65metres
Two/three lengths between  0.32 and  0.48metres
One/two very short lengths are necessary
Lengths for tests at  MEAN PRESSURE   - 4:
Two/three lengths between  1.28 and  1.92metres
Two/three lengths between  0.64 and  0.96metres
Two/three lengths between  0.42 and  0.64metres
Two/three lengths between  0.32 and  0.48metres
One/two very short lengths are necessary
Have you performed tests already?
(IN) y
```

```
  The length of pipes used and pressure points are:
Pipe test      L      X      Y
Pipe test 1  0.370  0.110  0.295
Pipe test 2  0.420  0.110  0.345
Pipe test 3  0.465  0.110  0.390
Pipe test 4  0.575  0.110  0.500
Pipe test 5  0.670  0.110  0.595
Pipe test 6  0.810  0.110  0.735
Pipe test 7  1.020  0.110  0.945
Pipe test 8  0.920  0.110  0.845
Pipe test 9  1.825  0.110  1.750
Pipe test10  1.720  0.110  1.645
  Do you want to change them?
(IN) no

The pressure readings are given in individual files by
AMPLITUDE and PHASE of all HARMONICS, for different
                MEAN PRESSURE
   (THE FILE NUMBERS MUST BE >=20 AND <=99)


The actual value of each file no.at mean press   is:
file no.at mean press  1 :   31
file no.at mean press  2 :   32
file no.at mean press  3 :   34
file no.at mean press  4 :   35
DO YOU WANT TO CHANGE THEM?
(IN) y
TYPE THE NEW VALUE OF file no.at mean press  - 1 :  (IN) 31
TYPE THE NEW VALUE OF file no.at mean press  - 2 :  (IN) 32
TYPE THE NEW VALUE OF file no.at mean press  - 3 :  (IN) 33
TYPE THE NEW VALUE OF file no.at mean press  - 4 :  (IN) 34
The actual value of each file no.at mean press   is:
file no.at mean press  1 :   31
file no.at mean press  2 :   32
file no.at mean press  3 :   33
file no.at mean press  4 :   34
DO YOU WANT TO CHANGE THEM?
(IN) no
  ARE EXPERIMENTAL DATA FILES ALREADY WRITTEN?
(IN) y
 Which units did you use for input data amplitude?
          1 - in VOLTS
          2 - in dB
(IN) dB                          <---(deliberate typing mistake)
  Please answer "1" or "2" only
(IN) 2
 Give overall calibration factors for pressure points in 'bar/volt':
 Calibration factor for pressure 1 =
(IN) 14.11
 Calibration factor for pressure 2=
(IN) 15.22
    Which scale do you want for Impedance Results?
          1 - SI units (Ns/m**5)
          2 - dB scale
(IN) 2
   Do you want to have:
          1- Results printed into a file (file14)
          2- Plotted results (output to attached file)
          3- Both
(IN) 3
```

```
Gino-f Mk 2.5c
 Do you want the flow plot to be:
    1 - vs time
    2 - vs pump angle of rotation
(IN) 1
  Give plotting time (in ms)
(IN) 30
Give mean pump flow in l/s;
 for  MEAN PRESSURE   =150.0 :  (IN) .45
Type number of pumping elements :  (IN) 8

WARNING: Insufficient number of lengths to define 'rhos'
 for harmonic number 9
 for  MEAN PRESSURE   =100.0
Give mean pump flow in l/s;
 for  MEAN PRESSURE   =100.0 :  (IN) .46
Give mean pump flow in l/s;
 for  MEAN PRESSURE   = 50.0 :  (IN) .47

WARNING: The value of |rhot|<0.3 for harmonic number 1
 for  MEAN PRESSURE   = 10.0

WARNING: The value of |rhot|<0.3 for harmonic number 2
 for  MEAN PRESSURE   = 10.0

WARNING: The value of |rhot|<0.3 for harmonic number 3
 for  MEAN PRESSURE   = 10.0

WARNING: The value of |rhot|>1.0 for harmonic number 6
 for  MEAN PRESSURE   = 10.0

WARNING: Insufficient number of lengths to define 'rhot'
 for harmonic number10
 for  MEAN PRESSURE   = 10.0
Give mean pump flow in l/s;
 for  MEAN PRESSURE   = 10.0 :  (IN) .48
 The analysis is complete


STOP
```

LISTING OF PART OF "file14"

AVERAGED RESULTS

FUNDAMENTAL FREQ.- 198.0 MEAN PRESSURE - 150.0

	RHOT		ZT		RHOS		ZS		QS	
H	AMP	PHA	AMP	PHA	AMP	PHA	AMP	PHA	AMP	PHA
1	0.82	-1.	216.112	-7.	0.90	-60.	201.100	-84.	0.522E-04	-174.
2	0.80	-7.	214.239	-29.	0.87	-85.	196.992	-83.	0.142E-04	83.
3	0.80	-7.	214.263	-27.	0.93	-106.	193.741	-86.	0.857E-05	-24.
4	0.81	-12.	212.734	-46.	0.92	-117.	191.963	-85.	0.650E-05	-135.
5	0.80	-16.	211.357	-52.	0.95	-125.	190.666	-87.	0.368E-05	123.
6	0.85	-24.	209.097	-69.	0.97	-128.	189.972	-88.	0.362E-05	3.
7	0.80	-16.	211.392	-51.	1.02	-138.	187.828	-92.	0.348E-05	-103.
8	1.00	-35.	206.214	-90.	0.87	-130.	189.621	-80.	0.261E-05	121.
9	0.81	3.	215.622	12.	0.90	167.	177.956	63.	0.553E-05	-147.
10	0.77	-7.	213.076	-25.	0.74	171.	180.742	26.	0.283E-05	-112.

AVERAGED RESULTS

FUNDAMENTAL FREQ.- 198.0 MEAN PRESSURE - 100.0

	RHOT		ZT		RHOS		ZS		QS	
H	AMP	PHA	AMP	PHA	AMP	PHA	AMP	PHA	AMP	PHA
1	0.73	-4.	212.081	-13.	0.89	-57.	201.344	-83.	0.502E-04	-171.
2	0.72	-9.	211.100	-25.	0.88	-86.	196.794	-83.	0.138E-04	91.
3	0.73	-11.	211.011	-32.	0.92	-106.	193.629	-86.	0.796E-05	-10.
4	0.74	-16.	209.683	-43.	0.92	-116.	191.982	-85.	0.573E-05	-119.
5	0.73	-19.	209.080	-46.	0.94	-127.	190.056	-86.	0.362E-05	145.
6	0.76	-22.	208.531	-55.	0.98	-130.	189.493	-89.	0.298E-05	27.
7	0.72	-21.	208.121	-47.	1.04	-143.	186.511	-94.	0.329E-05	-80.
8	0.80	-38.	205.034	-70.	0.94	-133.	188.911	-86.	0.217E-05	143.
10	0.82	-44.	203.742	-74.	0.87	-149.	185.227	-76.	0.290E-05	-33.

LISTING OF PART OF "file15"

RESULTS OF COMPONENTS CHARACTERISTICS

FUNDAMENTAL FREQ.- 198.0 MEAN PRESSURE - 150.0

TERMINATION REFLECTION COEFFICIENTS

PIPE	1		2		3		4		5	
2	0.00	0.	0.00	0.	0.00	0.	0.00	0.	0.80	-18.
3	0.00	0.	0.00	0.	0.00	0.	0.00	0.	0.80	-16.
4	0.00	0.	0.00	0.	0.79	-13.	0.79	-15.	0.81	-25.
5	0.00	0.	0.00	0.	0.81	-11.	0.84	-10.	0.00	0.
6	0.00	0.	0.80	-8.	0.80	-11.	0.00	0.	0.00	0.
7	0.00	0.	0.79	-6.	0.00	0.	0.00	0.	0.00	0.
8	0.00	0.	0.81	-7.	0.00	0.	0.00	0.	0.00	0.
9	0.82	-0.	0.00	0.	0.79	5.	0.00	0.	0.81	-4.
10	0.82	-2.	0.00	0.	0.81	-2.	0.00	0.	0.00	0.

PIPE	6		7		8		9		10	
1	0.00	0.	0.75	-19.	1.13	-47.	0.89	17.	0.88	-4.
2	0.89	-20.	0.64	-19.	0.97	-40.	0.94	-5.	0.00	0.
3	0.85	-27.	0.70	-21.	0.00	0.	0.00	0.	0.00	0.
5	0.00	0.	0.00	0.	0.00	0.	0.00	0.	0.68	-46.
6	0.00	0.	0.00	0.	0.88	-19.	0.00	0.	0.00	0.
7	0.82	-25.	0.00	0.	0.00	0.	0.00	0.	0.88	5.
8	0.00	0.	1.08	-20.	0.00	0.	0.00	0.	0.00	0.
9	0.00	0.	0.86	2.	0.00	0.	0.60	-5.	0.00	0.
10	0.00	0.	0.00	0.	0.00	0.	0.00	0.	0.64	16.

SOURCE REFLECTION COEFFICIENTS

l1	l2	1		2		3		4		5	
5	1	0.00	0.	0.00	0.	0.00	0.	0.93	-116.	0.95	-124.
5	1	0.00	0.	0.00	0.	0.00	0.	0.90	-119.	1.00	-128.
6	1	0.00	0.	0.00	0.	0.94	-105.	0.93	-114.	0.00	0.
6	1	0.00	0.	0.00	0.	0.91	-109.	0.81	-126.	0.00	0.
7	1	0.00	0.	0.87	-92.	0.94	-100.	0.00	0.	0.00	0.
7	1	0.00	0.	0.86	-89.	0.96	-105.	0.00	0.	0.00	0.
8	1	0.00	0.	0.00	0.	0.93	-103.	0.00	0.	0.00	0.
8	1	0.00	0.	0.00	0.	0.93	-108.	0.00	0.	0.00	0.
						!					
						!					
						V					
9	8	0.00	0.	0.88	-82.	0.00	0.	0.00	0.	0.93	-128.
9	8	0.00	0.	0.88	-84.	0.00	0.	0.00	0.	0.87	-111.
10	8	0.00	0.	0.88	-84.	0.00	0.	0.00	0.	0.00	0.
10	8	0.00	0.	0.89	-85.	0.00	0.	0.00	0.	0.00	0.

11	12	6		7		8		9		10	
4	1	1.01	-131.	1.00	-137.	0.80	-144.	0.75	164.	****	0.
4	1	0.89	-134.	1.04	-149.	0.83	-150.	0.61	150.	0.76	0.
5	1	0.97	-134.	0.88	-138.	0.00	0.	0.00	0.	0.00	0.
5	1	0.94	-130.	0.90	-140.	0.00	0.	0.00	0.	0.00	0.
7	1	0.00	0.	0.84	-134.	0.82	-136.	0.00	0.	0.00	0.
7	1	0.00	0.	0.57	-139.	0.95	-137.	0.00	0.	0.00	0.
9	8	1.28	-130.	0.00	0.	0.00	0.	0.97	179.	0.00	0.
9	8	0.88	-121.	0.00	0.	0.00	0.	0.97	171.	0.00	0.
10	8	1.36	-130.	0.00	0.	0.00	0.	0.00	0.	0.52	39.
10	8	0.80	-122.	0.00	0.	0.00	0.	0.00	0.	0.90	182.

LISTING OF INITIAL DATA FILE "file01"

(written by the program in interactive mode action)

```
  50  150   20
  10    4   10
   2    2
  31   32   33   34    0    0    0    0    0    0
150.0 100.0  50.0  10.0  20.0  20.0  20.0  20.0  20.0  20.0
198.0 198.0 198.0 198.0 198.0 198.0 198.0 198.0 198.0 198.0
   2
 14.110  15.220
0.370 0.110 0.295 0.420 0.110 0.345 0.465 0.110 0.390 0.575
0.110 0.500 0.670 0.110 0.595 0.810 0.110 0.735 1.020 0.110
0.945 0.920 0.110 0.845 1.825 0.110 1.750 1.720 0.110 1.645
2.150 0.000 0.285 0.000 0.000 0.000 0.000 0.000 0.000 0.000
0.000 0.000 0.000 0.000 0.000 0.000 0.000 0.000 0.000 0.000
0.000 0.000 0.000 0.000 0.000 0.000 0.000 0.000 0.000 0.000
```

EXAMPLE OF PART OF EXPERIMENTAL DATA FILE "file31"

84.8	-107.	84.9	-105.	¦
68.6	-1.	69.6	0.	¦
61.7	111.	64.7	114.	¦
58.4	-140.	64.7	-127.	¦
55.4	-23.	67.3	5.	¦ <-- ten harmonics
46.5	106.	62.2	-121.	¦
46.2	-156.	52.9	-7.	¦
47.	-44.	44.3	144.	¦
42.0	100.	46.9	-89.	¦
46.0	94.	44.8	-93.	¦
84.6	-105.	84.8	-104.	
68.3	0.	69.8	2.	
		¦		
		¦		
		V		
49.9	145.	45.4	-27.	
66.9	-170.	84.3	-90.	
72.4	-5.	71.9	175.	
56.9	87.	70.4	-48.	
61.1	-139.	60.4	-141.	
55.	-18.	65.8	13.	
53.7	88.	52.9	-93.	
58.7	-80.	63.5	117.	
49.1	-32.	47.3	-47.	
50.4	-138.	52.	-123.	
43.8	124.	43.7	-77.	

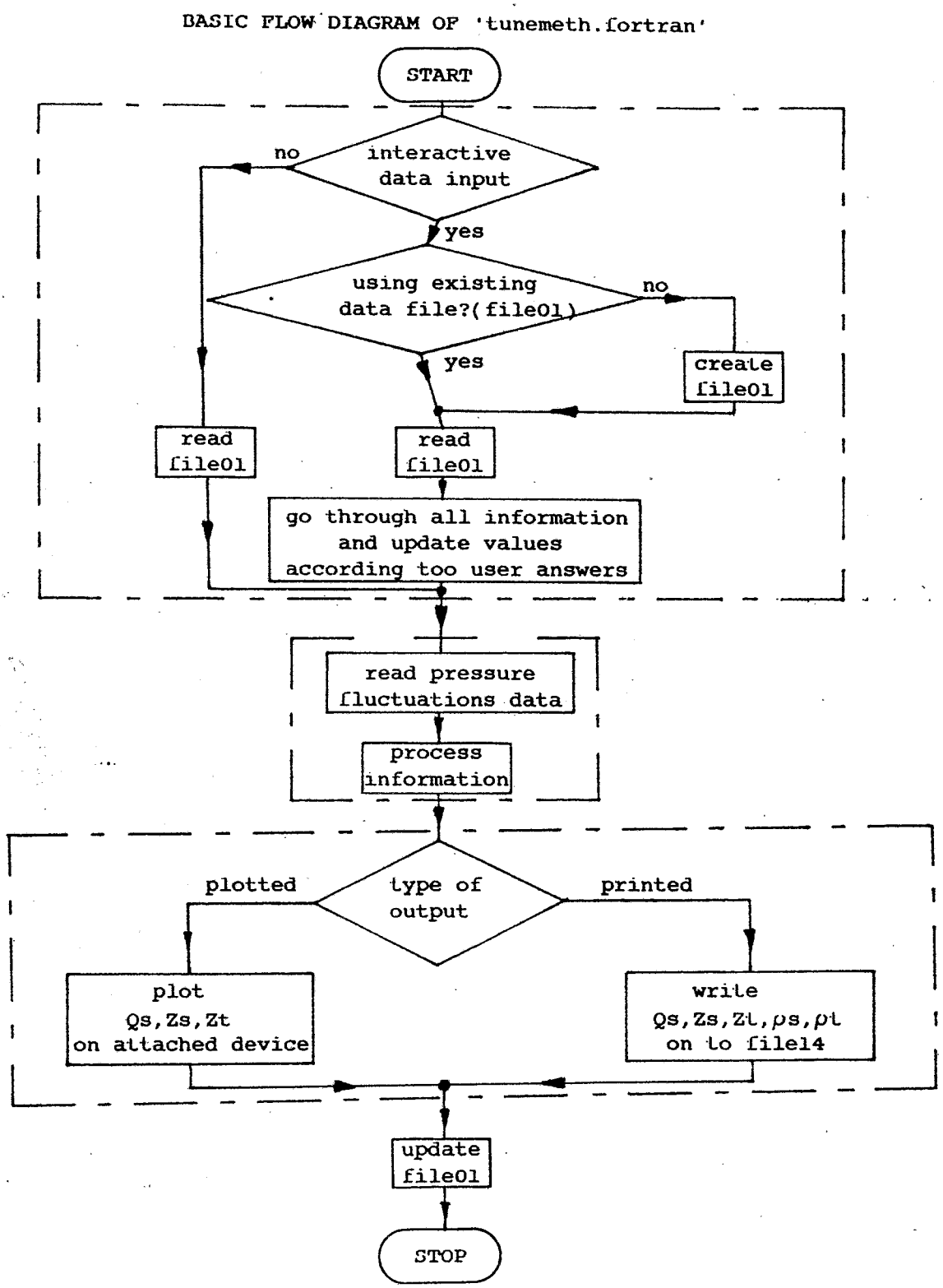

Fig.A3.1 Basic flow diagram of program 'tunemeth.fortran'

FLOW DIAGRAM OF PARTS b) AND c) OF 'tunemeth.fortran'

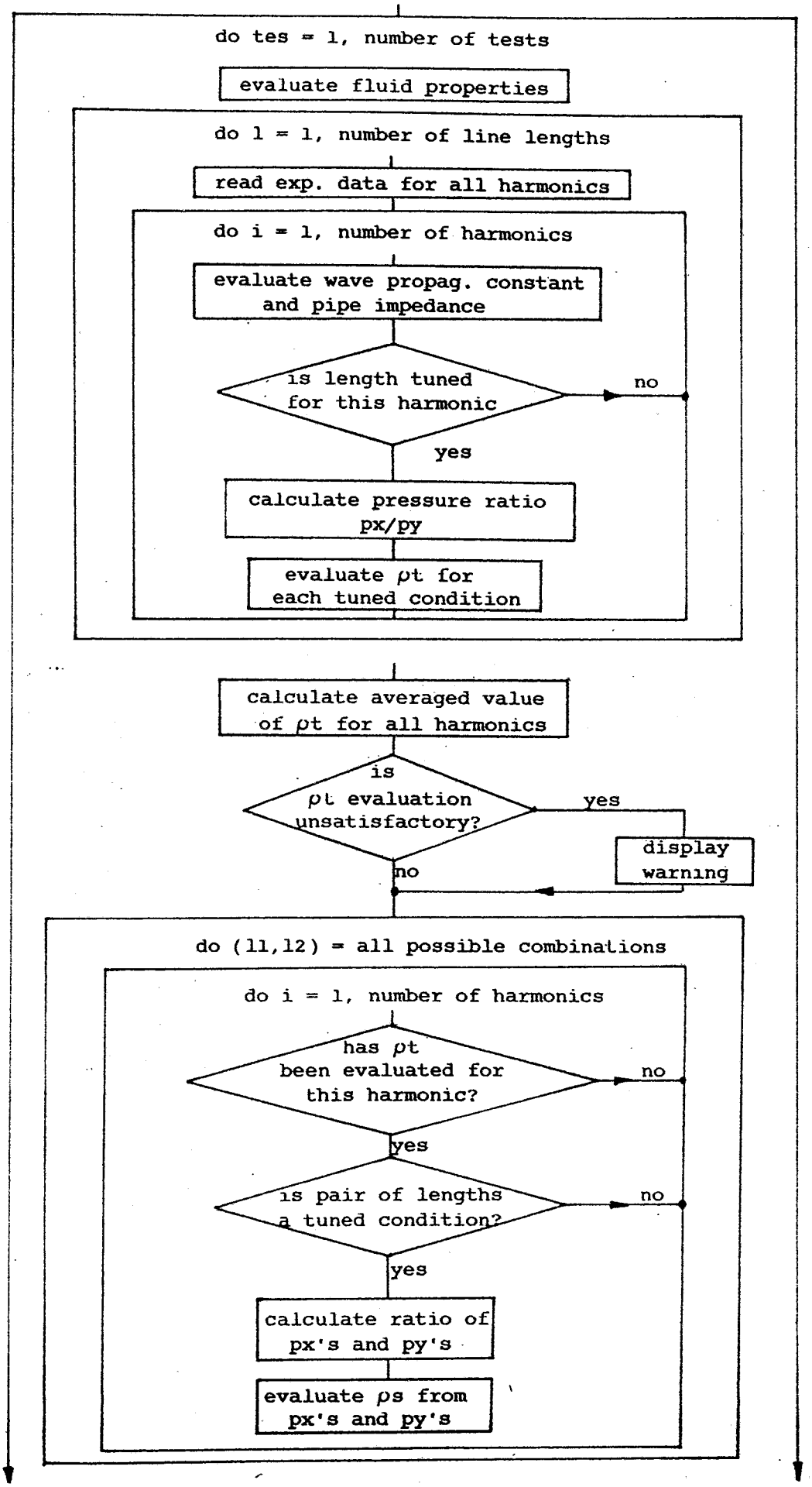

Fig.A3.2 Flow diagram of parts b) and c) of program 'tunemeth.fortran'

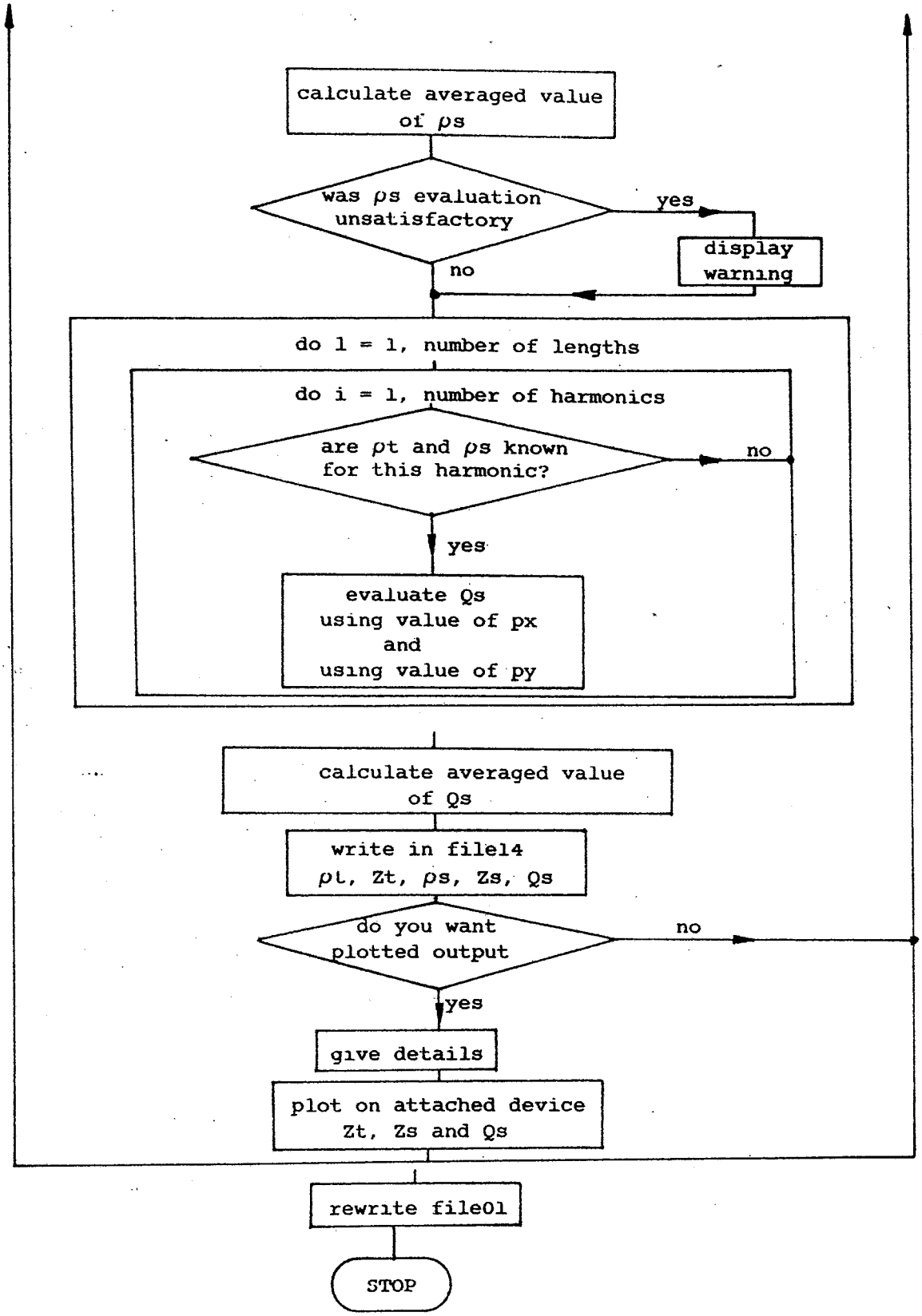

Fig.A3.2 Flow diagram of parts b) and c) of program 'tunemeth.fortran' (cont.)

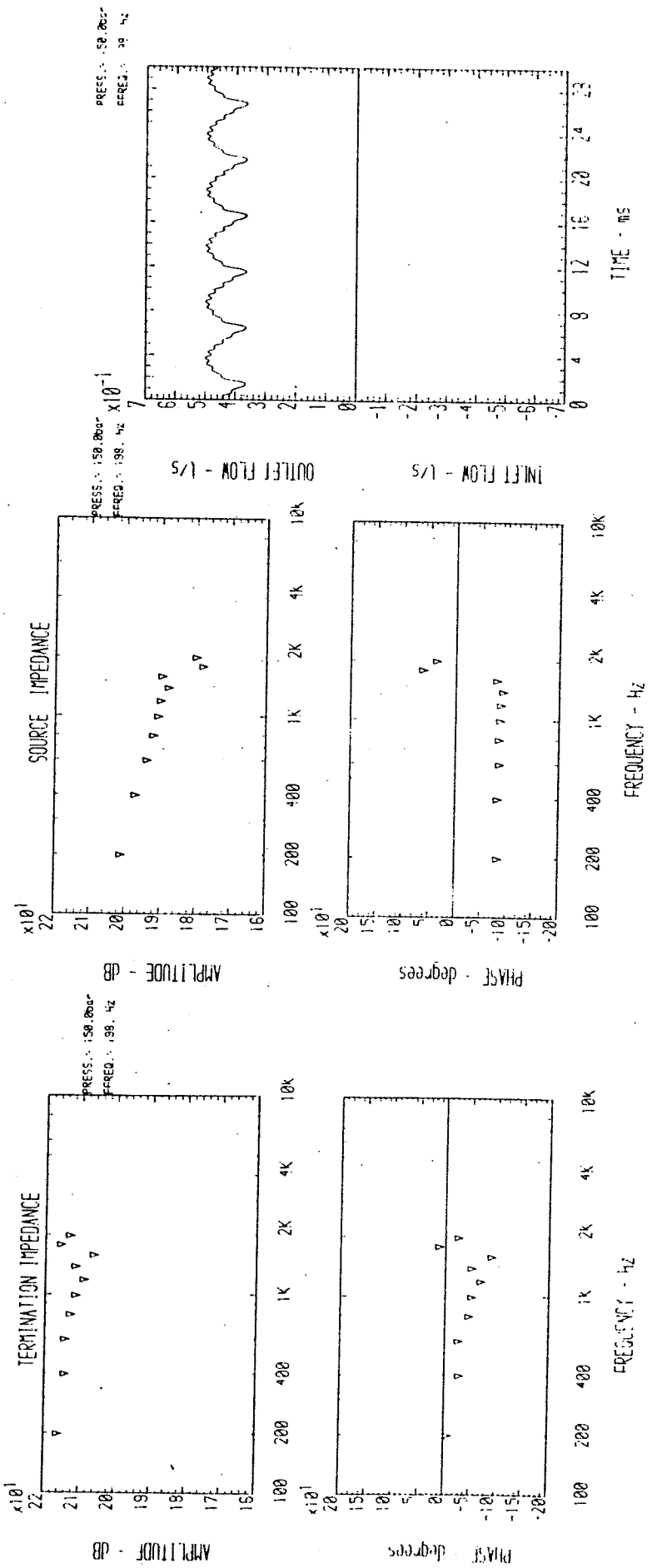

Fig.A3.3 Plotted results of typical run at 150 bar mean pressure

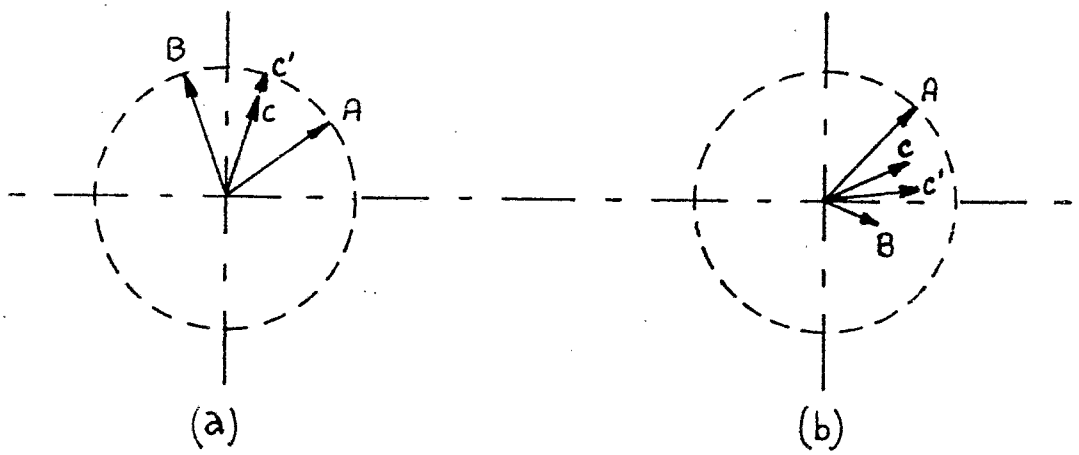

Fig.A3.4 Difference between 'real and imaginary parts' averaging (OC) and 'amplitude and phase' averaging (OC') of complex numbers

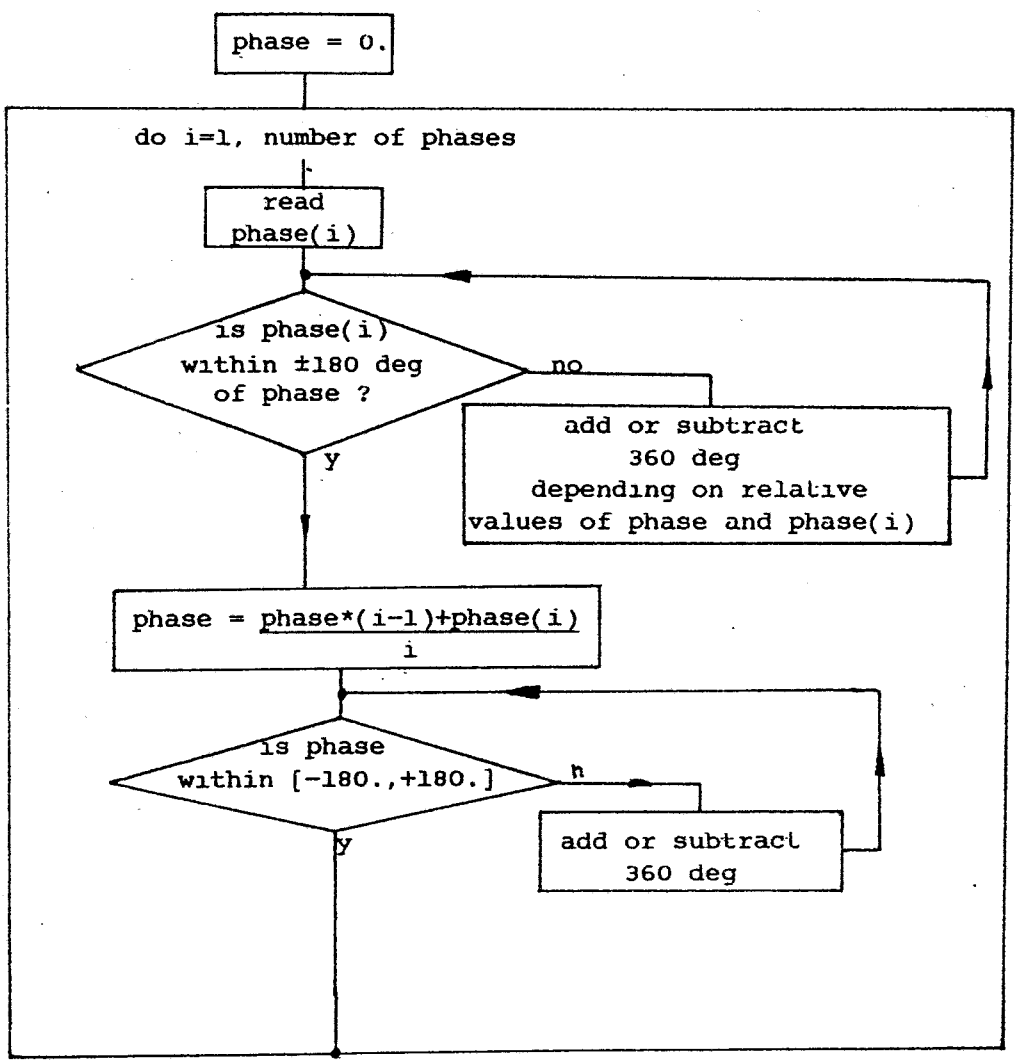

Fig.A3.5 Flow diagram of averaging of phases of complex data

COMPUTER PROGRAM DOCUMENTATION

FOR SUB-PROGRAM 'tunesub.fortran'

Library Classification

BENGF.tunesub.224.01

TITLE - Supporting Routines for Program 'tunemeth.fortran'

New Fortran 7a Multics 30/8/80

Author: F. Freitas

Purpose - The subroutines contained in this sub-program are used by the main program **tunemeth.fortran** for interactive data input and for plotted results output.

Inbuilt Sub-routines

ginoflow - plots pump displacement ripple vs pump rotation

ginotime - plots pump source flow vs time

insertion- prints on top right hand corner of each plot data details

quest1 - interactive questioning routine

quest2 - interactive questioning routine

quest3 - interactive questioning routine

quest4 - interactive questioning routine

Storage - 4 Records length

Subroutines Action

a) subroutine **ginoflow**

Purpose - Plot inlet and outlet displacement ripple of a hydraulic

pump by synthesis of Fourier harmonic components.

Associated Subroutines - gino library routines

All variables are transferred via argument list:

call ginoflow(qm,freq,nh,ampl,phase,np)

Input variables (transferred via argument list)

ampl	- amplitude of harm. of flow fluct.	[m^3/s]
freq	- harm. frequency	[Hz]
nh	- number of harmonics	-
np	- number of pumping elements	-
phase	- phase of harm. of flow fluct.	[deg]
qm	- mean flow	[ℓ/s]

Output Information

A typical example of the output of this subroutine is shown in fig.3.18.

The displacement ripple is plotted over half a revolution of the pump shaft using 360 points. The value of the high bound of YY-axis was fixed at 5cm^3/rad (in order to keep a common scale), for all the small size pumps. A value of 20cm^3/rad was used for larger pumps.

PROGRAM ACTION

The subroutine starts by setting up the axis and drawing the sign 'π', which is not supported by gino routines.

The displacement ripple is, then, given by:

$$d = \frac{n}{\omega} \left(q + \sum_{i=1}^{j} a_i \sin(ni\theta + p_i) \right) \qquad (A4.1)$$

where: ai - ampl of i'th harm comp of flow fluct. [m^3/s]

d - pump instantaneous displacement [m^3/rad]

i - harmonic number -

j - total number of harmonics -

n - number of pumping elements -

pi - phase of i'th harm comp of flow fluct. [deg]

q - mean pump flow at running speed [m^3/s]

θ - pump angle of rotation [rad]

ω - pump fundamental frequency [rad/s]

b) subroutine **insertion**

Purpose - To write on every plot details of mean pressure and fundamental frequency the system was run at.

Associated subroutines - gino library routines

All variables transferred via argument list:

call insertion(a,b)

Input variables (via argument list)

a - fundamental frequency [Hz]

b - mean pressure [bar]

Output Information

The output of this subroutine is printed on the top right hand corner of every plot output called by program **tunemeth.fortran** (see fig.A3.3).

c) subroutine **setgino**

Purpose - To plot impedance characteristics of pumps and terminations in a Bode-type diagram.

Associated subroutines - gino library routines

All variables transferred via argument list:

call setgino (ff,xa,xp,i,n)

Input variables (via argument list)

ff	- array containing harmonic frequencies	[Hz]
i	- number of harmonics	-
n	- n=1 for termination ; n=2 for source titles	-
xa	- amplitude of impedance	[Ns/m^5]
xp	- phase of impedance	[deg]

Output Information

The output of this subroutine (see fig.A3.3) consists of two plots, one of impedance amplitude and the other of phase versus frequency ([Hz]) in a $\log_{10}$ scale.

The title is either termination or source impedance depending upon the value of 'n'.

As it is possible, from **tunemeth** program, for a harmonic component not to be evaluated, the value is transferred as 140 dB which, when detected in the subroutine, is by-passed using the array variable 'no'.

d) subroutines **quest1, quest2, quest3, quest4**

Purpose - These subroutines print stored values of variables and update them according to user's answers.

Fig.A4.2 presents the flow diagram of **questl** as an example.

e) subroutine **ginotime**

Purpose - Plot inlet and outlet source flow of a pump vs time ([ms]).

PROGRAM ACTION

This subroutine is virtually identical to **ginoflow**, but eq.A4.1 is substituted by:

$$flow = q + \sum_{i=1}^{j} a_i \sin(ti\omega + p_i) \qquad (A4.2)$$

where: flow - instantaneous flow delivered by pump [m^3/s]

t - time [ms]

LISTING OF SUB-PROGRAM "tunesub.fortran"

```
*       PROGRAM NAME - tunesub.fortran
*
*       LIBRARY CLASSIFICATION -                    BENGP tunesub.224.01
*
*       TITLE - SUPPORTING ROUTINES FOR PROGRAM 'tunemeth.fortran'
*
*       New Fortran 5a Multics                                  30/8/80
*
*       A graphics terminal may be used to see output
*
*       Author - F.Freitas
*
*       Purpose - The subroutines contained in this sub-program are ued
*                 the main-program 'tunemeth' for interactive data input
*                 and for plotted output results.
*
*       Revisions -
*
*       This sub-program contains the following subroutines:
*
*       ginoflow  - plots displacement ripple vs pump rotation
*       ginotime  - plots source flow vs time (ms)
*       insertion - writes at top right corner of plot data details
*       questl    - questioning routine for interactive data input
*       quest2    - questioning routine for interactive data input
*       quest3    - questioning routine for interactive data input
*       quest4    - questioning routine for interactive data input
*       setgino   - plots source or termination impedance in
*                   dB vs frequency (log scale)
*
*
*
        subroutine ginoflow(qm,freq,nh,ampl,phase,np)
*
*       Input variables (transferred via argument list)
*
*       ampl  - amplitude of harm. of flow fluct.          [m3/s]
*       freq  - harm. frequency                            [Hz]
*       nh    - number of harmonics                        -
*       np    - number of pumping elements                 -
*       phase - phase of harm. of flow fluct.              [deg]
*       qm    - mean flow                                  [l/s]
*
*       Insource variables
*
*       i     - incremental variable                       -
*       j     - number of plotting points                  -
*       n     - incremental variable                       -
*       pi    - constant (=3.14159)                        -
*       r     - array containing instantaneous values of   [cu.cm/rad]
*               volume displacement/rad
*       t     - array containing values of pump rotation   [deg]
*       temp  - phase of each harmonic component           [rad]
*       xmax  - max value of pump angle                    [deg]
```

```
*         ymax  - max value of pump displacement                [cu.cm/rad]
*
          dimension freq(10),ampl(10),phase(10),r(600),t(600)
          external chahol(descriptors)
*
          call axipos(0,65.,80.,80.,1)
          call axipos(0,65.,80.,100.,2)
          call chasiz(2.0,4.)
          call chaang(90.)
          call movto2(50.,30.)
          call chahol("INLET FLOW - cu.cm/rad*.")
          call movto2(50.,85.)
          call chahol("OUTLET FLOW - cu.cm/rad*.")
          call chaang(0.)
          call movto2(64.,25.)
          call chahol("0.                                          *.")
*         draw symbol of 'pi'
          call movby2(.2,3.5)
          call linby2(2.,0.)
          call movby2(-1.5,0.)
          call linby2(0.,-3.5)
          call movby2(1.,0.)
          call linby2(0.,3.5)
          call movby2(.7,-3.5)
          call chahol(" rad.*.")
          call movto2(90.,15.)
          call chahol("PUMP ROTATION - rad*.")
          pi=3.14159
          ymax=5.
          j=360
          xmax=180.
          call axisca(1,36,0.,xmax,1)
          call axisca(1,10,-ymax,ymax,2)
          call grid(-2,0,1)
          do 5 i=1,nh
          phase(i)=phase(i)*pi/180.
5         continue
          do 10 n=1,j+1
          r(n)=0.0
          t(n)=(n-1)*xmax/j
          do 20 i=1,nh
          temp=i*t(n)*np*2*pi/360.+phase(i)
          r(n)=r(n)+ampl(i)*sin(temp)*1000.
20        continue
          r(n)=(qm+r(n))*np*1000./(freq(1)*2*pi)
10        continue
          call grapol(t,r,j+1)
          return
          end




          subroutine insertion(a,b)
*
*         Input variables (via argument list)
*
*         a  - fundamental frequency                              [Hz]
*         b  - mean pressure                                      [bar]
```

```
*
      external chahol(descriptors)
      call chasiz(1.5,2.0)
      call movto2(135.5,135.)
      call chahol("FFREQ.=*.")
      call chafix(a,5,0)
      call chahol(" Hz*.")
      call movto2(135.5,140.)
      call chahol("PRESS.=*.")
      call chafix(b,6,1)
      call chahol("bar*.")
      return
      end



      subroutine setgino(ff,xa,xp,i,n)
*
*     Input variables (via argument list)
*
*     ff - array containing harmonic frequencies          [Hz]
*     i  - number of harmonics                            -
*     n  - n=1 for termination ; n=2 for source titles    -
*     xa - amplitude of impedance                         [Ns/m5]
*     xp - phase of impedance                             [deg]
*
*     Insource variables
*
*     j  - incremental variable charactrizing harmonic number-
*     no - array which determines whether a value is to be   -
*          or not
*
      dimension ff(10),xa(10),xp(10),no(10)
      external chahol(descriptors)
      call axipos(1,40.,100.,95.,1)
      call axipos(1,40.,100.,50.,2)
      call axisca(4,5,100.,2000.,1)
      call axisca(1,6,160.,220.,2)
      call chasiz(2.0,4.0)
      call movto2(70.,152.)
      if(n.eq.2)go to 25
      call chahol("   SOURCE  IMPEDANCE *.")
      go to 26
25    call chahol("TERMINATION IMPEDANCE*.")
26    call chaang(90.)
      call movto2(28.,110.)
      call chahol("AMPLITUDE - dB*.")
      call chaang(0.)
      call chasiz(2.0,3.0)
      call grid(-2,0,1)
      call movto2(38.,92.)
      call chahol("100    200    400       1K      2K*.")
      call chahol("     4K       10K*.")
      do 30 j=1,i
      if(xa(j).le.141.)go to 40
      call grasym(ff(j),xa(j),1,2,0)
      go to 30
40    no(j)=1
30    continue
```

```
      call axipos(1,40.,30.,95.,1)
      call axipos(0,40.,55.,50.,2)
      call axisca(4,5,100.,2000.,1)
      call axisca(1,6,-180.,180.,2)
      call chaang(90.)
      call chasiz(2.0,4.0)
      call movto2(28.,38.)
      call chahol("PHASE - degrees*.")
      call chaang(0.)
      call movto2(70.,10.)
      call chahol("FREQUENCY - Hz*.")
      call chasiz(2.0,3.0)
      call grid(-2,0,1)
      call movto2(38.,20.)
      call chahol("100    200    400       1K      2K*.")
      call chahol("     4K      10K*.")
      do 50 j=1,i
      if(no(j).eq.1)go to 50
      call grasym(f(j),xp(j),1,2,0)
50    continue
100   continue
      return
      end
```

```
      subroutine questl(w,jj)
*
*     Input variables (via argument list)
*
*     jj - array of variables to be queried                    -
*     w  - array with name of variables                        -
*
*     Insource variables
*
*     aa - character string variable                           -
*     i  - incremental variable                                -
*     ty - character string variable                           -
*
      character*1 aa
      character*22 ty
      character*26 w(3)
      dimension jj(3)
*
80    print,"The values of the following variables are:"
      do 5 i=1,3
      write(6,100) i,w(i),jj(i)
5     continue
      ty="Type the new value of"
*
      print,"Do you want to change any?"
10    input,aa
      if(aa.eq."y") go to 20
      if(aa.eq."n") return
      print,'Please answer "yes" or "no"'
      go to 10
20    print,'Which parameter do you want to change? "1","2" or "3"'
30    input,aa
```

```
      if(aa.eq."1") go to 40
      if(aa.eq."2") go to 50
      if(aa.eq."3") go to 60
      print,' Please answer "1","2" or "3"'
      go to 30
40    print,ty,w(1)
      read(5,101,err=120)jj(1)
      go to 80
50    print,ty,w(2)
      read(5,101,err=120)jj(2)
      go to 80
60    print,ty,w(3)
      read(5,101,err=120)jj(3)
      go to 80
120   print,"  Wrong value. TRY AGAIN"
      go to 80
100   format(1h ,i1," - ",a26," = ",i4)
101   format(v)
      end



      subroutine quest2(w,n,rr)
*
*     Input variables (via argument list)
*
*     n  - dimension of array rr                                    -
*     rr - array containing variables to be queried                 -
*     w  - character string with name of variable                   -
*
*     Insource variables (via argument list)
*
*     i  - incremental variable                                     -
*     ty - character string variable                                -
*
      character *1 aa
      character *17 w
      character *23 ty
      dimension rr(10)
*
5     print,"The actual value of each ",w,"is:"
      do 10 i=1,n
      write(6,100)w,i,rr(i)
10    continue
      ty="TYPE THE NEW VALUE OF "
*
      print,"DO YOU WANT TO CHANGE THEM?"
20    input,aa
      if(aa.eq."y") go to 30
      if(aa.eq."n") return
      print,'   Please answer "yes" or "no"'
      go to 20
30    do 50 i=1,n
      write(6,110)ty,w,i
      read(5,101,err=120)rr(i)
50    continue
      go to 5
120   print," Wrong value. TRY AGAIN"
      go to 5
110   format(1h ,a23,a17," -",i2,"  : ")
100   format(1h ,a18,i2," is = ",f7.1)
```

```
101     format(v)
        end



        subroutine quest3(w,n,jj)
*
*       Input variables (via argument list)
*
*       jj - array containing values of variables to be queried-
*       n  - dimension of array jj                              -
*       w  - character string variable with name of jj          -
*
*       Insource variables
*
*       aa - character string variable                          -
*       i  - incremental variable                               -
*       ty - character string variable                          -
*
        character *1 aa
        character *22 ty
        character *23 w
        dimension jj(10)
*
5       print,"The actual value of each ",w," is:"
        do 10 i=1,n
        write(6,100)w,i,jj(i)
10      continue
        ty="TYPE THE NEW VALUE OF "
*
        print,"DO YOU WANT TO CHANGE THEM?"
20      input,aa
        if(aa.eq."y") go to 30
        if(aa.eq."n") return
        print,'   Please answer "yes" or "no"'
        go to 20
30      do 50 i=1,n
        write(6,102)ty,w,i
        read(5,101,err=120)jj(i)
50      continue
        go to 5
120     print," Wrong value.  TRY AGAIN"
        go to 5
100     format(1h ,a22,i2," :  ",i3)
101     format(v)
102     format(1h ,a22,a22," -",i2," :  ")
        end



        subroutine quest4(i)
*
*       Input variables (via argument list)
```

```
*
*       i  - integer =1 or =2
*
5       read(5,10,err=15)i
        if(i.eq.1.or.i.eq.2)return
15      print,'  Please answer "1" or "2" only'
        go to 5
10      format(v)
        end



        subroutine ginotime(qm,freq,nh,ampl,phase,time)
*
*       Input variables (transferred via argument list)
*
*       ampl  - amplitude of harm. of flow fluct.          [m3/s]
*       freq  - harm. frequency                            [Hz]
*       nh    - number of harmonics                        -
*       phase - phase of harm. of flow fluct.              [deg]
*       qm    - mean flow                                  [l/s]
*       time  - plotting time                              [ms]
*
*       Insource variables
*
*       i     - incremental variable                       -
*       j     - number of plotting points                  -
*       n     - incremental variable                       -
*       pi    - constant (=3.14159)                        -
*       r     - array containing instantaneous values of   [l/s]
*               source flow
*       t     - array containing values of pump rotation   [deg]
*       temp  - phase of each harmonic component           [rad]
*       xmax  - max value of pump angle                    [deg]
*       ymax  - max value of flow                          [l/s]
*
        dimension freq(10),ampl(10),phase(10),r(600),t(600)
        external chahol(descriptors)
*
        call axipos(0,65.,80.,80.,1)
        call axipos(0,65.,80.,100.,2)
        call chasiz(2.0,4.)
        call chaang(90.)
        call movto2(50.,35.)
        call chahol("INLET FLOW - l/s*.")
        call movto2(50.,90.)
        call chahol("OUTLET FLOW - l/s*.")
        call chaang(0.)
        call movto2(95.,15.)
        call chahol("TIME - ms*.")
        pi=3.14159
        ymax=0.7
        j=360
        xmax=time
        call axisca(1,10,0.,xmax,1)
        call axisca(1,10,-ymax,ymax,2)
        call grid(-2,1,1)
        do 5 i=1,nh
        phase(i)=phase(i)*pi/180.
```

```
5       continue
        do 10 n=1,j+1
        r(n)=0.0
        t(n)=(n-1)*xmax/j
        do 20 i=1,nh
        temp=2*pi*freq(i)*t(n)/1000.+phase(i)
        r(n)=r(n)+ampl(i)*sin(temp)*1000.
20      continue
        r(n)=qm+r(n)
10      continue
        call grapol(t,r,j+1)
        return
        end
```

FLOW DIAGRAM OF SUBROUTINE 'quest1'

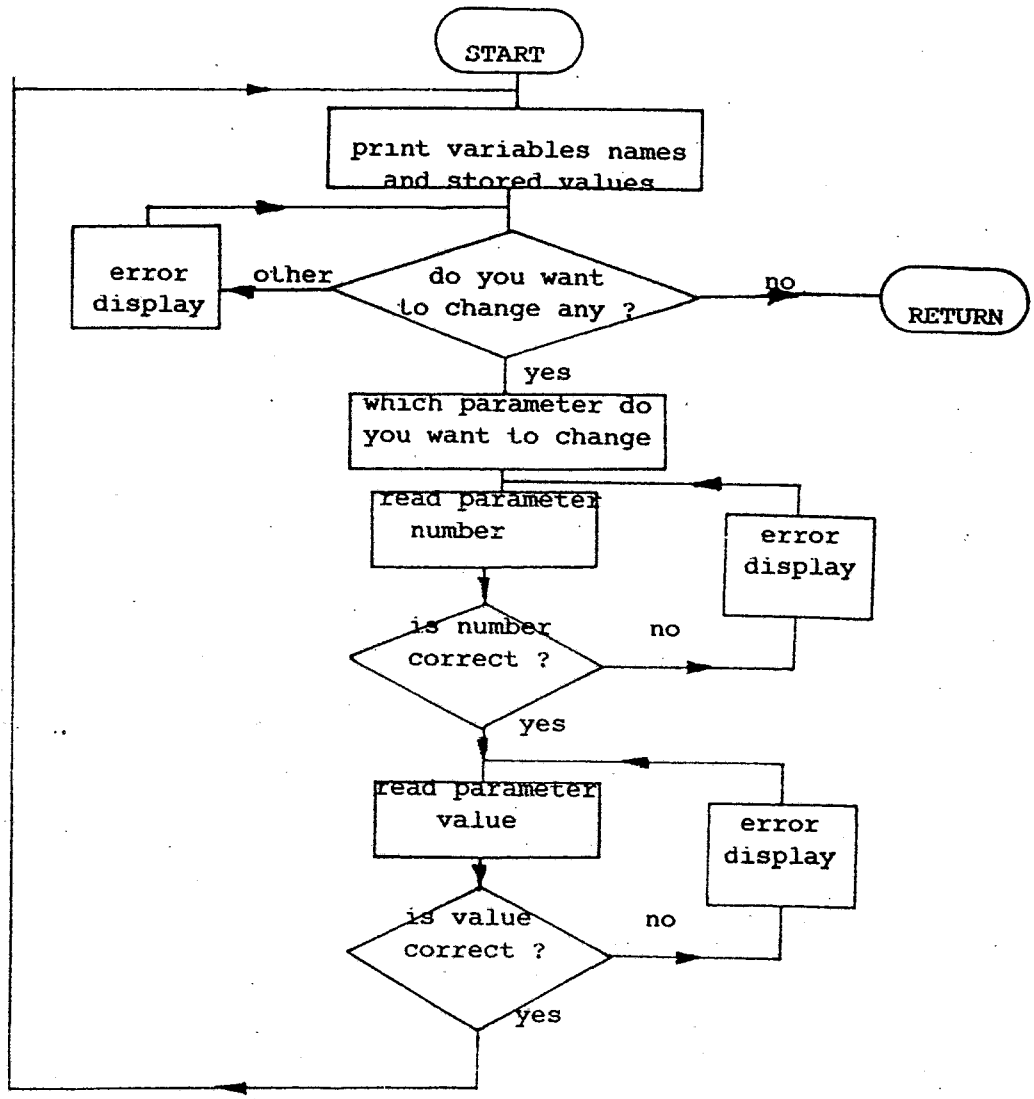

Fig.A4.1 Flow diagram of subroutine 'quest1'

APPENDIX V

SIZING OF A HYDRAULIC RESERVOIR

This appendix provides an illustration of the reservoir design procedures discussed in Chapter V.

Fig.A5.1 shows the circuit diagram of a hydraulic system for which a reservoir is to be sized.

The system is to be installed on mobile equipment and hence its shape may be determined by installation requirements, but a cylindrical shape will be assumed.

EXAMPLE DATA

Mean pump flow = 3 ℓ/s

Accumulator capacity = 1 ℓ

Actuator (single) : $\emptyset$ = 0.1 m ; ℓ = 0.2 m

Actuator (double) : $\emptyset$ = 0.1 m ; ℓ = 0.5 m ; $A_1 = 2 * A_2$

t_{min} = 0 C ; t_{max} = 120 C

Max tilting angle of vehicle = 30 deg

Fluid viscosity = 28 cSt (at working temp.)

SOLUTION

The return line is vertically orientated when entering the reservoir and sized to give a fluid velocity of 1m/s (return line diameter=0.06m).

At the end of the return line a diffuser is connected. The fluid velocity leaving the diffuser perforations must be between 0.1 and

0.5 m/s. Using data from Fitch [45] for woven wire cloth diffusers, a mesh with 36 perforations per inch, and 0.045 cm each perforation has a 41% of open area. If the fluid velocity is desired to be 0.3 m/s, it needs an area of 0.01 m^2 and hence the total diffuser area is:

$$\text{diffuser area} = \frac{\text{open area}}{41\%} = 0.0243 \ m^2$$

If the cylindrical shaped diffuser has its diameter equal to half its length, it must be:

$$\phi_{dif} = \frac{\ell_{dif}}{2} = \frac{0.0243}{2\,\pi} = 0.062 \ m$$

A deflector (see fig.A5.2) is used on the outside of the diffuser to direct the air bubbles upwards. If the anular area between the diffuser and deflector is made equal to the diffuser open area, the external diameter of the deflector is:

$$\phi_{defl} = 0.062^2 + \frac{0.01 * 4}{\pi} = 0.13 \ m$$

and its length is only half that of the diffuser.

The size of the air bubbles leaving the perforations of the diffuser are dependent upon the aperture of the perforations (0.045 cm), according to the formula [45]:

$$v_{bubble} = c \cdot \phi_{perf}$$

where, $c = 9.5*10^{-6}$ [m^2], for mineral oils. Hence, the air bubble volume is:

$$v_{bubble} = 4.28*10^{-9} \ m^3 \longrightarrow \phi_{bubble} = 1mm$$

The slip velocity of the bubbles is (see table 5.1):

$$V_{slip} = 11 \ mm/s$$

The tank diameter can, now, be evaluated at the point of highest fluid velocity in the tank (opposite deflector):

$$v_{slip} \cdot \frac{\pi (\phi^2_{tank} - \phi^2_{defl})}{4} = \text{pump flow}$$

hence, $\phi_{tank} = 0.6$ m.

Now that the tank diameter is determined from air release considerations, its minimum level must be set in order to accomodate the diffuser which must always be immersed. The diffuser is positioned one diameter away from the bottom of the tank and the minimum tank level is one diameter above the top of the diffuser.

An increase in this level may occur as a result of:

a) change in system capacity (actuators + accumulator):

$$\Delta v_{system} = 1.6 + 2.0 + 1.0 = 4.6 \ \ell$$

b) acceptable leakage in between inspections:

$$\Delta v_{leakage} = 1 \ \ell \text{ (assumed)}$$

c) thermal expansion, over 120 C, of fluid volume:

$$\Delta v_{expansion} = 80 * 2.4 \times 10^{-4} * 120 = 2.3 \ \ell$$

where, system volume = 70 ℓ (tank minimum level) + 10 ℓ (assumed system volume).

d) tilting of vehicle will increase the maximum level of the fluid by:

$$\Delta \ell_{tilt} = \frac{\phi_{tank}}{2} \cdot \frac{\sqrt{3}}{3} = 0.17 \text{ m}$$

or $\Delta v_{tilt} = 0.17 * A_{tank} = 48 \ \ell$

Hence, the distance between maximum and minimum levels in the tank must be:

$$\Delta \ell = \frac{4.6 + 1. + 2.3 + 48}{A_{tank}} = 20 \text{ cm}$$

If a 5cm clearance is allowed at the top, the overall length of the tank will be:

$$\ell = 20 + 5 + 12.4 + 6.2 + 6.2 = 50 \text{ cm}$$

and the overall tank capacity:

$$V_{tank} = 0.5 * A_{tank} = 141 \ \ell$$

The tank capacity evaluated in this manner is found to be much less than what would be recommended by AHEM [37]. Instead of the 'rule of thumb' of "three times the pump flow (ℓ/min)" the value was about 0.8 of the pump flow. On the other hand the normal practice in mobile equipment of using 5:1 ratio of pump flow to tank capacity [39] would give a considerably undersized tank in this case.

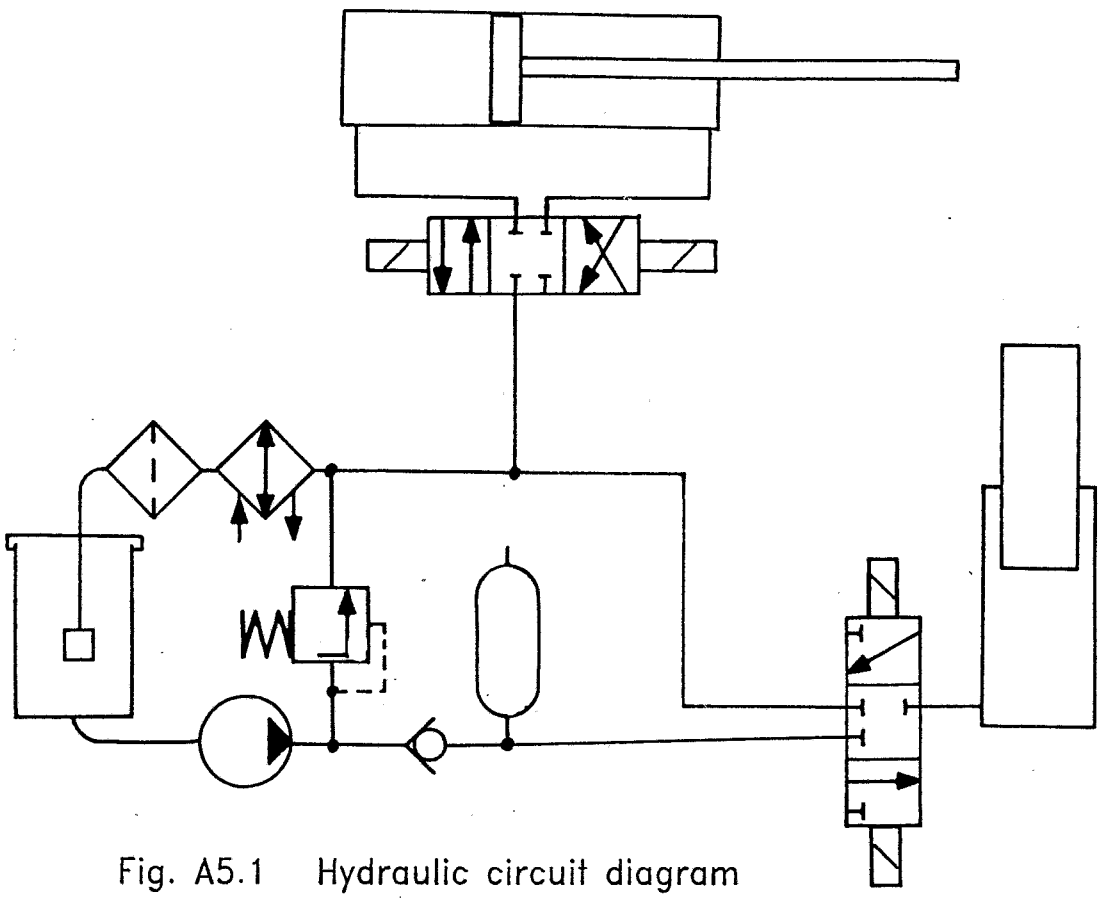

Fig. A5.1 Hydraulic circuit diagram

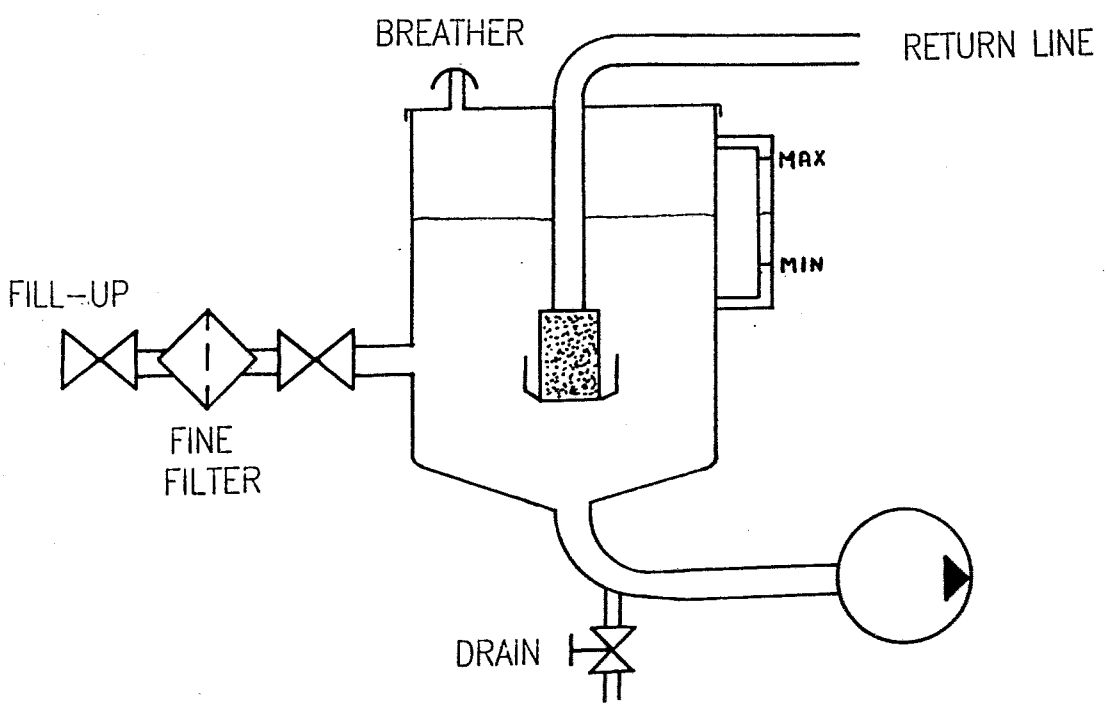

Fig. A5.2 Detail of hydraulic reservoir

APPENDIX VI

DESCRIPTION OF EXPERIMENTAL APPARATUS COMPONENTS

A6.1 HYDRAULIC COMPONENTS

Pump A

This was a variable displacement axial piston swash plate pump manufactured by Reyrolle Hydraulics Ltd., having the following specifications:

type	A200
theoretical max. displacement	$33cm^3/rev$
max. recommended speed	
a) unboosted	2500 rev/min
b) boosted	3500 rev/min
max. pressure for continuous operation	275 bar
number of pistons	7
weight	12 kg

This unit is reversible and was used as a motor as well as a pump. The swash control is manual, by rotation of a wheel. The very compact design of the unit lead to low dead volumes between port plate and pump flange.

Pump B

This was a large axial piston pump manufactured by Lucas Fluid Power. It was driven by a hydraulic motor on a variable speed rig. The pump has the following specifications:

type	HD900

theoretical displacement	68cm^3/rev
max. continuous speed	3000rev/min
max. pressure for continuous operation	270 bar
max. peak pressure	340 bar
number of pistons	9
weight	65.5 kg

This unit has very long internal passageways connecting the pump flange to the port plate and hence a large volume of fluid.

Pump C

This unit was a Dowty external gear pump with the following characteristics:

type	1P3060
theoretical displacement	19.2 cm^3/rev
max. working pressure	207 bar
max. rotational speed	3500 rev/min
number of gear teeth	8

This unit has hydraulically balanced side plates.

Pump E

This external gear pump was a large displacement unit manufactured by Hamworthy. The details of the unit are as follows:

type	P2C2125L
theoretical displacement	47 cm^3/rev
max. working pressure	207 bar
max. speed	2700 rev/min
number of teeth	10

Pump E was mounted on a variable speed rig, and driven by an external gear hydraulic motor of similar size to the pump.

Pump F

Pump F was an axial piston pump manufactured by Sperry Vickers, with the following specifications:

type	PVB 15
displacement	32 cm^3/rev
max. working pressure	210 bar
number of pistons	9

Pump F was used as boost pump during the tests reported in chapter VII. This unit had a pressure compensator control which was set to a very high pressure. Consequently, during the tests the pump always behaved as a fixed displacement unit.

Pump G

Pump G was an external gear pump of the P3000 range of pumps manufactured by Dowty. The details of the pump are:

type	2P3090
theoretical displacement	28.8 cm^3/rev
max. recommended speed	3000 rev/min
max. working pressure	207 bar
number of teeth	8

Valve A

Valve A is a restrictor valve produced by ACL and having 3/4" pipe connections.

Valve B

This valve is a cartridge type relief valve with two stages manufactured by Sterling Hydraulics Ltd. The specifications for the valve are:

type	A3A125

flow range	0 to 200 ℓ/min
pressure range	2 to 350 bar
temperature range	30 to 90 C
weight	0.26 kg
pipe connections	3/4"

This valve is of very light construction which allowed for easy fitting directly to the pipework.

A6.2 INSTRUMENTATION

Piezoelectric Pressure Transducer

The piezoelectric pressure transducers were manufactured by Vibrometer Ltd. having the following characteristics:

type	6QP500
max. working pressure	470 bar
max. working temperature	240 C
mass	negligible
linearity	$\ll \pm 1\%$
natural frequency	67 kHz
damping	0.3
insulation resistance	$2 \times 10^3\ \Omega$

These transducers are of very small size (see fig.2.1) and had sensitivities close to 7pCoulomb/bar.

Frequency Response Analyser (F.R.A.)

The F.R.A. was a Solartron 1170 capable of performing Fourier analysis of signals. This instrument analyses the signal up to the tenth harmonic of its fundamental frequency and the result (complex number) can be obtained in one of the following forms:

a) real and imaginary parts (a,b)

b) amplitude (volts) and phase (degrees) (A,θ)

c) amplitude (dB) and phase (degrees) $(dB;\theta)$

The logarithmic scale (dB) is defined relative to 10μV, according to the following equation:

$$amp(dB) = 20 \log_{10}(amp(volts)*10^5)$$

or

$$amp(dB) = 100 + 20 \log_{10}(amp(volts))$$

The F.R.A. uses the sine wave as the basis of the Fourier Analysis. The value of the phase displayed refers to the phase advance of the evaluated harmonic component compared to the reference signal, which is a square wave.

A digital interface was used to link the F.R.A. with a DEC PDP8 computer and automatic data acquisition was possible.

Storage Oscilloscope

This instrument was a Gould Digital Storage Oscilloscope with the following specifications:

type	OS4000
time base range	1μsec to 20sec/cm
input range sensitivity	5mv/cm to 20V/cm
maximum input voltage	400V DC or peak AC
screen resolution:	
single trace	100 points/cm
double trace	50 points/cm
digital storage size	1024 x 8 bits
plotter output (OS4001)	100mV/1cm of screen

The scope has a plotter interface which was used to record many of the time signals presented in this thesis.

Spectrum Analyser

The spectrum analyser is a Hewlett Packard instrument which accepts two signal inputs, performing a Fast Fourier Transform on each signal. The analyser displays then the amplitude and phase spectra of the signals over a selected frequency range. The instrument has the following characteristics:

frequency range (maximum)	0.02 Hz to 25kHz
amplitude display	10 dB scale
	2 dB scale
	linear scale
amplitude display	256 points (one channel)
amplitude range	+30 to -50dB (rel.to 1V)
	30Volts rms to 3mVolts

This instrument was used during tests to analyse pressure signals in a 2kHz frequency range to examine the main pumping component frequencies and in the 25kHz frequency range to search for the existence of cavitation.

Pressurized Tank Level Detection

The automatic control of fluid level in the pressurized tank was done through the use of an electronic control circuit connected to two light sensitive switches.

The control was designed to conform with the following requirements:

a) have manual or automatic selection

b) under automatic control the unit must:

i) start top-up pump when bottom detector is uncleared

ii) stop top-up pump when upper detector is covered

iii) actuate bleed valve if top detector is covered for over 15 sec

c) under manual control the actuation of top-up pump and bleed valve are independent.

The detectors were positioned around a transparent pipe in diametrical opposition to a light source. When the fluid is between the light source and the detector the switch is not activated but when the oil level drops the intensity of the light source is sufficient to activate the switch.

Figs.A6.1 and A6.2 show some details of the electronic circuitry used for the control and fig.5.9 shows the control box and the detectors positioned on the rig.

During the extensive tests performed the level detection proved very satisfactory. This made it possible to regard the pressurized reservoir as a normal reservoir.

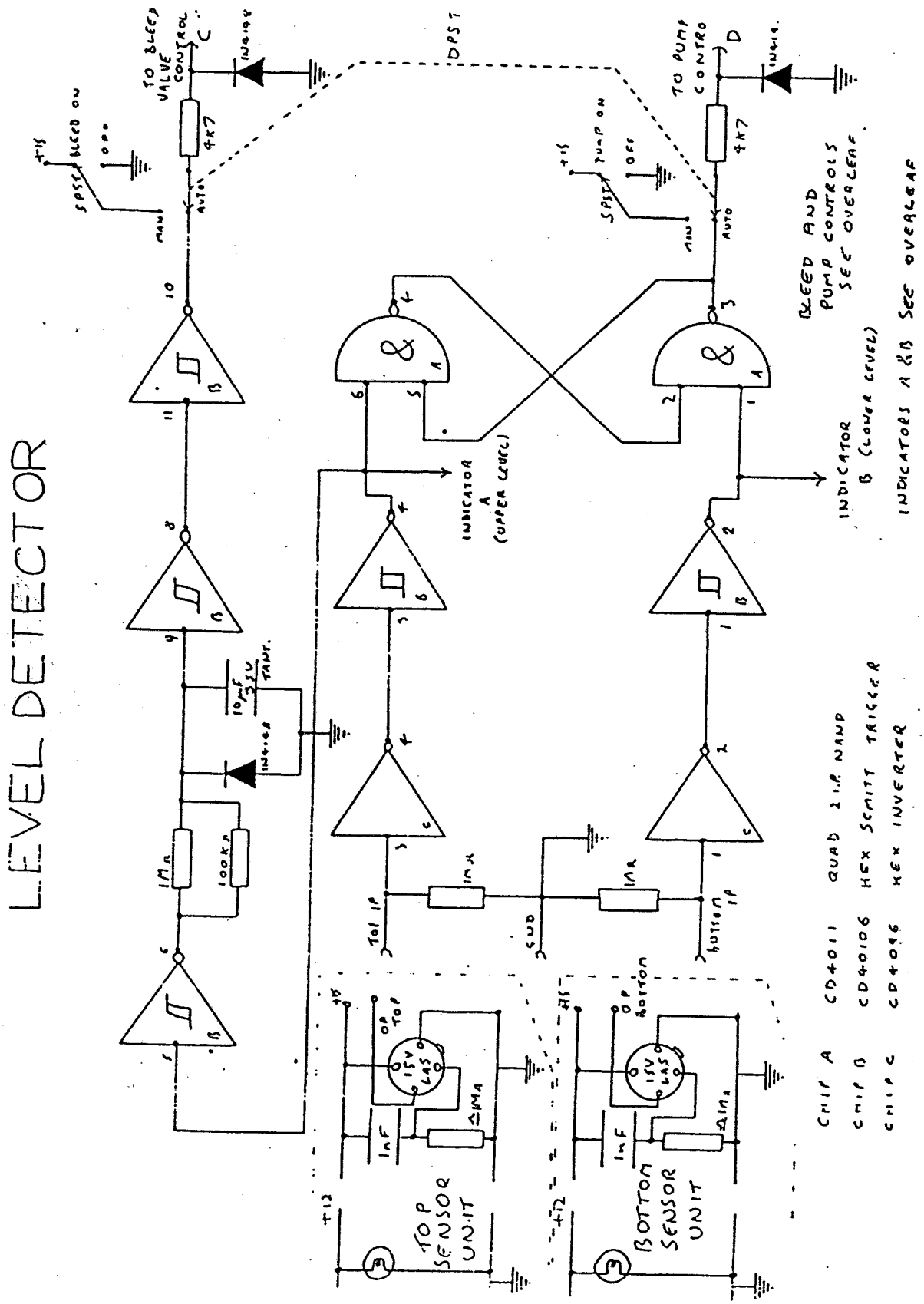

Fig. A6.1 Electronic circuit for tank level detection

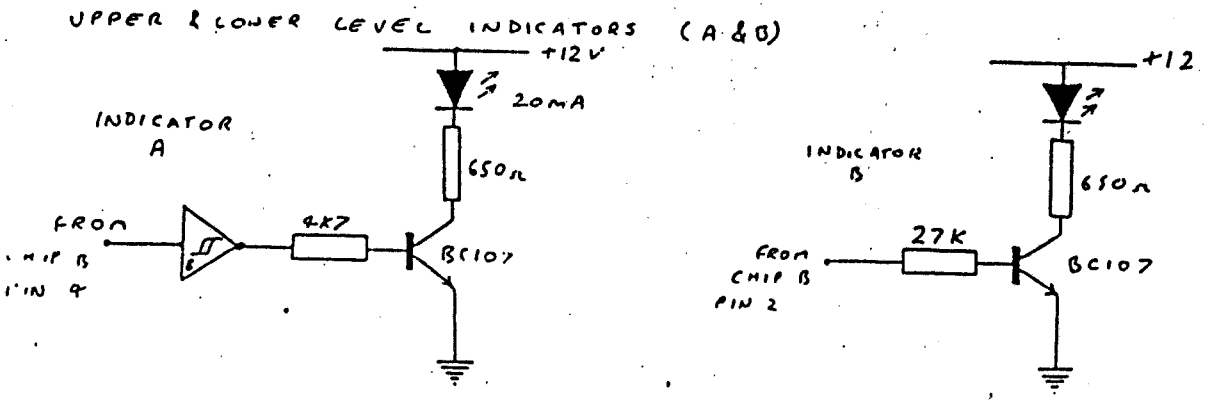

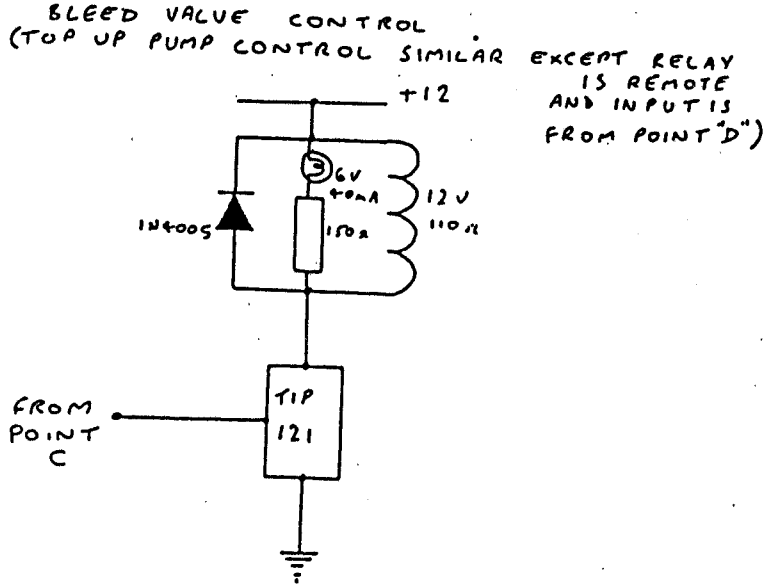

POWER REQUIREMENTS	
CIRCUIT	SUPPLY
DETECTOR CIRCUIT	±15V LASCAR 250mA PSU 106
SENSOR CIRCUIT (LIGHT ACTIVATED SWITCHES)	AS ABOVE
LEVEL INDICATORS	+12V KINGSHILL
PUMP AND BLEED CONTROLS (RELAYS & BULBS)	AS ABOVE
LIGHT BULBS IN SENSORS	AS ABOVE
BLEED VALVE SUPPLY	+27V KINGSHILL
TOP-UP PUMP SUPPLY	3 PHASE MAINS

Fig. A6.2 Electronic circuit for tank level detection (cont)